

Gold Nanoparticles: Assembly, Supramolecular Chemistry, Quantum-Size-Related Properties, and Applications toward Biology, Catalysis, and Nanotechnology

Marie-Christine Daniel and Didier Astruc*

Molecular Nanosciences and Catalysis Group, LCOO, UMR CNRS No. 5802, Université Bordeaux I, 33405 Talence Cedex, France

Received August 6, 2003

Contents

1. Historic Introduction	293	6.3. AuNP Sugar Sensors	323
2. General Background: Quantum Size Effect and Single-Electron Transitions	294	6.4. Other AuNP Bioconjugates: Peptides, Lipids, Enzymes, Drugs, and Viruses	324
3. Synthesis and Assembly	296	6.5. AuNP Biosynthesis	325
3.1. Citrate Reduction	296	7. Catalysis	325
3.2. The Brust–Schiffrin Method: Two-Phase Synthesis and Stabilization by Thiols	296	7.1. Catalysis of CO Oxidation	325
3.3. Other Sulfur Ligands	297	7.2. Electrochemical Redox Catalysis of CO and CH ₃ OH Oxidation and O ₂ Reduction	326
3.4. Other Ligands	298	7.3. Catalysis of Hydrogenation of Unsaturated Substrates	326
3.4.1. Phosphine, Phosphine Oxide, Amine, and Carboxylate Ligands	298	7.4. Catalysis by Functional Thiolate-Stabilized AuNPs	326
3.4.2. Isocyanide	298	7.5. Other Types of Catalysis	327
3.4.3. Acetone	298	8. Nonlinear Optics (NLO)	327
3.4.4. Iodine	298	9. Miscellaneous Applications	328
3.5. Microemulsion, Reversed Micelles, Surfactants, Membranes, and Polyelectrolytes	298	10. Conclusion and Perspectives	329
3.6. Seeding Growth	298	11. Acknowledgment	329
3.7. Physical Methods: Photochemistry (UV, Near-IR), Sonochemistry, Radiolysis, and Thermolysis	298	12. Abbreviations	329
3.8. Solubilization in Fluorous and Aqueous Media	299	13. References	330
3.9. Characterization Techniques	300		
3.10. Bimetallic Nanoparticles	303		
3.11. Polymers	304		
3.12. Dendrimers	307		
3.13. Surfaces, Films, Silica, and Other AuNP Materials	308		
4. Physical Properties	312		
4.1. The Surface Plasmon Band (SPB)	312		
4.2. Fluorescence	314		
4.3. Electrochemistry	315		
4.4. Electronic Properties Using Other Physical Methods	315		
5. Chemical, Supramolecular, and Recognition Properties	317		
5.1. Reactions of Thiolate-Stabilized AuNPs	317		
5.2. Supramolecular Chemistry	318		
5.3. Molecular Recognition	319		
5.3.1. Redox Recognition Using Functionalized AuNPs as Exoreceptors	319		
5.3.2. Miscellaneous Recognition and Sensors	320		
6. Biology	321		
6.1. DNA–AuNPs Assemblies and Sensors	321		
6.2. AuNP-Enhanced Immuno-Sensing	323		

1. Historic Introduction

Although gold is the subject of one of the most ancient themes of investigation in science, its renaissance now leads to an exponentially increasing number of publications, especially in the context of emerging nanoscience and nanotechnology with nanoparticles and self-assembled monolayers (SAMs). We will limit the present review to gold nanoparticles (AuNPs), also called gold colloids. AuNPs are the most stable metal nanoparticles, and they present fascinating aspects such as their assembly of multiple types involving materials science, the behavior of the individual particles, size-related electronic, magnetic and optical properties (quantum size effect), and their applications to catalysis and biology. Their promises are in these fields as well as in the bottom-up approach of nanotechnology, and they will be key materials and building block in the 21st century.

Whereas the extraction of gold started in the 5th millennium B.C. near Varna (Bulgaria) and reached 10 tons per year in Egypt around 1200–1300 B.C. when the marvelous statue of Touthankamon was constructed, it is probable that “soluble” gold appeared around the 5th or 4th century B.C. in Egypt and China. In antiquity, materials were used in an ecological sense for both aesthetic and curative purposes. Colloidal gold was used to make ruby glass



Marie-Christine Daniel was born in Vannes, France. She graduated from the University of Rennes (France). She is now finishing her Ph.D. on exoreceptors at the Bordeaux 1 University in the research group of Professor Didier Astruc. Her doctoral research is concerned with the recognition of anions of biological interest using fonctionalized gold nanoparticles and redox-active metalodendrimers.



Didier Astruc is Professor of Chemistry at the University Bordeaux I and has been a Senior Member of the Institut Universitaire de France since 1995. He studied in Rennes (thesis with R. Dabard), and then did his postdoctoral research at MIT with R. R. Schrock. He is the author of *Electron Transfer and Radical Processes in Transition-Metal Chemistry* (VCH, 1995, prefaced by Henry Taube) and *Chimie Organométallique* (EDP Science, 2000; Spanish version in 2003). His research interests are in organometallic chemistry at the interface with nanosciences, including sensing, catalysis, and molecular electronics.

and for coloring ceramics, and these applications are still continuing now. Perhaps the most famous example is the Lycurgus Cup that was manufactured in the 5th to 4th century B.C. It is ruby red in transmitted light and green in reflected light, due to the presence of gold colloids. The reputation of soluble gold until the Middle Ages was to disclose fabulous curative powers for various diseases, such as heart and venereal problems, dysentery, epilepsy, and tumors, and for diagnosis of syphilis. This is well detailed in what is considered as the first book on colloidal gold, published by the philosopher and medical doctor Francisci Antonii in 1618.¹ This book includes considerable information on the formation of colloidal gold sols and their medical uses, including successful practical cases. In 1676, the German chemist Johann Kunckels published another book,^{2a} whose chapter 7 concerned “drinkable gold that contains metallic gold in a neutral, slightly pink solution that exert curative properties for several diseases”. He concluded, well before Michael Faraday

(vide infra), that “gold must be present in such a degree of communitation that it is not visible to the human eye”. A colorant in glasses, “Purple of Cassius”, is a colloid resulting from the heterocoagulation of gold particles and tin dioxide, and it was popular in the 17th century.^{2b} A complete treatise on colloidal gold was published in 1718 by Hans Heinrich Helcher.³ In this treatise, this philosopher and doctor stated that the use of boiled starch in its drinkable gold preparation noticeably enhanced its stability. These ideas were common in the 18th century, as indicated in a French dictionary, dated 1769,⁴ under the heading “or potable”, where it was said that “drinkable gold contained gold in its elementary form but under extreme sub-division suspended in a liquid”. In 1794, Mrs. Fuhlame reported in a book⁵ that she had dyed silk with colloidal gold. In 1818, Jeremias Benjamin Richters suggested an explanation for the differences in color shown by various preparation of drinkable gold:⁶ pink or purple solutions contain gold in the finest degree of subdivision, whereas yellow solutions are found when the fine particles have aggregated.

In 1857, Faraday reported the formation of deep-red solutions of colloidal gold by reduction of an aqueous solution of chloroaurate (AuCl_4^-) using phosphorus in CS_2 (a two-phase system) in a well-known work. He investigated the optical properties of thin films prepared from dried colloidal solutions and observed reversible color changes of the films upon mechanical compression (from bluish-purple to green upon pressurizing).⁷ The term “colloid” (from the French, *colle*) was coined shortly thereafter by Graham, in 1861.⁸ Although the major use of gold colloids in medicine in the Middle Ages was perhaps for the diagnosis of syphilis, a method which remained in use until the 20th century, the test is not completely reliable.^{9–11}

In the 20th century, various methods for the preparation of gold colloids were reported and reviewed.^{11–17} In the past decade, gold colloids have been the subject of a considerably increased number of books and reviews,^{15–44} especially after the breakthroughs reported by Schmid^{17,19,21} and Brust et al.^{22,27} The subject is now so intensively investigated, due to fundamental and applied aspects relevant to the quantum size effect, that a majority of the references reported in the present review article have appeared in the 21st century. Readers interested in nanoparticles in general can consult the excellent books cited in refs 15, 24, 28, 33, and 43. The book by Hayat, published in 1989,¹⁴ essentially deals with biological aspects and imaging of AuNPs.

2. General Background: Quantum Size Effect and Single-Electron Transitions

Physicists predicted that nanoparticles in the diameter range 1–10 nm (intermediate between the size of small molecules and that of bulk metal) would display electronic structures, reflecting the electronic band structure of the nanoparticles, owing to quantum-mechanical rules.²⁹ The resulting physical properties are neither those of bulk metal nor those of molecular compounds, but they strongly depend on

the particle size, interparticle distance, nature of the protecting organic shell, and shape of the nanoparticles.²⁷ The few “last metallic electrons” are used for tunneling processes between neighboring particles, an effect that can be detected by impedance measurements that distinguish intra- and intermolecular processes. The *quantum size effect* is involved when the de Broglie wavelength of the valence electrons is of the same order as the size of the particle itself. Then, the particles behave electronically as zero-dimensional quantum dots (or quantum boxes) relevant to quantum-mechanical rules. Freely mobile electrons are trapped in such metal boxes and show a characteristic collective oscillation frequency of the plasma resonance, giving rise to the so-called plasmon resonance band (PRB) observed near 530 nm in the 5–20-nm-diameter range. In nanoparticles, there is a gap between the valence band and the conduction band, unlike in bulk metals. The size-induced metal–insulator transition, described in 1988, is observed if the metal particle is small enough (about 20 nm) that size-dependent quantization effects occur. Then, standing electron waves with discrete energy levels are formed. *Single-electron transitions* occur between a tip and a nanoparticle, causing the observation of so-called Coulomb blockades if the electrostatic energy, $E_{el} = e^2/2C$, is larger than the thermal energy, $E_T = kT$. The capacitance C becomes smaller with smaller particles. This means that single-electron transitions can be observed at a given temperature only if C is very small, i.e., for nanoparticles since they are small enough ($C < 10^{-18}$ F). Large variations of electrical and optical properties are observed when the energy level spacing exceeds the temperature, and this flexibility is of great practical interest for applications (transistors, switches, electrometers, oscillators, biosensors, catalysis).^{32–38} For instance, single-electron tunneling related to the electrical resistance of a single rod-shaped molecule provided a value of 18 ± 12 M Ω for self-assembled monolayers on gold (1,1,1) substrate used to tether AuNPs deposited from a cluster beam.³² The transition from metal-like capacitive charging to redox-like charging was observed with alkanethiolate–gold nanoparticles of low dispersity in an electrochemical setup for Coulomb staircase experiments.^{39,40} Indeed, it was initially indicated that these AuNPs could accommodate 10 redox states.^{39a} In a subsequent paper published in 2003, it was shown that lower temperatures enhance the resolution of quantized double-layer charging peaks in differential pulse voltammetry (DPV) observations. This led to the resolution of 13 peaks in CH₂Cl₂ at 263 K for Au₁₄₀ particles.^{39b} At the same time, however, a publication by Quinn’s group revealed remarkably well-resolved DPV of analogous Au₁₄₇ particles, showing 15 evenly spaced peaks at room temperature (295 K) corresponding to 15 oxidation states (Figure 1). It was also anticipated that, the number of observable charge states being limited by the size of the available potential window, additional peaks should be observed in controlled atmosphere and reduced temperature conditions.⁴⁰ Thus, AuNPs behave as other delocalized redox molecules, disclos-

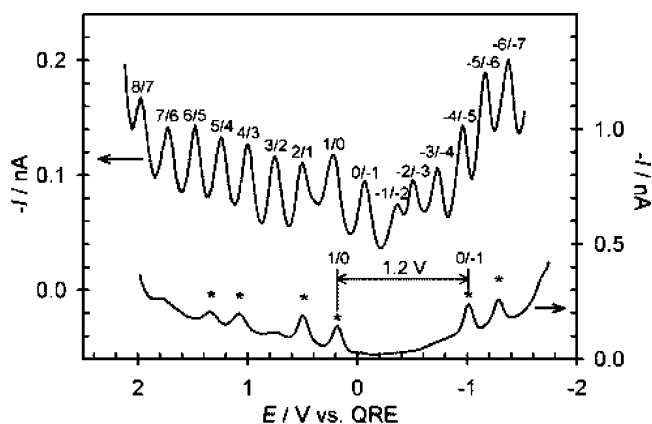


Figure 1. Differential pulse voltammetry (DPV) responses for AuNP solutions measured at a Pt microelectrode; (upper) as-prepared 177 μM hexanethiol-capped Au₁₄₇ showing 15 high-resolution quantized double-layer charging (QDL) peaks and (lower) 170 μM hexanethiol-capped Au₃₈ showing a HOMO–LUMO gap. It can be seen that the as-prepared solution contains a residual fraction of Au₃₈ that smears out the charging response in E regions where QDL peaks overlap. The electrode potential scanned negative to positive. Reprinted with permission from ref 40 (Quinn’s group). Copyright 2003 American Chemical Society.

ing redox cascades that are well known in inorganic and organometallic electrochemistry for other transition metal clusters and bi-sandwich complexes.

The pioneering work by Schmid and co-workers on well-defined phosphine-stabilized gold clusters showed the properties of quantum-dot particles for the first time.³⁰ The number of atoms in these gold clusters is based on the dense packing of atoms taken as spheres, each atom being surrounded by 12 nearest neighbors. Thus, the smallest cluster contains 13 atoms, and the following layers contain $10n^2 + 2$ atoms, n being the layer number. For instance, the second layer contains 42 atoms, which leads to a total of 55 atoms for a gold cluster, and the compound [Au₅₅(PPh₃)₁₂Cl₆] has been well characterized by Schmid’s group. Recently, spectroscopic data have revealed discrete energy level spacings of 170 meV that can be attributed to the Au₅₅ core.^{30c} Larger clusters containing, respectively, 147, 309, 561, 923, 1415, or 2057 ($n = 3–8$) atoms have been isolated.^{30,31} Discrete organogold clusters are also well known with small numbers of atoms and various geometries, and they will not be reviewed here.^{41,42} Large ones form a fuzzy frontier between clusters and colloids (AuNPs), the latter being defined by some dispersity materialized by a histogram determined using transmission electron microscopy (TEM) data.

Despite the considerable variety of contributions, we will focus first on synthesis, stabilization, and various types of assemblies, and then on physical properties and on chemical, supramolecular, and sensor properties, and finally on applications to biochemistry, catalysis, and nonlinear optical properties before concluding on the perspectives of AuNPs in nanosciences and nanotechnology. Many publications involve two or even sometimes several of these topics. Thus our classification is arbitrary, but the reader will often better understand the spirit of each paper from its title given in the reference section.

3. Synthesis and Assembly

3.1. Citrate Reduction

Among the conventional methods of synthesis of AuNPs by reduction of gold(III) derivatives, the most popular one for a long time has been that using citrate reduction of HAuCl_4 in water, which was introduced by Turkevitch in 1951.¹² It leads to AuNPs of ca. 20 nm. In an early effort, reported in 1973 by Frens,¹³ to obtain AuNPs of prechosen size (between 16 and 147 nm) via their controlled formation, a method was proposed where the ratio between the reducing/stabilizing agents (the trisodium citrate-to-gold ratio) was varied. This method is very often used even now when a rather loose shell of ligands is required around the gold core in order to prepare a precursor to valuable AuNP-based materials. Recently, a practical preparation of sodium 3-mercaptopropionate-stabilized AuNPs was reported in which simultaneous addition of citrate salt and an amphiphile surfactant was adopted; the size could be controlled by varying the stabilizer/gold ratio (Figure 2).⁴⁴

3.2. The Brust–Schiffrin Method: Two-Phase Synthesis and Stabilization by Thiols

Schmid's cluster $[\text{Au}_{55}(\text{PPh}_3)_{12}\text{Cl}_6]$, reported in 1981, long remained unique with its narrow dispersity (1.4 ± 0.4 nm) for the study of a quantum-dot nanomaterial, despite its delicate synthesis.⁴⁵ The stabilization of AuNPs with alkanethiols was first reported in 1993 by Mulvaney and Giersig, who showed the possibility of using thiols of different chain lengths and their analysis.^{46a} The Brust–Schiffrin method for AuNP synthesis, published in 1994, has had a considerable impact on the overall field in less than a decade, because it allowed the facile synthesis of thermally stable and air-stable AuNPs of reduced dispersity and controlled size for the first time (ranging in diameter between 1.5 and 5.2 nm). Indeed, these AuNPs can be repeatedly isolated and

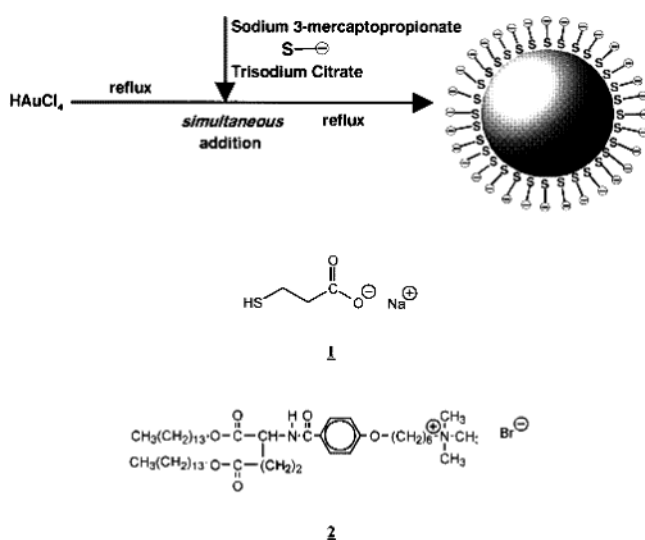


Figure 2. Preparation procedure of anionic mercapto-ligand-stabilized AuNPs in water. Reprinted with permission from ref 44 (Kunitake's group). Copyright 1999 Elsevier.

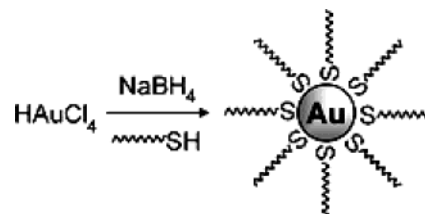
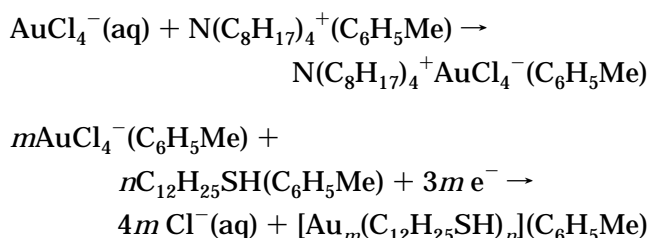


Figure 3. Formation of AuNPs coated with organic shells by reduction of Au^{III} compounds in the presence of thiols. Reprinted with permission from ref 73 (Crooks's group). Copyright 2001 Royal Society of Chemistry.

redissolved in common organic solvents without irreversible aggregation or decomposition, and they can be easily handled and functionalized just as stable organic and molecular compounds. The technique of synthesis is inspired by Faraday's two-phase system⁷ and uses the thiol ligands that strongly bind gold due to the soft character of both Au and S.⁴⁷ AuCl_4^- is transferred to toluene using tetraoctylammonium bromide as the phase-transfer reagent and reduced by NaBH_4 in the presence of dodecanethiol (Figure 3).^{47a} The organic phase changes color from orange to deep brown within a few seconds upon addition of NaBH_4 :



The TEM photographs showed that the diameters were in the range 1–3 nm, with a maximum in the particle size distribution at 2.0–2.5 nm, with a preponderance of cuboctahedral and icosahedral structures. Larger thiol/gold mole ratios give smaller average core sizes, and fast reductant addition and cooled solutions produced smaller, more monodisperse particles. A higher abundance of small core sizes (≤ 2 nm) is obtained by quenching the reaction immediately following reduction or by using sterically bulky ligands.^{48–50} Brust et al. extended this synthesis to *p*-mercaptophenol-stabilized AuNPs in a single-phase system,^{47b} which opened an avenue to the synthesis of AuNPs stabilized by a variety of functional thiol ligands.^{47,48} Subsequently, many publications appeared describing the use of the Brust–Schiffrin procedure for the synthesis of other stable AuNPs, also sometimes called monolayer-protected clusters (MPCs), of this kind that contained functional thiols.^{49–53} The proportion thiol: AuCl_4^- used in the synthesis controls the size of the AuNPs (for instance, a 1:6 ratio leads to the maximum average core diameter of 5.2 nm, i.e., ca. 2951 Au atoms and ca. 371 thiolate ligands; core diameter dispersity of $\sim \pm 10\%$). Murray et al. reported and studied the “place exchange” of a controlled proportion of thiol ligands by various functional thiols⁵² (Figures 4 and 5) and the subsequent reactions of these functional AuNPs.^{50,52} Schiffrin reported the purification of dodecanethiol-stabilized AuNPs from tetraoctylam-

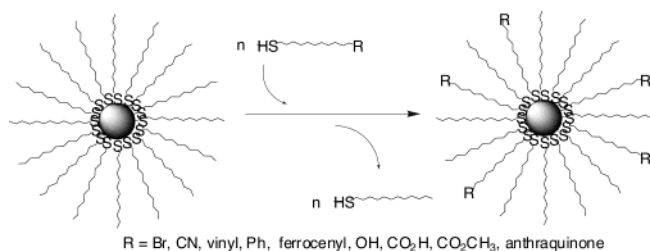


Figure 4. General scheme for the ligand-exchange reaction between alkanethiol-AuNPs of the Brust type and various functionalized thiols.

monium impurities by Soxhlet extraction.⁵⁴ The influence of nonionic surfactant polyoxoethylene(20) sorbitan monolaurate (Tween 20) on surface modification of AuNPs was studied with mercaptoalkanoic acids.⁵⁵ Digestive ripening, i.e., heating a colloidal suspension near the boiling point in the presence of alkanethiols (for instance, 138 °C for 2 min, followed by 5 h at 110 °C), significantly reduced the average particle size and polydispersity in a convenient and efficient way. This technique also led to the formation of 2D and 3D superlattices,^{56,57} a subject of intense investigation (see also section 3.13 on materials).^{58–63} For instance, AuNPs obtained using acid-facilitated transfer are free of tetraalkylammonium impurity, are remarkably monodisperse, and form crystalline superstructures.^{63a} The truncated icosahedron structure is formed in growth conditions in which the equilibrium shape is achieved.^{63b} Molecular dynamics simulations showed that AuNPs with 1157 Au atoms

attained an icosahedral structure upon freezing.^{63c} A single-toluene phase method was also reported whereby the ammonium salt-stabilized AuNPs were synthesized, followed by an exchange reaction with dodecanethiol.⁵⁸ Superhydride^{64a} and hexadecylaniline^{64b} (inter alia) have been used as alternative reagents to NaBH₄ for the reduction of gold(III) in the synthesis of thiol-stabilized AuNPs. Shape separation of suspended AuNPs by size-exclusion chromatography was monitored by examining the 3D chromatograms obtained by employing a diode-array detection system.⁶⁵

3.3. Other Sulfur Ligands

Other sulfur-containing ligands,^{67–70} such as xanthates⁶⁶ and disulfides,^{67–69} di-^{70a} and trithiols,^{70b} and resorcinarene tetrathiols,^{70d} have been used to stabilize AuNPs. Disulfides are not as good stabilizing agents as thiols,^{67–70} which is eventually useful for catalysis.⁷⁰ Similarly, thioethers do not bind AuNPs strongly,⁷¹ but the use of polythioethers by Rheinhout's group astutely circumvented this problem.^{72a} Tetradentate thiethers have also been used to reversibly form AuNP assemblies.^{72b} On the other hand, oxidation of thiol-stabilized AuNPs by iodine provokes their decomposition to gold iodide with formation of disulfides, which led Crooks to form polycyclodextrin hollow spheres by templating AuNPs.⁷³

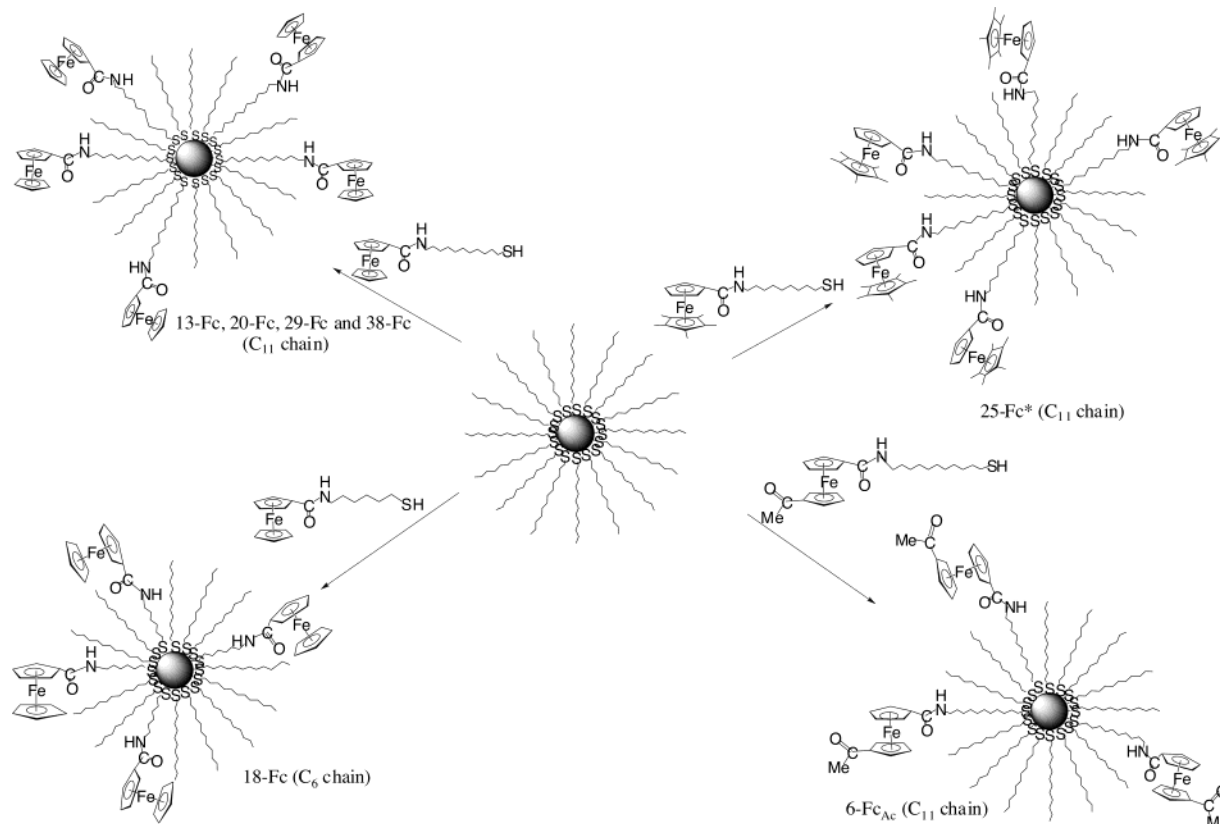


Figure 5. Ligand substitution reactions (CH₂Cl₂, 2 d, room temperature) for the syntheses of the AuNPs containing mixed dodecanethiol and (amidoferrocenyl) alkanethiol-type ligands with variation of the chain length (C₁₁ vs C₆) and ring structure of the ferrocenyl motif (Cp, Cp*, C₅H₄COMe). Reprinted with permission from ref 140 (Astruc's group). Copyright 2002 American Chemical Society.

3.4. Other Ligands

3.4.1. Phosphine, Phosphine Oxide, Amine, and Carboxylate Ligands

The Brust biphasic method of synthesis was applied to PPh_3 in order to improve the synthesis of Schmid's cluster $[\text{Au}_{55}(\text{PPh}_3)_{12}\text{Cl}_6]$, using $\text{HAuCl}_4 \cdot 3\text{H}_2\text{O}$ and $\text{N}(\text{C}_8\text{H}_{15})_4\text{Br}$ in a water–toluene mixture to which PPh_3 and then NaBH_4 were added. It was estimated that the cluster synthesized in this way had the formula $[\text{Au}_{101}(\text{PPh}_3)_{21}\text{Cl}_5]$ and contained 3.7 mass percent of $[\text{Au}(\text{PPh}_3)\text{Cl}]$ as an impurity.^{74a} Thermolysis of $[\text{Au}^{\text{I}}(\text{C}_{13}\text{H}_{27}\text{COO})(\text{PPh}_3)]$ at 180 °C under N_2 yielded monodispersed AuNPs capped by myristate and a small amount of PPh_3 ligands; the AuNP diameter increased with reaction time, from 12 nm for 1 h to 28 nm for 10 h, and with increasing temperature (42 nm for 5 h at 200 °C).^{74b} Various other gold complexes, in particular gold(I) amine complexes, have been used as precursors for the synthesis of amine-stabilized AuNPs.^{75,76a,b} Reduction of $\text{Au}^{\text{IV}}\text{Cl}_4$ by NaBH_4 in a mixture of tri-*n*-octylphosphine oxide (TOPO) and octadecylamine (1:0.57 molar ratio) at 190 °C resulted in the controlled growth of spherical AuNPs (8.59 ± 1.09 nm diameter) that are stable for months in toluene and were manipulated into crystals and 2D arrays (Figure 6).^{76c} Capping aqueous AuNPs with the amino acid lysine stabilizes the AuNPs in solution electrostatically and renders them air-stable and water-dispersible, a finding that is promising toward biologically relevant research.^{76d} Efficient synthesis of stable AuNPs by reaction of AuCl_4^- ions with the alkalothermophilic actinomycete *Thermomonospora* sp. has been described.^{76e}

3.4.2. Isocyanide

Aryl isocyanide thin films have attracted some attention, due to their potential application as mo-

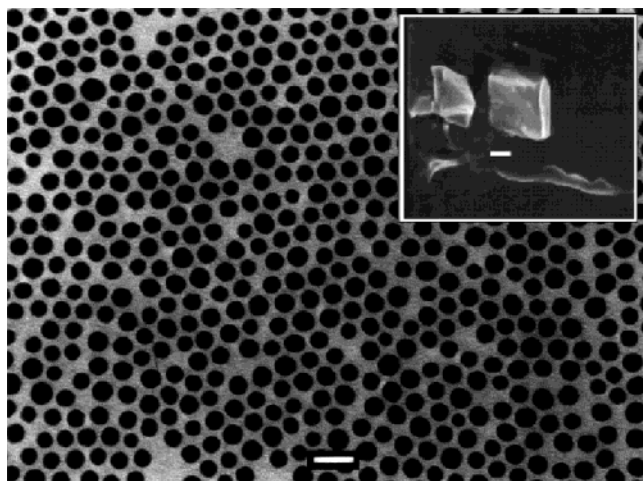


Figure 6. 2D lattice of octadecylamine/TOPO-capped AuNPs spontaneously formed when the latter are deposited on a copper grid; bar = 20 nm. (Inset) Scanning electron microscopy (SEM) image of a cubic colloidal crystal prepared from octadecylamine/TOPO-capped AuNPs (190 °C); bar = 80 μm. Reprinted with permission from ref 76c (O'Brien's group). Copyright 2000 The Royal Society of Chemistry.

lecular wires,^{76f} and 1,4-diisocyanide–AuNP forms large aggregate superstructures that have been examined by IR and Raman spectroscopy, showing bonding to the AuNP core via the carbon lone pair.^{76g,h}

3.4.3. Acetone

Pure Au^0NPs , obtained by replacement of citrate by acetone, were shown to be stable against attack by BH_4^- or HCl .⁷⁶ⁱ

3.4.4. Iodine

Iodine adsorption was shown to displace citrate ions from AuNPs, leading to superstructures that are also formed upon addition of KI .^{76j}

3.5. Microemulsion, Reversed Micelles, Surfactants, Membranes, and Polyelectrolytes

The use of microemulsions,⁷⁷ copolymer micelles,⁷⁸ reversed micelles,⁷⁷ surfactant, membranes, and other amphiphiles is a significant research field for the synthesis³⁸ of stabilized AuNPs in the presence or in the absence of thiol ligands.^{77–95} The syntheses involve a two-phase system with a surfactant that causes the formation of the microemulsion or the micelle maintaining a favorable microenvironment, together with the extraction of metal ions from the aqueous phase to the organic phase. This is an advantage over the conventional two-phase system. This dual role of the surfactant and the interaction between the thiol and the AuNP surface control the growth and stabilization of the AuNP or nanocrystal. The narrow size distribution allows the ordering of the particles into a 2D hexagonal close-packed array. AuNP sizes of the order of 4 nm diameter have been found.⁷⁹ Polyelectrolytes have also been extensively used for the synthesis of AuNPs (Figure 7).^{94,98–102} The polyelectrolyte coating of carboxylic acid-derivatized AuNPs with diameters less than 10 nm has been achieved by electrostatic self-assembly of oppositely charged polyelectrolytes.^{102b}

3.6. Seeding Growth

The seeding-growth procedure is another popular technique that has been used for a century. Recent studies have successfully led to control of the size distribution (typically 10–15%) in the range 5–40 nm, whereas the sizes can be manipulated by varying the ratio of seed to metal salt (Figure 8).^{103–105} The step-by-step particle enlargement is more effective than a one-step seeding method to avoid secondary nucleation.^{87a} Gold nanorods have been conveniently fabricated using the seeding-growth method.^{87b}

3.7. Physical Methods: Photochemistry (UV, Near-IR), Sonochemistry, Radiolysis, and Thermolysis

UV irradiation is another parameter that can improve the quality of the AuNPs,^{86,104,105} including when it is used in synergy with micelles⁸⁶ or seeds.¹⁰⁴ Near-IR laser irradiation provokes an enormous size growth of thiol-stabilized AuNPs.¹⁰⁶ The presence of an ultrasonic field (200 kHz) allowed the control of the rate of AuCl_4^- reduction in an aqueous solution containing only a small amount of 2-propanol and the

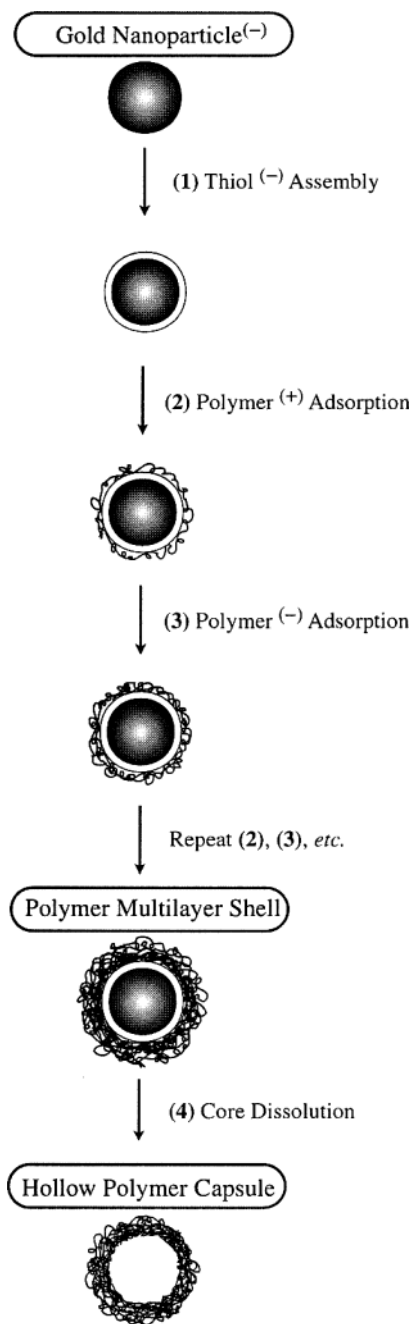


Figure 7. Schematic diagram illustrating the layer-by-layer polymer deposition process applied to AuNPs. Reprinted with permission from ref 98 (Caruso's group). Copyright 2001 American Chemical Society.

sizes of the formed AuNPs by using parameters such as the temperature of the solution, the intensity of the ultrasound, and the positioning of the reactor.^{107,108} Sonochemistry was also used for the synthesis of AuNPs within the pores of silica^{111–113} and for the synthesis of Au/Pd bimetallic particles.¹¹⁴ Radiolysis has been used to control the AuNP size^{115a} or to synthesize them in the presence of specific radicals,^{115b} and the mechanism of AuNP formation upon γ -irradiation has been carefully examined (Figure 9).¹¹⁶

AuNPs have been fabricated via decomposition of $[\text{AuCl}(\text{PPh}_3)]$ upon reduction in a monolayer at the gas/liquid interface.¹¹⁷ The thermolysis of $[\text{C}_{14}\text{H}_{29}\text{Me}_3\text{N}][\text{Au}(\text{SC}_{12}\text{H}_{25})_2]$ at 180 °C for 5 h under N_2

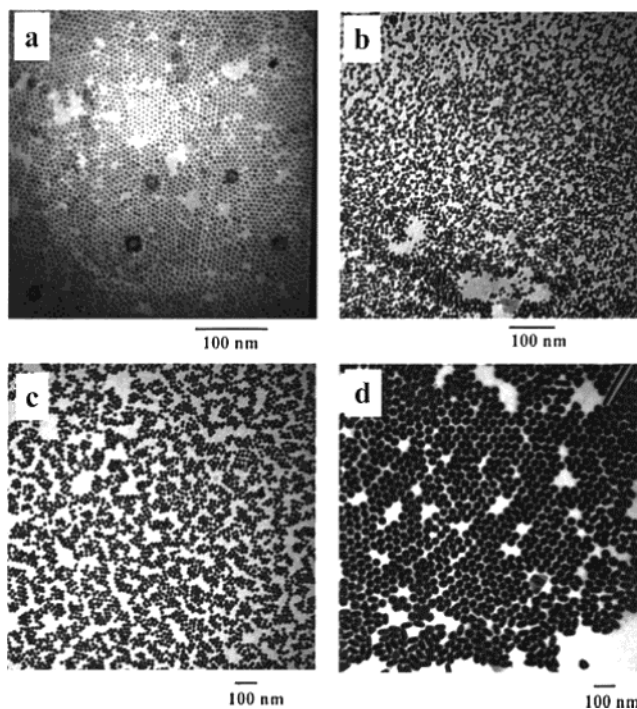


Figure 8. TEM image of larger gold particles prepared from seed: (a) 5.5 ± 0.6 , (b) 8.0 ± 0.8 , (c) 17 ± 2.5 , and (d) 37 ± 5 nm after separation of rods. The 5.5 ± 0.6 -nm AuNPs were extracted into toluene after thiol capping for TEM in order to remove excess surfactant. The other particles were separated from excess surfactant by centrifugation. Reprinted with permission from ref 89 (Murphy's group). Copyright 2001 American Chemical Society.

produced alkyl-groups-passivated AuNPs of 26 nm.^{118a} Thermolysis of crude preparations of Brust's AuNPs without removing the phase-transfer reagent, tetraoctylammonium bromide, to 150–25 °C led to an increase of the particle sizes to 3.4–9.7 nm, and this size evolution was discussed on the basis of a thermodynamic model. The heat-treated AuNPs formed 2D superlattices with hexagonal packing. The conformation of the alkanethiol is all-trans, and these ligands interpenetrate each other (Figure 10).^{118b} Laser photolysis has been used to form AuNPs in block copolymer micelles.¹¹⁹ Laser ablation is another technique of AuNP synthesis that has been used under various conditions whereby size control can be induced by the laser.^{120–122} The evolution of thiol-stabilized AuNPs has been induced by and observed upon heating.^{123–126,135} Structural changes of spherical aggregates composed of mercaptoacetate-stabilized AuNPs suspended in water were monitored by maintaining the spheroid suspension at a constant temperature, ranging from 65 to 91 °C, for 2–12 h. The spheroid diameter was reduced to almost 70% of the original size, due to an irreversible “coagulative” transition resulting from fusion among the nanocolloids in spheroids.^{126b} Morphology changes of AuNPs were also shown during sintering.^{126c} Sputtering AuNPs by single ions and clusters was shown to eject AuNPs.¹⁷⁸

3.8. Solubilization in Fluorous and Aqueous Media

AuNPs stabilized by perfluorodecanethiol or 1*H*,1*H*,2*H*,2*H*-perfluorooctathiol, with an average

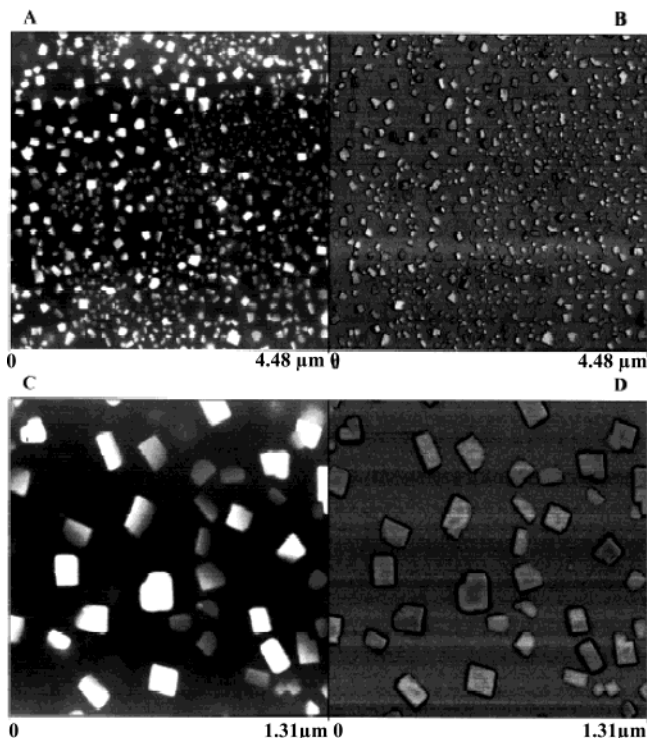


Figure 9. Taping-mode AFM images of the species formed in a solution irradiated with γ rays (1.5 kGy) and then deposited on highly ordered pyrolytic graphite (HOPG) 30 days after the irradiation and dried under a mild N_2 stream for visualization. The solution contains 10^{-3} mol·L $^{-1}$ Au III and poly(vinyl alcohol) but no alcohol. (A) Height-mode (z range 80.0 nm) image and (B) phase (z range 42.2°) image, run simultaneously on the same area of the sample. (C, D) Close-up images showing the same area as in (A) and (B), respectively. Reprinted from ref 116 (Belloni's group) by permission of The Royal Society of Chemistry (RSC) on behalf of the Centre National de la Recherche Scientifique (CNRS). Copyright 1998.

diameter of 2.4–2.6 nm, were prepared by reduction of $HAuCl_4$ by $NaBH_4$ (dropwise addition) in ethanol and were soluble only in fluorocarbon media.¹²⁷

Special emphasis has been placed on the synthesis of stable water-soluble thiol-stabilized AuNPs^{128–134} using thiols containing poly(ethylene oxide) chains^{128–130a} (Figure 11) or carboxylate modification (Figure 12).^{130b,134} Poly(*N*-vinyl-2-pyrrolidone) (PVP) is the polymer of choice for the stabilization in water of AuNPs prepared by reduction of $HAuCl_4$ (see the section on polymers).

3.9. Characterization Techniques

The most common characterization technique is high-resolution transmission electron microscopy (HRTEM), which gives a photograph of the gold core of the AuNPs,⁴⁶ but the core dimensions can also be determined using scanning tunneling microscopy (STM), atomic force microscopy (AFM), small-angle X-ray scattering (SAXS),^{50,137a} laser desorption–ionization mass spectrometry (LDI-MS),^{137b–139} and X-ray diffraction.¹³⁶ A detailed high-resolution study of the AuNP shape using HRTEM, reported by Brust et al., revealed that the truncated cuboctahedron predominated, and that decahedra, dodecahedra and icosahedra were also present in the same preparation of alkanethiol-stabilized AuNPs.⁴⁷ The histogram

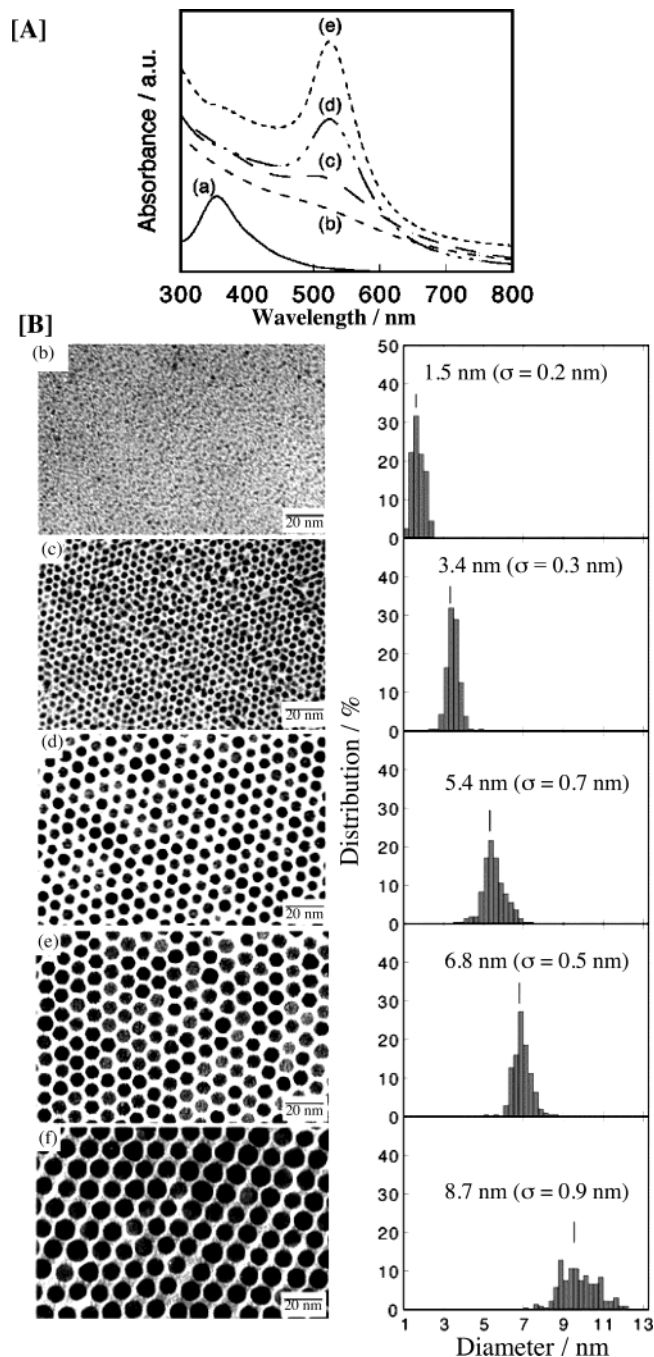


Figure 10. UV–vis spectra (A) and TEM images and size distributions (B) of (a) $[AuCl_4]^-$ before reduction; dodecanethiol-AuNPs (b) as prepared and after heat treatment at (c) 150, (d) 190, and (e) 230 °C; and (f) octadecanethiol-AuNPs heat-treated at 250 °C. Reprinted with permission from ref 188b (Miyake's group). Copyright 2003 American Chemical Society.

providing the size distribution of these cores gives crucial information on the dispersity of the sample that is usually obtained from TEM pictures.⁴⁷ The mean diameter, d , of the cores allows determination of the mean number of gold atoms, N_{Au} , in the cores:⁴⁷ $N_{Au} = 4\pi(d/2)^3/v_{Au}$. For instance, with $d = 2.06$ nm, $N_{Au} = 269$.¹⁴⁰ From these data, the elemental analysis, giving the Au/S ratio, allows calculation of the average number of S ligands. This number can also be deduced from X-ray photoelectron spectroscopy (XPS) or thermogravimetric analysis (TGA).⁵⁰

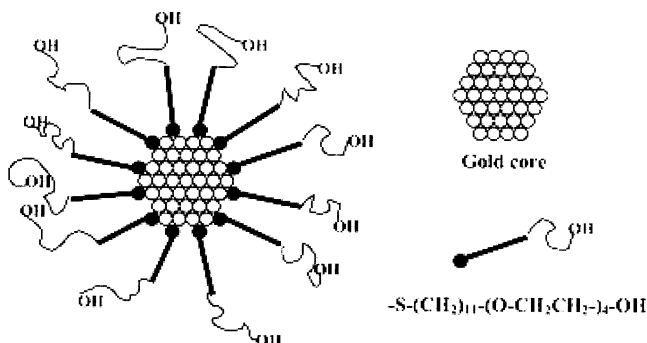


Figure 11. Schematic representation of a AuNP protected by a monolayer of monohydroxy (1-mercaptoundec-11-yl) tetraethylene glycol. The hydrophobic C₁₁ chain confers extreme stability to the cluster, while the hydrophilic tetraethylene glycol unit ensures solubility in water. Reprinted with permission from ref 129 (Brust's group). Copyright 2002 The Royal Society of Chemistry.

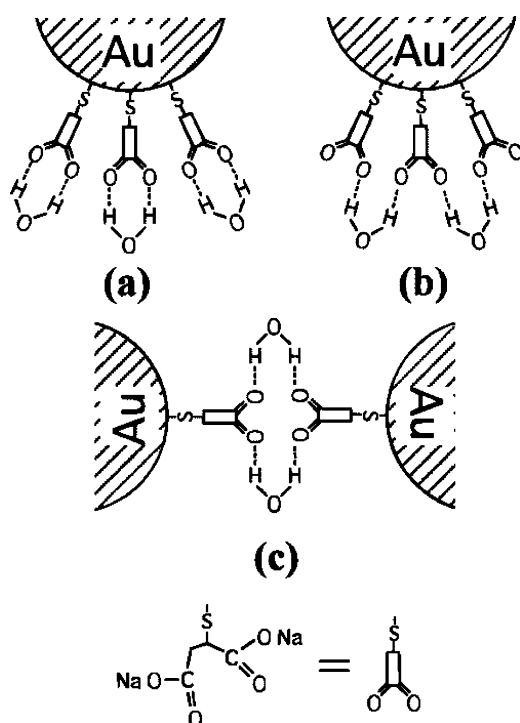


Figure 12. Possible combinations of H₂O molecules with mercaptosuccinic acid (MSA)-capped AuNPs: one H₂O molecule connected with two carbonyl groups in either (a) one MSA molecule, (b) adjoining MSA molecules on one AuNP, making a successive hydrogen-bonding network, or (c) MSA molecules from different AuNPs, the water acting as "glue" to join two neighboring particles. Reprinted with permission from ref 130b (Chen's group). Copyright 1999 American Chemical Society.

The oxidation state of the gold atoms of the core has been examined by Brust et al in their seminal article using X-ray photoelectron spectra that showed the binding energies of the doublet for Au 4f_{7/2} (83.8 eV) and Au 4f_{5/2} (87.5 eV) characteristic of Au⁰. No band was found for Au¹ at 84.9 eV, although one-third of the gold atoms are located at the surface and bonded to thiols for 2.0–2.5 nm sized particle cores. On this basis, Brust et al. suggested that the gold-thiol bond does not have the character of gold sulfide.^{46b} This matter of a thiol vs thiolate bond to the gold core atoms, however, has been debated. For instance, it was suggested that a high coverage of

gold cores by thiolate ligands¹³⁹ was due to large ligand/Au binding ratios on core edges and vertices (Figure 13), in accord with theoretical calculations.¹⁴⁰ Moreover, it was reported that thermolysis of the thiolate-stabilized AuNPs produces only the corresponding disulfide. The absence of thiol by thermal desorption mass spectrometry was considered to be evidence that the chemisorbed ligand consisted of an alkanethiolate (not thiol) fragment. This would mean that H₂ is produced during the reductive synthesis from thiols, but this formation has never been detected. Theoretical calculations suggested the formation of disulfides when the number of thiol molecules around a AuNP was enough to saturate the flat planes, whereas thiolate behavior was observed when the sulfur atoms were not enough.^{139a} This finding was reported¹³⁹ to corroborate the observation of a S–S distance of 2.32 Å from grazing incidence X-ray in self-assembly of *n*-alkanethiols on a (1,1,1) gold crystal surface.^{139b} Brust et al. recently provided ¹H NMR evidence for intact thiols adsorbed on AuNPs. They showed that the loss of hydrogen could be prevented to some extent as long as there is no easy reaction path for hydrogen removal.¹⁴⁰

X-ray diffraction also demonstrated the striking tendency of thiolates–AuNPs to spontaneously form highly ordered superlattices^{141–144} with periodicity extending to three dimensions up to several tens of micrometers.¹⁴³ These superlattices were obtained upon slow evaporation of the organic solvent or even water on a suitable surface.^{144b} Such self-organized superlattices of AuNPs on highly ordered pyrolytic graphite (HOPG) are also observable by STM (Figure 14).²⁷ Monodispersity is a very important criterion for the formation of ordered superlattices.^{145a} When the gas phase at the gas–suspension interface of a synthetic medium leading to sodium mercaptosuccinate–AuNPs contained nonpolar organic molecules, spherical AuNPs formed. On the other hand, when the gas phase contained polar organic vapors such as MeCN or CHCl₃, irregular-shaped AuNPs formed.^{145b}

Langmuir–Blodgett (LB) films of Schmid's Au₅₅ cluster were characterized by STM, Brewster angle microscopy (BAM), and scanning force microscopy (SFM). These techniques showed that the cluster formed monolayers, as indicated by the surface pressure–area (π –*A*) isotherms and the area–time (*A*–*t*) isobars between 20 and 30 °C and 15–30 nN/m of surface pressure, and the cluster size could be estimated from the π –*A* isotherms as 2.17 nm (calcd 2.1 nm).¹⁹ The Au₅₅ cluster has also been studied by Mössbauer spectroscopy, extended X-ray absorption fine structure (EXAFS), electron spectroscopy for chemical analysis (ESCA), and conductivity measurements. These techniques show that the Au₅₅ particles behave like a system with a few "last metallic electrons" that are used for tunneling between neighboring clusters. This "metallizing" situation was observed by applying an alternating current in the 10-kHz range as for impedance measurements.^{146,147} Scanning tunneling spectroscopy (STS) had been used to observe Coulomb blockade in metal nanoparticles. The tunneling current is induced by an

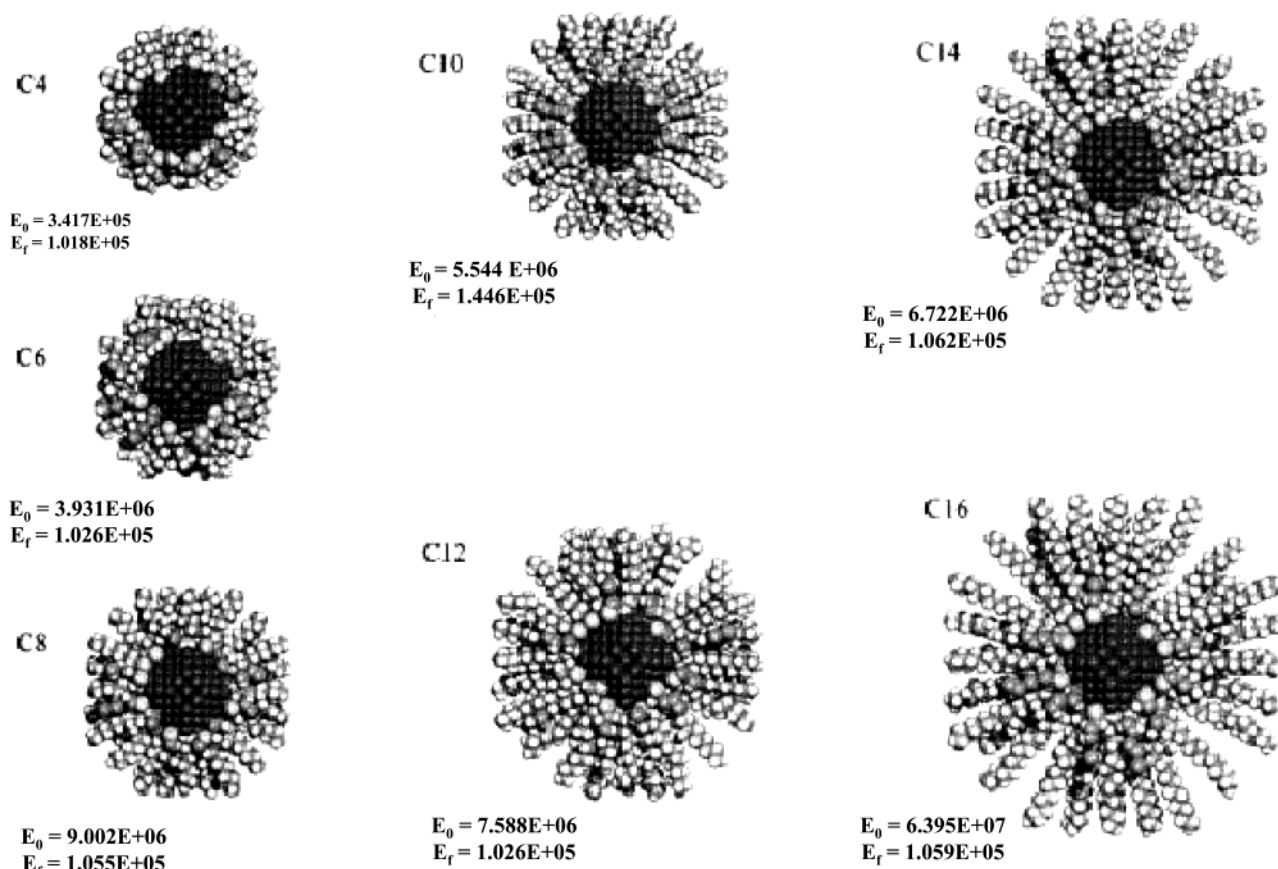


Figure 13. Stable configurations of AuNPs covered with n -alkanethiol molecules. The sequence shows $n = 4$ butanethiol, $n = 6$ hexanethiol, $n = 8$ octanethiol, $n = 10$ decanethiol, $n = 12$ dodecanethiol, $n = 14$ butanedecanethiol, and $n = 16$ hexanedecanethiol ($n =$ number of C atoms). Reprinted with permission from ref 139 (José-Yacamán's group). Copyright 1998 Kluwer.

applied voltage and leads to the charging of a metal particle with at least one single electron.^{148–150} Electrostatic trapping (ET) is a technique used to investigate isolated nanosize metal particles. It is based on moving a polarized particle in an electric field to the point of strongest field, which is the position between two electrodes (dipped in a solution of the particles) at a distance comparable to the particle diameter.^{27,148,149}

The UV–vis and IR spectra provide an identification of the ligand that is also confirmed by NMR spectroscopy, except that the ligand atoms close to the core give broad signals. This latter phenomenon is due to (i) spin–spin relaxational (T_2) broadening (main factor), (ii) variations among the gold–sulfur bonding sites around the particle, and (iii) a gradient in the packing density of the thiolate ligands from the core region to the ligand terminus at the periphery.^{151–153} The NMR spectra are very informative, as for all molecular compounds, for the part of the ligand remote from the core. The latter can also be more fully analyzed, if desired, after oxidative decomplexation using iodide.

IR spectroscopy shows that, as in SAMs,¹⁵⁴ the thiolate ligands of AuNPs are essentially in all-trans zigzag conformations, with 5–25% of gauche defects at both inner and terminal locations.^{50,152} IR and NMR spectroscopies allow, together with differential scanning calorimetry (DSC),^{152–155} the detection of order–disorder transitions in AuNPs in the solid

state. The temperature of the transition increases with the chain length, and FTIR shows the increasing amount of gauche defects. Variable-temperature deuterium NMR in the solid state shows that the disorder, materialized by the increased proportion of gauche bonds, propagates from the chain terminus toward the middle of the chain, but not further to the ligand atom, and causes chain melting.¹⁵² Calorimetric measurements led to the determination of the formation enthalpy of AuNPs in a water/sodium bis(2-ethylhexyl) sulfosuccinate/ n -heptane microemulsion. The results indicated that the energetic states and the dimensions of the AuNPs were influenced by the radii and concentrations of the reversed micelles.⁸⁰

Capillary zone electrophoresis in acetate buffer showed that the mobility of AuNPs with a given core diameter decreased with decreasing ionic strength. At the highest ionic strength investigated (6 mmol/L), a good linear dependence of the mobility on the reciprocal of the core radius allowed the characterization of the size of the AuNPs.¹⁵⁶

The AFM images of AuNPs operating in the contact mode in air at room temperature showed an attractive interaction among the particles, leading to the formation of aggregates and a mean size that is a function of the size of the reverse micelle used for the synthesis. This was taken into account in terms of the formation of an adsorbed layer of surfactant molecules at the particle surface.⁸¹

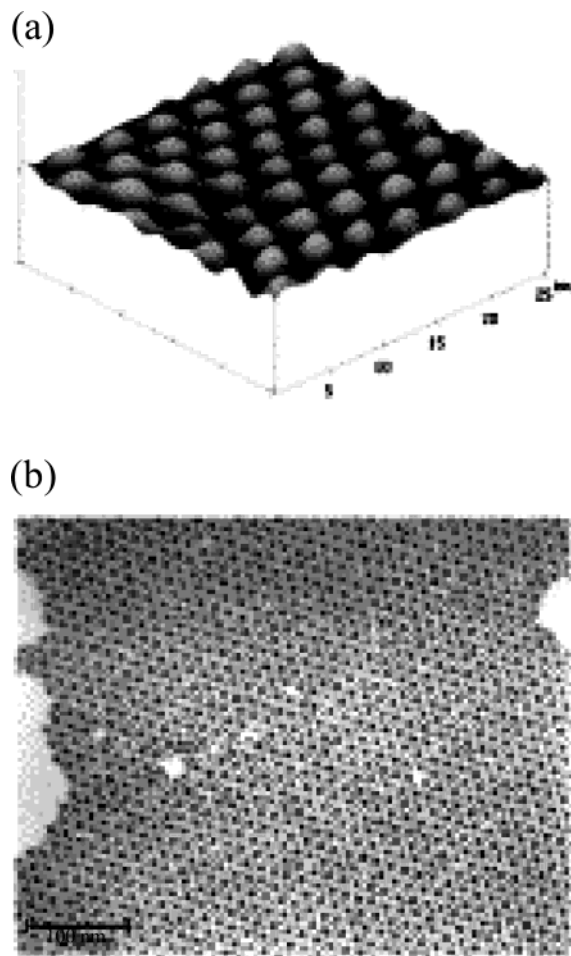


Figure 14. Nanostructure preparation from AuNPs: STM image of self-assembled superlattice of 3.5-nm gold particles on a HOPG substrate. The particles are stabilized by hexanethiol. TEM micrograph of an AB₂ superlattice of AuNPs having a bimodal size distribution (4.5 and 7.8 nm). The AuNPs are stabilized by decanethiol. Reprinted with permission from ref 27 (Brust's group). Copyright 2002 Elsevier.

The use of incoherent light experiments, performed in the vicinity of the surface plasmon resonance frequency, allowed measurement of the phase relaxation time and nonlinear susceptibility of AuNPs of 5–40 nm.¹⁵⁷

Surface-enhanced Raman scattering (SERS)^{70b} and XPS made it possible to analyze the chemisorptive properties of tetrathiol ligands and indicated that surface passivation was an important factor in the dispersibility of AuNPs in nonpolar solvents.^{70c}

EXAFS allowed investigation of the size-dependent distance contraction in thiol-stabilized AuNPs, and the short metal–ligand bond found suggested a rather strong surface interaction.¹⁵⁸

High-resolution time-of-flight mass spectroscopy analysis of alkanethiol-stabilized AuNPs allowed the assignment of the number of gold and sulfur atoms, although alkyl chains were not evident. Pure gold cluster ions of various sizes could be generated from the AuNPs in a two-laser experiment.¹⁵⁹

Small-angle X-ray scattering, STM, and AFM were consistent with a small, monodisperse (2.4 nm diameter) gold core.^{160a} The formation by physical vapor deposition and growth of AuNPs was studied by STM

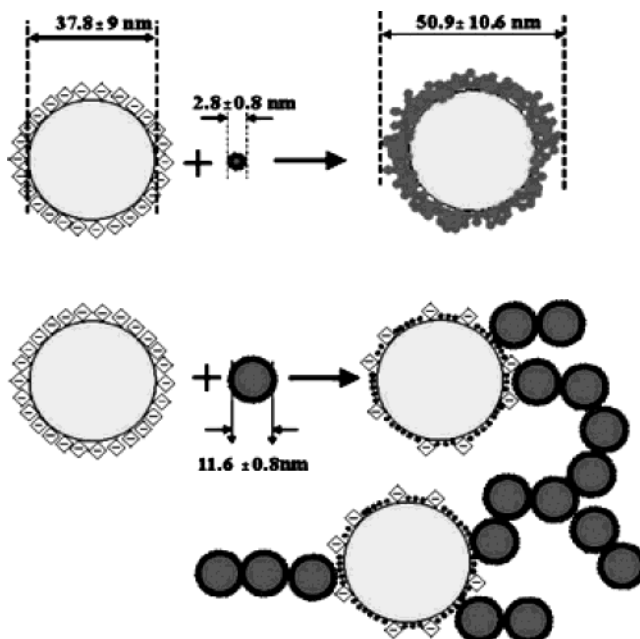


Figure 15. Schematic illustrating the proposed interactions of thiocyanate ion-coated 2.8 ± 0.8 - and 11.6 ± 0.8 -nm-diameter AuNPs with 37.8 ± 9 -nm-diameter ethylenediaminetetraacetic acid (EDTA)-covered AgNPs. Reprinted with permission from ref 164 (Fendler's group). Copyright 2002 The Royal Society of Chemistry.

on TiO₂ (1,1,0) surfaces.^{160b} The surface of AuNPs was analyzed using a phase reconstruction technique in TEM, extended to simultaneous correction of spherical aberration and two-fold astigmatism.^{160c} The vacancy formation energy of AuNPs has been shown to decrease with decreasing particle size.^{160d}

3.10. Bimetallic Nanoparticles

Bimetallic nanoparticles^{20,37} containing gold as one of the elements have been synthesized in a variety of ways. Bimetallic AuNPs have been reported with Ag (Figure 15),^{161–168} Pd (Figure 16),^{97,161,166,167} Pt,^{161,167} TiO₂,⁹⁹ Fe,^{169–171} Zn,¹⁶⁸ Cu,^{165,168} ZrO₂,¹⁷² CdS,^{173,174} Fe₂O₃,¹⁷⁵ and Eu.¹⁷⁶ Although bimetallic nanoparticles have been known for a long time, Schmid's group were the first to report the synthesis of core–shell bimetallic nanoparticles, the core–shell structure being demonstrated using HRTEM and energy-disperse X-ray (EDX) microanalysis. AuNPs of 18 nm diameter were covered with a Pd or Pt shell when an aqueous solution of these AuNPs was added to a solution of H₂PtCl₆ or H₂PdCl₄ and H₃NOHCl. The original color of the AuNPs then changed to brown-black. Addition of *p*-H₂NC₆H₄SO₃Na stabilized the generated particles in the same manner as P(*m*-C₆H₄-SO₃Na)₃ stabilized the AuNPs. The colloids showed a metallic luster and were of uniform 35 nm diameter. For instance, Au/Pt particles had an average gold content of 15% atom % located at the core surrounded by Pt crystals of about 5 nm that were pregrown before being added to the Au surface.¹⁶¹ Stabilization of the bimetallic particles could be achieved using the Brust procedure in the presence of thiols. Such stable bimetallic particles were synthesized with group 10 (Pd, Pt) and group 11 (Cu, Ag, Au) metals, all containing Au as one of the two

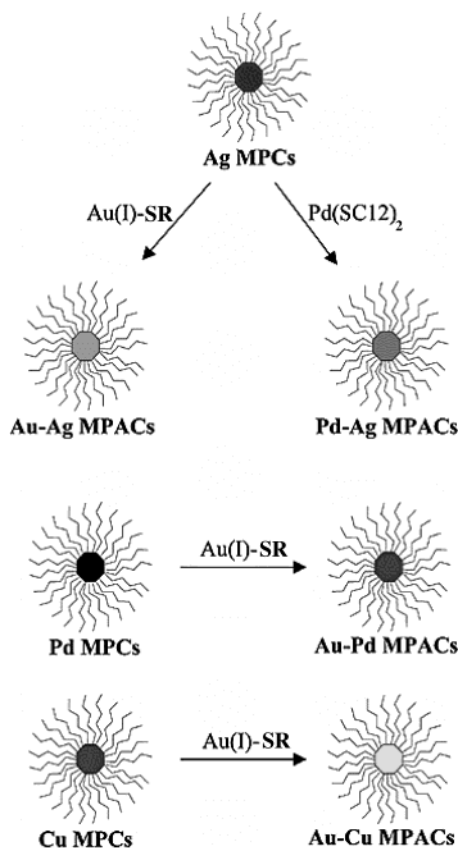


Figure 16. Cartoon diagram of core metal galvanic exchange reactions. MPC, monolayer-protected cluster; MPAC, monolayer-protected alloy cluster; SC12, $S(\text{CH}_2)_{11}\text{CH}_3$. Reprinted with permission from ref 166a (Murray's group). Copyright 2002 American Chemical Society.

metals, and were characterized using TEM, ^1H NMR line broadening, XPS, elemental analysis, and TGA. TEM showed that Pd/Au cores are small (1.7 nm) and relatively monodisperse (average 20% dispersity), while Ag/Au cores are larger (3.2 nm), and other bimetallic particles are of intermediate size. The mole ratios of metals both in and on the surface of the bimetallic cores differed significantly from the metal:salt ratio used in the bimetallic particle synthesis.¹⁶² Partially segregated alloys indeed form easily, and more noble metals prefer the nonsurface (core) location.²⁰ Metal galvanic exchange reactions are yet another quite facile way to synthesize stable bimetallic particles. This procedure relies on reactions of alkanethiolate–metal particles or other metal particles (Ag, Pd, Cu) with the complexes $[\text{Au}^{\text{I}}\text{SCH}_2(\text{C}_6\text{H}_4)\text{CMe}_3]$ and $[\text{Pd}^{\text{II}}\{\text{S}(\text{CH}_2)_{11}\text{Me}\}_2]$.^{163,166} Au core–Ag shell and Au core–Pt shell nanoparticles have been formed using photochemically reduced phosphotungstate Keggin ions.^{168b} Specific properties and functions of bimetallic nanoparticles will be discussed in the appropriate sections devoted to catalytic, electronic, and optical properties.

3.11. Polymers

Since the report in Helcher's treatise in 1718,³ indicating that starch stabilizes water-soluble gold particles, it has been known that such materials, recognized two centuries later as polymers, favor the isolation of AuNPs.^{14,179} With the considerably im-

proved recent understanding of the parameters leading to the stabilization of AuNPs and of their quantum-size-related interest, there has been a revival of activity in the field of polymer-stabilized AuNPs.^{33,177,180–181} The most commonly used polymers for the stabilization of AuNPs are PVP and poly(ethylene glycol).^{11b,14}

Although there are a variety of ways to achieve nanoparticle–polymer composites,^{182,183} two different approaches dominate. The first one consists of the in situ synthesis of the nanoparticles in the polymer matrix either by reduction of the metal salts dissolved in that matrix¹⁸⁴ or by evaporation of the metals on the heated polymer surface.¹⁸⁵ The second one, less frequently used, involves polymerization of the matrix around the nanoparticles.¹⁸⁶ Recently, however, blending of *premade* AuNPs into a *presynthesized* polystyrene polymer (synthesized by anionic polymerization) bound to a thiol group was also reported.¹⁸⁷ Whereas the physical process involving mechanical crushing or pulverization of bulk metals and arc discharge yielded large nanoparticles with a wide size distribution, nanoparticles prepared by reduction of metal salts are small, with a narrow size distribution. This reduction processes most often use a reagent such as NaBH_4 ¹⁸⁸ which is added in situ, or the reductant can also be the solvent, such as an alcohol.^{189,190} For instance, $\text{HAuCl}_4 \cdot 4\text{H}_2\text{O}$ gives stable AuNPs upon refluxing in methanol/water in the presence of PVP, even if NaOH is added subsequently to the preparation of the AuNPs.¹⁹¹ In poly(acrylamide), AuCl_4^- cannot be reduced by alcohol, but it can be reduced by NaBH_4 .¹⁹² Other reductants are generated involving radiolysis, photolysis,¹⁹³ or electrochemistry.¹⁹⁴ The polymer–nanoparticle composite can be generated from solution (the classic mode) or can involve the immobilization by a solid polymer such as poly(acrylic acid), poly(vinyl alcohol), or PVP frequently used. Reduction of metal ions in the presence of the polymer is most often chosen because the complexation of the metal cations by the ligand atoms of the polymer is crucial before reduction. In particular, it dramatically limits the particle size.¹⁹⁵

The most important role of the stabilizing polymer is to protect the nanoparticles from coagulation. Toshima has expressed this function quantitatively by the “gold number”, i.e. the number of milligrams of protective polymer that just prevents 10 mL of a red gold sol from changing color to violet upon addition of 1 mL of 10% aqueous NaCl. The “gold number” is smaller for protective polymers that are better stabilizers.¹⁸⁹ Core–shell PVP-stabilized Au/Pd¹⁹⁶ and Au/Pt^{197,198} nanoparticles were prepared by Yonezawa and Toshima by simultaneous alcohol reduction of the two corresponding metal salts and characterized by EXAFS. The relative order of reduction in alcohol/water is seemingly controlled by the relative redox potentials, HAuCl_4 being reduced more rapidly than $\text{Pd}(\text{OH})_2$ and PtCl_6^{2-} . The AuNPs form first, and then the Pd or Pt shell forms around the AuNPs to produce the core–shell bimetallic particles. In fact, the Pd⁰ formed reduces AuCl_4^- to Au^0 and thus acts as a mediator or redox catalyst for the reduction of AuCl_4^- , as long as any AuCl_4^- is left in

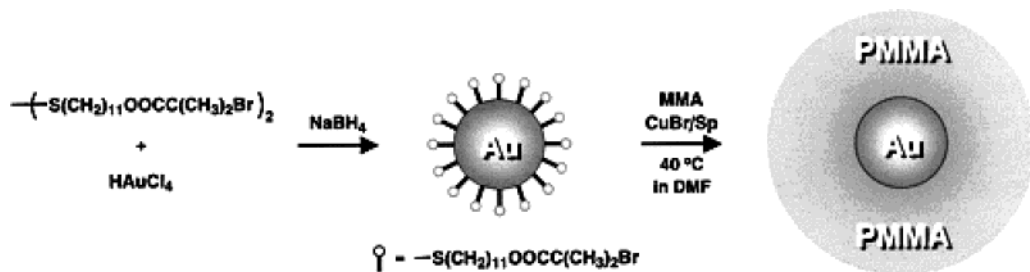


Figure 17. Schematic representation for the synthesis of polymer-coated AuNPs by surface-initiated living-radical polymerization (LRP). Reprinted with permission from ref 214 (Fukuda's group). Copyright 2002 American Chemical Society.

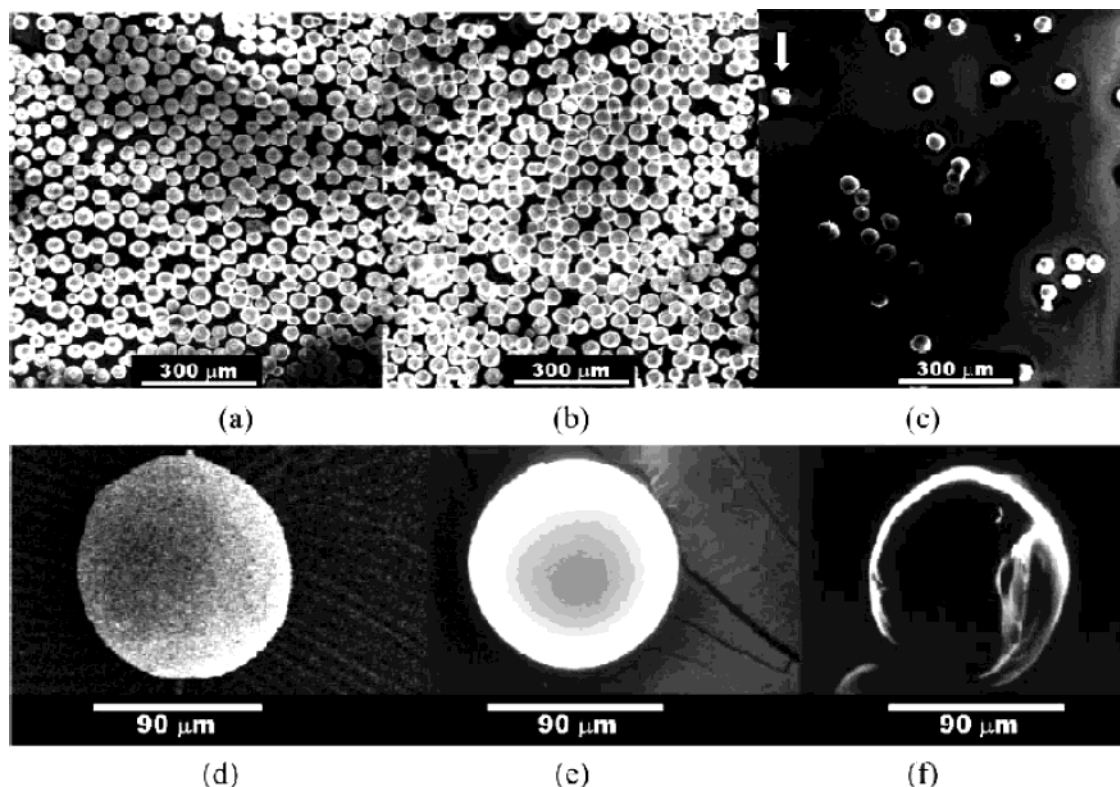


Figure 18. SEM image of (a) 50- μm ceramic hollow spheres (CHSs), (b) 50 μm gold-seeded CHSs, (c) 50- μm gold hollow spheres (GHSs) obtained by calcination and dissolution of gold-seeded CHSs, (d) a 100- μm CHS, (e) a 100- μm gold-seeded CHS, and (f) a 100- μm broken GHS. The arrow in (c) indicates a broken particle, which proves that it is hollow. From (f), it can be seen that the inside of GHS is empty. Reprinted with permission from ref 216b (Fendler's group). Copyright 2002 Elsevier.

the solution.^{199,200} Attempts to synthesize Pd-core/Au-shell bimetallic particles led instead to a remarkable cluster-in-cluster structure because of this redox priority (Figure 16).²⁰¹

Many ordered polymer-AuNPs are known. For instance, AuNPs in PVP were prepared by hydrazine reduction of incorporated HAuCl₄. The color of the solution of HAuCl₄-loaded block copolymer changed from yellow to purple, and then to bluish upon addition of a large excess of anhydrous hydrazine. The reduction can be stopped by addition of HCl, which protonates hydrazine in order to avoid coagulation of the AuNPs.^{202,203} These phenomena were also obtained with (styrene-*block*-ethylene oxide).^{204,205}

The use of a diaminotriazine-functionalized diblock copolymer led to size-controlled synthesis of AuNP aggregates in solution and in thin films with thymine functionality.²⁰⁶ AuNPs were generated in polymeric micelles composed of amphiphilic block copolymers,^{207,208} and amphiphilic star-block copolymers were

an ideal choice to serve as a confined reaction vessel.²⁰⁹ The formation of AuNPs was also controlled by using poly(methylphosphazene), whose lone pairs stabilized the AuNPs.²¹⁰ Functionalized polymers have also been used as stabilizers. Poly(ethylene glycol)-based polymer was used to fabricate an AuNP sensor that reversibly binds lectin for recognition and bioassay.²¹¹ The so-called "grafting from" technique has been used to construct highly dense polymer brushes. For instance, several methods,^{212–214} including the efficient living radical polymerization (LRP), have indeed been applied to the synthesis of AuNPs coated with such a high-density polymer brush. AuNP-based nanoscale architectures could be forecasted using this simple technique (Figure 17).²¹⁴

Polymer hollow spheres have been synthesized with movable AuNPs at their interiors.²¹⁵ AuNPs can serve as templates for the synthesis of conductive capsules²¹⁶ (Figure 18) and for the oligomerization of L-cysteine in aqueous solution (Figure 19).²¹⁷

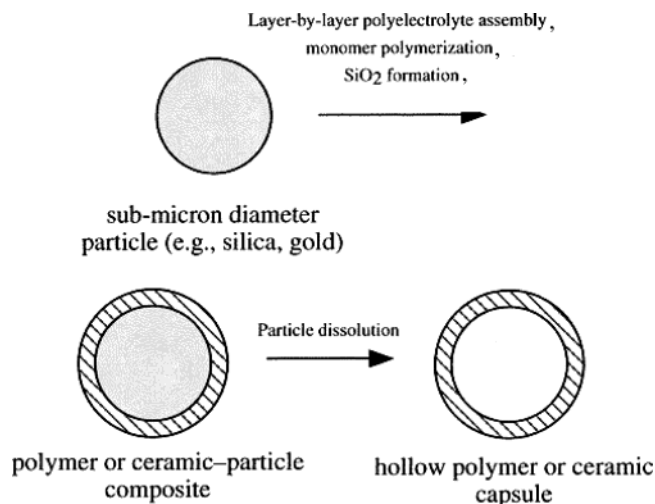


Figure 19. AuNPs as templates for the synthesis of hollow polymer capsules. Reprinted with permission from ref 216c (Feldheim's group). Copyright 1999 American Chemical Society.

Nanosized domains of block copolymers can be used as nanoreactors to synthesize AuNPs by expansion of the nanosized domains and period of block copolymers, such as polystyrene-*block*-poly(4-vinylpyridine) (PS-PVP) diblock copolymers.²¹⁸ Self-assemblies of AuNPs/polymer multilayer films have been formed using surface functionalization.^{219,220} AuNPs of average size between 1 and 50 nm have also been stabilized by many water-soluble polymers, and some of them have been shown to be stable after 9 months in air. The most stable ones were obtained with polymers possessing hydrophobic backbones and side groups, allowing good interactions with the AuCl₄⁻ ion. The preparations were carried out using either UV irradiation or KBH₄ to reduce HAuCl₄ in the presence of a mass ratio of polymer:gold 25:1.²²¹

Linear polymers having cyano or mercapto groups stabilize AuNPs of 1.5–3 nm diameter and narrow size distributions.²²² AuNPs of Brust type with some thiol chain termini bearing *exo*-norbornene units were polymerized using ring-opening metathesis polymerization (ROMP) to produce a block copolymer shell.^{223,224} Small AuNPs (5 nm diameter) stabilized with sodium citrate²²⁵ were attached to the surface of silica nanoparticles protected by polymer layers to provide contrast in the final TEM image, a strategy also used to obtain TEM contrast for many types of molecular⁹⁷ and biological materials.²²⁶ Solution behavior, i.e., transformation in the morphology from small spherical AuNPs to large anisotropic objects, was observed by decreasing the concentration of polystyrene-*block*-poly(2-vinylpyridine) micelles below the critical micelle concentration (Figure 20).⁸⁵

Networks of AuNPs prepared in water were observed by TEM upon adding poly(acrylic acid) to AuNPs stabilized by thiolated poly(ethylene oxide) chains of high molecular weight (necessary to stabilize AuNPs in water). Moreover, thin and linear thermally robust arrangements were formed when chondroitin sulfate c sodium salt (a polysaccharide carrying sulfuric acid groups and carboxylic acid groups) was added (Figure 21).²²⁷ AuNPs of about 20 nm size were formed upon reduction of AuCl₃ by polyaniline in *N*-methylpyrrolidinone.²²⁸ An amine-functionalized polymer was used to simultaneously assemble carboxylic-acid-functionalized AuNPs and silica nanoparticles into extended aggregates.²²⁹ Such a strategy also led to spherical silica templates (Figure 22).²²⁶ Macroporous Au spheres with a diameter ~9 μm have been formed by employing porous organic bead templates and preformed AuNPs.²³⁰ AuNPs were stabilized by the lone nitrogen pair on the backbone of polymethylphosphazene, [Me(Ph)PN]_n, and varying the ratio of [Me(Ph)PN]_n to HAuCl₄

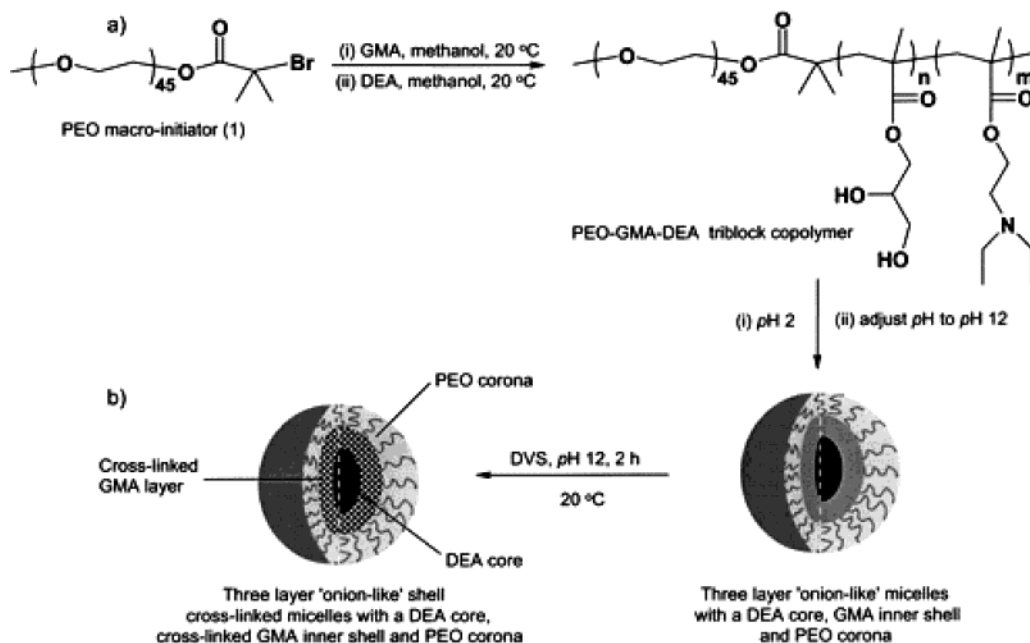


Figure 20. (a) Reaction scheme for the synthesis of the PEO-GMA-DEA^a triblock copolymers. (b) Schematic illustration of the formation of three-layer "onion-like" micelles and shell cross-linked micelles from PEO-GMA-DEA triblock copolymers. PEO-GMA-DEA, poly[(ethylene oxide)-*block*-glycerol monomethacrylate-*block*-2-(diethylamino)ethyl methacrylate]. Reprinted with permission from ref 85 (Armes's group). Copyright 2002 American Chemical Society.

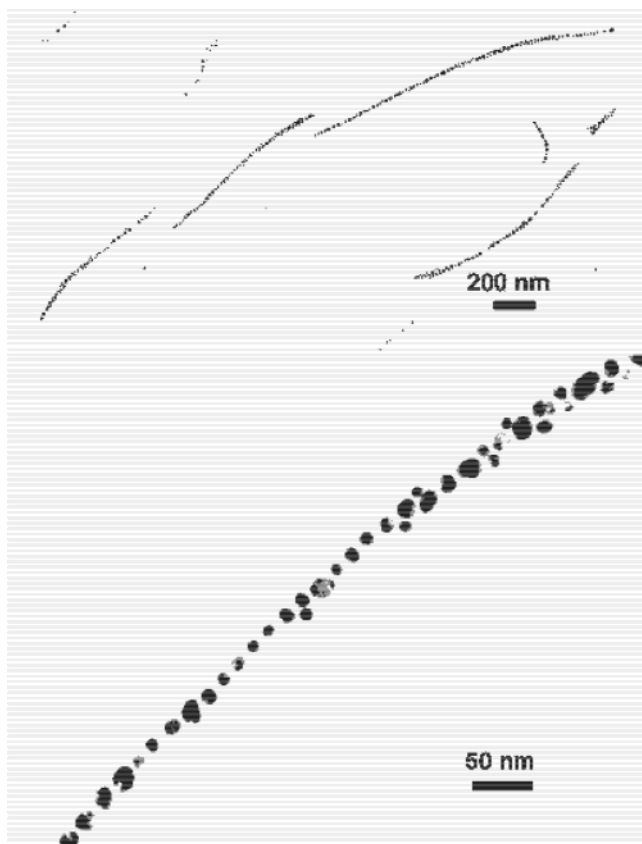


Figure 21. TEM images of AuNPs covered with PEGSH 2000, observed in the presence of chondroitin sulfate sodium salt (polysaccharide carrying sulfuric acid groups and carboxylic acid groups, which are expected to interact with the PEG chain). Reprinted with permission from ref 228 (Ishiwatari's group). Copyright 2002 The Chemical Society of Japan.

prior to reduction allowed control of the AuNP size.²³¹ AuNPs (4–12 nm) were associated with thiol-functionalized polyoxometalates γ -[SiW₁₀O₃₆(RSi)O]⁴⁻ (R = HSC₃H₆), where the R group played the role of both stabilizing the AuNPs via the thiolate ligand and forming a covalent link to the polyanion through the trimethoxysilane group.²³² The preparation of poly(*N*-isopropylacrylamide)-protected AuNPs has been carried out in a homogeneous phase using various methods, and this polymer was found to be a better passivant than alkanethiols.^{233a}

AuNPs were prepared in both aqueous and organic systems by reducing HAuCl₄ with *o*-anisidine in the presence of 1:1 *N*-methyl-2-pyrrolidone/toluene.^{233b} AuNPs of 6 nm diameter and narrow size distributions were stabilized by π -conjugated poly(dithiafulvene) polymers, and the oxidized form of this polymer induced a strong red shift of the absorption spectrum of the AuNPs to 550 nm (whereas the theory predicts 510–515 nm for the plasmon band in water).²³⁴ AuNPs with improved stability against long-term aggregation up to one month were prepared using poly(styrene)-*block*-poly(2-vinylpyridine) star-block copolymer.²³⁵

Water-soluble polymer-stabilized AuNPs were prepared from citrate-capped AuNPs by simple contact with dilute aqueous solutions of hydrophilic nonionic polymers based on the monomers *N*-[tris(hydroxymethyl)methyl]acrylamide and *N*-(isopropyl)acryl-

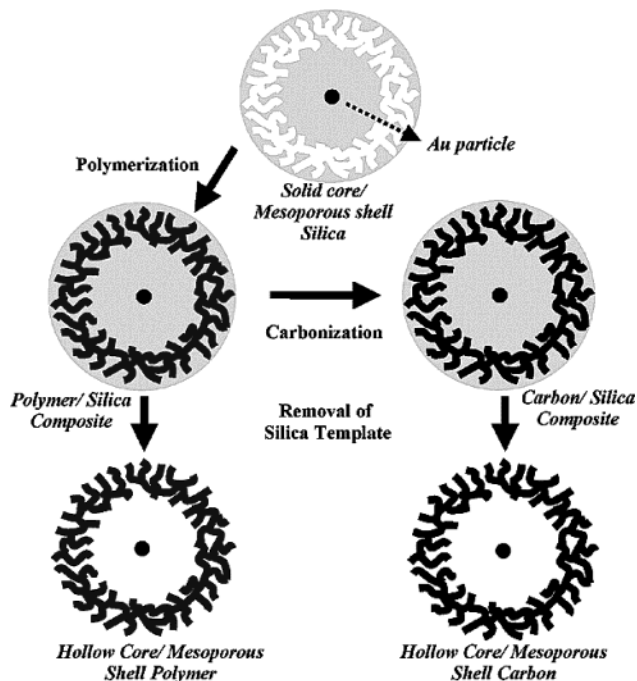


Figure 22. Schematic illustration for the synthesis of Au@HCMS (hollow core/mesoporous shell) polymer and carbon capsules. Reprinted with permission from ref 226 (Hyeon's group). Copyright 2002 American Chemical Society.

amide that were functionalized with disulfide anchoring groups. The resulting polymer-coated AuNPs could be stored in the dry state and redispersed in water to yield sterically stabilized AuNP suspensions. The disulfide-bearing polymers exhibited only a slightly larger affinity for the gold surface than those that do not have the disulfide groups. The polymer layers allowed the free diffusion of small solutes but efficiently minimized the nonspecific absorption of large molecules such as proteins, a promising property (Figure 23).^{236a} AuNPs have been synthesized in graft copolymer micelles,⁸⁷ and the diffusion of AuNPs in a polymer matrix has been analyzed.^{236b} Core-shell AuNPs have been prepared by the layer-by-layer technique, utilizing polyelectrolyte multilayers assembled onto polystyrene cores as thin films in which to infiltrate AuNPs, and hollow spheres were obtained by removal of the templated polystyrene cores.^{236c}

3.12. Dendrimers

A variety of assemblies between PAMAM dendrimers and AuNPs were reported in which the AuNPs were stabilized by the dendrimer that acted as both a polymer and a ligand. The AuNPs were stabilized only in the presence of excess PAMAM dendrimers and in solution, but PAMAM dendrimers functionalized with thiol termini could completely stabilize the AuNPs.²³⁷ PAMAM dendrimers were also functionalized with hydrophobic groups for solubilization of the AuNPs in organic solvents.^{238,368} Such dendrimer-AuNP assemblies were deposited as films on surfaces and used as sensors.^{239–241} AuNPs were synthesized from AuCl₃ in DMF using PAMAM dendrimers that were modified with surface methyl ester groups.²⁴² The use of PAMAM dendrimers for the stabilization of AuNPs allowed control of the

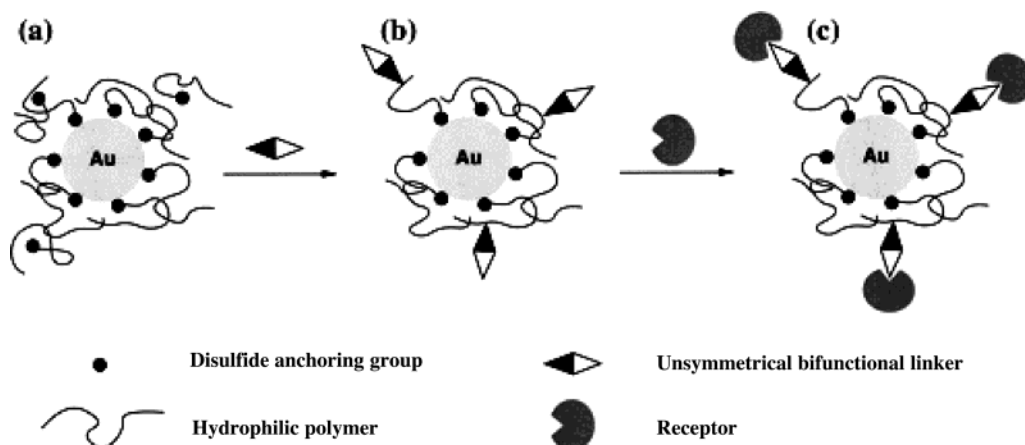


Figure 23. Stepwise "grafting-to" derivatization of AuNPs. (a) Fixation of the polymer with disulfide anchoring groups. (b) Activation of the polymer by unsymmetrical bifunctional linker groups. (c) Functionalization of the polymer by receptors. Step (b) is omitted when "activated" polymers are used. Reprinted with permission from ref 236a (Mangency's group). Copyright 2002 American Chemical Society.

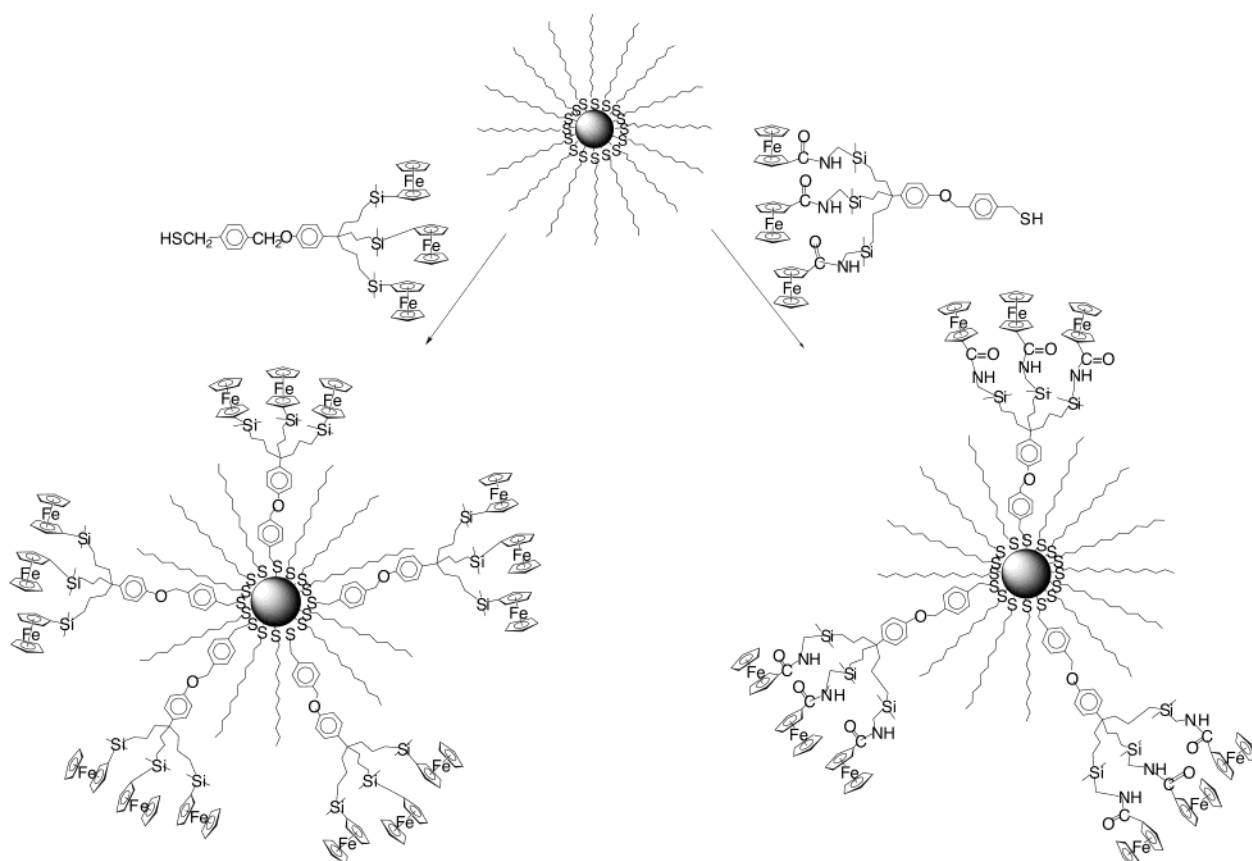


Figure 24. Syntheses of dendronized AuNPs using the thiol ligand substitution procedure. Reprinted with permission from ref 251 (Astruc's group). Copyright 2003 American Chemical Society.

interparticle distance.²⁴³ PAMAM-dendrimer-AuNPs assemblies were incorporated into SiO₂ matrices.²⁴⁴ The pH dependence of water-soluble PAMAM-dendrimer-stabilized AuNPs was examined,²⁴⁵ and such assemblies were used for imaging in cells.²⁴⁶ Bimetallic Au-Pd nanoparticles were synthesized by Crooks's group from PAMAM-dendrimer-Pd nanoparticles assemblies for a catalytic purpose.²⁴⁷⁻²⁴⁹ Dendrimers containing a AuNP core were synthesized by using the Brust-Schiffrin technique with dendrons that were functionalized with thiols at the focal point (Figures 24 and 25).²⁵⁰⁻²⁵⁴ PAMAM-dendrimer-AuNP composites were used as chemiresistor sensors

for the detection of volatile organic compounds and studied by specular neutron reflectometry.^{255a} AuNPs were formed in the presence of stiff polyphenylene dendrimer templates with 16 thiomethyl groups on the outside.^{255b}

3.13. Surfaces, Films, Silica, and Other AuNP Materials

AuNPs were deposited on surfaces for a number of purposes, including physical studies²⁵⁶⁻²⁷⁵ (Figures 26-28) and derivatization of self-assembled monolayers.²⁷⁶⁻²⁷⁸ Privileged materials for deposition are

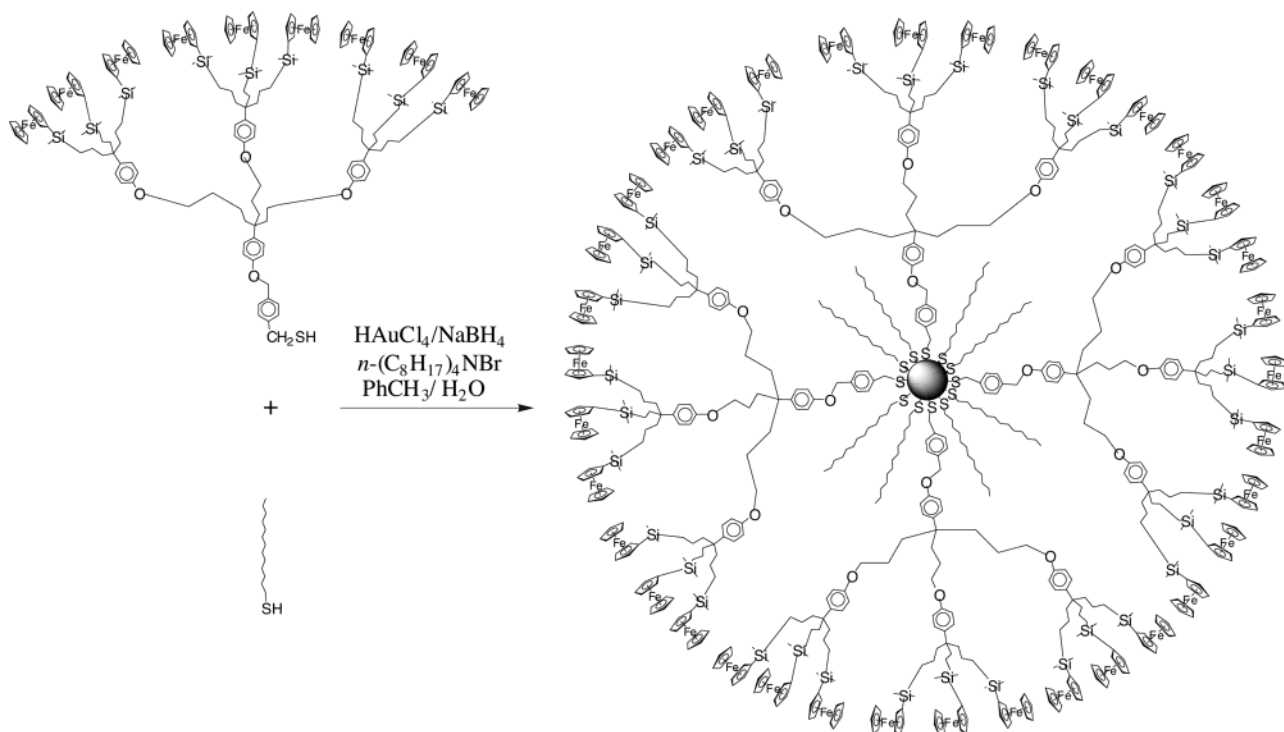


Figure 25. Direct syntheses of dendronized AuNPs containing a nonaferrocenyl thiol dendron (about 180 ferrocenyl groups). Reprinted with permission from ref 251 (Astruc's group). Copyright 2003 American Chemical Society.

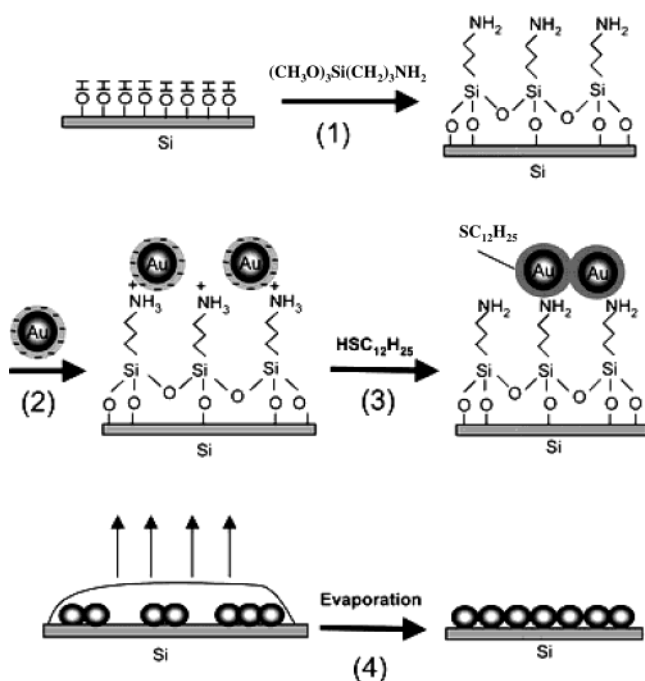


Figure 26. Schematic representation of the procedures developed for fabricating two-dimensional arrays of AuNPs on a silicon substrate in combination with self-assembly of an (aminopropyl)triethoxysilane monolayer, immobilization of nanoparticles, alkanethiol treatment, and solvent evaporation technique. Reprinted from ref 258 (Liu's group) by permission of the PCCP Owner Societies. Copyright 2002.

Si,²⁷⁹ various molecular silicon substrates,²⁸⁰ TiO₂ (Figure 29),^{281–285a} BaTiO₃,^{285b} SrTiO₃,^{285c} Al₂O₃ (Figure 30),²⁸⁶ ammonium salts,²⁸⁷ and various forms of carbon^{288–293} ([60] fullerene (Figure 31),^{288,289} nanotubes,^{290,291} and diamond²⁹²). AuNPs were also deposited together with [Ru^{II}tris(2,2'-bipyridine)] to

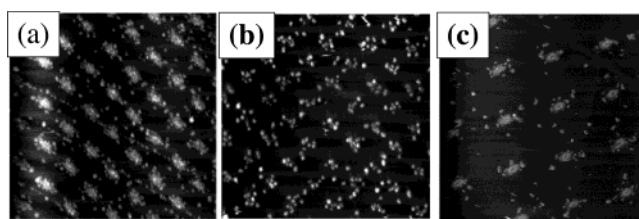


Figure 27. Tapping-mode AFM images ($2 \mu\text{m} \times 2 \mu\text{m}$) of the morphologies of a 0.02-mL gold film deposited on focused ion beam patterned surfaces for different ion fluences I_f and periodicities l_{def} : (a) $l_{\text{def}} = 300 \text{ nm}$, $I_f = 37\,500$ ions per point; (b) $l_{\text{def}} = 300 \text{ nm}$, $I_f = 3750$ ions per point; (c) $l_{\text{def}} = 500 \text{ nm}$, $I_f = 37\,500$ ions per point. Reprinted with permission from ref 262 (Bardotti's group). Copyright 2002 Elsevier.

form multistructures whose photocurrent responses were recorded.²⁹⁴

Thin films of AuNPs were prepared,^{126,295–309} in particular LB films^{310–319} (Figure 32) and monolayers³²⁰ at the liquid interface^{92,321} and from the gas phase.^{322a} Typically, the Brust–Schiffrin method was used to synthesize alkanethiol-stabilized AuNPs that were subsequently spread on the water surface. These totally hydrophobic films could sustain reasonable pressures, and the compressibility was high. It appeared likely that multilayers were generated above 6–8 mN/m.³¹⁷ Films of several tens of cm² in width and several microns in thickness were formed by cross-linking AuNPs with alkanedithiols, followed by filtration onto nanoporous supports.^{322b} A conducting AuNP film is simply produced by rinsing a polystyrene plate with ethanol and water, followed by stirring it at room temperature in an aqueous solution consisting of a thiol and a AuNP solution.³²³ AuNPs were dispersed into Nylon-1,1 thin films, and the resulting materials were studied during heat treatment.^{324–326} Phase transfer of AuNPs across a

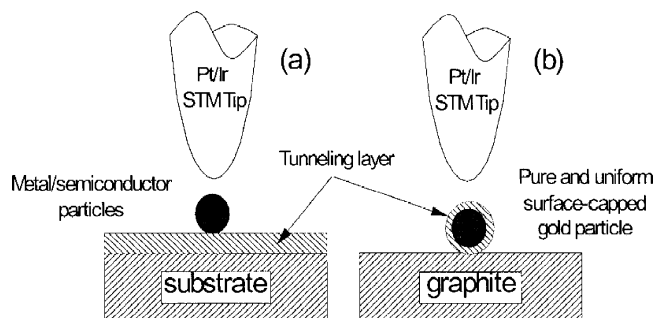


Figure 28. Schematic configuration of the experimental apparatus for measuring current–voltage characteristics by an STM tip. (a) Conventional structure of single-electron tunneling (SET) devices in which a small AuNP is separated from a substrate electrode by an ultrathin tunneling layer. (b) Current structure of the SET devices in which a small AuNP is separated from a HOPG ground plane by a surface-capped tunneling layer on the gold particle. Reprinted with permission from ref 272 (Huang's group). Copyright 1998 Elsevier.

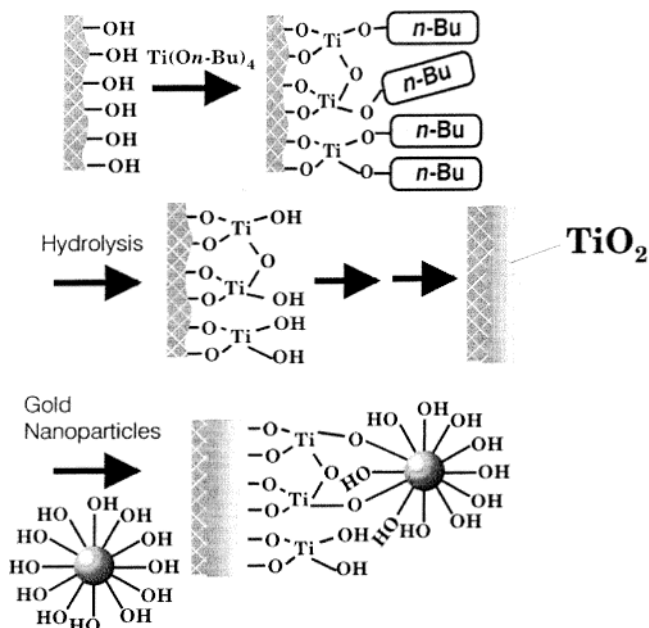


Figure 29. Schematic illustration of sequential surface sol–gel technique and alternate assembly. Reprinted with permission from ref 284a (Kunitake's group). Copyright 1999 American Chemical Society.

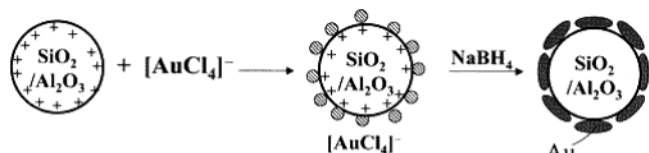


Figure 30. AuNP deposits on SiO₂/Al₂O₃ nanoparticles produced by reduction of [AuCl₄][−] with freshly prepared sodium borohydride solution. Reprinted with permission from ref 115b (Kamat's group). Copyright 2000 American Chemical Society.

water/oil interface was achieved by stoichiometric ion-pair formation between carboxylate anions on particle surfaces and tetraoctylammonium cations and revealed by TEM, IR, UV–vis absorption, and EDX.^{327a} Complete phase transfer of negatively charged (–CO₂[−] or –SO₃[−]), surface-modified AuNPs from the aqueous phase to the organic phase was carried out by hydrophobization using primary

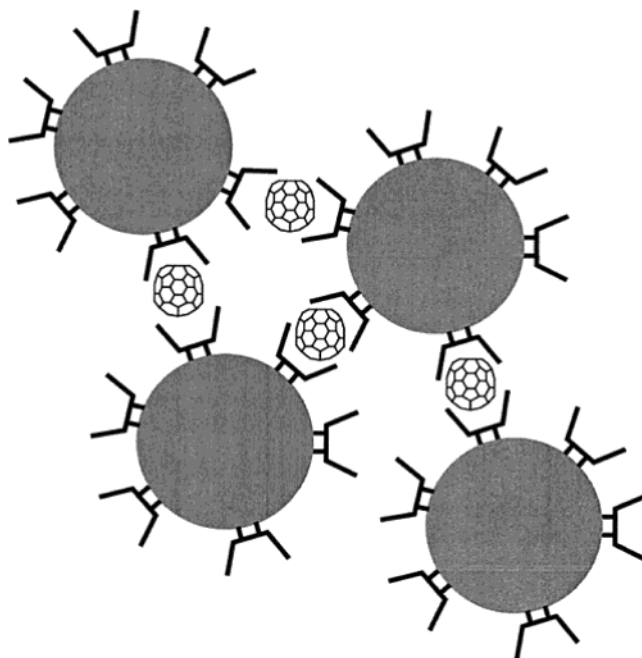


Figure 31. Fullerene-induced network of γ -cyclodextrin-capped AuNPs in aqueous solution. Reprinted with permission from ref 288a (Kaifer's group). Copyright 2001 American Chemical Society.

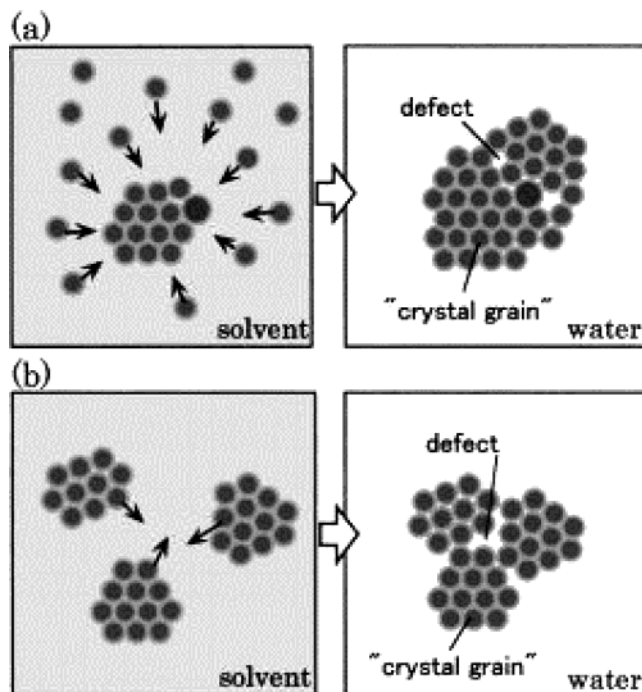


Figure 32. Schematics of the formation of the defects in LB monolayers prepared from (a) a low particle concentration and (b) a high AuNP concentration of LB spreading suspensions. Reprinted with permission from ref 312 (Huang's group). Copyright 2001 American Institute of Physics.

amines.^{327b} AuP nanowires that are between 100 and 200 nm wide could be formed by ultrashort laser pulses.^{327c}

There are many reports of the preparation, characterization, and study of AuNPs dispersed within mesoporous silica, Au@SiO₂.^{111–113,125,328–360} The influence of size,^{328,329} the biofunctionalization,³³¹ the crystal growth,³³² the organization in high order

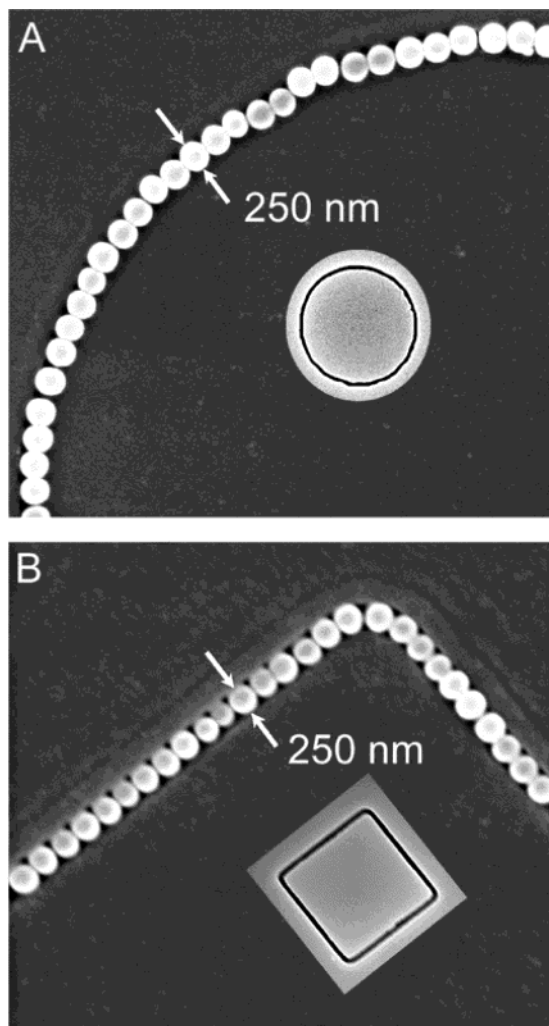


Figure 33. SEM images of plasmonic waveguide structures fabricated by assembling the Au@SiO₂ core-shell AuNP against templates (see insets) patterned in thin films of photoresist. These core-shell AuNPs had a core diameter of 50 nm and a shell thickness of ~100 nm. Reprinted with permission from ref 329a (Xia's group). Copyright 2002 American Chemical Society.

(Figure 33),³³³ the influence of radiations on the nucleation,³⁴² and the sol-gel approach^{354,359} have been examined in the preparations of Au@SiO₂. The two most common synthetic methods to form sol-gel matrices of AuNPs are the citrate route followed by stabilization by a (3-aminopropyl)trimethoxysilane (APTMS)-derived aminosilicate and the sol-gel processing in inverse micelles (Figure 34).³⁵⁴ For instance, 2- and 5-nm AuNPs have been inserted in mesoporous silica materials MCM-41 and MCM-48 by the Somorjai group.³⁵² Another simple and successful method involves tetramethoxysilane, partially hydrolyzed tetrakis(hydroxymethyl)phosphonium chloride, and HAuCl₄ in aqueous solution to produce Au@SiO₂ containing up to 1% weight Au.³⁴² Reduction of HAuCl₄ using H₂ at 973 K for 1 h was also successfully used.³⁴⁴ The sonochemical approach of HAuCl₄ reduction leads to the deposition of AuNPs on the surface of the silica spheres¹¹³ or within the pores of mesoporous silica.^{111,112} Some methods for the engineering of the AuNP surface have been described.³⁵⁵ The homogeneous incorporation of silica-coated AuNPs into a transparent silica gel without

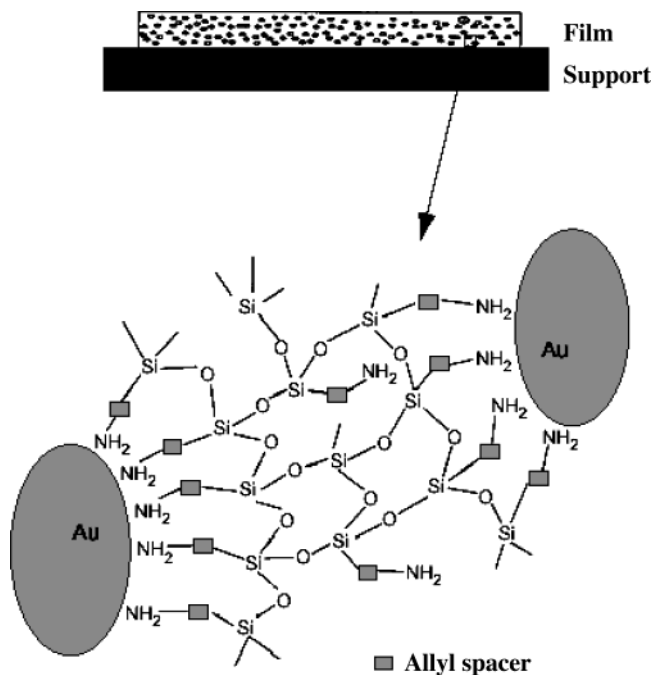


Figure 34. Schematic illustration of AuNPs in a silicate matrix. Reprinted with permission from ref 353 (Lev's group). Copyright 1997 The Royal Society of Chemistry.

any aggregation of particles has been reported.³³⁵ There is growing interest for the assembly and study of AuNPs on silanized glass plates,^{295,300,347,360,492,645-648}

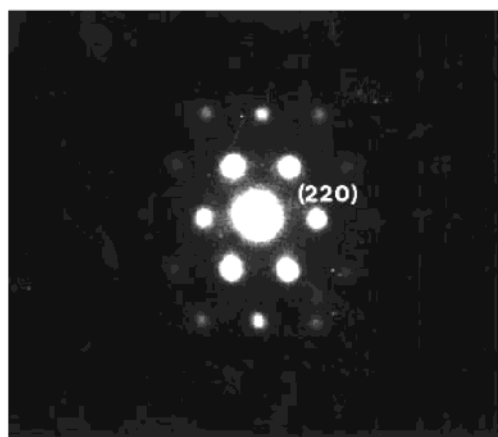
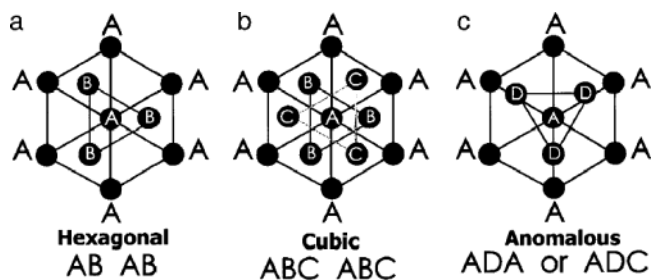


Figure 35. AuNP superlattices. (Top) Packing sequences observed in AuNP superlattices: (a) hexagonal close-packing ABAB, (b) cubic close-packing ABC ABC, and (c) anomalous packing in which AuNPs sit on two fold saddle positions D. The packing becomes ADA or ADC. (Bottom) High-dispersion diffraction patterns from an FCC AuNP superlattice on the [111] zone axis. The reflections (220), corresponding to the second row of reflections, correspond to the void superlattice. Reprinted with permission from ref 366 (José-Yacamán's group). Copyright 2000 Springer.

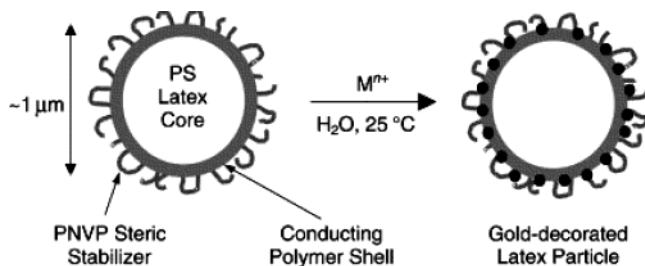


Figure 36. Synthesis of gold-decorated latexes via electroless deposition of gold from aqueous solution, using the conducting polymer overlayer as a redox template. PNVP, poly(*N*-vinylpyrrolidone). Reprinted with permission from ref 372a (Armes's group). Copyright 2001 The Royal Society of Chemistry.

and highly stable AuNPs have been prepared inside HY zeolite supercages.³⁶¹

AuNPs have been manipulated to form highly ordered 1D,^{65,362–364} 2D,^{141,365} or 3D^{59,366,367} (Figure 35) nanonetworks and superstructures.^{60,368} Synthetic opals^{369,370} were fabricated using a layer-by-layer process.³⁷⁰ AuNPs have been formed in lipids following electrostatic entrapment of AuCl_4^- ,³⁷¹ and biomolecular templating allowed site-specific organization of AuNPs.³⁷² AuNPs have been used to decorate latexes via conducting polymer templates (Figure 36).^{373a} The spin-coating method was shown to be far superior to the traditional immersion method for the fast fabrication of AuNPs attached to APTMS-modified fused silica.^{373b}

AuNP-containing materials, whose assembly is mentioned in this section, will be also discussed for their applications in the sensors and catalysis sections.

4. Physical Properties

4.1. The Surface Plasmon Band (SPB)

The deep-red color of AuNP sols in water and glasses reflects the surface plasmon band (SPB; see also section 2 for background), a broad absorption band in the visible region around 520 nm. The SPB is due to the collective oscillations of the electron gas at the surface of nanoparticles (6s electrons of the conduction band for AuNPs) that is correlated with the electromagnetic field of the incoming light, i.e., the excitation of the coherent oscillation of the conduction band. The study of the SPB has remained an area of very active research from both scientific and technological standpoints, especially when the particles are embedded in ionic matrices and glasses.^{374,375} For instance, a driving force for this interest is the application to the photographic process.³⁷⁶ Thus, the SPB provides a considerable body of information on the development of the band structure in metals and has been the subject of extensive study of optical spectroscopic properties of AuNPs.^{375,377–379}

The nature of the SPB was rationalized in a master publication authored by Mie in 1908.³⁷⁹ According to Mie theory, the total cross section composed of the SP absorption and scattering is given as a summation over all electric and magnetic oscillations. The resonances denoted as surface plasmons were described

quantitatively by solving Maxwell's equations for spherical particles with the appropriate boundary conditions. Mie theory attributes the plasmon band of spherical particles to the dipole oscillations of the free electrons in the conduction band occupying the energy states immediately above the Fermi energy level.³⁸⁰ All the numerous subsequent and recent reports correlate the spectroscopic behavior of AuNPs with the Mie theory.^{24,375,380–383} The main characteristics of the SPB are (i) its position around 520 nm; (ii) its sharp decrease with decreasing core size for AuNPs with 1.4–3.2-nm core diameters due to the onset of quantum size effects that become important for particles with core sizes <3 nm in diameter and also cause a slight blue shift (the damping of the SP mode follows a 1/radius dependence due essentially to surface scattering of the conduction electrons;^{381,384} this decrease of intensity of the SPB as particle size decreases is accompanied by broadening of the plasmon bandwidth); and (iii) steplike spectral structures indicating transitions to the discrete unoccupied levels of the conduction band with monodispersed AuNPs with core diameters between 1.1 and 1.9 nm.^{382,383}

Thus, the SPB is absent for AuNPs with core diameter less than 2 nm, as well as for bulk gold. For AuNPs of mean diameter of 9, 15, 22, 48, and 99 nm, the SPB maximum λ_{max} was observed at 517, 520, 521, 533, and 575 nm, respectively, in aqueous media. The SPB maximum and bandwidth are also influenced by the particle shape, medium dielectric constant, and temperature. The refractive index of the solvent has been shown to induce a shift of the SPB, as predicted by Mie theory.^{385,386} For instance, solutions of dodecanethiolate AuNPs of 5.2 nm average diameter reveal an 8-nm shift in SPB as the solvent refractive index is varied from $n_d^{20} = 1.33$ to 1.55. The ligand shell alters the refractive index and causes either a red or blue shift, so that the spectroscopic data obtained often deviate from the prediction of Mie theory that deals with naked nanoparticles. The agreement with Mie theory is obtained only when the shift induced by this ligand shell is taken into account. This shift is especially significant with thiolate ligands, which are responsible for a strong ligand field interacting with the surface electron cloud. In fact, since all AuNPs need some kind of stabilizing ligands or polymer, the band energy is rarely exactly as predicted by Mie theory if the shift of this stabilizer is not considered. With elliptical particles, the SPB is shifted to higher wavelength as the spacing between particles is reduced, and this shift is well described as an exponential function of the gap between the two particles. It becomes negligible when the gap is larger than about 2.5 times the short-axis length.^{386c} A red shift for a polarization parallel to the long particle axis and a blue shift for the orthogonal polarization were reported and rationalized by a dipolar interaction mechanism.^{386d} The optical thickness could be used as a measure of efficiency, this parameter being critically dependent on particle size and refractive index. Therefore, impurities can be easily detected since the refractive index of AuNPs greatly differs from that of gold oxide

or gold chloride.^{386g}

Another influential parameter is the core charge. Excess electronic charge causes shifts to higher energy, whereas electron deficiency causes shifts to lower energy.^{386,387} A convenient theoretical expression has been derived for the SPB position as a function of the changes in free electron concentration:

$$\lambda_{\text{final}}/\lambda_{\text{initial}} = (N_{\text{initial}}/N_{\text{final}})^{1/2}$$

For instance, in the AuNPs of 5.2 nm diameter containing 2951 Au atoms, the authors assume that there is one free electron per Au atom (e.g., $N_{\text{initial}} = 2951$ free electrons per AuNP); AuNPs charged to +0.82 V vs Ag leads to the removal of 19 electrons per AuNP, and thus N_{final} is 19 electrons less ($N_{\text{final}} = 2932$). This corresponds to a predicted red shift of 1.7 nm, which is much smaller than that observed experimentally (9 nm from 516 to 525 nm, which would theoretically correspond to the removal of 100 electrons from the AuNP). The reason for this difference is not clear, and tentative explanations involve a much reduced number of free electrons and large shift amplification by the thiolate ligand shell.³⁸⁶

The SPB width was found to increase with decreasing size in the intrinsic size region (mean diameter smaller than 25 nm) and also to increase with increasing size in the extrinsic region (mean diameter larger than 25 nm). A small temperature effect was also found. It was proposed that the dominant electronic dephasing mechanism involves electron–electron interactions rather than electron–phonon coupling.^{387a} Femtosecond light scattering of AuNPs of 80 nm diameter showed, on the other hand, that both electron–phonon and phonon–phonon coupling processes occur in the individual AuNPs.^{387b} In Au–SiO₂ core–shell particles (Au@SiO₂), varying the SiO₂ shell thickness and the refractive index of the solvent allowed control over the optical properties of the dispersions, and the optical spectra were in good agreement with Mie theory.³⁵⁶ The SPB position in Au@SiO₂ (including films) was accurately predicted by the Maxwell–Garnett model, and it was concluded that it is possible to synthesize composite materials with optical properties that lie anywhere between those of transparent glass and those of metallic gold.^{388–390}

A near-field optical antenna effect was used to measure the line shape of the SPB in single AuNPs, and the results were found to be in agreement with Mie theory; double-peak shapes caused by electromagnetic coupling between close-lying particles were observed.³⁹¹

From optical spectra of oriented AuNPs/polyethylene, the SPB extinction maxima of AuNPs for incident fields polarized parallel to the direction of nanoparticle orientation ($\lambda_{\text{max}} - (0)$) were found to be red-shifted relative to the extinction maxima for perpendicular polarization ($\lambda_{\text{max}} - (90)$).³⁹² For rodlike particles, the extinction maximum for incident electric fields polarized along the long axis occurs at a longer wavelength than the λ_{max} for polarization along the particle radius.³⁹³ Selective suppression of

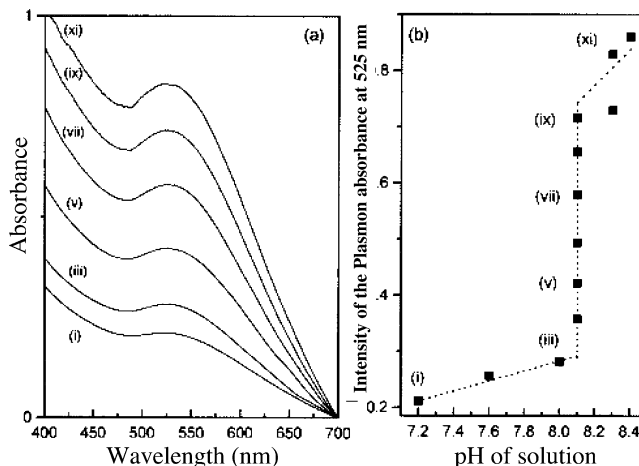


Figure 37. (a) UV/vis solution spectra of 4-mercaptopropionic acid-capped AuNPs as a function of the addition of NaOH(aq) and (b) the variation of the intensity of the plasmon absorbance, at 525 nm, as a function of the pH of the solution. Points i, iii, v, vii, ix, and xi in (b) were obtained from curves i, iii, v, vii, ix, and xi in (a), respectively. Reprinted with permission from ref 93 (Evans's group). Copyright 1998 American Chemical Society.

extinction of the SPB was observed.^{394,395} Picosecond dynamics of AuNPs was studied by laser excitation close to the SPB at 66 nm, leading to the formation of “hot” non-Fermi electronic distribution within the AuNPs.³⁹⁶ Visible–laser-induced fusion and fragmentation could be induced by thionicotamide, and aggregation effects disappear following laser pulse excitation.^{397a} Softening of the coherently excited breathing mode on AuNPs was observed by time-resolved spectroscopy, showing that the period of breathing mode increases with pump laser power.^{397b} The coagulation (along with Oswald ripening) of AuNPs dispersed in organic liquids was dramatically accelerated by visible light, and the process was shown to be wavelength dependent; UV irradiation caused coalescence.³⁹⁸ Laser irradiation at the SPB of suspended AuNPs in 2-propanol causes coagulation or dispersion, depending on concentration, the photochemical reaction being due to electron transfer from a solvent molecule to the AuNP.³⁹⁹ AuNPs were pulverized into smaller AuNPs with a desired average diameter and a narrow distribution by a suitable selection of laser irradiation.⁴⁰⁰ When a molecular linker, 4-aminobenzenethiol, attached several AuNPs together, the optical absorption differed, consistent with plasmon–plasmon interactions between the AuNPs of the assembly (Figure 37).⁴⁰¹

Applications of the sensitivity of the position of the SPB are known, especially in the fields of sensors and biology. A shift of the SPB of AuNPs has been measured upon adsorption of gelatin, and quantitative yield measurements of the adsorbed amount were obtained.⁴⁰² Rhodamine 6G was shown to provoke morphological changes and particle growth upon laser irradiation of the SPB as a result of melting and fusion of AuNPs, and the multiphoton process leading to the fusion process has been elucidated using picosecond laser flash photolysis (Figure 38).⁴⁰³ Increasing the solution temperature from 10 to 40 °C thermally triggered the reversible hydrophilic-to-hydrophobic phase transition of the adsorbed elastin-

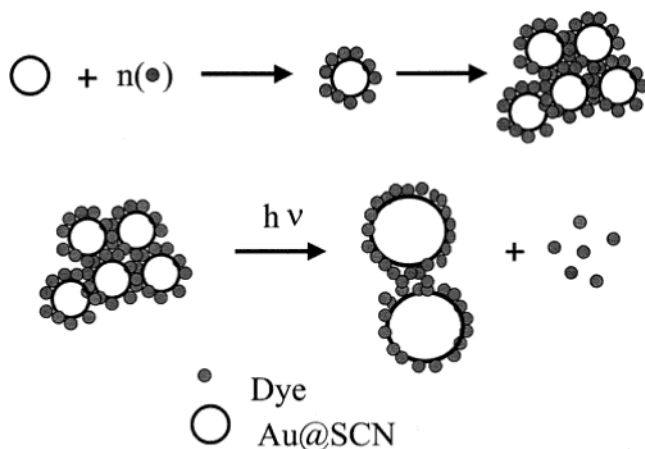


Figure 38. Schematic diagram illustrating the possible morphological changes associated with laser irradiation of the AuNP-dye assembly. Au@SCN, AuNPs obtained by reduction of AuCl_4^- with SCN^- . Reprinted with permission from ref 402 (Kamat's group). Copyright 2000 American Chemical Society.

like polypeptide, a thermally responsive biopolymer.⁴⁰⁴ Formation of large aggregates caused a reversible change in color of the AuNP suspension from red to violet due to coupling to surface plasmons in aggregated colloids. The SPB was used to study the dispersibility of AuNPs in a variety of solvents (Figure 39).⁴⁰⁵ Phase transfer of dodecylamine-capped AuNPs dispersed in an organic solvent into water containing the surfactant cetyltrimethylammonium bromide (CTAB) was monitored by color changes initiated upon shaking.⁴⁰⁶ Surface interaction of AuNPs with functional organic molecules was probed using the shifts of the SPB. For instance, a red shift was observed with an increase of the solvent dielectric constant with solvents that do not coordinate the gold core, but the SPB is unaffected in polar solvents that do not bind to the core.⁴⁰⁷ AuNPs consisting of a mixture of triangular/hexagonal and smaller, close-to-spherical particles display two SPBs at 540 and 680 nm, respectively, as expected. UV-visible data indicate preferential adsorption of the flat AuNPs on polyelectrolyte films and the development of a new band at 650 nm as the number of bilayers increased.^{408a} Compared to solid AuNPs of similar size, nanorings produced on soda-glass substrates using colloidal lithography exhibit a red-shifted localized SPB that could be tuned over an extended wavelength range by varying the ratio of the ring thickness to its radius.^{408b}

The magnetic circular dichroism (MCD) spectra of AuNPs and $\text{Au}_9(\text{PPh}_3)_8^{3+}$ encapsulated in optically transparent xerogels have been shown to be temperature dependent between 5 and 295 K only for the former, and indicate that the MCD spectra of the latter reflect an excited-state phenomenon with a strong intermixing of the excited spin-orbit states.^{382b} The hot electron dynamics of AuNPs was characterized using femtosecond two-color pump-probe spectroscopy in the SPB region.^{382c}

4.2. Fluorescence

Fluorescence studies of AuNPs have been carried out under various conditions,^{409–419} including femtosecond emission⁴¹⁰ and steady-state investigation of

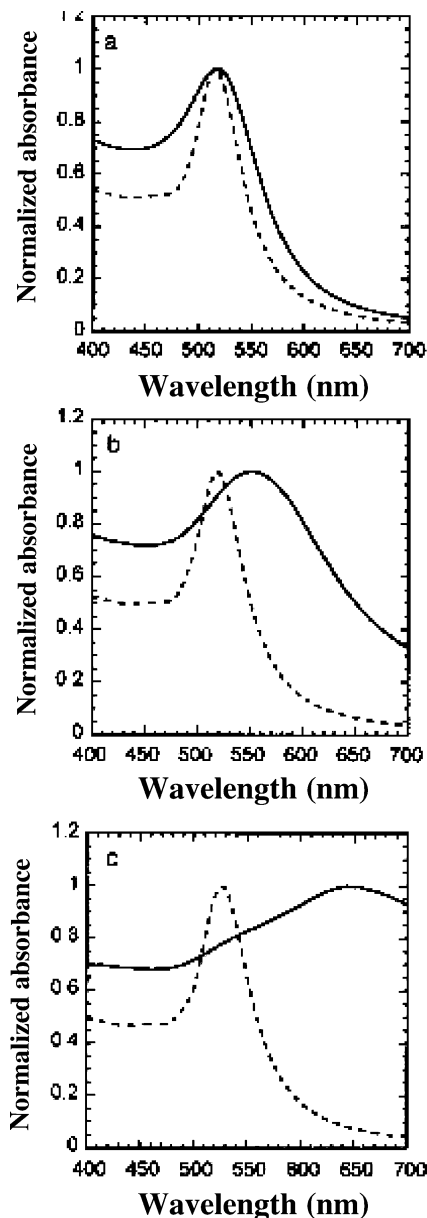


Figure 39. Optical absorption spectra of AuNPs 8.3 nm in diameter dispersed in (a) water, (b) ethanol, and (c) chloroform. The dashed lines represent the values calculated from the Mie equation. The solid lines represent the experimental data. Reprinted with permission from ref 404 (Huang's group). Copyright 2002 American Institute of Physics.

the interaction between thiolate ligands and the gold core.⁴¹¹ Capping fluorescent groups are pyrenyl,⁴¹³ polyoctylthiophenyl,⁴¹⁵ fluorenyl,⁴¹⁹ and other probes.^{414,416–418} Indeed, resonant energy transfer was observed in fluorescent ligand-capped AuNPs, this phenomenon being of great interest in biophotonics⁴²⁰ and materials science.^{421–423} Both radiative and non-radiative rates critically depend on the size and shape of the AuNPs, the distance between the dye molecules, the orientation of the dipole with respect to the dye-nanoparticle axis, and the overlap of the molecule's emission with the nanoparticle's absorption spectrum.⁴¹⁸ Orders-of-magnitude higher efficiencies were obtained with nanometer-dimension metal samples.^{424–426} The observed increase in the fluorescence yield reflected the suppression of the

nonradiative decay upon binding to AuNPs.⁴¹⁴ Visible luminescence has been reported for water-soluble AuNPs, for which a hypothetical mechanism involving $5d^{10} \rightarrow 6(sp)^1$ interband transition has been suggested.⁴⁰⁹ On the basis of the ability of discrete photoisomeric states of spiropyrans to exhibit distinct physical properties, photoswitchable AuNP assemblies of various amino acids were designed by anchoring spiropyrans to allow the release of the outer sphere of amino acids on irradiation.⁴²⁷

4.3. Electrochemistry

The electrochemistry of thiolate-stabilized AuNPs showing the formation of core charge has been indicated in section 2 (staircase blockade).^{39,40} Moreover, the quantized capacitance charging of AuNPs self-assembled monolayers on electrode surfaces could be rectified by certain hydrophobic electrolyte ions, such as PF_6^- , in aqueous solution (Figure 40).^{39c} In the presence of some *p*-nitrothiophenolate ligands, the peak spacings corresponding to the quantized capacitance charging were found to decrease slightly compared to those obtained in the absence of *p*-nitrothiophenolate ligands, corresponding to a small decrease of the particle capacitance due to the presence of more polar ligands.^{428a} Magneto-electrochemistry of AuNP quantized capacitance charging showed the influence of a magnetic field on the electrochemistry of AuNPs, and in particular the effect of electron parity upon their charging states.^{428b} Double-layer capacitance was obtained in aqueous media by differential pulse voltammetry.^{428c} The voltammetry of small AuNPs containing respectively 11^{429a} and 38^{429b} core Au atoms has been reported.

Viologen thiols and dithiols have been synthesized and connected to AuNPs.^{430,431} In particular, viologen thiols have been used as redox-active linkers in order to study electron transfer between the linked AuNPs.^{430a} AuNPs have been shown to tune the electrochemical properties of the electrode/solution interface using the $Fe(CN)_6^{3-/4-}$ redox system.⁴³²

The electrochemistry of functional AuNPs containing thiolate ligands bearing ferrocenyl^{49b} or amido- or silylferrocenyl^{140,250–252,433} and biferrocenyl groups has been reported, and these ferrocenyl- or biferrocenyl-derived AuNPs have been deposited on elec-

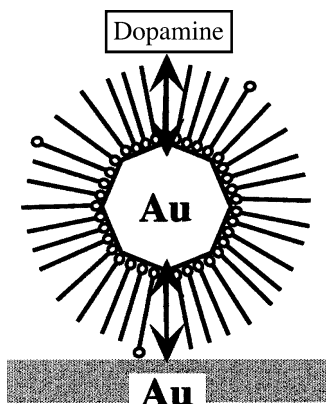


Figure 40. Schematic chart of electron tunneling through surface-confined AuNP layers. Reprinted with permission from ref 39c (Chen's group). Copyright 2001 American Chemical Society.

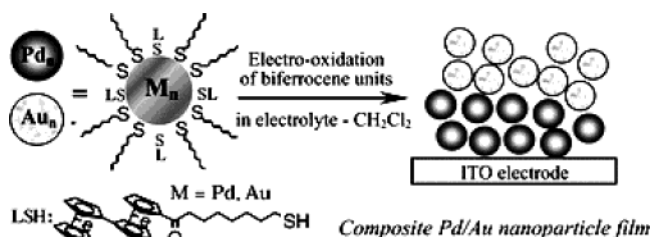


Figure 41. Combination of electro-oxidative deposition of PdNPs attached with biferrocene-terminated thiolates and that of AuNPs with the same thiolates, to form a thin redox-active film with a layered hybrid structure. Reprinted with permission from ref 440 (Nishihara's group). Copyright 2002 The Royal Society of Chemistry.

trodes by scanning around the potential region around the Fe^{II}/Fe^{III} waves.^{251,252} Nishihara's group has modified alkanethiol-stabilized AuNPs by thiol ligands bearing biferrocenyl^{434–437} or anthraquinone^{436,437} using the thiolate-exchange method. The second oxidation process of the biferrocenyl units of AuNPs–biferrocenylthiolate led to a uniform redox-active AuNP film on an electrode. AuNPs–anthraquinonethiolate was found to be aggregated by two-electron reduction of anthraquinone groups. These findings confirmed that AuNPs containing multiple redox molecules could assemble according to charge accumulation. The multielectron system seemed to be indispensable for these deposition phenomena, as they were not observed for AuNPs linked via thiolate ligands with a single redox species such as ferrocenyl.^{49b} This property also allowed Yamada and Nishihara to construct alternating multilayered structures of palladium and gold nanoparticles connected with biferrocenyl groups (Figure 41).⁴⁴⁰ Ferrocenyl-dendronized AuNPs also adsorb very well, a useful property for molecular recognition (vide infra).^{251,252} C_{60} -functionalized AuNPs, synthesized using the ligand-exchange procedure, can form a derivatized electrode upon immersion of a gold electrode, and this modified electrode showed two peaks corresponding to the reduction of C_{60} that were stable upon scanning.^{441a} The charge injection energetics between a solution redox couple and hexanethiol–AuNPs has been probed by scanning electrochemical microscopy.^{441b} Altogether, electrochemistry has been used in several ways to fabricate and deposit AuNPs,^{251,252,436–441} inter alia on porous silicon.^{441c} A APTMS-supported AuNP electrode was constructed; therefore, the preparation procedure using 3-mercaptopropionic acid-bridged copper hexacyanoferrate multilayers on a planar macroelectrode was copied to the as-prepared AuNP electrode.^{441d} AuNPs formed from ferrocenylthiophenol (2.5 nm) were studied inter alia by voltammetry, showing only 15% coverage with the composition $Au_{490}Fc_{80}$.^{441e} AuNP microelectrodes have been prepared with uniform Pt group over-

4.4. Electronic Properties Using Other Physical Methods

It was found that, for 2D superlattices consisting of large (5 nm) AuNPs, the electronic behavior was dominated by the Coulomb blockade effect at low temperature, while the $I-V$ response was ohmic at

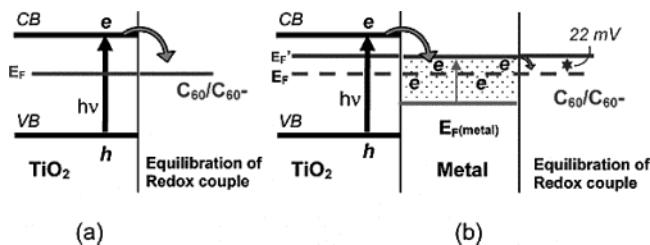


Figure 42. Charge distribution between TiO_2 and AuNPs, leading to equilibration with the $\text{C}_{60}/\text{C}_{60}^-$ redox couple (a) in the absence and (b) in the presence of metal nanoparticles. E_F and E_F' refer to the Fermi levels of TiO_2 before and after attaining equilibrium, respectively. Reprinted with permission from ref 442b (Kamat's group). Copyright 2003 American Chemical Society.

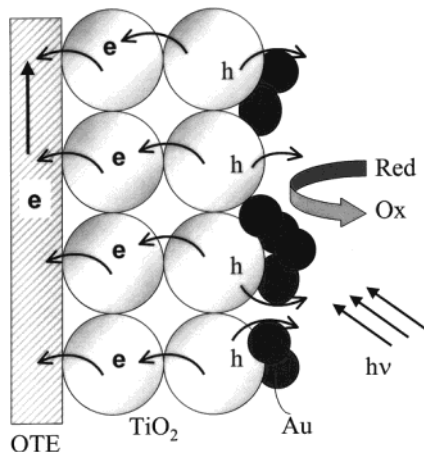


Figure 43. Charge separation in a AuNP-modified nanostructured TiO_2 electrode. OTE, optically transparent electrode. Reprinted with permission from ref 459 (Kamat's group). Copyright 2000 American Chemical Society.

room temperature.⁶¹ TiO_2 nanoparticles exhibited a blue coloration due to stored electrons within the particles when subjected to UV. A partial disappearance of the blue color was seen upon contact with

AuNPs as electrons were transferred from TiO_2 to AuNPs (Figure 42).^{442b} TiO_2 films cast on conducting glass plates were modified by adsorbing AuNPs (5 nm diameter) from a toluene solution, and selective formation of Au islands and larger particles on the TiO_2 surface was observed by TEM and AFM (Figure 43).⁴⁵⁹ A technique was described in which a AuNP was connected to two Cr electrodes, and electron transport in this sample could be fitted to orthodox theory of electron tunneling.^{443a} Scanning electrochemical microscopy was used to investigate the kinetics of electron-transfer reactions between methyl viologen (MV^{2+}) and protons, giving H_2 and MV^+ , catalyzed by AuNPs supported on an insulating substrate. This technique allows investigation of AuNP size effects on the kinetics and study of reactions at semiconductor nanoparticle surfaces in the absence of a metallic conductor.^{443b} An electronic conductivity study of composites made from 1,10-decanethiol and AuNPs using pressed pellets between 1- μm electrode gaps showed that the I - V curve was sigmoidal (Figure 44).⁴³⁸ The rectifying effects of electrolyte ions on interfacial electron transfer were investigated with AuNP monolayers anchored by bifunctional chemical bridges containing viologen groups (Figure 45).⁴³⁹ X-ray absorption near-edge structure (XANES) of 2-nm AuNPs capped with dendrimer and thiol revealed the gain of a 5d electron relative to the bulk when capped with weakly interacting dendrimers and the loss of a 5d electron when capped with strongly interacting thiol ligands.^{444a} The chemical states of the self-assembled AuNPs absorbed onto the surface of a silane were studied by angle-resolved X-ray photoelectron spectroscopy, which made it possible to distinguish bound thiolate ligands and unbound thiols^{444b} and to investigate the size-dependent systematics of lattice contraction and charge redistribution.^{444c} Using a pump-probe technique, the dynamics of the hot carriers in nanodots induced by femtosecond laser pulses showed that

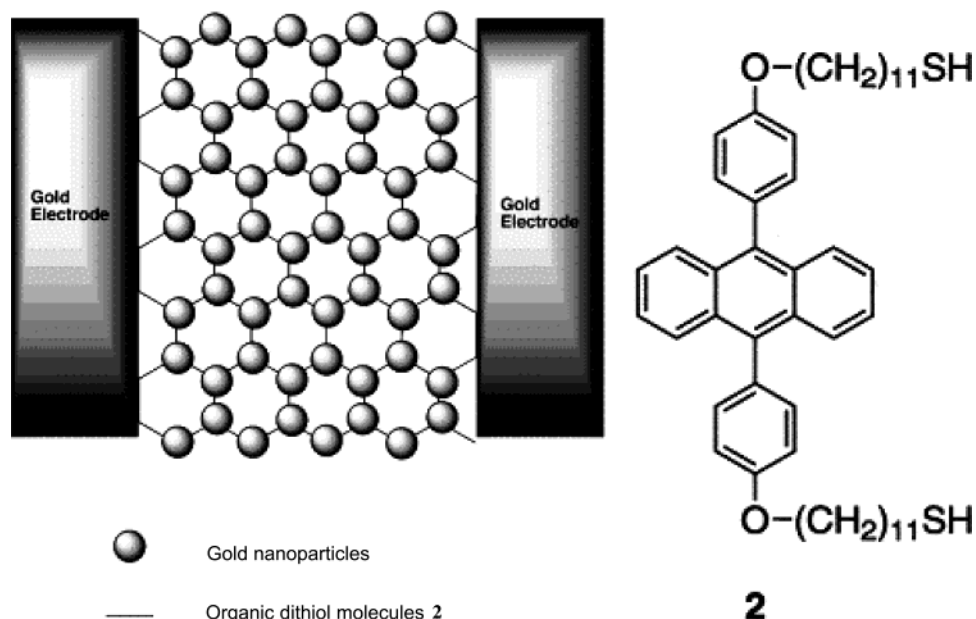


Figure 44. Schematic illustration of the micro-gap electrodes which are connected with the network of organic dithiols and AuNPs. Shaded circles indicate AuNPs, and lines indicate organic dithiol molecules. Reprinted with permission from ref 438 (Ogawa's group). Copyright 2001 Elsevier.

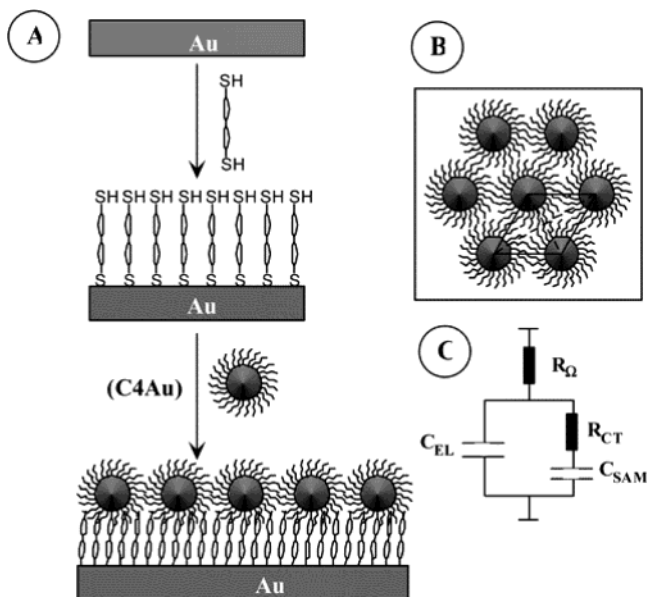


Figure 45. (A) Sequential anchoring of AuNPs to viologen dithiol self-assembled monolayers, (B) hypothetical hexagonal distribution of surface-immobilized AuNPs, and (C) Randle's equivalent circuit, where R_{Ω} is the solution (uncompensated) resistance, R_{CT} is the charge-transfer resistance, and C_{SAM} and C_{EL} are the interfacial capacitances from the collective contributions of all surface-anchored AuNPs and the interparticle void space, respectively. Reprinted with permission from ref 439 (Chen's group). Copyright 2002 American Chemical Society.

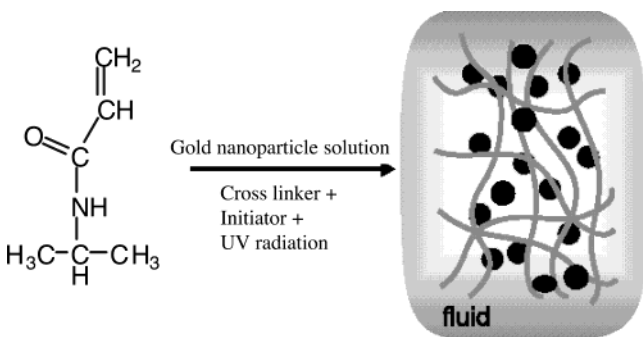


Figure 46. Scheme showing how the AuNPs are locked in the hydrogel network. Reprinted with permission from ref 445 (El-Sayed's group). Copyright 2001 Elsevier.

changing the surrounding matrix led to large variations in the relaxation times of both the electron-phonon and phonon-phonon coupling (Figure 46).⁴⁴⁵ High-resolution electron energy loss spectroscopy (HREELS) was used to study low-energy electron impact on films of AuNPs passivated with dialkyl sulfide.^{446a} Metal-containing molecular rods were self-assembled on a Au disk electrode, and AuNPs were deposited electrochemically; cyclic voltammetry indicated that the electron could transport rapidly through this structure between the Au electrode and $Fe(CN)_6^{3-/4-}$.^{446b} The effect of spin-orbit scattering on discrete energy levels in AuNPs and other nanoparticles showed level-to-level fluctuations of the effective g -factor from Zeeman splitting, and the statistics were found to be well characterized by random matrix predictions.^{447a} Energy transfer from a surface-bound arene to the gold core was observed

upon photoirradiation.⁴¹⁹

AuNPs have a remarkably low melting temperature (between 300 and 400 °C), due to the large ratio of surface atoms to inner atoms, compared to that of bulk gold (1064 °C). This property was used in the process of printing and laser-curing of AuNP solutions, a laser irradiation time of 1 ms being sufficient.^{447b}

5. Chemical, Supramolecular, and Recognition Properties

5.1. Reactions of Thiolate-Stabilized AuNPs

Some of the thiolate ligands in alkanethiolate-stabilized AuNPs can be substituted by reaction with other thiols at rates depending on the chain length⁵⁰ and steric bulk⁵³ of the leaving thiolate and incoming thiols^{448a} and on the charge of the AuNPs. For instance, oxidation of the AuNPs largely enhances the proportion of thiolate ligands that can be replaced.^{448b} Various functional thiols could be partially incorporated into AuNPs using this efficient reaction. For instance, incorporation of 11-mercaptoundecanoic acid gave amphiphilic AuNPs that were soluble in basic aqueous media but aggregated in acidic media due to hydrogen-bonding. This property was controlled by adjusting the pH,¹³³ and in particular biomimetic ion-gating recognition has been reported.^{449a} The chelating properties of the carboxylate group with metal have been used for metal detection^{449b} and formation of AuNP films.^{450,451} Complexation of pyridine-functionalized thiol AuNPs also led to solid substrate assembly,⁴⁵² and such bifunctional ligands were used to link AuNPs, which led to electron-hopping studies and applications as sensors.⁴⁵³ Various other electroactive^{45,455-460} and photoactive groups,⁴⁶⁰⁻⁴⁶⁷ spin labels,⁴⁶⁸ and catalysts,^{469,470} as well as simple groups such as halides, nitriles, alkenes, and sulfonates,^{48,471} were similarly introduced using this ligand-exchange reaction.^{52c}

Nucleophilic substitution of bromide in ω -bromoalkanethiolate-functionalized AuNPs follows an S_N2 mechanism with alkylamines, the rate being largely dependent on the steric bulk (Figure 47). Similarly, nucleophilic substitution of the hydroxy group by alkyl halides could be carried out with ω -hydroxy-functionalized AuNPs.^{52c} C_{60} was introduced into AuNPs by nucleophilic addition of 4-aminophenoxide ligands to C_{60} double bonds (Figure 48).²⁸⁸ Nucleophilic addition of ω -maleimido thiol-AuNPs onto a sulfidryl group was used to attach AuNPs to proteins, peptides, and oligonucleotides.^{472,473} The nucleophilic reaction of amino groups of SAMs on a gold surface with carbonyl groups of functional AuNPs was used to attach AuNPs onto the SAMs.²⁷⁶ Nucleophilic reaction of the amino group of ω -aminothiols-AuNPs with the aldehyde group of glycoproteins, generated by oxidation of ribose cis-diols, could be used to label carbohydrates.⁴⁷⁴ Carboxylic acid-alcohol coupling was used to link 2-naphthaleneethanol, ferrocenemethanol, phenothiazine, anthraquinone, α -D-glucose, and uridine to AuNPs.⁴⁷⁵ Propionic anhydride reacted with p -mercatophenol-AuNPs, giving only partial esterification due to the steric constraint.⁴⁷

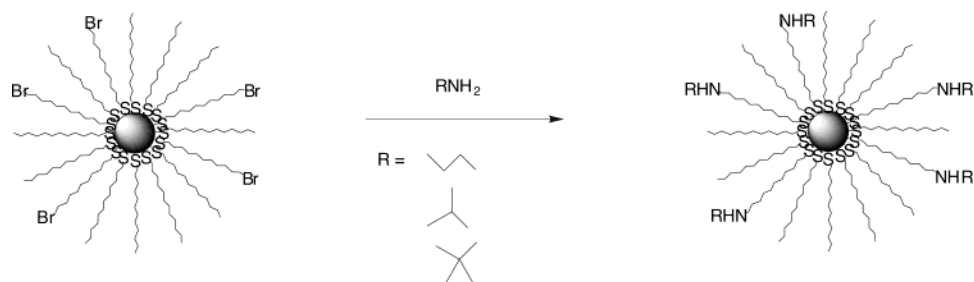


Figure 47. Nucleophilic substitution reaction between AuNPs containing alkanethiol bromide and alkylamines.

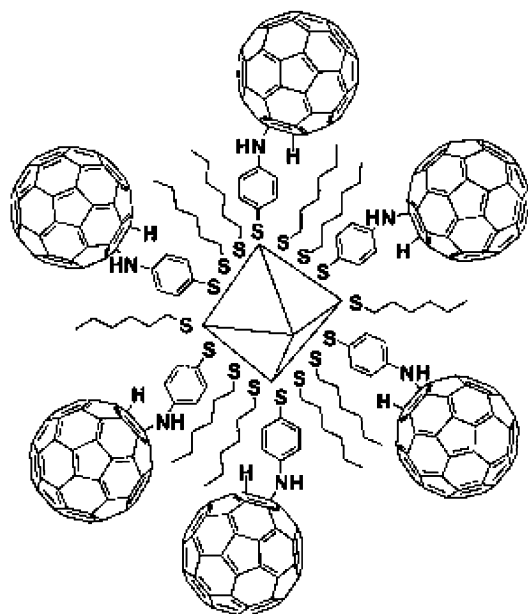


Figure 48. C₆₀-linked AuNPs. Reprinted with permission from ref 287 (Shon's group). Copyright 2002 The Royal Society of Chemistry.

The radical polymerization precursor 2-bromoisobutyronitrile reacted with 11-mercaptoundecanol-AuNPs, providing the ester linkage.⁴⁷⁶ Carboxylic acid-amine coupling was used to link TEMPO, pyridine, glutamic acid, pyrene, fluorescein,^{50,475} carbon nanotubes,^{477,478} ferrocenyl, and viologen to AuNPs (Figure 49).⁴⁷⁹ AuNPs functionalized with sulfo-*N*-hydroxysuccinimide react with primary amines, which allows any protein bearing a primary amine to be linked to AuNPs. AuNPs could be polymerized when they bore a thiol functionalized with an atom-transfer-radical (ATR) polymerization initiator such as CuBr/tris(2-dimethylaminoethyl)amine²¹² or CuBr/1,4,8,11-tetraethyl-1,4,8,11-tetraazacyclotetradecane.⁴⁷⁶ AuNPs could be subjected to cationic polymerization, giving dense brushes if they were functionalized with *ω*-trifluoromethanesulfonate, using 2-phenyl-2-oxazoline or *N,N*-di-*n*-octadecylamine as a monomer and terminating agent, respectively. AuNPs functionalized with a thiolate ligand bearing a norbornyl group could be submitted to ROMP using Grubb's catalyst [RuCl₂(PCy₃)₂(=CHPh)], and two kinds of electroactive ferrocenyl groups could be incorporated. Spherical hollow-sphere capsules were formed by ROMP of AuNPs functionalized with a tripodal ligand followed by etching.⁴⁸⁰ Polymerization of *ω*-siloxane-AuNPs formed AuNPs that were surrounded by polysiloxane shells.⁴⁸¹

The thiolate-stabilized AuNPs can be decomposed inter alia by reaction of cyanide to give mononuclear gold cyanide and the free thiols or by photoirradiation in the presence of bromine-containing trihalomethanes.⁴⁸²

5.2. Supramolecular Chemistry

Acid-base chemistry^{483,484} has been involved in molecular recognition and has been studied using various techniques.^{484,485} For instance, the structures formed by adsorption of carboxyalkylphosphonic acids on metal oxides were compared to those formed with *ω*-mercaptocarboxylic acids and AuNP cores using ¹H fast magic angle spinning (MAS), heteronuclear correlation (HETCOR), and ¹H double-quantum (DQ) MAS solid-state NMR.⁴⁸⁶ Infrared reflection spectroscopic data were used to characterize the interfacial structures derived from the interfacial reactivity at the interconnecting linkages of core-shell nanoparticle networks and pH-tunable networks consisting of head-to-head hydrogen-bonded carboxylic acid terminals.^{487,488} Nanoparticle arrays obtained by mixing anionic bilayer membranes and cationic, quaternary ammonium-stabilized AuNPs were immobilized densely into the hydrophilic interlayers of dispersed lamellar structures to form a quasi-1D structure.⁴⁸⁹ A pseudorotaxane assembly was achieved at the surface of AuNPs, pointing to similarities with the binding of a drug molecule by the receptor sites on the surface of a cell (Figure 50).⁴⁹⁰ Evidence for film formation was also found in the case of AuNPs terminated by carboxylic acid groups.⁴⁹¹⁻⁴⁹³

For amide-functionalized AuNPs, IR and ¹H NMR studies revealed that intramolecular H-bonding was highly dependent on the distance of the amide from the core.⁴⁹⁴ Polyhedral oligomeric silsesquioxanes functionalized by diaminopyridines self-assembled with complementary thymines into spherical aggregates.⁴⁹⁵ IR spectroscopy and cyanide-mediated decomposition of the gold cores of amide-stabilized AuNPs showed a strong correlation between the strength of the intramolecular H-bonding and the rate of decomposition.⁴⁹⁶ Interaction of nitroxyl radicals with AuNPs, monitored by paramagnetic probes, resulted in loss of the EPR signal, due to exchange interaction of the unpaired electron with conduction band electrons of the AuNPs. Catalytic oxidation of a probe was also found when dioxygen was present.⁴⁹⁷

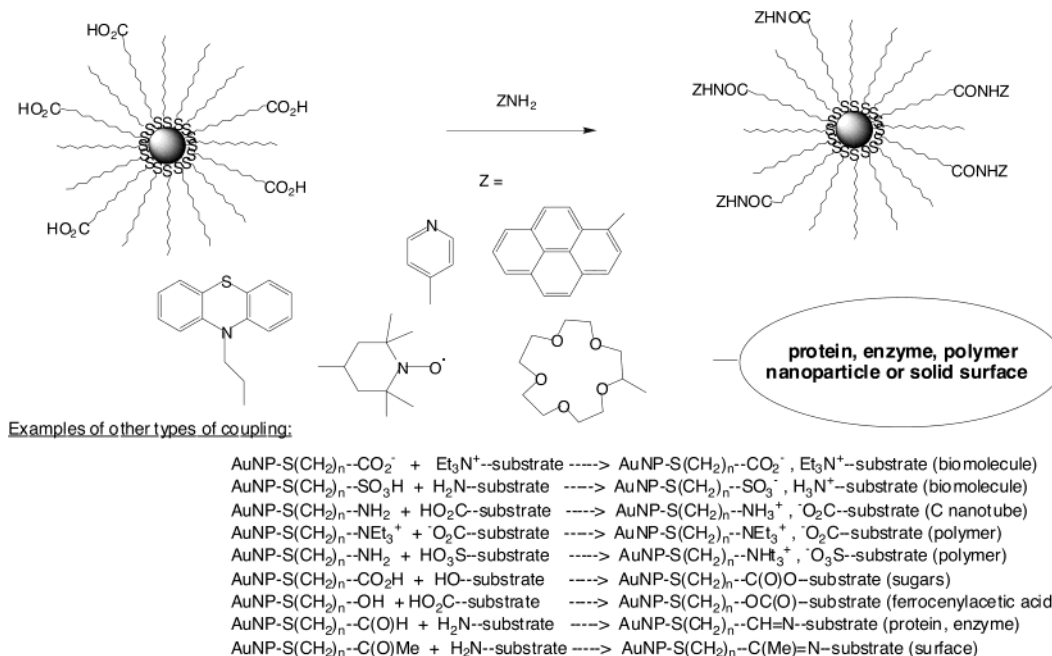


Figure 49. Examples of amide coupling reactions between AuNPs containing carboxylic acid termini and amine derivatives.

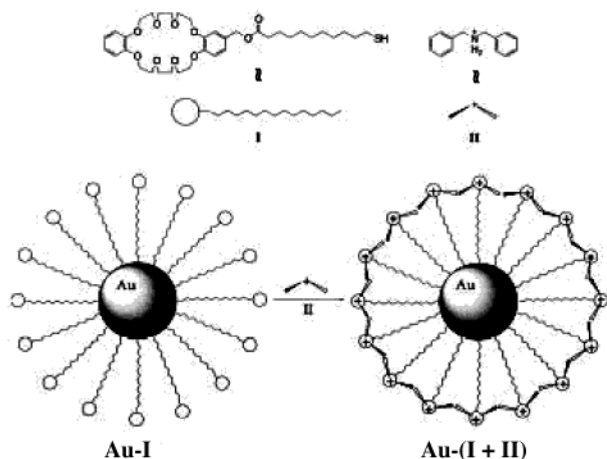


Figure 50. Programmed pseudorotaxane assembly at the surface of AuNPs by heterosupramolecular chemistry. Reprinted with permission from ref 490 (Fitzmaurice's group). Copyright 1999 Wiley-VCH.

5.3. Molecular Recognition

5.3.1. Redox Recognition Using Functionalized AuNPs as Exoreceptors

Alkanethiolate-stabilized AuNPs in which a proportion of the alkanethiolate ligands have been exchanged by amidoferrocenyl-alkanethiol recognize H_2PO_4^- and HSO_4^- as their $n\text{-Bu}_4\text{N}^+$ salts using the variation of the ferrocenyl redox potential.⁴³³ Thus, they are exo-receptors^{501a} for these anions. These salts can be titrated by cyclic voltammetry using this variation of redox potential as a function of the addition of the salt, since a one-to-one interaction occurs between each amidoferrocenyl group and the anion. The case of H_2PO_4^- corresponds to a square scheme with a strong interaction in the Echegoyen–Kaifer model, whereby a new ferrocenyl wave is

obtained upon addition of the salt.⁴⁹⁸ The difference of potential, $\Delta E^{\circ} = E^{\circ}_{\text{free}} - E^{\circ}_{\text{bound}}$, between these two waves is 220 mV and provides access to the ratio of apparent association constants between the AuNPs and the salt in the ferrocenyl (K_0) and ferrocenium (K_+) forms:

$$\Delta E^{\circ} = E^{\circ}_{\text{free}} - E^{\circ}_{\text{bound}} = 0.059 \log(K_+/K_0) = 6210 \pm 620 \quad \text{at } 25 \text{ }^{\circ}\text{C}$$

The hydrogen-bonding between the amido group and the H_2PO_4^- anion and the electrostatic attraction between the anion and the cationic ferrocenium form upon anodic oxidation are two factors partly responsible for the variation of redox potential signifying recognition.⁴⁹⁹ The addition of the salt $[n\text{-Bu}_4\text{N}^+][\text{H}_2\text{PO}_4^-]$ to a monomeric amidoferrocenyl derivative that is not connected to the AuNP provokes only a weak shift of 45 mV. Thus, an additional key factor is the topological one created by the AuNP environment, i.e. the dense thiolate ligand shell that forces the anion to penetrate into a narrow channel between the thiolate ligands. This steric factor compares with that of a nonakis-amidoferrocenyl dendrimer, but is less marked than that in an 18-amidoferrocenyl dendrimer, because the recognition process follows a positive dendritic effect in dendrimers due to the increased steric bulk at the periphery.⁵⁰⁰ AuNPs containing various proportions of amidoferrocenyl-alkanethiolates and similar ligands with various chain lengths were synthesized as well as analogues containing the pentamethylamidoferrocenyl-alkanethiolate ligand or the 1-acetyl-1'-amidoferrocenyl-alkanethiolate ligand in order to study the influence of the stereoelectronic factors on the recognition. The chain proportion and length did not show a significant influence, but the electron-withdrawing acetyl group of the amidoferrocenyl system favored the recognition, whereas the electron-releasing methyl

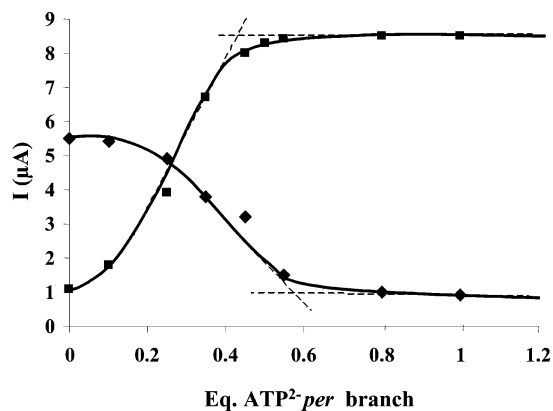


Figure 51. Titration of ATP^{2-} with ferrocenyl-dendronized AuNPs. Decrease of the intensity of the initial CV wave (♦) and increase of the intensity of the new CV wave (■) vs the number of equivalents of $[\textit{n}\text{-Bu}_4\text{N}]_2[\text{ATP}]$ added per ferrocenyl branch. Nanoparticles, 3.8×10^{-6} M in CH_2Cl_2 . Conditions: supporting electrolyte, $[\textit{n}\text{-Bu}_4\text{N}][\text{PF}_6]$ 0.1 M; reference electrode, Ag; auxiliary and working electrodes, Pt; scan rate, 0.2 V/s; solution of $[\textit{n}\text{-Bu}_4\text{N}]_2[\text{ATP}]$, 5×10^{-3} M; internal reference, FeCp_2^* . Reprinted with permission from ref 251 (Astruc's group). Copyright 2003 American Chemical Society.

substituents provided a decrease of the ΔE° values. This latter finding indicated that the most important hydrogen-bonding interaction in the chelating group was that between the negatively charged oxygen atom of the anion and the positively charged NH group of the AuNP ligand.¹⁴⁰

The case of HSO_4^- corresponds to the square scheme, with a weak interaction in the Echevoyen–Kaifer model ($K_0 \ll 1$), whereby there is no new ferrocenyl wave upon addition of the salt, but only a cathodic shift of the original wave. ΔE° is now the potential shift of this wave at the equivalence point, and its measure now gives access to the absolute value of K_+ .⁴⁹⁸

$$\Delta E^\circ = 0.059 \log [cK_+] \quad \text{at } 25^\circ \text{C}$$

This shift (30 mV) was smaller than that found in polyamidoferrocenyl dendrimers and only equal to that of a tripodal tris-amidoferrocenyl derivative, although it was larger than that in monoamidoferrocene (<10 mV). To combine the advantages of both AuNPs and dendrimers, dendronized AuNPs were synthesized with amidoferrocenyl groups or silylferrocenyl groups at the periphery. For this purpose, the direct synthetic method proved more useful than the place ligand substitution method, the latter being marred by the steric effect in this case. These ferrocenyl dendrimers with an AuNP core contained up to 360 ferrocenyl groups and were more efficient than the ferrocenyl-alkanethiolate-containing AuNPs. Positive dendritic effects were observed; i.e., AuNP-cored ferrocenyl dendrimers assembled with nonakisilylferrocenyl dendrons showed larger values than those assembled with tris-silylferrocenyl dendrons (Figures 51 and 52). In addition, one of the most interesting properties of these AuNP-cored large ferrocenyl dendrimers was their great ability to adsorb on metal surfaces. For instance, very stable platinum electrodes modified with these AuNP-cored

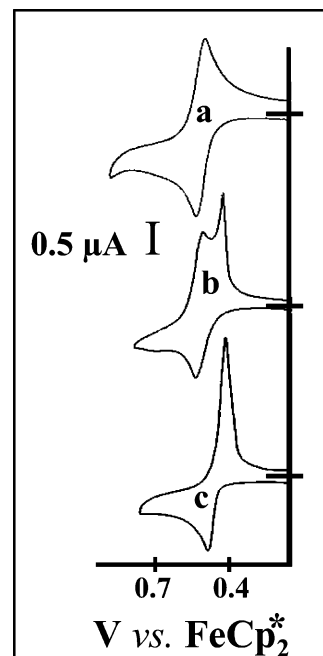


Figure 52. Titration of ATP^{2-} with dendronized AuNPs in the presence of $[\textit{n}\text{-Bu}_4\text{N}][\text{Cl}]$ and $[\textit{n}\text{-Bu}_4\text{N}][\text{HSO}_4]$ (both anions, 5×10^{-2} M, 0.5 equiv per ferrocenyl branch). Cyclic voltammograms of AuNPs (a) alone, (b) in the course of the titration, and (c) with an excess of $[\textit{n}\text{-Bu}_4\text{N}]_2[\text{ATP}]$. Reprinted with permission from ref 251 (Astruc's group). Copyright 2003 American Chemical Society.

dendrimers were prepared upon cycling the potential region around the ferrocenyl redox potential. These platinum electrodes modified with the large AuNP-cored silylferrocenyl dendrimers easily and selectively recognize the anion in a mixture of several anions, such as HSO_4^- and halides. Gratifyingly, the recognized salt could be removed by washing with methylene chloride, but the attached AuNP-cored silylferrocenyl dendrimer remained attached, and the modified electrodes could be reused many times for the recognition procedure (Figure 53).¹⁴⁰

5.3.2. Miscellaneous Recognition and Sensors

The controlled assembly of nanoparticles in solution based on supramolecular chemistry, i.e., non-covalent bonding,^{501a} is a general strategy leading to well-organized AuNP materials. Thus, approaches have been reported using hydrogen-bonding,^{501b} π - π ,^{501c} host-guest,^{501d} van der Waals,^{501e} electrostatic,^{501f} charge-transfer,^{501g} and antigen-antibody^{501h} interactions.

Amide-functionalized AuNPs were also used as optical sensors for anions.⁵⁰² AuNPs functionalized with 15-crown-5 recognize K^+ in water,^{503a} and Li^+ ^{503b} (Figure 54) and heavy metal ions^{28,504} were recognized using AuNP-based sensors. The recognition properties based on H-bonding were used to assemble AuNPs into micelles using polymers (Figure 55).⁵⁰⁵ AuNPs have also been used for vapor sensing.^{507a,b} The sensitivity of the plasmon band with the core environment is obviously a source of sensing, and the optical response (SPB) has been modeled.⁵⁰⁶ (See also the SPB section and that on biological applica-

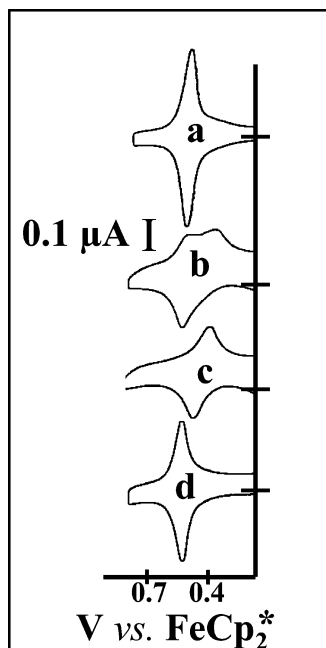


Figure 53. Recognition of ATP^{2-} with a Pt electrode modified with dendronized AuNPs. Cyclic voltammograms of dendronized AuNP-modified electrodes (a) alone, (b) in the course of the titration, (c) with an excess of $[\textit{n}\text{-Bu}_4\text{N}]_2\text{-[ATP]}$, and (d) after removal of ATP^{2-} by washing the modified electrode with CH_2Cl_2 . Reprinted with permission from ref 251 (Astruc's group). Copyright 2003 American Chemical Society.

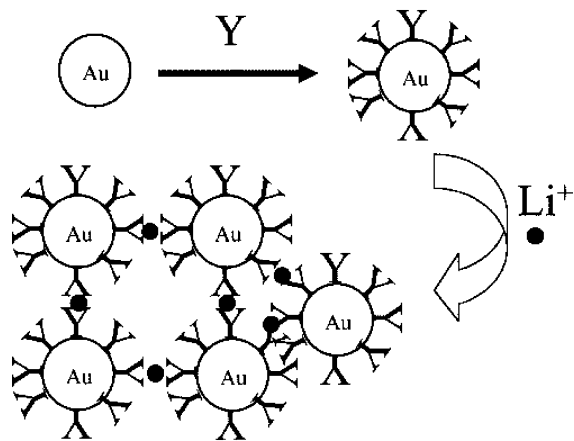


Figure 54. Detection scheme for Li^+ with functionalized AuNPs. AuNPs are surface-derivatized with a ligand Y that binds to lithium ions in a bidentate fashion. Upon introduction of lithium ion (small dark circles) into the solution, AuNP aggregation is induced, which is manifested as a visible color change in the solution. Reprinted with permission from ref 503b (Murphy's group). Copyright 2002 American Chemical Society.

tions, in particular the color sensitivity of the AuNP–DNA assemblies.) Electrochemical genosensors for the detection of the Factor V Leiden mutation from polymerase chain reaction amplicons using the oxidation signal of AuNPs at +1.20 V were described.^{507c} DNA–AuNP assemblies, which are discussed in the next section, have also been used as colorimetric lead biosensors.^{507d} *N*-Methylimidazole-functionalized AuNPs were reported to recognize bis- and tris-Zn-porphyrins.^{507e}

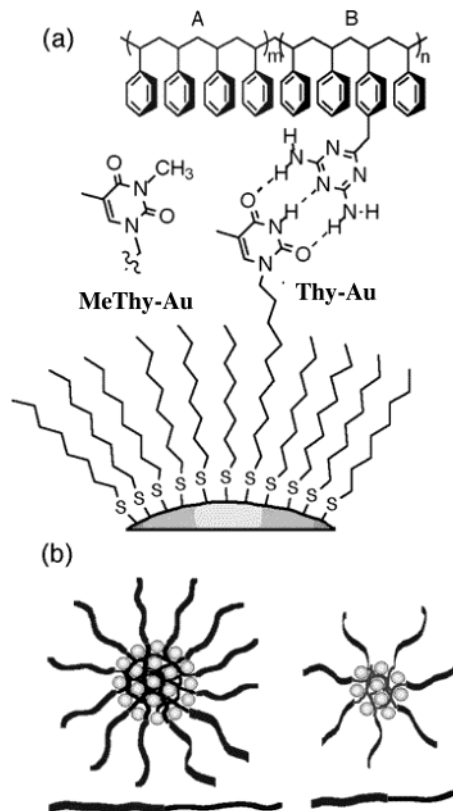


Figure 55. (a) Diblock copolymers 1–3, Thy-Au, and non-hydrogen-bonding control MeThy-Au. (b) Scheme demonstrating an increase in both core diameter and outer corona as the polymer size increases. Reprinted with permission from ref 505 (Rotello's group). Copyright 2002 American Chemical Society.

6. Biology

6.1. DNA–AuNPs Assemblies and Sensors

Conjugates of AuNPs–oligonucleotides are of great current interest because of the potential use of the programmability of DNA base-pairing to organize nanocrystals in space and the multiple ways of providing a signature for the detection of precise DNA sequences. Applications in the fields of biosensors, disease diagnosis, and gene expression are clearly called for. The two groups of Mirkin–Letsinger at Northwestern^{508–516} and Alivisatos–Schultz at Berkeley⁴⁷³ have pioneered strategies for the organization of functionalization of AuNPs with oligonucleotides. The former group used DNA as a linker to form macroscopic assemblies consisting in discrete 13-nm-diameter particles. The DNA attached to the nanoparticles retained its ability to hybridize with complementary DNA, and the annealing process was thermally reversible and nondestructive. The reaction was sequence-specific (Figure 56).⁵⁰⁹ The latter group used DNA as a template to prepare nanocrystal molecules consisting of two or three 1.4-nm-diameter particles on a single oligonucleotide strand.⁴⁷³ DNA-driven assemblies of AuNPs have indeed attracted considerable interest,^{510–536} and a new colorimetric technique based on the sensitivity of the SPB to monitor DNA modification was designed by the Mirkin–Letsinger group.^{508–517} In this strategy, AuNPs are used as building blocks, allowing the assembly of alkanethiol-capped oligonucleotides

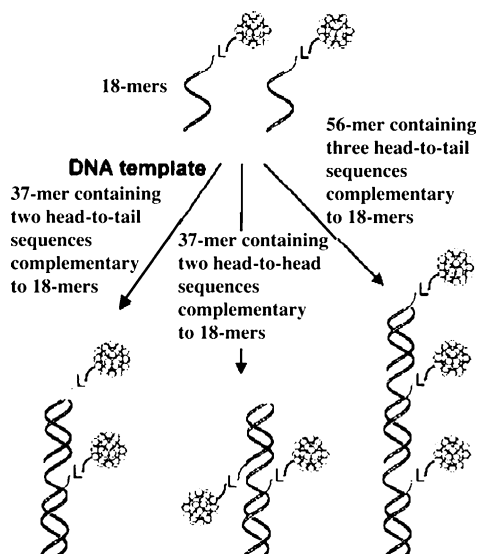


Figure 56. Preparation of “nanocrystal molecules” consisting of two or three DNA modified Au particles attached to a complementary DNA template, using phosphine-stabilized 1.40 nm AuNPs modified with a single thiol-capped oligonucleotide and two different DNA template lengths and sequences. Reprinted with permission from ref 509 (Mirkin’s group). Copyright 1997 Kluwer.

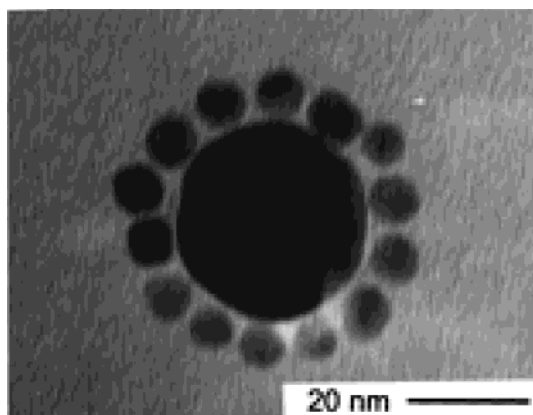


Figure 57. TEM images of the binary AuNPs network materials supported on holey carbon grids: a AuNP satellite structure obtained from the reaction involving 120/1 1-modified 8-nm particles/2-modified 31-nm AuNPs and linking oligonucleotide. Reprinted with permission from ref 511b (Mirkin’s group). Copyright 1998 American Chemical Society.

such as single-stranded DNA and complementary linker oligonucleotide (DNA) strands (Figure 57).

Aggregation of AuNPs linked by the oligonucleotides provokes a red-to-blue color change (red shift from 520 to 600 nm of the SPB) that is most useful for this DNA-sensing method. The parameters that are controlled are the AuNP composition, the periodicity, and the aggregate thermal stability. These parameters are organized in order to influence the optical, mechanical, and electrical properties of the AuNPs. In particular, the optical properties due to the SPB of AuNPs from 13 to 17 nm diameter led to the development of a highly selective diagnostic method for DNA, based on the distance-related SPB of AuNPs (Figure 58). The effect of the length of the DNA strands that control the interparticle distance was studied, and it was found that the SPB frequency

changes are inversely dependent on the oligonucleotide linker length (between 24 and 72 base pairs, i.e., from 80 to 24 Å). An interesting result was that the most important parameter that controls the SPB shift of these AuNPs–DNA materials is the aggregate size. This aggregate size is under kinetic control, and it is the growth rate that depends on the linker length. Annealing of the kinetic structures formed at temperatures just below their melting points lead to a SPB shift. This growth, leading to the red shift of the SPB, occurs through an Oswald ripening mechanism whereby larger aggregates grow at the expense of smaller ones.

Electrodynamics modeling contributes to show that these SPB shifts are much more consistent with changes in aggregate size than with interparticle distance. Thus, DNA linkers could be more useful as kinetic controllers of aggregate growth than as spacer units, a valuable indication for the development of quantitative assays for DNA.⁵¹⁵

Another important characteristic of the AuNP-based pair detection is the “melting” transition of the complementary DNA strand. The AuNPs are linked in the presence of the complementary strand. These H-bonded connections of the links are broken at sufficiently high temperatures, which unzips the oligonucleotides, “melting” the DNA and releasing the particles.⁵¹³ Calculations using AuNP polarizabilities determined from Mie theory, an iterative conjugate-gradient solution algorithm, and fast Fourier transform methods for efficient solution of the electrostatics of interacting AuNP equations show that the UV extinction lowering and the shift and broadening of the SPB of the DNA-linked AuNPs are explained as the collective electromagnetic response of thousands of AuNPs.⁵¹⁰

Supramolecular aggregates were shown to form by self-assembly of DNA–streptavidin adducts.⁵¹⁹ Heterologous chemical systems including DNA have been scaffolded into precise 2D geometrical arrangements.⁵²⁴ The conformation of oligonucleotides attached to AuNPs has been probed by the electrophoretic mobility determined on 2% agarose gels, and the effective diameter of the DNA–AuNP conjugates has been determined (Figure 59).⁵²⁵

Multiple thiolate and phosphine anchors improved the AuNP–nucleotide stability.^{529,530} DNA was coated with cationic, metastable AuNPs.⁵³⁷ Several reports indeed showed the efficacy of electrostatic AuNP–DNA assembly,^{537–539} including for the fabrication of linear superstructures.⁵³⁸ Interestingly, however, DNA also wraps around negatively charged AuNP cores.⁵³⁰ Ring aggregation of AuNPs can be induced by DNA hybridization even without cross linking.^{539c}

DNA–nucleotides and AuNP–DNA nanostructures were analyzed using electrochemical techniques,^{540–546} including scanning electrochemical microscopy.^{544a} Imaging of DNA–AuNPs assemblies by TEM, AFM, and near-field scanning optical microscopy was provided.^{544b} Other techniques used were SPB (Figure 60),^{510–514} luminescence,⁴²⁰ Fourier transform infrared and Raman spectroscopy,^{533,540} surface-enhanced Raman spectroscopy,⁵⁴⁷ labeling and scanning force microscopy,^{533,548} differential light-

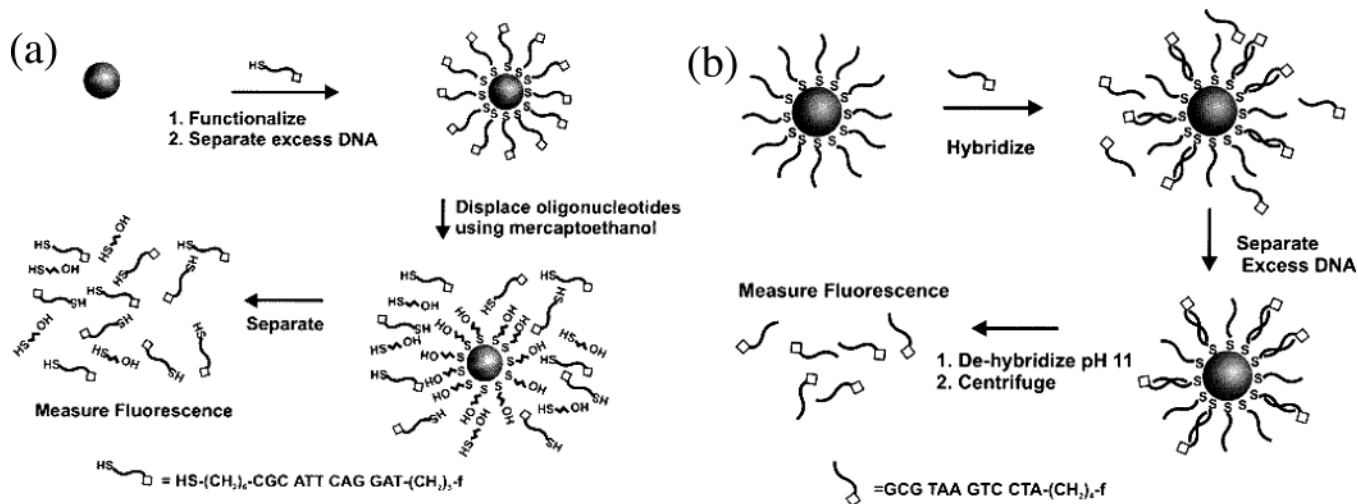


Figure 58. Fluorescence-based method for determining (a) the surface coverage and (b) the hybridization efficiency of thiol-capped oligonucleotides bound to gold thin films and AuNPs. Reprinted with permission from ref 516 (Mirkin's group). Copyright 2000 American Chemical Society.

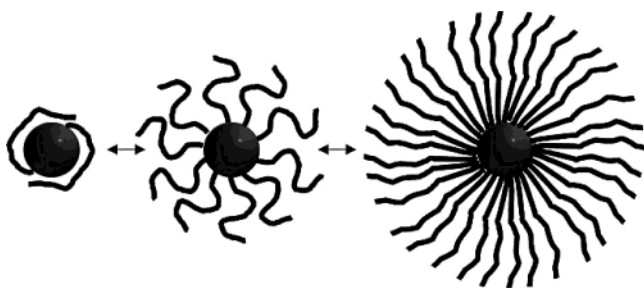


Figure 59. Different possible configurations of DNA molecules attached to the surface of AuNPs. Reprinted with permission from ref 525 (Alivisatos's group). Copyright 2003 American Chemical Society.

scattering spectroscopy,^{549a} and quartz-crystal microbalance (QCM).^{535,536,549} The latter technique was shown to be especially useful for the design of new DNA sensors^{535,536} involving dendritic amplification of DNA analysis.⁵³⁶ Using 50-nm-diameter AuNPs, with QCM it was also possible to reach a sensitivity of 10^{-14} M of DNA analyte, a fragment of P 53 gene near codon 248 which has significance in cancer diagnosis.⁵³⁵ Microcantilevers were used to detect DNA strands with a specific sequence using AuNP-modified DNA. This method is analogous to QCM in the vibration-working mode, but it has various advantages over QCM.^{549b} When the size of the AuNPs is 50 nm, a sensitivity of 10^{-15} M for single-base mutation detection has been achieved with this method.^{549c} Dry-reagent strip-type biosensors based on AuNP-DNA interaction enabled visual detection within minutes, and quantitative data were obtained by densitometric analysis.^{549d} AuNP-streptavidin conjugates covered with 6-ferrocenylhexanethiol were attached onto a biotinylated DNA detection probe of a sandwich DNA complex, and the amplified voltammetric signal was recorded. A detection level down to 2.0 pM for oligonucleotide was obtained.^{549e} Single-stranded and double-stranded DNA were shown by electrophoresis and fluorescence to bind nonspecifically to the AuNP surface, despite their negative charge.^{549f} Nonspecific binding of biological molecules

can be eliminated, however, using ethylene glycol core protection.^{549g}

6.2. AuNP-Enhanced Immuno-Sensing

Immunolabeling with AuNPs and imaging of cells, biomolecules, and other biological components have been extensively reviewed in the book edited by Hayat in 1989,¹⁴ and this area continues to attract the attention of biochemists and biophysicists.⁵⁵⁵ The recognition of proteins has been for some time the subject of research of biodevices for diagnostics based on the interaction between AuNP-antibody conjugates and their antigens.¹⁴ Only recent progress is reviewed here. The great sensitivity of the SPB by AuNP adsorption led to their use in bioassay applications. The investigated AuNP-protein conjugate architectures involve either direct binding of antigen: AuNP-bioconjugate to an antibody-modified surface or the exposure of an antibody-derived surface to free antigen and then to a secondary antibody-AuNP conjugate. This classic type of immunoassay allows the evaluation of AuNP tags in a standard mode of antigen detection.⁵⁵⁰⁻⁵⁵² Biosensors for immunoassays in human serum have been developed.^{553,554}

6.3. AuNP Sugar Sensors

AuNPs coupled with biomolecules are attracting increasing attention because of the potential applications of these new materials in biology-related challenges.^{555,556} Mannose-encapsulated AuNPs have been shown by TEM to specifically bind FimH adhesin of bacterial type 1 pili in *Escherichia coli*, and to do so more strongly than free mannose in the competition assay. This process represents a new method of labeling specific proteins on the cell surface using carbohydrate-conjugated AuNPs, whereby the visualization of the target receptor on the cell surface is relatively easy under an electron microscope.⁵⁵ AuNPs functionalized with a monolayer of 11-thioacetate-undecanol-derivatized neoglycoconjugates of lactose disaccharide and trisaccharide antigens can be used to mimic glycopospholipid clusters in plasma

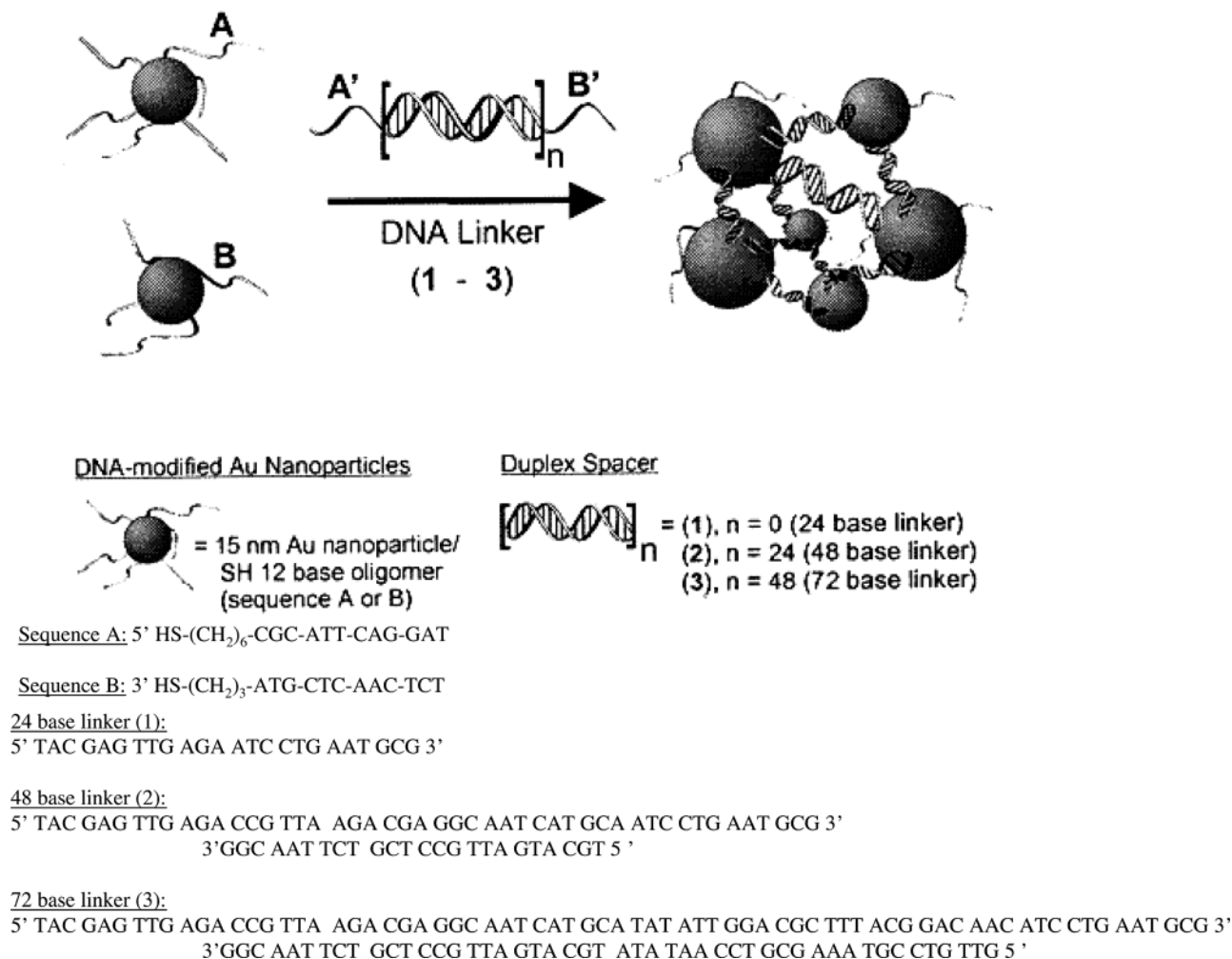


Figure 60. Control of the optical properties of DNA-linked AuNPs assemblies by modulating the length of the DNA linker molecule (1, 2, 3) and the thiol 12 base oligomer (A and B) one. Reprinted with permission from ref 514 (Mirkin's group). Copyright 2000 American Chemical Society.

membranes in order to investigate a new mechanism of cell adhesion through carbohydrate-carbohydrate interactions.^{558,559} Spontaneous formation of AuNPs was observed in aqueous solutions of sugar-persubstituted PAMAM dendrimers without the addition of any additional reductant.⁵⁶⁰ AuNPs coated with haptenated mercaptodextrans containing 15 mercapto groups bind specifically to paramagnetic beads coated with the corresponding antibody.^{561a} A mannose derivative has been self-assembled onto preformed, citrate-capped water-soluble AuNPs, and, through the use of a C₂ tether, a rapid colorimetric detection test has been developed for the protein canavalinin A.^{561b} Multivalent interactions of glycono-AuNPs containing galactosyl and glucosyl headgroups with the HIV-associated recombinant glycoprotein gp 120 have been studied.^{561c}

6.4. Other AuNP Bioconjugates: Peptides, Lipids, Enzymes, Drugs, and Viruses

Phospholipids were used for the formation of AuNPs,⁵⁶³⁻⁵⁶⁵ in particular as dispersants in the preparation of AuNPs.⁵⁶² Helically patterned arrays of AuNPs were formed using lipid tubules as templates.⁵⁶³ The assembly of relatively short polypeptides on a template can provide protein-like complex

structures and properties, especially in conjugates with AuNPs.^{566,567} Water-soluble AuNPs based on thiopronin have been prepared.^{568,569} Other Au-NP-based receptors providing H-bonds recognize flavin.^{570,571} Ligand design optimizes bioconjugation in various AuNPs frameworks.⁵⁷²⁻⁵⁷⁶ Enzymatic activity of fungal protease-AuNP bioconjugates was reported⁵⁷⁷ as well as a method to construct a third-generation horseradish peroxidase biosensor by self-assembling AuNPs.⁵⁷⁸ Phthalocyanine-stabilized AuNPs were shown to be a potential delivery vehicle for photodynamic therapy.⁵⁷⁹ The biochemical preparation of AuNPs was reported whereby the biological organisms played the roles of reductant, protecting agent, and precipitating agent.^{175b,580-582} AuNPs bound on APTMS-functionalized Na-Y zeolite could be used for the immobilization of pepsin, whose catalytic activity in the bioconjugate was comparable to that of the free enzyme.^{583a} Assembly of AuNPs on polyurethane spheres could be used to immobilize enzymes such as pepsin; these bioconjugate catalysts can also be reused as free enzymes.^{583b} Raleigh resonance spectroscopy was reported on single bromo mosaic virus capsids (28 nm) with AuNPs (2.5-4.5 nm) inside.^{583c}

Control over the morphology of ceramic crystals by biomimetic processes is of increasing interest. For instance, large changes in the morphology of barite crystals occur on templates of varying dimensionality.^{584a} In a strategy aimed at nuclear targeting in biological systems mimicking viruses, the most capable peptides were combined on a 20-nm bovine serum albumin–AuNP platform, and the trajectories inside cells of these assemblies were monitored using a combination of video-enhanced color microscopy and differential interference contrast microscopy.^{584b}

6.5. AuNP Biosynthesis

Macroscopic quantities of microorganisms such as fungi could be used as living templates with AuNPs to organize presynthesized nanoscale components into ordered structures.^{584c} Reaction of AuCl_4^- ions with the extract of geranium leaves and an endophytic fungus, *Colletotrichum* sp., present in the leaves, leads to the formation of AuNPs.^{584d}

7. Catalysis

Gold is very popular for being chemically inert. It is indeed one of the most stable metals in the group 8 elements, and it is resistant to oxidation. In the 1970s, however, Parravano's group reported the investigation of the activity of gold in oxygen/hydrogen-transfer reactions^{585,586} and the reduction of NO by dihydrogen,⁵⁸⁷ but these studies remained isolated. Therefore, the discovery by Haruta et al., reported in 1989, that AuNPs supported on Co_3O_4 , Fe_2O_3 , or TiO_2 were highly active catalysts, under high dispersion, for CO and H_2 oxidation,^{588,589} NO reduction,⁵⁹⁰ water–gas shift reaction,⁵⁹¹ CO_2 hydrogenation,⁵⁹² and catalytic combustion of methanol⁵⁹³ was a surprise, and was considered important by the chemical community. Catalysis with AuNPs, in particular the very active oxide-supported ones, is now an expanding area, and a large number of new catalytic systems for various reactions are now being explored.

7.1. Catalysis of CO Oxidation

Most of the recent research on the catalytic activity of oxide-supported AuNPs concerned CO oxidation.^{588–621} In particular, the mechanism of the catalytic process was actively investigated, and particle size effects and metal/support interactions were examined. The gold cluster $[\text{Au}_9(\text{PPh}_3)_8(\text{NO}_3)_3]$ was highly dispersed by impregnating Mn, Fe, Co, Ni, Cu, or Cu hydroxide with a solution of this cluster, and activity in CO oxidation was found even at subambient temperatures (below 0 °C and even at –70 °C).⁵⁹⁵ Further studies on the AuNP/ $\text{Fe}(\text{OH})_3$ system showed that the catalytic activity was extremely high after calcination, which was ascribed to the stabilization of $[\text{Au}(\text{PPh}_3)]^+$, leading to small particles.⁵⁹⁶ Alternatively, it was suggested that the catalytic activity was due to the presence of ferrihydrate activating O_2 ,⁵⁹⁷ and Au^+ species were found to be more active than Au^0 particles.⁵⁹⁸ Small AuNPs were stabilized by insertion into zeolite supercages, and ^{129}Xe and DRIF studies showed the presence of $\text{Au}^{\delta+}$ species,⁵⁹⁹ which were found to be highly active.^{599,600}

With AuNPs impregnated on $\text{Mg}(\text{OH})_2$, it was indicated that, below 1 nm diameter, AuNPs have icosahedral symmetry, whereas above 1 nm, the AuNPs are in face-centered cubic cuboctahedral symmetry. This showed that the geometrical factor is also important in catalytic activity.⁶⁰¹ New methods for preparation of AuNPs for catalytic oxidation of CO include arc melting, chemical vapor deposition, co-sputtering,⁶⁰² and pulsed laser deposition (PLD).⁶⁰³ The exceptionally high catalytic activity of the AuNPs deposited onto Fe_2O_3 , Co_2O_3 , and TiO_2 ^{604–607} supports was interpreted in terms of the formation of an active AuNP/support interface along the perimeter of AuNPs.^{608,609} The morphology, electronic structure, and catalytic activity in CO oxidation over a $\text{Au}/\text{FeO}_x/\text{SiO}_2/\text{Si}(100)$ model sample prepared by PLD have been investigated by X-ray photoelectron spectroscopy and TEM, which showed that activity in CO oxidation increased after oxidation, the higher activity being associated with amorphous iron oxide with Fe 2p binding energy = 711.3 eV.^{610–613} The intrinsic catalytic activity of the AuNPs was shown to increase with decreasing particle size. When an Au/FeO_x interface was created by FeO_x deposition on large AuNPs, a significant increase in the rate of the CO oxidation was observed, and these data correlate the catalytic activity with the valence bond density of states of the AuNPs.⁶¹⁴ Spherical aberration-free phase image analysis showed that catalytically active AuNPs form single crystals having a cuboctahedral shape, and that the atomic structure on the surface and interface is largely deformed from the bulk structure by stress produced by the atom-missing structure, the reconstructed structure surface, and strong interaction with the substrate.⁶¹⁵ It has been suggested that a synergistic mechanism occurs at the AuNP–metal oxide interface, with the oxide support being part of the catalytic process. Adsorption of CO would proceed on the AuNP on a site adjacent to a metal oxide site occupied by an adsorbed O_2 molecule. The reaction would involve an intermediate carbonate-like species decomposing to CO_2 upon desorption from the surface.⁵⁹³ AuNP– FeO_x catalysts, prepared by coprecipitation, containing ferrihydrite, a structurally disordered material with approximate composition $\text{Fe}_5\text{HO}_8 \cdot 4\text{H}_2\text{O}$, and a noncrystalline phase $\text{AuOOH} \cdot x\text{H}_2\text{O}$, showed 100% conversion after 20 min at room temperature.⁶¹⁶ AuNPs prepared by chemical vapor deposition (CVD) of dimethyl gold acetylacetonate are active catalysts for CO oxidation below 0 °C.⁶¹⁷ Extensively varying the conditions of preparation of AuNP– MO_x catalysts (M = Si, Ti, Zr, Al) of 1–6 nm size, followed by characterization using TEM, XPS, and EPR, made it possible to investigate the structure–reactivity of the catalysts.⁶¹⁸ AuNPs supported on a TiO_2 surface by calcination first at 500 °C under vacuum and then at 400 °C in air showed low-temperature activity on CO oxidation (Figure 61).⁶²¹ The size of the most active AuNPs was determined by low-frequency Raman modes, providing a signal at $11 \pm 1 \text{ cm}^{-1}$ that corresponded to a particle diameter of $8 \pm 1 \text{ nm}$, and combination of this technique with microscopy techniques gave information on size distribution and structural 3D

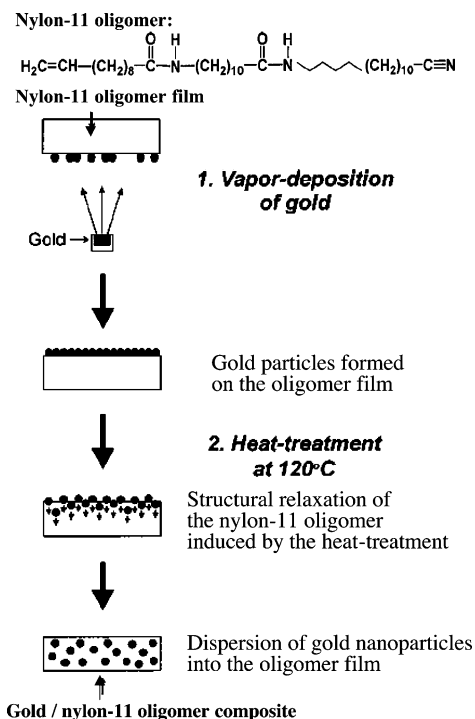
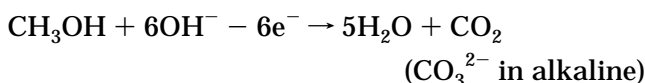
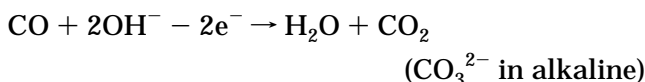


Figure 61. Novel method of preparation of a AuNP catalyst supported on TiO_2 . Reprinted with permission from ref 621 (Sayo's group). Copyright 1999 Elsevier.

arrangement.⁶²² DFT calculation for O_2 chemisorption showed a typical binding energy of 0.5–1.5 eV, increasing for negatively charged clusters.⁶²³

7.2. Electrochemical Redox Catalysis of CO and CH_3OH Oxidation and O_2 Reduction

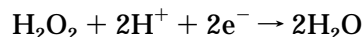
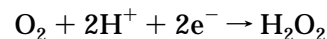
The electrooxidation of CO⁶²⁴ and CH_3OH ,^{126,625,626} both leading to CO_2 (CO_3^{2-} in alkaline medium), i.e.,



has been reported using alkanethiolate–AuNPs that were precipitated onto a glassy carbon electrode by cross-linking the AuNPs with 9-nonanedithiol, leading to a 3D network thin film. The electrocatalytic processes were shown by cyclic voltammetry. A wave observed at +50 mV on the negative sweeping in the presence of CO was characteristic of CO oxidation, whereas a wave observed at +250 mV in the presence of MeOH was characteristic of MeOH oxidation. The oxidation current was found to increase with concentration of CO or MeOH, observed only after a potential polarization around +800 mV that provoked catalytic activation. This activation was confirmed by matching the oxidation potential with that of Au oxide formation, and by quartz-crystal microbalance, infrared reflection spectroscopy, and AFM experiments.^{627a} This electrocatalytic CO oxidation was also demonstrated using AuNPs synthesized by block copolymer micelle encapsulation, whereby the dip-coating method of synthesis produced a highly dis-

perse, quasi-regular array of AuNPs (diameter 4.8 ± 1.3 nm).^{627b}

AuNPs electrodeposited on a gold electrode by applying a 5-s potential step from 1.1 to 0 V with a 0.5 M H_2SO_4 solution containing 0.11 mM $\text{Na}[\text{AuCl}_4]$ were shown to be very active catalysts for the reduction of O_2 . Two electrocatalytic reduction waves recorded at +50 and –250 mV indicated a two-step, four-electron reduction path of O_2 .^{628a}



AuNPs deposited on boron-doped diamond with an average diameter of 60 nm were shown to be 20 times more active than polycrystalline gold for the electrocatalytic O_2 reduction.^{628a}

7.3. Catalysis of Hydrogenation of Unsaturated Substrates

More recent investigations have shown that AuNPs that were adsorbed and dispersed on oxide support by reduction of AuCl_4^- or AuCl_3 , and then calcinated, were also efficient catalysts for other reactions, including hydrogenation of unsaturated substrates. For instance, such AuNPs of 1–5 nm diameter, supported on titania or zirconia, were active in the regioselective hydrogenation of acrolein to allylic alcohol at 180–280 °C (total pressure, 2 MPa), a particularly difficult reaction. Following TEM and EPR studies, it was suggested that the origin of the selectivity of C=O vs C=C hydrogenation might be attributed to quantum size effects that alter the electronic properties of sufficiently small AuNPs.^{629–631} Active sites were identified as edges.⁶³¹ AuNPs were prepared by dispersion on an amorphous silica support, wherein silanol groups of the surface of fumed silica spontaneously reduced AuCl_4^- ions. These supported AuNPs were found to be catalytically active in the hydrogenation of cyclohexene at 80 °C and 200 psi H_2 .⁶³² PVP-stabilized Au/Pd bimetallic nanoparticles²⁰¹ showed high activity for the hydrogenation of cycloocta-1,3-diene (COD), with 100% selectivity for cyclooctene formation. The high activity was ascribed to electronic deficiency of the active surface Pd atoms (required for π back-donation from the coordinated olefin) due to electron transfer to the gold atoms (Figure 62).^{26,180} Reduction of eosin by NaBH_4 at 29 °C was catalyzed by AuNPs of 10–46 nm diameter, prepared by a seed-mediated growth method, and the reaction rates were shown to increase both above and below 15 nm diameter.⁶³³

7.4. Catalysis by Functional Thiolate-Stabilized AuNPs

Since imidazoles play a key role as catalysts in many hydrolytic systems, *N*-imidazole-functionalized thiolate–AuNPs were investigated as catalysts, in 6:4 methanol–water solution, for the cleavage of 2,4-dinitrophenyl acetate with more than an order-of-magnitude rate acceleration with respect to acetyl-*N*-methylhistamine.⁴⁷⁰ A thiol terminated with a

Polymer-Protected Au/Pd Bimetallic Clusters

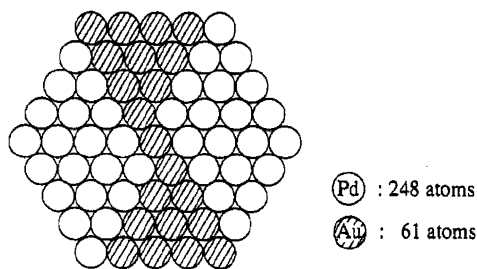


Figure 62. Cross section of a model for Au/Pt (1/4) AuNPs catalytically active for hydrogenation reaction, prepared by a successive (Pt then Au) reduction. Reprinted with permission from ref 196b (Toshima's group). Copyright 1993 American Chemical Society.

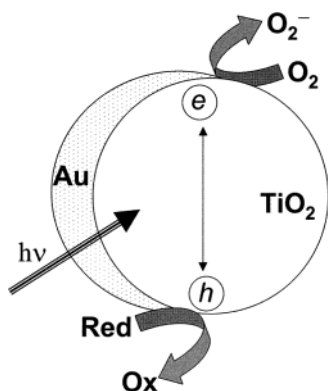


Figure 63. Interfacial charge-transfer processes in a metal-semiconductor nanoparticle. Reprinted with permission from ref 461b (Kamat's group). Copyright 2001 American Chemical Society.

hexadiene functionality was coordinated to alkanethiolate-AuNPs and to RuCl_3 , and the functional AuNPs catalyzed the heterogeneous polymerization of norbornene. The FTIR spectra are consistent with the presence of Cl-bridged dimeric Ru catalytic species.⁶³⁴

7.5. Other Types of Catalysis

AuNPs supported on highly hydrophobic ethane-bridged Ti-incorporated mesoporous organosilica catalyzed vapor-phase epoxidation of propene using H_2 and O_2 at 90–120 °C.⁶³⁵ Clear red-gold microemulsions of $\text{Na}[\text{AuCl}_4]$ and NaBH_4 supported on activated carbon were active catalysts for the oxidation of glycol to glycolate by O_2 ,⁸² although Au/C catalysts of comparable medium-size particles show higher conversion.^{636,637} Semiconductor/AuNP composites synthesized by reducing HAuCl_4 on the surface of preformed TiO_2 nanoparticles of 10–40 nm diameter were grown by laser-induced melting/fusion, and the particles modified by this treatment were shown to undergo photocatalytic charge transfer, probed using thiocyanate oxidation at the semiconductor interface (Figure 63).⁴⁶¹ Miscellaneous catalytic applications involve lithography,⁶³⁸ synthesis of onions,^{639a} combustion,^{639b} and the reaction between CS_2 and NaBH_4 .^{69b} AuNPs-dendrimer composites prepared by laser irradiation were shown to catalyze the reduction of 4-nitrophenol by NaBH_4 at rates de-

pending on the dendrimer structure (PPI more efficient than PAMAM).⁶⁴⁰

8. Nonlinear Optics (NLO)

Glasses, polymers, and other shell materials with NLO properties are becoming viable alternatives to the expensive inorganic crystals LiNbO_3 , KH_2PO_4 , and BaB_2O_4 to change the wavelength of laser light through parametric processes. Indeed, the latter crystals are also cumbersome to tailor into the waveguide configurations that are compatible with optical fiber systems. Besides organic chromophores, nanoparticles including AuNPs represent a very important category of NLO dopants.

The nonlinear response of glasses containing metal nanoparticles is dominated by two relaxation processes:⁶⁴¹ (i) a fast relaxation process due to electron-phonon coupling, leading to thermal equilibrium between the electron and lattice in a metal nanoparticle system after excitation of the hot electron by the incident pulse, and (ii) a slow relaxation process due to thermal diffusion of the excess heat from metal nanoparticles to the matrix.

AuNPs have a large third-order nonlinear susceptibility and a near-resonance nonlinear response⁶⁴² that is fast on the 50-ps time scale, and glass with dispersed AuNPs is therefore a candidate material for use in nonlinear optical devices.⁶⁴³ Their production requires the dispersion of a large amount of AuNPs. Although the AuNP concentration is low in glasses prepared by conventional methods due to the vaporization and low solubility of raw materials, a large amount of AuNPs can be dispersed in matrices by ion implantation, because this technique is free of these restrictions.⁶⁴⁴ Glass produced by ion implantation has a large third-order nonlinear optical susceptibility ($\chi^{(3)} = 1.2 \times 10^{-7}$ esu).⁶⁴⁵ In glass with dispersed AuNPs, the growth of AuNPs leads to an increase in third-order optical susceptibility and concurrently an increase in absorption coefficient.⁶⁴⁴ For practical applications, it is desirable to have a low absorption coefficient and a large third-order optical susceptibility. With silica glass in which AuNPs were synthesized by ion implantation, AuNPs were found to grow through an Ostwald ripening mechanism controlled by diffusion in the silica glass.^{645,646} The third-order nonlinear optical susceptibility, $\chi^{(3)}$, of this glass was found to be proportional to the fourth power of the radius of the colloid particles or the fourth power of the absorption coefficient at the peak of the SPB when the total volume of the AuNPs was constant. $\chi^{(3)}$ was also inversely proportional to the third power of the total volume of AuNPs when the absorption coefficient of the SPB was constant.⁶⁴⁶ Crystallization effects were found to influence the NLO response of transparent glass-ceramics with AuNP nuclei. The temporal absorption change at the SPB showed that the fast component of the relaxation process was hardly changed with crystallization, while the relaxation time of the tail component decreased with an increase in crystallite size.⁶⁴⁷ The relaxation time was also found to increase with a decrease of the AuNP radius, and the tail of the decay curve due to the slow

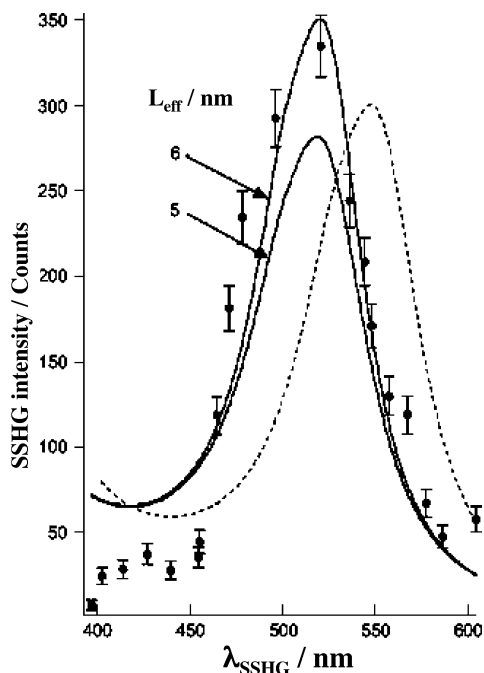


Figure 64. SSHG spectrum for the underivatized AuNPs at the air/toluene interface (circles). The adsorption band corresponds to surface plasmon excitations and has a maximum at 520 nm. The solid line represents the calculated SSHG spectrum for AuNPs in toluene, taking size effects into account ($L_{\text{eff}} = 6$ and 5 nm). The solid line is for $\lambda_p = 138.5$ nm, corresponding to bulk gold; the dotted line is for a material with a free electron concentration 10% lower than that of bulk gold, for $\lambda_p' = 146$ nm and $v_f' = 1.342 \times 10^6 \text{ ms}^{-1}$ (and $L_{\text{eff}} = 6$ nm). Reprinted with permission from ref 652 (Schiffrin's group). Copyright 1997 The Royal Society of Chemistry.

relaxation component increased with an increase of the AuNP size.⁶⁴⁸ Dielectric periodic structures in which some frequencies of light cannot penetrate because photon modes at these frequencies do not exist in the structure were called photonic crystals. In such photonic crystals with AuNPs dispersed in layers as a defect structure, the defect mode shift could be attributed to the Kerr effect inside the defect structure. NLO effects were found in these photonic crystals.⁶⁴⁹

Although glass–AuNPs have attracted the most attention, other AuNP materials with interesting NLO properties are also known in which the AuNPs are in suspension⁶⁵⁰ or embedded in other supports, such as pores of mesoporous silica,¹¹² polymer matrices,⁶⁵¹ and thiolate ligand shells.^{652–656} Indeed, second-order NLO activity for liquid dispersion of AuNPs has been disclosed.^{657,658} AuNPs in polydiacetylenes induce an enhancement of the third-order susceptibility, $\chi^{(3)}$, by 2 orders of magnitude in comparison with that of the polymer alone.⁶⁵⁹ In addition, hyper-Raleigh scattering (HRS) has been used to study the NLO response of AuNP suspensions,⁶⁵⁰ and molecularly bridged thiolate–AuNPs showed very large responses. Both symmetry and distance were found to be key factors in determining NLO behavior.⁶⁵³ NLO-active chromophores have also been anchored onto AuNPs in order to combine the NLO properties of both the core and ligand components of thiolate-stabilized AuNPs.⁶⁵¹ Surface second harmonic generation (SSHG) was used as a new technique, sensitive to resonant plasmon excitation, to characterize AuNPs at the air/toluene interface. Wavelength analysis of these thiolate-stabilized AuNPs indicated the narrow frequency band of the AuNP surface plasmon (Figure 64).⁶⁵² NLO properties of C₆₀-containing nitrogen ligands bound to AuNPs were investigated, and optical limiting effects were measured for 8 ns at 532 nm. The NLO properties of these composites, investigated by the Z-scan technique, could be attributed to the strong excited-state absorption of the ligands and the SP resonance of the AuNPs. The main absorptive mechanisms are the nonlinear absorption and the absorption-induced nonlinear scattering. The stronger nonlinear refractions enhance further the refractive optical linear effects (Figure 65).^{654–656}

9. Miscellaneous Applications

AuNPs have been used to manipulate the selectivity between solutes in capillary electrophoresis. Therefore, the AuNPs serve as large surface area platforms for organofunctional groups that interact with the capillary surface, the analytes, or both. The apparent mobilities of target analytes as well as the electro-

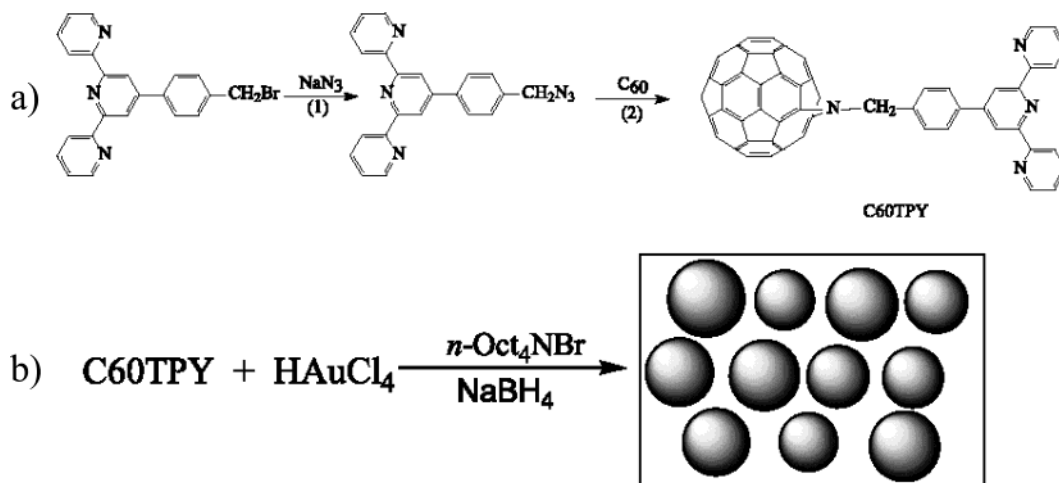


Figure 65. Synthetic routes leading to (a) a [60]fullerene-substituted oligopyridine and (b) the AuNPs stabilized by it. Reprinted with permission from ref 656 (Li's group). Copyright 2002 Elsevier.

osmotic flow could be altered, which led to enhanced selectivities.⁶⁶⁰ The use of AuNPs has also been extended to chip-based capillary electrophoresis devices, the AuNPs in the microchannels acting as a rectifier.⁶⁶¹ Electromagnetic coupling effects with lithographically produced AuNPs were investigated by photon scanning tunneling microscopy. The surface plasmon propagation on microstructured metal thin films was examined in order to provide an interface between the nano-optical device and classical far-field optics.⁶⁶²

The optical manipulation of particles on waveguide surfaces offers a controllable tool for application to particle sorting, sensing, and atomic mirrors. In this context, potassium-ion-exchanged optical waveguides in glass for evanescent field propulsion of AuNPs were optimized.⁶⁶³

Encapsulation techniques are currently used to reduce photo-oxidation in commercial devices. In particular, utilization of AuNPs in optoelectronic devices often enhances the optical and electrical properties as well as the stability; this technique effectively inhibits photoluminescence decay.⁶⁶⁴

10. Conclusion and Perspectives

AuNPs, which have been known for 2500 years, are the subject of an exponentially increasing number of reports and are full of promises for optical, electronic, magnetic, catalytic, and biomedical applications in the 21st century, using the “bottom-up” approach with the hybrid organic–inorganic and biological–inorganic building blocks derived therefrom. From the fascination produced by the more or less virtual medical uses of soluble gold in the past millenaries, it remains at least that AuNPs are completely biocompatible. The reasons for the present excitement in AuNP research are also the stability of AuNPs, the extraordinary diversity of their modes of preparations (including biosynthetic modes and template synthesis) involving ceramics, glasses, polymers, ligands, surfaces, films, oxides, zeolithes, biomolecules, and bioorganisms, and their essential properties and role in nanoscience and future nanotechnology.

The classic Turkevitch–Frens synthesis with citrate stabilizer is practical and still very much used to prepare precursors. However, the stabilization of AuNPs by alkanethiolate and various functional thiolate ligands forming very stable, relatively monodisperse materials and the two-phase Schiffrin synthesis have been a breakthrough. These facile syntheses have been shown to be particularly favorable for easy manipulations, such as place-exchange reactions and extensive physical characterizations, formation of superlattices and crystals, and rich molecular chemistry. For instance, multiple redox states (up to 15!) of AuNP–alkanethiolate were beautifully characterized at room temperature as charge injection in the core is quantized, and 2D and 3D AuNP superlattices are now common, easily controlled assemblies that use supramolecular principles and are characterized by spectacular imaging and microscopy techniques.

Fascinating aspects are the optoelectronic properties of AuNPs related to the surface plasmon absorption, reflecting the collective oscillation of the conducting electrons of the gold core, a feature relevant to the quantum size effect. NLO applications of AuNPs are also rapidly growing. The combination of this photonics discipline with biology and medicine has already been demonstrated by the seminal work on AuNP–DNA assemblies and is very promising for future biomolecular manipulations and applications, such as labeling, detection, and transfer of drugs, including genetic materials.

Electronic conduction correlated with single-electron tunneling is a possible basis for future nano-electronic digital circuits in connection with self-assembled monolayers, although the quantized capacitance involved will require ultrapure AuNP materials.

Excellent sensory and environmental devices are becoming available by tuning the spectroscopy, fluorescence, luminescence, and electrochemical characteristics of AuNPs with those of substrates including DNA, sugars, and other biological molecules or systems. Another promising electrochemical field that has just started to develop is that of AuNP ultramicroelectrodes. Thus, it is becoming possible to control molecules at a resolution well below that offered by photolithography. In particular, DNA is a candidate for this task because of its excellent specificity in base pairing, and it can be easily addressed at the nanoscale for applications in biosensing and bionanotechnology.

Finally, although bulk gold is well known for being inert, the reactivity of the gold cores in AuNPs has recently proven very useful in catalytic applications, even at subambient temperatures, and the field of AuNP-catalyzed CO and methanol oxidation and O₂ reduction is now also developing at a rapid rate. Here again, the variety of synthetic possibilities using AuNP components and the understanding of the AuNP nanostructures and their role on the catalytic events is a key toward future applications.

In conclusion, an extraordinary variety of structures, properties, and applications is available for AuNPs and will motivate fundamental studies and applications in connection with those of other molecular, inorganic, and biological nanomaterial components in interdisciplinary research involving chemistry, physics, biology, and medicine.⁶⁶⁵

11. Acknowledgment

The helpful assistance of Jocelyne Moncada for the preparation of this manuscript and financial support from the Institut Universitaire de France (IUF), the University Bordeaux I, and the Centre National de la Recherche Scientifique (CNRS) are gratefully acknowledged.

12. Abbreviations

2D	two-dimensional
3D	three-dimensional
AFM	atomic force microscopy
APTMS	(3-aminopropyl)trimethoxysilane

ATR	atom-transfer radical
Au@SiO ₂	Au–SiO ₂ core–shell particles
AuNP	gold nanoparticle
BAM	Brewster angle microscopy
CVD	chemical vapor deposition
DFT	density functional theory
DNA	desoxyribonucleic acid
DPV	differential pulse voltammetry
DQ	double quantum
DSC	differential scanning calorimetry
EDX	energy-disperse X-ray
EPR	electronic paramagnetic resonance
ESCA	electron spectroscopy for chemical analysis
ET	electrostatic trapping
EXAFS	extended X-ray absorption fine structure
FTIR	Fourier transform infrared
HETCOR	heteronuclear correlation
HIV	human immunodeficiency virus
HOPG	highly ordered pyrolytic graphite
HREELS	high-resolution electron energy loss spectroscopy
HRS	hyper-Raleigh scattering
HRTEM	high-resolution transmission electron microscopy
LB	Langmuir–Blodgett
LDI-MS	laser desorption–ionization mass spectrometry
LRP	living radical polymerization
MAS	magic angle spinning
MCD	magnetic circular dichroism
MPC	monolayer-protected cluster
NLO	nonlinear optics
PAMAM	polyamidoamine
PLD	pulsed laser deposition
PRB	plasmon resonance band
PS–PVP	polystyrene– <i>block</i> -poly(4-vinylpyridine)
PVP	poly(<i>N</i> -vinyl-2-pyrrolidone)
QCM	quartz crystal microbalance
ROMP	ring-opening metathesis polymerization
SAM	self-assembled monolayer
SAXS	small-angle X-ray scattering
SEM	scanning electron microscopy
SERS	surface-enhanced Raman scattering
SFM	scanning force microscopy
SP	surface plasmon
SPB	surface plasmon band
SSHG	surface second harmonic generation
STM	scanning tunneling microscopy
STS	scanning tunneling spectroscopy
TEM	transmission electron microscopy
TEMPO	2,2,6,6-tetramethyl-1-piperidinyloxy
TGA	thermogravimetric analysis
TOPO	tri- <i>n</i> -octylphosphine oxide
XANES	X-ray absorption near-edge structure
XPS	X-ray photoelectron spectroscopy

13. References

- Antonii, F. *Panacea Aurea-Auro Potabile*; Bibliopolio Frobeniano: Hamburg, 1618.
- (a) Kunkels, J. *Nuetliche Observationes oder Anmerkungen von Auro und Argento Potabili*; Schutzens: Hamburg, 1676. (b) Savage, G. *Glass and Glassware*; Octopus Book: London, 1975.
- Helcher, H. H. *Aurum Potabile oder Gold Tinstur*; J. Herbord Klossen: Breslau and Leipzig, 1718.
- Dictionnaire de Chymie*; Lacombe: Paris, 1769.
- Fulhame, Mrs. *An Essay on Combustion with a View to a New Art of Dying and Painting*; J. Cooper: London, 1794.
- Ostwald, W. Zur Geschichte des Colloiden Goldes. *Kolloid Z.* **1909**, 4, 5.
- Faraday, M. Experimental Relations of Gold (and other Metals) to Light. *Philos. Trans.* **1857**, 147, 145–181.
- Graham, T. *Philos. Trans. R. Soc.* **1861**, 151, 183–190.
- Kahn, R. L. Serum Diagnosis for Syphilis. In *Colloid Chemistry*; Alexander, J., Ed.; The Chemical Catalog Co.: New York, 1928; Vol. II, p 757.
- Hauser, E. A. Aurum Potabile. *J. Chem. Educ.* **1952**, 456–458.
- (a) Brown, D. H.; Smith, W. E. The Chemistry of the Gold Drugs Used in the Treatment of Rheumatoid Arthritis. *Chem. Soc. Rev.* **1980**, 9, 217–240. (b) *Immuno-Gold Electron Microscopy in Virus Diagnosis and Research*; Hyatt, A. D., Eaton, B. T., Eds.; CRC Press: Boca Raton, FL, 1993.
- Turkevitch, J.; Stevenson, P. C.; Hillier, J. Nucleation and Growth Process in the Synthesis of Colloidal Gold. *Discuss. Faraday Soc.* **1951**, 11, 55–75.
- Frens, G. Controlled Nucleation for the Regulation of the Particle Size in Monodisperse Gold Suspensions. *Nature: Phys. Sci.* **1973**, 241, 20–22. For a more recent report on citrate-stabilized AuNPs, see ref 223.
- Hayat, M. A. *Colloidal Gold. Principles, Methods and Applications*; Academic Press: New York, 1989.
- Clusters and Colloids*; Schmid, G., Ed.; VCH: Weinheim, 1994.
- Bradley, J. S. In *Clusters and Colloids*; Schmid, G., Ed.; VCH: Weinheim, 1994; Chapter 6, pp 459–544.
- Schmid, G. Large Clusters and Colloids. *Chem. Rev.* **1992**, 92, 1709–1727.
- Fendler, J. H.; Meldrum, F. C. The Colloidal Chemical Approach to Nanostructured Materials. *Adv. Mater.* **1995**, 7, 607–632.
- Schmid, G.; Chi, L. F. Metal Clusters and Colloids. *Adv. Mater.* **1998**, 10, 515–527.
- Edelstein, A. S.; Cammarata, R. C. *Nanoparticle: Synthesis, Properties and Applications*; Institute of Physics Publishing: Bristol, 1996.
- Schmid, G. In *Nanoscale Materials in Chemistry*; Klabunde, K. J., Ed.; Wiley: New York, 2001.
- Bethell, D.; Brust, M.; Schiffrin, D. J.; Kiely, C. From Monolayers to Nanostructured Materials: An Organic Chemist's View of Self-Assembly. *J. Electroanal. Chem.* **1996**, 409, 137–143.
- Matijevic, E. Controlled Colloid Formation. *Curr. Opin. Colloid Interface Sci.* **1996**, 1, 176–183.
- Optical Properties of Metal Clusters*; Freibig, U., Vollmer, M., Eds.; Springer-Verlag: New York, 1995.
- Ung, T.; Liz-Marzán, L. M.; Mulvaney, P. Gold Nanoparticle Thin Films. *Colloids Surf. A: Physicochem. Eng. Asp.* **2002**, 202, 119–126.
- Yonezawa, T.; Toshima, N. Polymer-Stabilized Metal Nanoparticles: Preparation, Characterization and Applications. In *Advanced Functional Molecules and Polymers*; Nalwa, H. S., Ed.; Gordon & Breach: Reading, UK, 2001; Vol. 2, Chapter 3, pp 65–86.
- Brust, M.; Kiely, C. J. Some Recent Advances in Nanostructure Preparation from Gold and Silver: A Short Topical Review. *Colloids Surf. A: Physicochem. Eng. Asp.* **2002**, 202, 175–186.
- Metal Nanoparticles—Synthesis, Characterization and Applications*; Feldheim, D. L., Colby, A. F., Jr., Eds.; Marcel Dekker: New York, 2002.
- Alivisatos, A. P. Semiconductor Clusters, Nanocrystals, and Quantum Dots. *Science* **1996**, 271, 933–937.
- (a) Schmid, G.; Bäuml, M.; Geerkens, M.; Heim, I.; Osemann, C.; Sawitowski, T. Current and Future Applications of Nanoclusters. *Chem. Soc. Rev.* **1999**, 28, 179–185. (b) Schmid, G.; Corain, B. Nanoparticulated Gold: Syntheses, Structures, Electronics, and Reactivities. *Eur. J. Inorg. Chem.* **2003**, 3081–3098. (c) Zhang, H.; Schmid, G.; Hartmann, U. Reduced Metallic Properties of Ligand-Stabilized Small Metal Clusters. *Nano Lett.* **2003**, 3, 305–307.
- Schmid, G.; Harms, M.; Malm, J. O.; Bovin, J. O.; Van Ruitenbeck, J.; Zandbergen, H. W.; Fu, W. T. Ligand-stabilized Giant Palladium Clusters: Promising Candidates in Heterogeneous Catalysis. *J. Am. Chem. Soc.* **1993**, 115, 2046–2048.
- Andres, R. P.; Bein, T.; Dorogi, M.; Feng, S.; Jenderson, J. I.; Kubiak, C. P.; Mahoney, W.; Osifchin, R. G.; Reifenvenger, R. “Coulomb Staircase” at Room Temperature in a Self-Assembled Molecular Nanostructure. *Science* **1996**, 272, 1323–1325.
- (a) *Fine Particles Sciences and Technology—From Micro- to New Particles*; Pellizzetti, E., Ed.; Kluwer: Dordrecht, 1996. (b) Toshima, N. In *Fine Particles Sciences and Technology—From Micro- to New Particles*; Pellizzetti, E., Ed.; Kluwer: Dordrecht, 1996; pp 371–383.
- Beesley, J. E. *Colloidal Gold. A New Perspective for Cytochemical Marking*; Royal Microscopical Society Handbook 17; Oxford Science Publication, Oxford University Press: Oxford, 1989.
- Toshima, N.; Yonezawa, T. Bimetallic Nanoparticles—Novel Materials for Chemical and Physical Applications. *New J. Chem.* **1998**, 1179–1201.
- Fendler, J. H. Self-Assembled Nanostructured Materials. *Chem. Mater.* **1996**, 8, 1616–1624.
- Henglein, A. Physicochemical Properties of Small Metal Particles and the Atom-to-Metal Transition. *J. Phys. Chem.* **1993**, 97, 5457–5471.
- Belloni, J. Metal Nanocolloids. *Curr. Opin. Colloid Interface Sci.* **1996**, 1, 184–196.

- (39) (a) Chen, S.; Ingram, R. S.; Hostetler, M. J.; Pietron, J. J.; Murray, R. W.; Schaaff, T. G.; Khoury, J. T.; Alvarez, M. M.; Whetten, R. L. Gold Nanoelectrodes of Varied Size: Transition to Molecule-Like Charging. *Science* **1998**, *280*, 2098–2101. (b) Miles, D. T.; Murray, R. W. Temperature-Dependent Quantized Double Layer Charging of Monolayer-Protected Gold Clusters. *Anal. Chem.* **2003**, *75*, 1251–1257. (c) Chen, S.; Pei, R. Ion-Induced Rectification of Nanoparticle Quantized Capacitance Charging in Aqueous Solutions. *J. Am. Chem. Soc.* **2001**, *123*, 10607–10615.
- (40) Quinn, B. M.; Liljeroth, P.; Ruiz, V.; Laaksonen, T.; Kontturi, K. Electrochemical Resolution of 15 Oxidation States for Monolayer Protected Gold Nanoparticles. *J. Am. Chem. Soc.* **2003**, *125*, 6644–6645.
- (41) (a) Puddephat, R. J. *The Chemistry of Gold*; Elsevier: Amsterdam, 1978. (b) *Gold, Progress in Chemistry, Biochemistry and Technology*; Schmidbauer, H., Ed.; Wiley: Chichester, 1999.
- (42) Laguna, A. In *Metal Clusters in Chemistry*; Braunstein, P., Oro, L., Raithby, P. R., Eds; Wiley-VCH: Weinheim, 1999.
- (43) *Nanoparticles and Nanostructured Films*; Fendler, J. H., Ed.; Wiley-VCH: Weinheim, 1998.
- (44) Yonezawa, T.; Kunitake, T. Practical Preparation of Anionic Mercapto Ligand-Stabilized Gold Nanoparticles and Their Immobilization. *Colloids Surf. A: Physicochem. Eng. Asp.* **1999**, *149*, 193–199.
- (45) Schmid, G.; Pfeil, R.; Boese, R.; Bandermann, F.; Meyer, S.; Calis, G. H. M.; van der Velden, J. W. A. $[\text{Au}_{55}(\text{P}(\text{C}_6\text{H}_5)_3)_{12}\text{Cl}_6]$ – A Gold Cluster of Unusual Size. *Chem. Ber.* **1981**, *114*, 3634–3642.
- (46) (a) Giersig, M.; Mulvaney, P. Preparation of ordered colloid monolayers by electrophoretic deposition. *Langmuir* **1993**, *9*, 3408–3413. (b) Hasan, M.; Bethell, D.; Brust, M. The Fate of Sulfur-Bound Hydrogen on Formation of Self-Assembled Thiol Monolayers on Gold: ^1H NMR Spectroscopic Evidence from Solutions of Gold Clusters. *J. Am. Chem. Soc.* **2003**, *125*, 1132–1133.
- (47) (a) Brust, M.; Walker, M.; Bethell, D.; Schiffrin, D. J.; Whyman, R. J. Synthesis of Thiol-Derivatized Gold Nanoparticles in a Two-phase Liquid–Liquid System. *J. Chem. Soc., Chem. Commun.* **1994**, 801–802. (b) Brust, M.; Fink, J.; Bethell, D.; Schiffrin, D. J.; Kiely, C. J. Synthesis and Reactions of Functionalised Gold Nanoparticles. *J. Chem. Soc., Chem. Commun.* **1995**, 1655–1656.
- (48) (a) Chen, S. 4-Hydroxythiophenol-Protected Gold Nanoclusters in Aqueous Media. *Langmuir* **1999**, *15*, 7551–7557. (b) Chen, S.; Murray, R. W. Arenethiolate Monolayer-Protected Gold Clusters. *Langmuir* **1999**, *15*, 682–689.
- (49) (a) Hostetler, M. J.; Green, S. J.; Stokes, J. J.; Murray, R. W. Monolayers in Three Dimensions: Synthesis and Electrochemistry of ω -Functionalized Alkanethiolate-Stabilized Gold Cluster Compounds. *J. Am. Chem. Soc.* **1996**, *118*, 4212–4213. (b) Ingram, R. S.; Hostetler, M. J.; Murray, R. W. Poly-hetero- ω -functionalized Alkanethiolate-Stabilized Gold Cluster Compounds. *J. Am. Chem. Soc.* **1997**, *119*, 9175–9178.
- (50) Templeton, A. C.; Wuelfing, W. P.; Murray, R. W. Monolayer-Protected Cluster Molecules. *Acc. Chem. Res.* **2000**, *33*, 27–36.
- (51) Hostetler, M. J.; Wingate, J. E.; Zhong, C.-J.; Harris, J. E.; Vachet, R. W.; Clark, M. R.; Londono, J. D.; Green, S. J.; Stokes, J. J.; Wignall, G. D.; Glish, G. L.; Porter, M. D.; Evans, N. D.; Murray, R. W. Alkanethiolate Gold Cluster Molecules with Core Diameters from 1.5 to 5.2 nm: Core and Monolayer Properties as a Function of Core Size. *Langmuir* **1998**, *14*, 17–30.
- (52) (a) Templeton, A. C.; Hostetler, M. J.; Kraft, C. T.; Murray, R. W. Reactivity of Monolayer-Protected Gold Cluster Molecules: Steric Effects. *J. Am. Chem. Soc.* **1998**, *120*, 1906–1911. (b) Hostetler, M. J.; Templeton, A. C.; Murray, R. W. Dynamics of Place-Exchange Reactions on Monolayer-Protected Gold Cluster Molecules. *Langmuir* **1999**, *15*, 3782–3789.
- (53) Hostetler, M. J.; Templeton, A. C.; Murray, R. W. Dynamics of Place-Exchange Reactions on Monolayer-Protected Gold Cluster Molecules. *Langmuir* **1999**, *15*, 3782–3789.
- (54) Waters, C. A.; Mills, A. J.; Johnson, K. A.; Schiffrin, D. J. Purification of Dodecanethiol Derivatized Gold Nanoparticles. *Chem. Commun.* **2003**, 540–541.
- (55) Aslan, K.; Pérez-Luna, V. H. Surface Modification of Colloidal Gold by Chemisorption of Alkanethiols in the Presence of a Nonionic Surfactant. *Langmuir* **2002**, *18*, 6059–6065.
- (56) Prasad, B. L. V.; Stoeva, S. I.; Sorensen, C. M.; Klabunde, K. J. Digestive Ripening of Thiolated Gold Nanoparticles: The Effect of Alkyl Chain Length. *Langmuir* **2002**, *18*, 7515–7520.
- (57) Prasad, B. L. V.; Stoeva, S. I.; Sorensen, C. M.; Klabunde, K. J. Digestive-Ripening Agents for Gold Nanoparticles: Alternatives to Thiols. *Chem. Mater.* **2003**, *15*, 935–942.
- (58) (a) Andres, R. P.; Bielefeld, J. D.; Henderson, J. I.; Janes, D. B.; Kolagunta, V. R.; Kubiak, C. P.; Mahoney, W. J.; O. R. G. Self-Assembly of a Two-Dimensional Superlattice of Molecularly Linked Metal Clusters. *Science* **1996**, *273*, 1690–1693. (b) Lin, X. M.; Sorensen, C. M. Ligand-Induced Gold Nanocrystal Superlattice Formation in Colloidal Solution. *Chem. Mater.* **1999**, *11*, 198–202.
- (59) (a) Brown, L. O.; Hutchison, J. E. Formation and Electron Diffraction Studies of Ordered 2-D and 3-D Superlattices of Amine-Stabilized Gold Nanocrystals. *J. Phys. Chem. B* **2001**, *105*, 8911–8916. (b) Stoeva, S. I.; Prasad, B. L. V.; Uma, S.; Stoimenov, P. K.; Zaikovskiy, V.; Sorensen, C. M.; Klabunde, K. J. Face-Centered Cubic and Hexagonal Closed-Packed Nanocrystal Superlattice of Gold Nanoparticles Prepared by Different Methods. *J. Phys. Chem. B* **2003**, *107*, 7441–7448.
- (60) (a) Li, W.; Huo, L.; Wang, D.; Zeng, G.; Xi, S.; Zhao, B.; Zhu, J.; Wang, J.; Shen, Y.; Lu, Z. Self-Assembled Multilayers of Alternating Gold Nanoparticles and Dithiols: Approaching to Superlattice. *Colloids Surf.* **2000**, *175*, 217–223. (b) Wang, T.; Zhang, D.; Xu, W.; Zhu, D. Self-Organization of Gold Nanoparticles into 2D Superlattice through π - π Interaction. *Synth. Met.* **2003**, *135–136*, 835–836.
- (61) (a) Kanehara, M.; Oumi, Y.; Sano, T.; Teranishi, T. Formation of Low-Symmetric 2D Superlattices of Gold Nanoparticles through Surface Modification by Acid–Base Interaction. *J. Am. Chem. Soc.* **2003**, *125*, 8708. (b) Teranishi, T. Fabrication and Electronic Properties of Gold Nanoparticles. In *Dendrimers and Nanoscience*; Astruc, D., Ed.; Comptes-Rendus Chimie, Elsevier: Paris, 2003 (in press).
- (62) Dieluweit, S.; Pum, D.; Sleytr, U. B. Formation of a Gold Superlattice on an S–Layer with Square Lattice Symmetry. *Supramol. Sci.* **1998**, *5*, 15–19.
- (63) (a) Sarathy, K. V.; Kulkarni, G. U.; Rao, C. N. R. A Novel Method of Preparing Thiol-Derivatized Nanoparticles of Gold, Platinum and Silver Forming Superstructures. *Chem. Commun.* **1997**, 537–538. (b) Ascencio, J. A.; Pérez, M.; José-Yacamán, M. A Truncated Icosahedral Structure Observed in Gold Nanoparticles. *Surf. Sci.* **2000**, *447*, 73–80. (c) Chushak, Y.; Bartell, L. S. Molecular Dynamics Simulations of the Freezing of Gold Nanoparticles. *Eur. Phys. J. D* **2001**, *16*, 43–46.
- (64) (a) Yee, C. K.; Jordan, R.; Ulman, A.; White, H.; King, A.; Rafailovich, M.; Sokolov, J. Novel One-Phase Synthesis of Thiol-Functionalized Gold, Palladium, and Iridium Nanoparticles Using Superhydride. *Langmuir* **1999**, *15*, 3486–3491. (b) Selvakannan, P. R.; Mandal, S.; Pasricha, R.; Adyanthaya, S. D.; Sastry, M. One-Step Synthesis of Hydrophobized Gold Nanoparticles of Controllable Size by the Reduction of Aqueous Chloroaurate Ions by Hexadecylaniline at the Liquid–Liquid Interface. *Chem. Commun.* **2002**, 1334–1335.
- (65) Wei, G.-T.; Liu, F.-K.; Wang, C. R. C. Shape Separation of Nanometer Gold Particles by Size-Exclusion Chromatography. *Anal. Chem.* **1999**, *71*, 2085–2091.
- (66) Tzhayik, O.; Sawant, P.; Efrima, S.; Kovalev, E.; Klug, J. T. Xanthate Capping of Silver, Copper, and Gold Colloids. *Langmuir* **2002**, *18*, 3364–3369.
- (67) Porter, L. A., Jr.; Ji, D.; Westcott, S. L.; Graupe, M.; Czernuszewicz, R. S.; Halas, N. J.; Lee, T. R. Gold and Silver Nanoparticles Functionalized by the Adsorption of Dialkyl Disulfides. *Langmuir* **1998**, *14*, 7378–7386.
- (68) Yonezawa, T.; Yasui, K.; Kimizuka, N. Controlled Formation of Smaller Gold Nanoparticles by the Use of Four-Chained Disulfide Stabilizer. *Langmuir* **2001**, *17*, 271–273.
- (69) (a) Manna, A.; Chen, P.-L.; Akiyama, H.; Wei, T.-X.; Tamada, K.; Knoll, W. Optimized Photoisomerization on Gold Nanoparticles Capped by Unsymmetrical Azobenzene Disulfides. *Chem. Mater.* **2003**, *15*, 20–28. (b) Torigoe, K.; Esumi, K. Preparation and Catalytic Effect of Gold Nanoparticles in Water Dissolving Carbon Disulfide. *J. Phys. Chem. B* **1999**, *103*, 2862–2866.
- (70) (a) Resch, R.; Baur, C.; Bugacov, A.; Koel, B. E.; Echterneck, P. M.; Madhukar, A.; Montoya, N.; Requicha, A. A. G.; Will, P. Linking and Manipulation of Gold Multinanoparticle Structures Using Dithiols and Scanning Force Microscopy. *J. Phys. Chem. B* **1999**, *103*, 3647–3650. (b) Félijd, N.; Aubard, J.; Lévi, G.; Krenn, J. R.; Hohenau, A.; Schider, G.; Leitner, A.; Ausenegg, F. R. Optimized Surface-Enhanced Raman Scattering on Gold Nanoparticle Arrays. *Appl. Phys. Lett.* **2003**, *82*, 3095–3097. (c) Tan, Y.; Li, Y.; Zhu, D. Fabrication of Gold Nanoparticles Using a Trithiol (Thiocyanuric Acid) as the Capping Agent. *Langmuir* **2002**, *18*, 3392–3395. (d) Balasubramanian, R.; Kim, B.; Tripp, S. L.; Wang, X.; Lieberman, M.; Wei, A. Dispersion and Stability Studies of Resorcinarene-Encapsulated Gold Nanoparticles. *Langmuir* **2002**, *18*, 3676–3681.
- (71) Shelley, E. J.; Ryan, D.; Johnson, S. R.; Couillard, M.; Fitzmaurice, D.; Nellist, P. D.; Chen, Y.; Palmer, R. E.; Preece, J. A. Dialkyl Sulfides: Novel Passivating Agents for Gold Nanoparticles. *Langmuir* **2002**, *18*, 1791–1795.
- (72) Li, X.-M.; de Jong, M. R.; Inoue, K.; Shinkai, S.; Huskens, J.; Reinhoudt, D. N. Formation of Gold Colloids Using Thioether Derivatives as Stabilizing Ligands. *J. Mater. Chem.* **2001**, *11*, 1919–1923. (b) Maye, M. M.; Chun, S. C.; Han, L.; Rabinovitch, D.; Zhong, C.-J. Novel Spherical Assembly of Gold Nanoparticles Mediated by a Tetradentate Thioether. *J. Am. Chem. Soc.* **2002**, *124*, 4958–4959.
- (73) Sun, L.; Crooks, R. M.; Chechik, V. Preparation of Polycyclodextrin Hollow Spheres by Templating Gold Nanoparticles. *Chem. Commun.* **2001**, 359–360.

- (74) (a) Weare, W. W.; Reed, S. M.; Warner, M. G.; Hutchison, J. E. Improved Synthesis of Small ($d_{\text{CORE}} \approx 1.5$ nm) Phosphine-Stabilized Gold Nanoparticles. *J. Am. Chem. Soc.* **2000**, *122*, 12890–12891. (b) Yamamoto, M.; Nakamoto, M. New Type of Monodispersed Gold Nanoparticles Capped by Myristate and PPh_3 Ligands Prepared by Controlled Thermolysis of $[\text{Au}(\text{C}_{13}\text{H}_{27}\text{COO})(\text{PPh}_3)]$. *Chem. Lett.* **2003**, *32*, 452–453.
- (75) (a) Heath, J. R.; Brandt, L.; Leff, D. V. Synthesis and Characterization of Hydrophobic, Organically-Soluble Gold Nanocrystals Functionalized with Primary Amines. *Langmuir* **1996**, *12*, 4723–4730. (b) Heath, J. R.; Knobler, C. M.; Leff, D. V. Pressure/Temperature Phase Diagrams and Superlattices of Organically Functionalized Metal Nanocrystal Monolayers: The Influence of Particle Size, Size Distribution, and Surface Passivant. *J. Phys. Chem. B* **1997**, *101*, 189–197.
- (76) (a) Gomez, S.; Philippot, K.; Collière, V.; Chaudret, B.; Senocq, F.; Lecante, P. Gold Nanoparticles from Self-Assembled Gold (I) Amine Precursors. *Chem. Commun.* **2000**, 1945–1946. (b) Bardaji, M.; Uznanski, P.; Amiens, C.; Chaudret, B.; Laguna, A. Auophilic Complexes as Gold Atom Sources in Organic Media. *Chem. Commun.* **2002**, 598–599. (c) Green, M.; O'Brien, P. A Simple One Phase Preparation of Organically Capped Gold Nanocrystals. *Chem. Commun.* **2000**, 183–184. (d) Selvakannan, P. R.; Mandal, S.; Phadtare, S.; Pasricha, R.; Sastry, M. Capping of Gold Nanoparticles by the Amino Acid Lysine Renders Them Water-Dispersible. *Langmuir* **2003**, *19*, 3545–3549. (e) Ahmad, A.; Senapati, S.; Khan, M. I.; Kumar, R.; Sastry, M. Extracellular Biosynthesis of Monodisperse Gold Nanoparticles by a Novel Extremophilic Actinomycete, *Thermomonospora* sp. *Langmuir* **2003**, *19*, 3550–3553. (f) Chen, J.; Calvet, L. C.; Reed, M. A.; Carr, D. W.; Grushiba, D. S.; Bennett, D. W. *Chem. Phys. Lett.* **1999**, *313*, 741. (g) Kim, H. S.; Lee, S. J.; Kim, N. H.; Yoon, J. K.; Park, H. K.; Kim, K. Adsorption Characteristics of 1,4-Phenylene Diisocyanide on Gold Nanoparticles: Infrared and Raman Spectroscopy Study. *Langmuir* **2003**, *19*, 6701–6710. (h) Joo, S.-W.; Kim, W.-J.; Yoon, W. S.; Choi, I. S. Adsorption of 4,4'-Biphenyl Diisocyanide on Gold Nanoparticle Surfaces Investigated by Surface-Enhanced Raman Scattering. *J. Raman Spectrosc.* **2003**, *34*, 271–275. (i) Li, G.; Lauer, M.; Schulz, A.; Boettcher, C.; Li, F.; Fuhrhop, J.-H. Spherical and Planar Gold (0) Nanoparticles with a Rigid Gold(I)-Anion or a Fluid Gold(0)-Acetone Surface. *Langmuir* **2003**, *19*, 6483–6491. (j) Cheng, W.; Dong, S.; Wang, E. Iodine-Induced Gold Nanoparticle Fusion/Fragmentation/Aggregation and Iodine-Linked Nanostructured Assemblies on a Glass Substrate. *Angew. Chem., Int. Ed.* **2003**, *42*, 449–452.
- (77) (a) Lattes, A.; Rico, I.; de Savignac, A.; Samii, A. Formamide, a Water Substitute in Micelles and Microemulsions: Structural Analysis Using a Diels–Alder Reaction as a Chemical Probe. *Tetrahedron* **1987**, *43*, 1725–1735. (b) Taleb, A.; Petit, C.; Pileni, M. P. J. Optical Properties of Self-Assembled 2D and 3D Superlattices of Silver Nanoparticles. *Phys. Chem. B* **1998**, *102*, 2214–2220. (c) Chen, F.; Xu, G.-Q.; Hor, T. S. A. Preparation and Assembly of Colloidal Gold Nanoparticles in CTAB-Stabilized Reverse Microemulsion. *Mater. Lett.* **2003**, *57*, 3282–3286.
- (78) Sohn, B.-H.; Choi, J.-M.; Yoo, S., II; Yun, S.-H.; Zin, W.-C.; Jung, J. C.; Kanehara, M.; Hirata, T.; Teranishi, T. Directed Self-Assembly of Two Kinds of Nanoparticles Utilizing Monolayer Films of Diblock Copolymer Micelles. *J. Am. Chem. Soc.* **2003**, *125*, 6368–6369.
- (79) Manna, A.; Imae, T.; Yogo, T.; Aoi, K.; Okazaki, M. Synthesis of Gold Nanoparticles in a Winsor II Type Microemulsion and Their Characterization. *J. Colloid Interface Sci.* **2002**, *256*, 297–303.
- (80) Aliotta, F.; Arcoleo, V.; Buccoleri, S.; La Manna, G.; Liveri, V. T. Calorimetric Investigation on the Formation of Gold Nanoparticles in Water/AOT/*n*-heptane Microemulsions. *Thermochim. Acta* **1995**, *265*, 15–23.
- (81) Arcoleo, V.; Liveri, V. T. AFM Investigation of Gold Nanoparticles Synthesized in Water/AOT/*n*-heptanes. *Chem. Phys. Lett.* **1996**, *258*, 223–227.
- (82) Porta, F.; Prati, L.; Rossi, M.; Scari, G. Synthesis of Au (0) Nanoparticles from W/O Microemulsions. *Colloids Surf.* **2002**, *211*, 43–48.
- (83) Chiang, C.-L. Controlled Growth of Gold Nanoparticles in AOT/ C_{12}E_4 /Isooctane Mixed Reverse Micelles. *J. Colloid Surf. Sci.* **2001**, *239*, 334–341.
- (84) Chiang, C.-L. Controlled Growth of Gold Nanoparticles in Aerosol-OT/Sorbitan Monooleate/Isooctane Mixed Reverse Micelles. *J. Colloid Interface Sci.* **2000**, *230*, 60–66.
- (85) Liu, S.; Weaver, J. V. M.; Save, M.; Armes, S. P. Synthesis of pH-Responsive Shell Cross-Linked Micelles and Their Use as Nanoreactors for the Preparation of Gold Nanoparticles. *Langmuir* **2002**, *18*, 8350–8357.
- (86) Mössmer, S.; Spatz, J. P.; Möller, M.; Aberle, T.; Schmidt, J.; Burchard, W. Solution Behavior of Poly(styrene)-*block*-poly(2-vinylpyridine) Micelles Containing Gold Nanoparticles. *Macromolecules* **2000**, *33*, 4791–4798.
- (87) (a) Carrot, G.; Valmalette, J. C.; Plummer, C. J. G.; Scholz, S. M.; Dutta, J.; Hofmann, H.; Hilborn, J. G. Gold Nanoparticle Synthesis in Graft Copolymer Micelles. *Colloid Polym. Sci.* **1998**, *276*, 853–859. (b) Busbee, B. D.; Obare, S. O.; Murphy, C. J. An Improved Synthesis of High-Aspect-Ratio Gold Nanorods. *Adv. Mater.* **2003**, *15*, 414–416.
- (88) Mandal, M.; Ghosh, S. K.; Kundu, S.; Esumi, K.; Pal, T. UV Photoactivation for Size and Shape Controlled Synthesis and Coalescence of Gold Nanoparticles in Micelles. *Langmuir* **2002**, *18*, 7792–7797.
- (89) Jana, N. R.; Gearheart, L.; Murphy, C. J. Seeding Growth for Size Control of 5–40 nm Diameter Gold Nanoparticles. *Langmuir* **2001**, *17*, 6782–6786.
- (90) Jana, N. R.; Gearheart, L.; Murphy, C. J. Seed-Mediated Growth Approach for Shape-Controlled Synthesis of Spheroidal and Rodlike Gold Nanoparticles Using a Surfactant Template. *Adv. Mater.* **2001**, *13*, 1389–1393.
- (91) Markowitz, M. A.; Dunn, D. N.; Chow, G. M.; Zhang, J. The Effect of Membrane Charge on Gold Nanoparticle Synthesis via Surfactant Membranes. *J. Colloid Interface Sci.* **1999**, *210*, 73–85.
- (92) Johnson, S. R.; Evans, S. D.; Mahon, S. W.; Ulman, A. Synthesis and Characterization of Surfactant-Stabilized Gold Nanoparticles. *Supramol. Sci.* **1997**, *4*, 329–333.
- (93) Johnson, S. R.; Evans, S. D.; Brydson, R. Influence of a Terminal Functionality on the Physical Properties of Surfactant-Stabilized Gold Nanoparticles. *Langmuir* **1998**, *14*, 6639–6647.
- (94) Hassenkam, T.; Nørgaard, K.; Iversen, L.; Kiely, C. J.; Bjørholm, T. Fabrication of 2D Gold Nanowires by Self-Assembly of Gold Nanoparticles on Water Surfaces in the Presence of Surfactants. *Adv. Mater.* **2002**, *14*, 1126–1130.
- (95) Kawai, T.; Neivandt, D. J.; Davies, P. B. Sum Frequency Generation on Surfactant-Coated Gold Nanoparticles. *J. Am. Chem. Soc.* **2000**, *122*, 12031–12032.
- (96) Youk, J. H.; Locklin, J.; Xia, C.; Park, M.-K.; Advincula, R. Preparation of Gold Nanoparticles from a Polyelectrolyte Complex Solution of Terthiophene Amphiphiles. *Langmuir* **2001**, *17*, 4681–4683.
- (97) Yonezawa, T.; Onoue, S.-Y.; Kunitake, T. Preparation of Cationic Gold Nanoparticles and Their Monolayer Formation on an Anionic Amphiphile Layer. *Chem. Lett.* **1999**, 1061–1062.
- (98) Gittins, D. I.; Caruso, F. Tailoring the Polyelectrolyte Coating of Metal Nanoparticles. *J. Phys. Chem. B* **2001**, *105*, 6846–6852.
- (99) Gohy, J.-F.; Varshney, S. K.; Jérôme, R. Morphology of Water-Soluble Interpolyelectrolyte Complexes Formed by Poly(2-vinylpyridinium)-*block*-poly(ethylene oxide) Diblocks and Poly(4-styrenesulfonate) Polyanions. *Macromolecules* **2001**, *34*, 2745–2747.
- (100) Svergun, D. I.; Shtykova, E. V.; Dembo, A. T.; Bronstein, L. M.; Platonova, O. A.; Yakunin, A. N.; Valetsky, P. M.; Khokhlov, A. R. Size Distributions of Metal Nanoparticles in Polyelectrolyte Gels. *J. Chem. Phys.* **1998**, *109*, 111109–11116.
- (101) Mayya, K. S.; Gittins, D. I.; Caruso, F. Gold-Titania Core–Shell Nanoparticles by Polyelectrolyte Complexation with a Titania Precursor. *Chem. Mater.* **2001**, *13*, 3833–3836.
- (102) (a) Mayer, A. B. R.; Mark, J. E. Colloidal Gold Nanoparticles Protected by Cationic Polyelectrolytes. *Pure Appl. Chem.* **1997**, *11*, A34, 2151–2164. (b) Mayya, K. S.; Schoeler, B.; Caruso, F. Preparation and Organization of Nanoscale Polyelectrolyte-Coated Gold Nanoparticles. *Adv. Funct. Mater.* **2003**, *13*, 183–188.
- (103) Jana, N. R.; Gearheart, L.; Murphy, C. J. Evidence for Seed-Mediated Nucleation in the Chemical Reduction of Gold Salts to Gold Nanoparticles. *Chem. Mater.* **2001**, *13*, 2313–2322.
- (104) Sau, T. K.; Pal, A.; Jana, N. R.; Wang, Z. L.; Pal, T. Size Controlled Synthesis of Gold Nanoparticles Using Photochemically Prepared Seed Particles. *J. Nanopart. Res.* **2001**, *3*, 257–261.
- (105) Meltzer, S.; Resch, R.; Koel, B. E.; Thompson, M. E.; Madhukar, A.; Requicha, A. A. G.; Will, P. Fabrication of Nanostructures by Hydroxylamine Seeding of Gold Nanoparticle Templates. *Langmuir* **2001**, *17*, 1713–1718.
- (106) Mallick, K.; Wang, Z. L.; Pal, T. Seed-Mediated Successive Growth of Gold Particles Accomplished by UV Irradiation: a Photochemical Approach for Size-Controlled Synthesis. *J. Photochem. Photobiol.* **2001**, *140*, 75–80.
- (107) Zhou, Y.; Wang, C. Y.; Zhu, Y. R.; Chen, Z. Y. A Novel Ultraviolet Irradiation Technique for Shape-Controlled Synthesis of Gold Nanoparticles at Room Temperature. *Chem. Mater.* **1999**, *11*, 2310–2312.
- (108) (a) Niidome, Y.; Hori, A.; Sato, T.; Yamada, S. Enormous Size Growth of Thiol-passivated Gold Nanoparticles Induced by Near-IR Laser Light. *Chem. Lett.* **2000**, 310–311. (b) Reed, J. A.; Cook, A.; Halaas, D. J.; Parazolli, P.; Robinson, A.; Matula, T. J.; Griezler, F. The Effects of Microgravity on Nanoparticle Size Distributions Generated by the Ultrasonic Reduction of an Aqueous Gold-Chloride Solution. *Ultrason. Sonochem.* **2003**, *10*, 285–289.

- (109) Okitsu, K.; Yue, A.; Tanabe, S.; Matsumoto, H.; Yobiko, Y. Formation of Colloidal Gold Nanoparticles in an Ultrasonic Field: Control of Rate of Gold (III) Reduction and Size of Formed Gold Particles. *Langmuir* **2001**, *17*, 7717–7720.
- (110) Okitsu, K. Sonolytic Control of Rate of Gold (III) Reduction and Size of Formed Gold Nanoparticles: Relation between Reduction Rates and Sizes of Formed Nanoparticles. *Bull. Chem. Soc. Jpn.* **2002**, *75*, 2289–2296.
- (111) Chen, W.; Cai, W. P.; Liang, C. H.; Zhang, L. D. Synthesis of Gold Nanoparticles Dispersed Within Pores of Mesoporous Silica Induced by Ultrasonic Irradiation and its Characterization. *Mater. Res. Bull.* **2001**, *36*, 335–342.
- (112) Chen, W.; Cai, W.; Zhang, L.; Wang, G.; Zhang, L. Sonochemical Processes and Formation of Gold Nanoparticles within Pores of Mesoporous Silica. *J. Colloid Surf. Sci.* **2001**, *238*, 291–295.
- (113) Pol, V. G.; Gedanken, A.; Calderro-Moreno, J. Deposition of Gold Nanoparticles on Silica Spheres: A Sonochemical Approach. *Chem. Mater.* **2003**, *15*, 1111–1118.
- (114) Mizukoshi, Y.; Okitsu, K.; Maeda, Y.; Yamamoto, T. A.; Oshima, R.; Nagata, Y. Sonochemical Preparation of Bimetallic Nanoparticles of Gold/Palladium in Aqueous Solution. *J. Phys. Chem. B* **1997**, *101*, 7033–7037.
- (115) (a) Henglein, A.; Meisel, D. Radiolytic Control of the Size of Colloidal Gold Nanoparticles. *Langmuir* **1998**, *14*, 7392–7396. (b) Dawson, A.; Kamat, P. V. Complexation of Gold Nanoparticles with Radiolytically Generated Thiocyanate Radicals (SCN)₂⁻. *J. Phys. Chem. B* **2000**, *104*, 11842–11846.
- (116) Gachard, E.; Remita, H.; Khatouri, J.; Keita, B.; Nadjio, L.; Belloni, J. Radiation-Induced and Chemical Formation of Gold Clusters. *New J. Chem.* **1998**, 1257–1265.
- (117) Khomutov, G. B. Two-Dimensional Synthesis of Anisotropic Nanoparticles. *Colloids Surf.* **2002**, 243–267.
- (118) (a) Nakamoto, M.; Yamamoto, M.; Fukusumi, M. Thermolysis of Gold (I) Thiolate Complexes Producing Novel Gold Nanoparticles Passivated by Alkyl Groups. *Chem. Commun.* **2002**, 1622–1623. (b) Shimizu, T.; Teranishi, T.; Hasegawa, S.; Miyake, M. Size Evolution of Alkanethiol-Protected Gold Nanoparticles by Heat Treatment in the Solid State. *J. Phys. Chem. B* **2003**, *107*, 2719–2724. (c) Teranishi, T.; Hasegawa, S.; Shimizu, T.; Miyake, M. Heat-Induced Size Evolution of Gold Nanoparticles in the Solid State. *Adv. Mater.* **2001**, *13*, 1699–1701.
- (119) Bronstein, L.; Chernyshov, D.; Valetsky, P.; Tkachenko, N.; Lemmetyinen, H.; Hartmann, J.; Förster, S. Laser Photolysis Formation of Gold Colloids in Block Copolymer Micelles. *Langmuir* **1999**, *15*, 83–91.
- (120) (a) Mafumé, F.; Kohno, J.-Y.; Takeda, Y.; Kondow, T. Full Physical Preparation of Size-Selected Gold Nanoparticles in Solution: Laser Ablation and Laser-Induced Size Control. *J. Phys. Chem. B* **2002**, *106*, 7575–7577. (b) Mafuné, F.; Kondow, T. Formation of Small Gold Clusters in Solution by Laser Excitation of Interband Transition. *Chem. Phys. Lett.* **2003**, *372*, 199–204.
- (121) Mafumé, F.; Kohno, J.-Y.; Takeda, Y.; Kondow, T.; Sawabe, H. Formation of Gold Nanoparticles by Laser Ablation in Aqueous Solution of Surfactant. *J. Phys. Chem. B* **2001**, *105*, 5114–5120.
- (122) Kawakami, Y.; Seto, T.; Yoshida, T.; Ozawa, E. Gold Nanoparticles and Films Produced by a Laser Ablation/Gas Deposition (LAGD) Methodology. *Appl. Surf. Sci.* **2002**, *197–198*, 587–593.
- (123) Maye, M. M.; Zheng, W.; Leibowitz, F. L.; Ly, N. K.; Zhong, C.-J. Heating-Induced Evolution of Thiolate-Encapsulated Gold Nanoparticles: A Strategy for Size and Shape Manipulations. *Langmuir* **2000**, *16*, 490–497.
- (124) Magnusson, M. H. Gold Nanoparticles: Production, Reshaping, and Thermal Charging. *J. Nanopart. Res.* **1999**, *1*, 243–251.
- (125) De Marchi, G.; Mattei, G.; Mazzoli, P.; Sada, C.; Miotello, A. Two Stages in the Kinetics of Gold Cluster Growth in Ion-Implanted Silica During Isothermal Annealing in Oxidizing Atmosphere. *J. Appl. Phys.* **2002**, *92*, 4249–4254.
- (126) (a) Luo, J.; Jones, V. W.; Maye, M. M.; Han, L.; Kariuki, N. N.; Zhong, C.-J. Thermal Activation of Molecularly-Wired Gold Nanoparticles on a Substrate as Catalyst. *J. Am. Chem. Soc.* **2002**, *124*, 13988–13989. (b) Adachi, E. Coagulative Transition of Gold Nanoparticle Spheroids into Monolithic Colloids: Structure, Lifetime, and Transition Model. *Langmuir* **2001**, *17*, 3863–3870. (c) Nakaso, K.; Shimada, M.; Okuyama, K.; Deppert, K. Evaluation of the Change in the Morphology of Gold Nanoparticles During Sintering. *Aerosol Sci.* **2002**, *33*, 1061–1074.
- (127) Yonezawa, T.; Onoue, S.-Y.; Kimizuka, N. Formation of Uniform Fluorinated Gold Nanoparticles and Their Highly Ordered Hexagonally Packed Monolayer. *Langmuir* **2001**, *17*, 2291–2293.
- (128) Foos, E. E.; Snow, A. W.; Twigg, M. E.; Ancona, M. G. Thiol-Terminated Di-, Tri-, and Tetraethylene Oxide Functionalized Gold Nanoparticles: A Water-Soluble, Charge-Neutral Cluster. *Chem. Mater.* **2002**, *14*, 2401–2408.
- (129) Kanaras, A. G.; Kamounah, F. S.; Schaumburg, K.; Kiely, C. J.; Brust, M. Thioalkylated Tetraethylene Glycol: a New Ligand for Water Soluble Monolayer Protected Gold Clusters. *Chem. Commun.* **2002**, 2294–2295.
- (130) (a) Wuelfing, W. P.; Gross, S. M.; Miles, D. T.; Murray, R. W. Nanometer Gold Clusters Protected by Surface-Bound Monolayers of Thiolated Poly(ethylene glycol) Polymer Electrolyte. *J. Am. Chem. Soc.* **1998**, *120*, 12696–12697. (b) Chen, S.; Kimura, K. Synthesis and Characterization of Carboxylate-Modified Gold Nanoparticles Powders Dispersible in Water. *Langmuir* **1999**, *15*, 1075–1082. (c) Kimura, K.; Sato, S.; Yao, H. Particle Crystals of Surface Modified Gold Nanoparticles Grown From Water. *Chem. Lett.* **2001**, 372–373.
- (131) Yonezawa, T.; Sutoh, M.; Kunitake, T. Practical Preparation of Size-Controlled Gold Nanoparticles in Water. *Chem. Lett.* **1997**, 619–620.
- (132) Warner, M. G.; Reed, S. M.; Hutchison, J. E. Small, Water-Soluble, Ligand-Stabilized Gold Nanoparticles Synthesized by Interfacial Ligand Exchange Reactions. *Chem. Mater.* **2000**, *12*, 3316–3320.
- (133) Simard, J.; Briggs, C.; Boal, A. K.; Rotello, V. M. Formation and pH-controlled Assembly of Amphiphilic Gold Nanoparticles. *Chem. Commun.* **2000**, 1943–1944.
- (134) Yao, H.; Momozawa, O.; Hamatani, T.; Kimura, K. Stepwise Size-Selective Extraction of Carboxylate-Modified Gold Nanoparticles from an Aqueous Suspension into Toluene with Tetraoctylammonium Cations. *Chem. Mater.* **2001**, *13*, 4692–4697.
- (135) Jana, N. R.; Peng, X. Single-Phase and Gram-Scale Routes toward Nearly Monodisperse Au and Other Noble Metal Nanocrystals. *J. Am. Chem. Soc.* **2003**, *125*, 14280–14281.
- (136) Leff, D. V.; Ohara, P. C.; Heath, J. R.; Gelbart, W. M. Thermodynamic Control of Gold Nanocrystal Size: Experiment and Theory. *J. Phys. Chem.* **1995**, *99*, 7036–7041.
- (137) (a) Nakamura, K.; Kawabata, T.; Mori, Y. Size Distribution Analysis of Colloidal Gold by Small-Angle X-ray Scattering and Light Absorbance. *Powder Technol.* **2003**, *131*, 120–128. (b) Cleveland, C. L.; Landman, U.; Shafiqullin, M. N.; Stephens, P. M.; Whetten, R. L. Structural Evolution of Larger Gold Clusters. *Z. Phys. D* **1997**, *40*, 503–508. (c) Koga, K.; Sugawara, K. Population Statistics of Gold Nanoparticle Morphologies: Direct Determination by HRTEM Observations. *Surf. Sci.* **2003**, *529*, 23–35.
- (138) Fenter, P.; Eberhardt, A.; Eiseberger, P. Self-Assembly of *n*-alkyl Thiols as Disulfides on Au(111). *Science* **1994**, *266*, 1216–1218.
- (139) Gutiérrez-Wing, C.; Ascencio, J. A.; Pérez-Alvarez, M.; Marin-Almazo, M.; José-Yacamán, M. On the Structure and Formation of Self-Assembled Lattices of Gold Nanoparticles. *J. Cluster Sci.* **1998**, *9*, 529–545.
- (140) Labande, A.; Ruiz, J.; Astruc, D. Supramolecular Gold Nanoparticles for the Redox Recognition of Oxoanions: Syntheses, Titrations, Stereoelectronic Effects, and Selectivity. *J. Am. Chem. Soc.* **2002**, *124*, 1782–1789.
- (141) Whetten, R. L.; Khoury, J. T.; Alvarez, M.; Murthy, S.; Vezmar, I.; Wang, Z. L.; Stephens, P. W.; Cleveland, C. L.; Luetke, W. D.; Landman, U. Nanocrystal Gold Molecules. *Adv. Mater.* **1996**, *8*, 428–433.
- (142) Whetten, R. L.; Shafiqullin, M. N.; Khoury, J. T.; Schaaf, T. G.; Vezmar, I.; Alvarez, M. M.; Wilkinson, A. Crystal Structures of Molecular Gold Nanocrystal Arrays. *Acc. Chem. Res.* **1999**, *32*, 397–406.
- (143) Kiely, C. J.; Fink, J.; Brust, M.; Bethell, D.; Schiffrin, D. J. Spontaneous Ordering of Bimodal Ensembles of Nanoscopic Gold Clusters. *Nature* **1998**, *396*, 444–446.
- (144) (a) Schmid, G.; Meyer-Zaika, W.; Pugin, R.; Sawitowski, T.; Majoral, J. P.; Caminade, A. M.; Turrin, C. O. Naked Au₅₅ Clusters: Dramatic Effect of a Thiol-Terminated Dendrimer. *Chem.-Eur. J.* **2000**, *6*, 1693–1697. (b) Wang, S.; Sato, S.; Kimura, K. Preparation of Hexagonal-Close-Packed Colloidal Crystals of Hydrophilic Monodisperse Gold Nanoparticles in Bulk Aqueous Solution. *Chem. Mater.* **2003**, *15*, 2445–2448.
- (145) (a) Zanchet, D.; Hall, B. D.; Ugarte, D. Structure Population in Thiol-Passivated Gold Nanoparticles. *J. Phys. Chem. B* **2000**, *104*, 11013–11018. (b) Wang, S.; Sato, S.; Kimura, K. Influence of Organic Vapors on the Self-assembly of Gold Nanoparticles at Solution-gas Interfaces. *Chem. Lett.* **2003**, *32*, 520–521.
- (146) Schön, G.; Simon, U. A Fascinating New Field in Colloid Science: Small Ligand-Stabilized Metal Clusters and Possible Application in Microelectronics. Part I. State of the Art. *Colloid Polym. Sci.* **1995**, *273*, 101–117.
- (147) Schön, G.; Simon, U. A Fascinating New Field in Colloid Science: Small Ligand-Stabilized Metal Clusters and Their Possible Application in Microelectronics. Part II. Future Directions. *Colloid Polym. Sci.* **1995**, *273*, 202–218.
- (148) Van Kempen, H.; Dubois, J. G. A.; Gerritsen, J. W.; Schmid, G. Small Metallic Particles Studied by Scanning Tunneling Microscopy. *Physica B* **1995**, *204*, 51–56.
- (149) Dubois, J. G. A.; Gerritsen, J. W.; Shafraanjuk, S. E.; Boon, E. F. G.; Schmid, G.; van Kempen. Coulomb Staircases and Quantum Size Effects in Tunneling Spectroscopy on Ligand-Stabilized Metal Clusters. *Europhys. Lett.* **1996**, *33*, 279–284.

- (150) Bzryadin, A.; Dekker, C.; Schmid, G. Electrostatic Trapping of Single Conducting Nanoparticles Between Nanoelectrodes. *Appl. Phys. Lett.* **1997**, *71*, 1273–1275.
- (151) Templeton, A. C.; Hostetler, M. J.; Kraft, C. T.; Murray, R. W. Reactivity of Monolayer-Protected Gold Cluster Molecules: Steric Effects. *J. Am. Chem. Soc.* **1998**, *120*, 1906–1911.
- (152) Badia, A.; Cuccia, L.; Demers, L.; Morin, F.; Lennox, R. B. Structure and Dynamics in Alkanethiolate Monolayers Self-Assembled on Gold Nanoparticles: A DSC, FT-IR, and Deuterium NMR Study. *J. Am. Chem. Soc.* **1997**, *119*, 2682–2692.
- (153) Badia, A.; Demers, L.; Dickinson, L.; Morin, F. G.; Lennox, R. B.; Reven, L. Gold–Sulfur Interactions in Alkylthiol Self-Assembled Monolayers Formed on Gold Nanoparticles Studied by Solid-State NMR. *J. Am. Chem. Soc.* **1997**, *119*, 11104–11105.
- (154) Ulman, A. Formation and Structure of Self-Assembled Monolayers. *Chem. Rev.* **1996**, *96*, 1533–1554.
- (155) de Dios, A. C.; Abraham, A. E. ¹³C Chemical Shifts in Octanethiols Adsorbed on Gold: a Theoretical Study. *J. Mol. Struct.* **2002**, *602–603*, 209–214.
- (156) Schnabel, U.; Fischer, C.-H.; Kenndler, E. Characterization of Colloidal Gold Nanoparticles According to Size by Capillary Zone Electrophoresis. *J. Microcolumn Sep.* **1997**, *9*, 529–534.
- (157) Puech, K.; Henari, F. Z.; Blau, W. J.; Duff, D.; Schmid, G. Investigation of the Ultrafast Dephasing Time of Gold Nanoparticles Using Incoherent Light. *Chem. Phys. Lett.* **1995**, *247*, 13–17.
- (158) Zanchet, D.; Tolentino, H.; Alves, M. C. M.; Alves, O. L.; Ugarte, D. Inter-Atomic Distance Contraction in Thiol-Passivated Gold Nanoparticles. *Chem. Phys. Lett.* **2000**, *323*, 167–172.
- (159) Arnold, R. J.; Reilly, J. P. High-Resolution Time-of-Flight Mass Spectra of Alkanethiolate-Coated Gold Nanocrystals. *J. Am. Chem. Soc.* **1998**, *120*, 1528–1532.
- (160) (a) Terrill, R. H.; Postlethwaite, T. A.; Chen, C.-H.; Poon, C.-D.; Terzis, A.; Chen, A.; Hutchison, J. E.; Clark, M. R.; Wignall, G.; Londono, J. D.; Superfine, R.; Falvo, M.; Johnson, C. S., Jr.; Samulski, E. T.; Murray, R. W. Monolayers in Three Dimensions: NMR, SAXS, Thermal, and Electron Hopping Studies of Alkanethiol Stabilized Gold Clusters. *J. Am. Chem. Soc.* **1995**, *117*, 12537–12548. (b) Kitchin, J. R.; Barteau, M. A.; Chen, J. G. A Comparison of Gold and Molybdenum Nanoparticles on TiO₂(110) 1 × 2 Reconstructed Single-Crystal Surfaces. *Surf. Sci.* **2003**, *526*, 323–331. (c) Kawasaki, T.; Takai, Y. Phase Reconstruction with Simultaneous Correction of Spherical and Astigmatic Aberrations by Three-Dimensional Fourier Filtering Methodology. *Surf. Interface Anal.* **2003**, *35*, 51–54. (d) Qi, W. H.; Wang, M. P. Size Dependence of Vacancy Formation Energy of Metallic Nanoparticles. *Physica B* **2003**, *334*, 432–435.
- (161) Schmid, G.; Lehnert, A.; Malm, J.-O.; Bovin, J.-O. Ligand-Stabilized Bimetallic Colloids Identified by HRTEM and EDX. *Angew. Chem., Int. Ed. Engl.* **1991**, *30*, 874–876.
- (162) Schierhorn, M.; Marzán-Liz, L. M. Synthesis of Bimetallic Colloids with Tailored Intermetallic Separation. *Nano Lett.* **2002**, *2*, 13–16.
- (163) Cao, Y. W.; Jin, R.; Mirkin, C. A. DNA-Modified Core–Shell Ag/Au Nanoparticles. *J. Am. Chem. Soc.* **2001**, *123*, 7961–7962.
- (164) Hutter, E.; Fendler, J. H. Size Quantized Formation and Self-Assembly of Gold Encased Silver Nanoparticles. *Chem. Commun.* **2002**, 378–379.
- (165) Moskovits, M.; Srnová-Sloufová, I.; Vlcková, B. Bimetallic Ag–Au Nanoparticles: Extracting Meaningful Optical Constants from the Surface-Plasmon Extinction Spectrum. *J. Chem. Phys.* **2002**, *116*, 10435–10446.
- (166) (a) Shon, Y.-S.; Dawson, G. B.; Porter, M.; Murray, R. W. Monolayer-Protected Bimetal Cluster Synthesis by Core Metal Galvanic Exchange Reaction. *Langmuir* **2002**, *18*, 3880–3885. (b) Huang, T.; Murray, R. W. Luminescence of Topronin Monolayer-Protected Silver Clusters Changes To That of Gold Clusters upon Galvanic Core Metal Exchange. *J. Phys. Chem. B* **2003**, *107*, 7434–7440.
- (167) Hostetler, M. J.; Zhong, C.-J.; Yen, B. K. H.; Andereg, J.; Gross, S. M.; Evans, N. D.; Porter, M.; Murray, R. W. Stable, Monolayer-Protected Metal Alloy Clusters. *J. Am. Chem. Soc.* **1998**, *120*, 9396–9697.
- (168) (a) Shibata, T.; Bunker, B. A.; Zhang, Z.; Meisel, D.; Vardeman, C. F., II; Gezelter, J. D. Size-Dependent Spontaneous Alloying of Au–Ag Nanoparticles. *J. Am. Chem. Soc.* **2002**, *124*, 11989–11996. (b) Mandal, S.; Selvakannan, P. R.; Pasricha, R.; Sastry, M. Keggin Ions as UV–Switchable Reducing Agents in the Synthesis of Au Core–Ag Shell Nanoparticles. *J. Am. Chem. Soc.* **2003**, *125*, 8440–8441.
- (169) Norsten, T. B.; Frankamp, B. L.; Rotello, V. M. Metal Directed Assembly of Terpyridine-Functionalized Gold Nanoparticles. *Nano Lett.* **2002**, *2*, 1345–1348.
- (170) Ravel, B.; Carpenter, E. E.; Harris, V. G. Oxidation of Iron in Iron/Gold Core/Shell Nanoparticles. *J. Appl. Phys.* **2002**, *91*, 8195–8197.
- (171) Bian, B.; Hirotsu, Y. Preparation of Thin Films of Oriented Iron Nanocrystals. *Jpn. J. Appl. Phys.* **1997**, *36*, 1232–1235.
- (172) Vacassy, R.; Lemaire, L.; Valmalette, J.-C.; Dutta, J.; Hofmann, H. Synthesis of Zirconia-Coated Gold Nanoparticles. *J. Mater. Sci. Lett.* **1998**, *17*, 1665–1667.
- (173) Kolny, J.; Kornowski, A.; Weller, H. Self-Organization of Cadmium Sulfide and Gold Nanoparticles by Electrostatic Interaction. *Nano Lett.* **2002**, *2*, 361–364.
- (174) Yang, Y.; Shi, J.; Chen, H.; Dai, S.; Liu, Y. Enhanced Off-Resonance Optical Nonlinearities of Au@CdS Core–Shell Nanoparticles Embedded in BaTiO₃ Thin Films. *Chem. Phys. Lett.* **2003**, *370*, 1–6.
- (175) Horváth, D.; Toth, L.; Gucci, L. Gold Nanoparticles: Effect of Treatment on Structure and Catalytic Activity of Au/Fe₂O₃ Catalyst Prepared by Co–Precipitation. *Catal. Lett.* **2000**, *67*, 117–128.
- (176) Ascencio, J. A.; Mejia, Y.; Liu, H. B.; Angeles, C.; Canizal, G. Bioreduction Synthesis of Eu–Au Nanoparticles. *Langmuir* **2003**, *19*, 5882–5886.
- (177) Tuzar, Z.; Kratochvil, P. *Surface and Colloid Science*; Plenum Press: New York, 1993; Vol. 15.
- (178) Birtcher, R. C.; McCormick, A. W.; Baldo, P. M.; Toyoda, N.; Yamada, I.; Matsuo, J. Gold Nanoparticles Sputtered by Single Ions and Clusters. *NIM Phys. Res. B* **2003**, *206*, 851–854.
- (179) Napper, D. H. *Polymeric Stabilization of Colloidal Dispersions*; Academic Press: London, 1983.
- (180) Mayer, A. B. R.; Mark, J. E. In *Nanotechnology, Molecularly Designed Materials*; Chow, G. M., Gonsalves, K. E., Eds.; ACS Symposium Series 622; American Chemical Society: Washington, DC, 1996.
- (181) Roucoux, A.; Schulz, J.; Patin, H. Reduced Transition Metal Colloids: A Novel Family of Reusable Catalysts? *Chem. Rev.* **2002**, *102*, 3757–3778.
- (182) Ziolo, R. F.; Giannelis, E. P.; Weinstein, B. A.; O'Horo, M. P.; Gamguly, B. N.; Mehrota, V.; Russel, M. W.; Huffman, D. R. Matrix-Mediated Synthesis of Nanocrystalline γ -Fe₂O₃: A New Optically Transparent Magnetic Material. *Science* **1992**, *257*, 219–223.
- (183) Jordan, R.; West, N.; Chou, Y.-M.; Nuyken, O. Nanocomposites by Surface-Initiated Living Cationic Polymerization of 2-Oxazolines on Functionalized Gold Nanoparticles. *Macromolecules* **2001**, *34*, 1606–1611.
- (184) Selvan, S. T.; Spatz, J. P.; Klock, H.-A.; Möller, M. Gold-Polypyrrole Core–Shell Particles in Diblock Copolymer Micelles. *Adv. Mater.* **1998**, *10*, 132–134.
- (185) Sayo, K.; Deki, S.; Hayashi, S. A Novel Method of Preparing Nano-Sized Gold and Palladium Particles Dispersed in Composites That Uses the Thermal Relaxation Technique. *Eur. Phys. J. D* **1999**, *9*, 429–432.
- (186) (a) Lee, J.; Sundar, V. C.; Heine, J. R.; Bawendi, M. G.; Jensen, K. F. Full Color Emission from II–VI Semiconductor Quantum Dot-Polymer Composites. *Adv. Mater.* **2000**, *12*, 1102–1105. (b) Teichroeb, J. H.; Forrest, J. A. Direct Imaging of Nanoparticle Embedding to Probe Viscoelasticity of Polymer Surfaces. *Phys. Rev. Lett.* **2003**, *91*, 016104-1–016104-4. (c) Raula, J.; Shan, J.; Nuopponen, M.; Niskanen, A.; Jiang, H.; Kauppinen, E. I.; Tenhu, H. Synthesis of Gold Nanoparticles Grafted with a Thermoresponsive Polymer by Surface-Induced Reversible-Addition-Fragmentation Chain-Transfer Polymerization. *Langmuir* **2003**, *19*, 3499–3504.
- (187) Corbier, M. K.; Cameron, N. S.; Sutton, M.; Mochrie, S. G. J.; Lurio, L. B.; Rühm, A.; Lennox, R. B. Polymer-Stabilized Gold Nanoparticles and Their Incorporation into Polymer Matrices. *J. Am. Chem. Soc.* **2001**, *123*, 10411–10412.
- (188) Kolb, U.; Quaiser, S. A.; Winter, M.; Reetz, M. T. Investigation of Tetraalkylammonium Bromide Stabilized Palladium/Platinum Bimetallic Clusters Using Extended X-ray Absorption Fine Structure Spectroscopy. *Chem. Mater.* **1996**, *8*, 1889–1894.
- (189) Hirai, H.; Toshima, N. In *Polymer-Attached Catalysts*; Iwasawa, Y., Ed.; Kluwer: Dordrecht, 1986.
- (190) Toshima, N.; Yonezawa, T. Bimetallic Nanoparticles–Novel Materials for Chemical and Physical Applications. *New J. Chem.* **1998**, 1179–1201.
- (191) Hirai, H.; Nakao, Y.; Toshima, N. Preparation of Colloidal Transition Metals in Polymers by Reduction with Alcohols or Ethers. *J. Macromol. Sci. Chem.* **1979**, *A13*, 727–750.
- (192) Teranishi, T.; Miyake, M. Size Control of Metal Nanoparticles with Aid of Surface Protection by Polymer. *Hyomen* **1997**, *35*, 439–452.
- (193) Esumi, K.; Susuki, A.; Aihara, N.; Usui, K.; Torigoe, K. Preparation of Gold Colloids with UV Irradiation Using Dendrimers as Stabilizer. *Langmuir* **1998**, *14*, 3157–3159.
- (194) Reetz, M. T.; Helbig, W. Size-Selective Synthesis of Nanostructured Transition Metal Clusters. *J. Am. Chem. Soc.* **1994**, *116*, 7401–7402.
- (195) Schaaf, T. G.; Whetten, R. L. Giant Gold-Glutathione Cluster Compounds: Intense Optical Activity in Metal-Based Transitions. *J. Phys. Chem. B* **2000**, *104*, 2630–2641.
- (196) (a) Toshima, N.; Harada, M.; Yamazaki, Y.; Asakura, K. Catalytic Activity and Structural Analysis of Polymer-Protected Gold–Palladium Bimetallic Clusters Prepared by the Simultaneous

- Reduction of Hydrogen Tetrachloroaurate and Palladium Dichloride. *J. Phys. Chem.* **1992**, *96*, 9927–9933. (b) Harada, M.; Asakura, K.; Toshima, N. Catalytic Activity and Structural Analysis of Polymer-Protected Au/Pd Bimetallic Clusters Prepared by the Successive Reduction of H₂AuCl₄ and PdCl₂. *J. Phys. Chem.* **1993**, *97*, 5103–5114.
- (197) Toshima, N.; Yonezawa, T. Preparation of Polymer-Protected Gold/Platinum Bimetallic Clusters and Their Application to Visible Light-Induced Hydrogen Evolution. *Makromol. Chem., Macromol. Symp.* **1992**, *59*, 281–295.
- (198) Yonezawa, T.; Toshima, N. Polymer- and Micelle-Protected Gold/Platinum Bimetallic Systems. Preparation, Application to Catalysis for Visible-Light-Induced Hydrogen Evolution, and Analysis of Formation Process with Optical Methods. *J. Mol. Catal.* **1993**, *83*, 167–181.
- (199) Yonezawa, T.; Toshima, N. Mechanistic Consideration of Formation of Polymer-Protected Nanoscopic Bimetallic Clusters. *J. Chem. Soc., Faraday Trans.* **1995**, *91*, 4111–4119.
- (200) Astruc, D. Redox Catalysis. *Electron Transfer and Radical Processes in Transition Metal Chemistry*; VCH: New York, 1995; Chapter 7.
- (201) Harada, M.; Asakura, K.; Toshima, N. J. Catalytic Activity and Structural Analysis of Polymer-Protected Gold/Palladium Bimetallic Clusters Prepared by the Successive Reduction of Hydrogen Tetrachloroaurate(III) and Palladium Dichloride. *J. Phys. Chem.* **1993**, *97*, 5103.
- (202) Spatz, J. P.; Mössmer, S.; Möller, M. Mineralization of Gold Nanoparticles in a Block Copolymer Microemulsion. *Chem.–Eur. J.* **1996**, *12*, 1552–1555.
- (203) Spatz, J. P.; Mössmer, S.; Möller, M. Metastable Reverse Globular Micelles and Giant Micellar Wires from Block Copolymers. *Angew. Chem., Int. Ed. Engl.* **1996**, *35*, 1510–1512.
- (204) Spatz, J. P.; Roescher, A.; Möller, M. Gold Nanoparticles in Micellar Poly(Styrene)-*b*-Poly(Ethyleneoxide) Films. *Adv. Mater.* **1996**, *8*, 337–340.
- (205) Bronstein, L. M.; Chernyshov, D. M.; Timofeeva, G. I.; Dubrovina, L. V.; Valetsky, P. M.; Obolonkova, E. S.; Khokhlov, A. R. Interaction of Polystyrene-Block-Poly(Ethylene Oxide) Micelles with Cationic Surfactant in Aqueous Solutions. Metal Colloid Formation in Hybrid Systems. *Langmuir* **2000**, *16*, 3626–3632.
- (206) Frankamp, B. L.; Uzun, O.; Ilhan, F.; Boal, A. K.; Rotello, V. M. Recognition-Mediated Assembly of Nanoparticles into Micellar Structures with Diblock Copolymers. *J. Am. Chem. Soc.* **2002**, *124*, 892–893.
- (207) Spatz, J. P.; Mössmer, S.; Harmann, C.; Möller, M.; Herzog, T.; Krieger, M.; Boyen, H.-G.; Ziemann, P.; Kabius, B. Ordered Deposition of Inorganic Clusters from Micellar Block Copolymer Films. *Langmuir* **2000**, *16*, 407–415.
- (208) Gohy, J. F.; Willet, N.; Varshney, S.; Zhang, J.-X.; Jérôme, R. Core–Shell–Corona Micelles with a Responsive Shell. *Angew. Chem., Int. Ed.* **2001**, *40*, 3214–3216.
- (209) Youk, J. H.; Park, M. K.; Locklin, J.; Advincula, R.; Yang, J.; Mays, J. Preparation of Aggregation Stable Gold Nanoparticles Using Star-Block Copolymers. *Langmuir* **2002**, *18*, 2455–2458.
- (210) Walker, C. H.; St John, J. V.; Wisian-Neilson, P. Synthesis and Size Control of Gold Nanoparticles Stabilized by Poly(Methylphenylphosphazene). *J. Am. Chem. Soc.* **2001**, *123*, 3846–3847.
- (211) Otsuka, H.; Akiyama, Y.; Nagasaki, Y.; Kataoka, K. Quantitative and Reversible Lectin-Induced Association of Gold Nanoparticles Modified with γ -Lactosyl-Mercapto-Poly(Ethylene Glycol). *J. Am. Chem. Soc.* **2001**, *123*, 8226–8230.
- (212) Nuss, S.; Böttcher, H.; Wurm, H.; Hallensleben, M. L. Gold Nanoparticles with Covalently Attached Polymer Chains. *Angew. Chem., Int. Ed.* **2001**, *40*, 4016–4018.
- (213) Mandal, T. K.; Fleming, M. S.; Walt, D. R. Preparation of Polymer Coated Gold Nanoparticles by Surface-Confined Living Radical Polymerization at Ambient Temperature. *Nano Lett.* **2002**, *2*, 3–7.
- (214) Ohno, K.; Hoh, K.-m.; Tsuji, Y.; Fukuda, T. Synthesis of Gold Nanoparticles Coated with Well-Defined, High-Density Polymer Brushes by Surface-Initiated Living Radical Polymerization. *Macromolecules* **2002**, *35*, 8989–8993.
- (215) Kamata, K.; Lu, Y.; Xia, Y. Synthesis and Characterization of Monodispersed Core–Shell Spherical Colloids with Movable Cores. *J. Am. Chem. Soc.* **2003**, *125*, 2384–2385.
- (216) (a) Marinakos, S. M.; Shultz, D. A.; Feldheim, D. L. Gold Nanoparticles as Templates for the Synthesis of Hollow Nanometer-Sized Conductive Polymer Capsules. *Adv. Mater.* **1999**, *11*, 34–37. (b) Chah, S.; Fendler, J. H.; Yi, J. Nanostructured Gold Hollow Microspheres Prepared on Dissolvable Ceramic Hollow Sphere Templates. *J. Colloid Interface Sci.* **2002**, *250*, 142–148. (c) Marinakos, S. M.; Novak, J. P.; Brousseau, L. C., III; House, A. B.; Edeki, E. M.; Feldhaus, J. C.; Feldheim, D. L. Gold Particles as Templates for the Synthesis of Hollow Polymer Capsules. Control of Capsule Dimensions and Guest Encapsulation. *J. Am. Chem. Soc.* **1999**, *121*, 8518–8522.
- (217) Naka, K.; Itoh, H.; Chujo, Y. Effect of Gold Nanoparticles as a Support for the Oligomerization of L-Cysteine in an Aqueous Solution. *Langmuir* **2003**, *19*, 5546–5549.
- (218) Sohn, B.-H.; Seo, B.-W.; Yoo, S.-I. Changes of the Lamellar Period by Nanoparticles in the Nanoreactor Scheme of Thin Films of Symmetric Diblock Copolymers. *J. Mater. Chem.* **2002**, *12*, 1730–1734.
- (219) Cant, N. E.; Critchley, K.; Zhang, H.-L.; Evans, S. D. Surface Functionalization for the Self-Assembly of Nanoparticle/Polymer Multilayer Films. *Thin Solid Films* **2003**, *426*, 31–39.
- (220) Gonsalves, K. E.; Carlson, G.; Chen, X.; Kumar, J.; Aranda, F.; Perez, R.; Jose-Yacamán, M. Surface-Functionalized Nanostructured Gold/Polymer Composite Films. *J. Mater. Sci. Lett.* **1996**, *15*, 948–951.
- (221) Mayer, A. B. R.; Mark, J. E. Colloidal Gold Nanoparticles Protected by Water-Soluble Homopolymers and Random Copolymers. *Eur. Polym. J.* **1998**, *34*, 103–108.
- (222) Teranishi, T.; Kiyokawa, I.; Miyake, M. Synthesis of Monodisperse Gold Nanoparticles Using Linear Polymers as Protective Agents. *Adv. Mater.* **1998**, *10*, 596–599.
- (223) Watson, K. J.; Zhu, J.; Nguyen, S. B. T.; Mirkin, C. A. Hybrid Nanoparticles with Block Copolymer Shell Structures. *J. Am. Chem. Soc.* **1999**, *121*, 462–463.
- (224) Watson, K. J.; Zhu, J.; Nguyen, S. B. T.; Mirkin, C. A. Redox-Active Polymer-Nanoparticle Hybrid Materials. *Pure Appl. Chem.* **2000**, *72*, 67–72.
- (225) Grabar, K. C.; Allison, K. J.; Baker, B. E.; Bright, R. M.; Brown, K. R.; Freeman, R. G.; Fox, A. P.; Keating, C. D.; Musick, M. D.; Natan, M. J. Two-Dimensional Arrays of Colloidal Gold Particles: A Flexible Approach to Macroscopic Metal Surfaces. *Langmuir* **1996**, *12*, 2353–2361.
- (226) Kim, M.; Sohn, K.; Na, H. B.; Hyeon, T. Synthesis of Nanorattles Composed of Gold Nanoparticles Encapsulated in Mesoporous Carbon and Polymer Shells. *Nano Lett.* **2002**, *2*, 1383–1387.
- (227) Wolfe, D. B.; Oldenburg, S. J.; Westcott, S. L.; Jackson, J. B.; Paley, M. S.; Halas, N. J. Photodeposition of Molecular Layers on Nanoparticle Substrates. *Langmuir* **1999**, *15*, 2745–2748.
- (228) Takagi, K.; Ishiwatari, T. Polymer Chain-Guided Arrangement of Gold Nanoparticles. *Chem. Lett.* **2002**, 990–991.
- (229) Wang, J.; Neoh, K. G.; Kang, E. T. Preparation of Nanosized Metallic Particles in Polyaniline. *J. Colloid Surf. Sci.* **2001**, *239*, 78–86.
- (230) Shchukin, D. G.; Caruso, R. A. Template Synthesis of Porous Gold Microspheres. *Chem. Commun.* **2003**, 1478–1479.
- (231) Walker, C. H.; St. John, J. V.; Wisian-Neilson, P. Synthesis and Size Control of Gold Nanoparticles Stabilized by Poly(methylphenylphosphazene). *J. Am. Chem. Soc.* **2001**, *123*, 3846–3847.
- (232) (a) Mayer, C. R.; Neveu, S.; Cabuil, V. A Nanoscale Hybrid System Based on Gold Nanoparticles and Heteropolyanions. *Angew. Chem., Int. Ed.* **2002**, *41*, 501–503. (b) Mayer, C. R.; Neveu, S.; Simonnet-Jégat, C.; Debiemme-Chouvy, C.; Cabuil, V.; Secheresse, F. Nanocomposite Systems Based on Gold Nanoparticles and Thiometalates. From Colloids to Networks. *J. Mater. Chem.* **2003**, *13*, 338–341.
- (233) (a) Shan, J.; Nuopponen, M.; Jiang, H.; Kauppinen, E.; Tenhu, H. Preparation of Poly(*N*-isopropylacrylamide)-Monolayer-Protected Gold Clusters: Synthesis Methods, Core Size, and Thickness of Monolayer. *Macromolecules* **2003**, *36*, 4526–4533. (b) Dai, X.; Tan, Y.; Xu, J. Formation of Gold Nanoparticles in the Presence of *o*-Anisidine and the Dependence of the Structure of Poly(*o*-anisidine) on Synthetic Conditions. *Langmuir* **2002**, *18*, 9010–9016.
- (234) Zhou, Y.; Itoh, H.; Uemura, T.; Naka, K.; Chujo, Y. Preparation of π -Conjugated Polymer-Protected Gold Nanoparticles in Stable Colloidal Form. *Chem. Commun.* **2001**, 613–614.
- (235) Youk, J. H.; Park, M.-K.; Locklin, J.; Advincula, R.; Yang, J.; Mays, J. Preparation of Aggregation Stable Gold Nanoparticles Using Star-Block Copolymers. *Langmuir* **2002**, *18*, 2455–2458.
- (236) (a) Mangeney, C.; Ferrage, F.; Aujard, I.; Marchi-Artzner, V.; Jullien, L.; Ouari, O.; El Rekaï, D.; Laschewsky, A.; Vikholm, I.; Sadowski, J. W. Synthesis and Properties of Water-Soluble Gold Colloids Covalently Derivatized with Neutral Polymer Monolayers. *J. Am. Chem. Soc.* **2002**, *124*, 5811–5821. (b) Cole, D. H.; Shull, K. R.; Rehn, L. E.; Baldo, P. M. RBS Analysis of the Diffusion of Nano-Size Spheres in a Polymer Matrix. *Nucl. Instrum. Methods Phys. Res. B* **1998**, *136–138*, 283–289. (c) Liang, Z.; Susha, A.; Caruso, F. Gold Nanoparticle-Based Core–Shell and Hollow Spheres and Ordered Assemblies Thereof. *Chem. Mater.* **2003**, *15*, 3176–3183.
- (237) Chechik, V.; Crooks, R. M. Monolayers of Thiol-Terminated Dendrimers on the Surface of Planar and Colloidal Gold. *Langmuir* **1999**, *15*, 6364–6369.
- (238) Esumi, K.; Hosoya, T.; Suzuki, A.; Torigoe, K. Preparation of Hydrophobically Modified Poly(amidoamine) Dendrimer-Encapsulated Gold Nanoparticles in Organic Solvents. *J. Colloid Interface Sci.* **2000**, *229*, 303–306.
- (239) Krasteva, N.; Besnard, I.; Guse, B.; Bauer, R. E.; Müllen, K.; Yasuda, A.; Vossmeier, T. Self-Assembled Gold Nanoparticle/

- Dendrimer Composite Films for Vapor Sensing Applications. *Nano Lett.* **2002**, *2*, 551–555.
- (240) He, J.-A.; Valluzzi, R.; Yang, K.; Dolukhanyan, T.; Sung, C.; Kumar, J.; Tripathy, S. K. Electrostatic Multilayer Deposition of a Gold-Dendrimer Nanocomposite. *Chem. Mater.* **1999**, *11*, 3268–3274.
- (241) Won, J.; Ihn, K. J.; Kang, Y. S. Gold Nanoparticle Patterns of Polymer Films in the Presence of Poly(amidoamine) Dendrimers. *Langmuir* **2002**, *18*, 8246–8249.
- (242) Esumi, K.; Kameo, A.; Suzuki, A.; Torigoe, K. Preparation of Gold Nanoparticles in Formamide and *N,N*-dimethylformamide in the Presence of Poly(amidoamine) Dendrimers with Surface Methyl Ester Groups. *Colloids Surf.* **2001**, *189*, 155–161.
- (243) Frankamp, B. L.; Boal, A. K.; Rotello, V. M. Controlled Interparticle Spacing through Self-Assembly of Au Nanoparticles and Poly(amidoamine) Dendrimers. *J. Am. Chem. Soc.* **2002**, *124*, 15146–15147.
- (244) Zhou, Y.; Ma, C.; Itoh, H.; Naka, K.; Chujo, Y. A Simple In Situ Hydrogen Interaction to Homogeneous Dispersion of Gold Nanoparticles in SiO₂ Matrix Using Dendrimer as Template. *Chem. Lett.* **2002**, 1170–1171.
- (245) Zheng, J.; Stevenson, M. S.; Hikida, R. S.; Van Patten, G. P. Influence of pH on Dendrimer-Protected Nanoparticles. *J. Phys. Chem. B* **2002**, *106*, 1252–1255.
- (246) Bielinska, A.; Eichman, J. D.; Lee, I.; Baker, J. R., Jr.; Balogh, L. Imaging {Au⁰-PANAM} Gold-Dendrimer Nanocomposites in Cells. *J. Nanopart. Res.* **2002**, *4*, 395–403.
- (247) (a) Zhao, M.; Crooks, R. M. Intradendrimer Exchange of Metal Nanoparticles. *Chem. Mater.* **1999**, *11*, 3379–3385. (b) Gröhn, F.; Bauer, B. J.; Akpalu, Y. A.; Jackson, C. L.; Amis, E. J. Dendrimer Templates for the Formation of Gold Nanoclusters. *Macromolecules* **2000**, *33*, 6042–6050.
- (248) Crooks, R. M.; Zhao, M.; Sun, L.; Chechik, V.; Yeung, L. K. Dendrimers-Encapsulated Metal Nanoparticles: Synthesis, Characterization, and Applications to Catalysis. *Acc. Chem. Res.* **2001**, *34*, 181–190.
- (249) Niu, Y.; Crooks, R. M. Dendrimer-Encapsulated Metal Nanoparticles and Their Applications to Catalysis. In *Dendrimers and Nanoscience*; Astruc, D., Ed.; Comptes-Rendus Chimie, Elsevier: Paris, 2003; in press.
- (250) Daniel, M.-C.; Ruiz, J.; Nlate, J.; Palumbo, J.; Blais, J.-C.; Astruc, D. Gold Nanoparticles Containing Redox-Active Supramolecular Dendrons that Recognize H₂PO₄⁻. *Chem. Commun.* **2001**, 2000–2001.
- (251) Daniel, M.-C.; Ruiz, J.; Nlate, S.; Blais, J.-C.; Astruc, D. Nanoscopic Assemblies Between Supramolecular Redox Active Metallodendrons and Gold Nanoparticles: Synthesis, Characterisation and Selective Recognition of H₂PO₄⁻, HSO₄⁻ and Adenosine-5'-Triphosphate (ATP²⁻) Anions. *J. Am. Chem. Soc.* **2003**, *125*, 2617–2628.
- (252) Astruc, D.; Blais, J.-C.; Daniel, M.-C.; Nlate, S.; Ruiz, J. Metallodendrimers and Dendronized Gold Colloids as Nanocatalysts, Nanosensors and Nanomaterials for Molecular Electronics. In *Dendrimers and Nanosciences*, *Comptes Rendus Chimie*; Astruc, D., Ed.; Elsevier: Paris, 2003; in press.
- (253) Wang, R.; Yang, J.; Zheng, Z.; Carducci, M. D.; Jiao, J.; Seraphin, S. Dendron-Controlled Nucleation and Growth of Gold Nanoparticles. *Angew. Chem., Int. Ed.* **2001**, *40*, 549–552.
- (254) Kim, M.-K.; Jeon, Y.-M.; Jeon, W. S.; Kim, H.-J.; Hong, S. G.; Park, C. G.; Kim, K. Novel Dendron-Stabilized Gold Nanoparticles with High Stability and Narrow Size Distribution. *Chem. Commun.* **2001**, 667–668. (b) Gopidas, K. R.; Whitesell, J. K.; Fox, M.-A. Nanoparticle-Cored Dendrimers: Synthesis and Characterization. *J. Am. Chem. Soc.* **2003**, *125*, 6491–6502.
- (255) (a) Krastena, N.; Krustev, R.; Yasuda, A.; Vossmeier, T. Vapor Sorption in Self-Assembled Gold Nanoparticle/Dendrimer Films Studied by Specular Neutron Reflectometry. *Langmuir* **2003**, *19*, 7754–7760. (b) Kimura, K.; Takashima, S.; Ohshima, H. Molecular Approach to the Surface Potential Estimate of Thiolate-Modified Gold Nanoparticles. *J. Phys. Chem. B* **2002**, *106*, 7260–7266. (c) Taubert, A.; Wiesler, U.-M.; Müllen, K. Dendrimer-Controlled One-Pot Synthesis of Gold Nanoparticles with a Bimodal Size Distribution and their Self-Assembly in the Solid State. *J. Mater. Chem.* **2003**, *13*, 1090–1093.
- (256) Bhat, R. R.; Fischer, D. A.; Genzer, J. Fabricating Planar Nanoparticle Assemblies with Number Density Gradients. *Langmuir* **2002**, *18*, 5640–5643.
- (257) Nagle, L.; Ryan, D.; Cobbe, S.; Fitzmaurice, D. Templated Nanoparticle Assembly on the Surface of a Patterned Nanosphere. *Nano Lett.* **2003**, *3*, 51–53.
- (258) Liu, S.; Zhu, T.; Hu, R.; Liu, Z. Evaporation-Induced Self-Assembly of Gold Nanoparticles Into a Highly Organized Two-Dimensional Array. *Phys. Chem. Chem. Phys.* **2002**, *4*, 6059–6062.
- (259) Radnik, J.; Mohr, C.; Claus, P. On the Origin of Binding Energy Shifts of Core Levels of Supported Gold Nanoparticles and Dependence of Pretreatment and Material Synthesis. *Phys. Chem. Chem. Phys.* **2003**, *5*, 172–177.
- (260) Paraschiv, V.; Zapotoczny, S.; de Jong, M. R.; Vancso, G. J.; Huskens, J.; Reinhoudt, D. N. Functional Group Transfer from Gold Nanoparticles to Flat Gold Surfaces for the Creation of Molecular Anchoring Points on Surfaces. *Adv. Mater.* **2002**, *14*, 722–726.
- (261) Geng, J.; Johnson, B. F. G.; Thomas, M. D. R.; Shephard, D. S.; Jiang, L. Behaviour of Two-Dimensional Arrays of Gold Nanoparticles Under H₂S: Agglomeration and Regeneration. *Inorg. Chim. Acta* **2002**, *330*, 33–37.
- (262) Bardotti, L.; Prével, B.; Jensen, P.; Treilleux, M.; Mélinon, P.; Perez, A.; Gierak, J.; Faini, G.; Maily, D. Organizing Nanoclusters on Functionalized Surfaces. *Appl. Surf. Sci.* **2002**, *191*, 205–210.
- (263) Haidara, H.; Mougín, K.; Schultz, J. Spontaneous Growth of Two-Dimensional Complex Patterns of Nanoparticles at Model Molecular Surfaces. *Langmuir* **2001**, *17*, 659–663.
- (264) Mougín, K.; Haidara, H.; Castelein, G. Controlling the Two-dimensional Adhesion and Organization of Colloidal Gold Nanoparticles. *Colloids Surf.* **2001**, *193*, 231–237.
- (265) Ito, S.; Yoshikawa, H.; Masuhara, H. Laser Manipulation and Fixation of Single Gold Nanoparticles in Solution at Room Temperature. *J. Appl. Phys.* **2002**, *80*, 482–484.
- (266) Murakoshi, K.; Nakato, Y. Formation of Linearly Arrayed Gold Nanoparticles on Gold Single-Crystal Surfaces. *Adv. Mater.* **2000**, *12*, 791–795.
- (267) Resch, R.; Lewis, D.; Meltzer, S.; Montoya, N.; Koel, B. E.; Madhukar, A.; Requicha, A. A. G.; Will, P. Manipulation of Gold Nanoparticles in Liquid Environments Using Scanning Force Microscopy. *Ultramicroscopy* **2000**, *82*, 135–139.
- (268) Lei, S.; Zhao, S.; Chen, S.; Ai, Z.; Wang, S. Effect of Square Wave Pulse on the Deposition Structure of Gold Nanoparticles. *J. Serb. Chem. Soc.* **1999**, *64*, 259–263.
- (269) Rudoy, V. M.; Dement'eva, O. V.; Yaminskii, I. V.; Sukhov, V. M.; Kartseva, M. E.; Ogarev, V. A. Metal Nanoparticles on Polymer Surfaces: 1. A New Method of Determining Glass Transition Temperature of the Surface Layer. *Colloid J.* **2002**, *64*, 746–754.
- (270) Schulz, F.; Franzka, S.; Schmid, G. Nanostructured Surfaces by Deposition of Metal Nanoparticles by Means of Spray Techniques. *Adv. Funct. Mater.* **2002**, *12*, 532–536.
- (271) Baur, C.; Gazen, B. C.; Koel, B. C.; Ramachandran, T. R.; Requicha, A. A. G.; Zini, L. Robotic Nanomanipulation with a Scanning Probe Microscope in a Networked Computing Environment. *J. Vac. Sci. Technol. B* **1997**, *15*, 1577–1580.
- (272) Han, M. Y.; Zhou, L.; Quek, C. H.; Li, S. F. Y.; Huang, W. Room-Temperature Coulomb Staircase on Pure and Uniform Surface-Capped Gold Nanoparticles. *Chem. Phys. Lett.* **1998**, *287*, 47–52.
- (273) Garino, J. C.; Yang, Y.; Amro, N. A.; Cruchon-Dupeyrat, S.; Chen, S.; Liu, G.-Y. Precise Positioning of Nanoparticles on Surfaces Using Scanning Probe Lithography. *Nano Lett.* **2003**, *3*, 389–395.
- (274) Zhu, T.; Fu, X.; Mu, T.; Wang, J.; Liu, Z. pH-Dependent Adsorption of Gold Nanoparticles on *p*-Aminothiophenol-Modified Gold Substrates. *Langmuir* **1999**, *15*, 5197–5199.
- (275) Chan, E. W. L.; Yu, L. Chemoselective Immobilization of Gold Nanoparticles onto Self-Assembled Monolayers. *Langmuir* **2002**, *18*, 311–313.
- (276) Menzel, H.; Mowery, M. D.; Cai, M.; Evans, C. E. Surface-Confining Nanoparticles as Substrates for Photopolymerizable Self-Assembled Monolayers. *Adv. Mater.* **1999**, *11*, 131–134.
- (277) Zhu, T.; Zhang, X.; Wang, J.; Fu, X.; Liu, Z. Assembling Colloidal Au Nanoparticles with Functionalized Self-Assembled Monolayers. *Thin Solid Films* **1998**, *327–329*, 595–598.
- (278) (a) Li, Q.; Zheng, J.; Liu, Z. Site-Selective Assemblies of Gold Nanoparticles on an AFM Tip-Defined Silicon Template. *Langmuir* **2003**, *19*, 166–171. (b) Zheng, J.; Chen, Z.; Liu, Z. Atomic Force Microscopy-Based Nanolithography on Silicon Using Colloidal Au Nanoparticles As a Nanooxidation Mask. *Langmuir* **2000**, *16*, 9673–9676. (c) Lee, K.-B.; Lim, J.-H.; Mirkin, C. A. Protein Nanostructures Formed via Direct-Write Dip-Pen Nanolithography. *J. Am. Chem. Soc.* **2003**, *125*, 5588–5589.
- (279) Tilley, R. D.; Saito, S. Preparation of Large Scale Monolayers of Gold Nanoparticles on Modified Silicon Substrates Using a Controlled Pulling Methodology. *Langmuir* **2003**, *19*, 5115–5120.
- (280) Zanella, R.; Giorgio, S.; Henry, C. R.; Louis, C. Alternative Methods for the Preparation of Gold Nanoparticles Supported on TiO₂. *J. Phys. Chem. B* **2002**, *106*, 7634–7642.
- (281) Schaaff, T. G.; Blom, D. A. Deposition of Au–Nanocrystals on TiO₂ Crystallites. *Nano Lett.* **2002**, *2*, 507–511.
- (282) Bocuzzi, F.; Chiorino, A.; Manzoli, M. FTIR Study of the Cationic Effects of CO adsorbed on Gold Nanoparticles Supported on Titania. *Surf. Sci.* **2000**, *454–456*, 942–946.
- (283) Qian, W.; Lin, L.; Deng, Y. J.; Xia, J. J.; Zou, Y. H.; Wong, G. K. L. Femtosecond Studies of Coherent Acoustic Phonons in Gold Nanoparticles Embedded in TiO₂ Thin Films. *J. Appl. Phys.* **2000**, *87*, 612–614.

- (284) (a) Yonezawa, T.; Matsune, H.; Kunitake, T. Layered Nanocomposite of Close-Packed Gold Nanoparticles and TiO₂ Gel Layers. *Chem. Mater.* **1999**, *11*, 33–35. (b) Yang, Y.; Shi, J.; Huang, W.; Dai, S.; Wang, L. Preparation and Optical Properties of Gold Nanoparticles Embedded in Barium Titanate Thin Films. *J. Mater. Sci.* **2003**, *38*, 1243–1248. (c) Lengel, G.; Ziemann, P.; Banhart, F.; Walther, P. Anomalous Behavior of Gold Nanoislands on Top of SrTiO₃(001) During their Overgrowth by Thin YBaCuO Films. *Physica C* **2003**, *390*, 175–184.
- (285) (a) Winkler, C.; Carew, A. J.; Haq, S.; Raval, R. Carbon Monoxide on γ -Alumina Single-Crystal Surfaces with Gold Nanoparticles. *Langmuir* **2003**, *19*, 717–721. (b) Hultheen, J. C.; Patrissi, C. J.; Miner, D. L.; Crosthwait, E. R.; Oberhauser, E. B.; Martin, C. R. Changes in the Shape and Optical Properties of Gold Nanoparticles Contained Within Alumina Membranes Due to Low-Temperature Annealing. *J. Phys. Chem. B* **1997**, *101*, 7727–7731. (c) García-Serrano, J.; Pal, U. Synthesis and Characterization of Au Nanoparticles in Al₂O₃ Matrix. *Hydrogen Energy* **2003**, *28*, 637–640.
- (286) Yonezawa, T.; Onoue, S.-y.; Kunitake, T. Growth of Closely Packed Layers of Gold Nanoparticles on an Aligned Ammonium Surface. *Adv. Mater.* **1998**, *10*, 414–416.
- (287) Shon, Y.-S.; Choo, H. [60]Fullerene-Linked Gold Nanoparticles: Synthesis and Layer-by-Layer Growth on a Solid Surface. *Chem. Commun.* **2002**, 2560–2561.
- (288) (a) Liu, J.; Alvarez, J.; Ong, W.; Kaifer, A. E. Network Aggregates Formed by C₆₀ and Gold Nanoparticles Capped with γ -Cyclodextrin Hosts. *Nano Lett.* **2001**, *1*, 57–60. (b) Zhu, D.; Li, Y.; Wang, S.; Shi, Z.; Du, C.; Xiao, S.; Fang, H.; Zhou, Y. Design, Synthesis and Properties of Functional Materials Based on Fullerene. *Synth. Met.* **2003**, *133–134*, 679–683.
- (289) Liu, L.; Wang, T.; Li, J.; Guo, Z.-X.; Dai, L.; Zhang, D.; Zhu, D. Self-Assembly of Gold Nanoparticles to Carbon Nanotubes Using a Thiol-Terminated Pyrene as Interlinker. *Chem. Phys. Lett.* **2003**, *367*, 747–752.
- (290) Jiang, K.; Eitan, A.; Schädler, L. S.; Ajayan, P. M.; Siegel, R. W.; Grobert, N.; Mayne, M.; Reyes-Reyes, M.; Terrones, H.; Terrones, M. Selective Attachment of Gold Nanoparticles to Nitrogen-Doped Carbon Nanotubes. *Nano Lett.* **2003**, *3*, 275–277.
- (291) Boyen, H.-G.; Herzog, Th.; Käppler, G.; Weigl, F.; Ziemann, P. X-Ray Photoelectron Spectroscopy Study on Gold Nanoparticles Supported on Diamond. *Phys. Rev. B* **2002**, *65*, 0754121–0754125.
- (292) Teranishi, T.; Sugawara, A.; Shimizu, T.; Miyake, M. Planar Array of 1D Gold Nanoparticles on Ridge-and-Valley Structured Carbon. *J. Am. Chem. Soc.* **2002**, *124*, 4210–4211.
- (293) (a) Kuwahara, Y.; Akiyama, T.; Yamada, S. Construction of Gold Nanoparticle-Ruthenium (II) Tris(2,2'-bipyridine) Self-Assembled Multistructures and Their Photocurrent Responses. *Thin Solid Films* **2001**, *393*, 273–277. (b) Gittins, D. I.; Susha, A. S.; Schoeler, B.; Caruso, F. Dense Nanoparticulate Thin Films via Gold Nanoparticle Self-Assembly. *Adv. Mater.* **2002**, *14*, 508–512.
- (294) (a) Seitz, O.; Chehimi, M. M.; Cabot-Deliry, E.; Truong, S.; Felidj, N.; Perruchot, C.; Greaves, S. J.; Watts, J. F. Preparation and Characterization of Gold Nanoparticles Assemblies on Silanised Glass Plates. *Colloids Surf.* **2003**, *218*, 225–239. (b) Hrapovic, S.; Liu, Y.; Enright, G.; Bensebaa, F.; Luong, J. H. T. New Strategy for Preparing Thin Gold Films on Modified Glass Surfaces by Electroless Deposition. *Langmuir* **2003**, *19*, 3958–3965.
- (295) Gu, Z.-Z.; Horie, R.; Kubo, S.; Yamada, Y.; Fujishima, A.; Sato, O. Fabrication of a Metal-Coated Three-Dimensionally Ordered Macroporous Film and its Application as a Refractive Index Sensor. *Angew. Chem., Int. Ed.* **2002**, *41*, 1153–1156.
- (296) He, T.; Ma, Y.; Cao, Y.-A. C.; Yang, W.-S.; Yao, J.-N. Improved Photochromism of WO₃ Thin Films by Addition of Au Nanoparticles. *Phys. Chem. Chem. Phys.* **2002**, *4*, 1637–1639.
- (297) (a) Deki, S.; Ko, H. Y. Y.; Fujita, T.; Akamatsu, K.; Mizuhata, M.; Kajinami, A. Synthesis and Microstructure of Metal Oxide Thin Films Containing Metal Nanoparticles by Liquid-Phase Deposition (LPD) Methodology. *Eur. Phys. J. D* **2001**, *16*, 325–328. (b) Deki, S.; Nabika, H.; Akamatsu, K.; Mizuhata, M.; Kajinami, A.; Tomita, S.; Fujii, M.; Hayashi, S. Fabrication and Characterization of PAN-Derived Carbon Thin Films Containing Au Nanoparticles. *Thin Solid Films* **2002**, *408*, 59–63.
- (298) (a) Raguse, B.; Müller, K.-H.; Wiecezorek, L. Nanoparticle Actuators. *Adv. Mater.* **2003**, *15*, 922–926. (b) Zhang, H.-L.; Evans, S. D.; Henderson, J. R. Spectroscopic Ellipsometric Evaluation of Gold Nanoparticle Thin Films Fabricated Using Layer-by-Layer Self-Assembly. *Adv. Mater.* **2003**, *15*, 531–534.
- (299) Yanagi, H.; Ohno, T. Nanofabrication of Gold Particles in Glass Films by AFM-Assisted Local Reduction. *Langmuir* **1999**, *15*, 4773–4776.
- (300) Huang, W.; Shi, J. Synthesis and Properties of ZrO₂ Films Dispersed with Au Nanoparticles. *J. Sol-Gel Sci. Technol.* **2001**, *20*, 145–151.
- (301) Diao, J. J.; Qiu, F. S.; Chen, G. D.; Reeves, M. E. Surface Vertical Deposition of Gold Nanoparticle Film. *J. Phys. D: Appl. Phys.* **2003**, *36*, L25–L27.
- (302) Ko, H. Y. Y.; Mizuhata, M.; Kajinami, A.; Deki, S. Fabrication of High Performance Thin Films from Metal Fluorocomplex Aqueous Solution by the Liquid-Phase Deposition. *J. Fluorine Chem.* **2003**, *120*, 157–163.
- (303) Lu, A. H.; Lu, G. H.; Kessinger, A. M.; Foss, C. A., Jr. Dichroic Thin Layer Films Prepared from Alkanethiol-Coated Gold Nanoparticles. *J. Phys. Chem. B* **1997**, *101*, 9140–9142.
- (304) Yang, W.; Inoue, H.; Chow, T. Y.; Samura, H.; Saegusa, T. Metal Oxide Thin Films Containing Au Nano-Particles Prepared with Gas Diffusion Methodology. *J. Sol-Gel Sci. Technol.* **1998**, *11*, 117–124.
- (305) Compagnini, G.; Scalisi, A. A.; Puglisi, O. Ablation of Noble Metals in Liquids: a Method to Obtain Nanoparticles in a Thin Polymeric Film. *Phys. Chem. Chem. Phys.* **2002**, *4*, 2787–2791.
- (306) Kariuki, N. N.; Han, L.; Ly, N. K.; Patterson, M. J.; Maye, M. M.; Liu, G.; Zhong, C.-J. Preparation and Characterization of Gold Nanoparticles Dispersed in Poly(2-hydroxyethyl methacrylate). *Langmuir* **2002**, *18*, 8255–8259.
- (307) (a) He, T.; Ma, Y.; Cao, Y.; Jiang, P.; Zhang, X.; Yang, W.; Yao, J. Enhancement Effect of Gold Nanoparticles on the UV–Light Photochromism of Molybdenum Trioxide Thin Films. *Langmuir* **2001**, *17*, 8024–8027. (b) Hussain, I.; Brust, M.; Papworth, A. J.; Cooper, A. I. Preparation of Acrylate-Stabilized Gold and Silver Hydrosols and Gold-Polymer Composite Films. *Langmuir* **2003**, *19*, 4831–4835.
- (308) (a) Gittins, D. I.; Susha, A. S.; Schoeler, B.; Caruso, F. Dense Nanoparticulate Thin Films via Gold Nanoparticle Self-Assembly. *Adv. Mater.* **2002**, *14*, 508–512. (b) Joseph, Y.; Besnard, I.; Rosenberger, M.; Guse, B.; Nothofer, H.-G.; Wessels, J.-M.; Ute, W.; Knop-Gericke, A.; Su, D.; Schlögl, R.; Yasuda, A.; Vossmeier, T. Self-assembled Gold Nanoparticles/Alkanedithiol Films: Preparation, Electron Microscopy, XPS-Analysis, Charge Transport, and Vapor-Sensing Properties. *J. Phys. Chem. B* **2003**, *107*, 7406–7413.
- (309) (a) Werts, M. H.; Lambert, M.; Bourgoin, J.-P.; Brust, M. Nanometer Scale Patterning of Langmuir-Blodgett Films of Gold Nanoparticles by Electron Beam Lithography. *Nano Lett.* **2002**, *2*, 43–47. (b) Paul, S.; Pearson, C.; Molloy, A.; Cousins, M. A.; Green, M.; Koliopoulou, S.; Dimitrakis, P.; Normand, P.; Tsoukalas, D.; Petty, M. C. Langmuir–Blodgett Film Deposition of Metallic Nanoparticles and Their Application to Electronic Memory Structures. *Nano Lett.* **2003**, *3*, 533–536.
- (310) Brust, M.; Stühr-Hansen, N.; Nørgaard, K.; Christensen, J. B.; Nielsen, L. K.; Bjørnholm, T. Langmuir–Blodgett Films of Alkane Chalcogenide (S, Se, Te) Stabilized Gold Nanoparticles. *Nano Lett.* **2001**, *1*, 189–191.
- (311) Sastry, M.; Gole, A.; Patil, V. Lamellar Langmuir–Blodgett Films of Hydrophobized Colloidal Gold Nanoparticles by Organization at the Air–Water Interface. *Thin Solid Films* **2001**, *384*, 125–131.
- (312) Huang, S.; Tsutsui, G.; Sakaue, H.; Shingubara, S.; Takahagi, T. Experimental Conditions for a Highly Ordered Monolayer of Gold Nanoparticles Fabricated by the Langmuir–Blodgett Methodology. *J. Vac. Sci. Technol. B* **2001**, *19*, 2045–2049.
- (313) Kalinina, M. A.; Arslanov, V. V.; Tsar'kova, L. A.; Dolzhikova, V. D.; Rakhnyanskaya, A. A. Langmuir–Blodgett Monolayers and Films of Alkylated Tetraazacrowns Containing Metal Ions and Nanoparticles. *Colloid J.* **2001**, *63*, 312–317.
- (314) Sbrana, F.; Parodi, M. T.; Ricci, D.; Di Zitti, E. Langmuir Films of Thiolated Gold Nanoparticles Transferred onto Functionalized Substrate: 2-D Local Organization. *Mater. Sci. Eng. C* **2002**, *22*, 187–191.
- (315) Ravaine, S.; Fanucci, G. E.; Seip, C. T.; Adair, J. H.; Talham, D. R. Photochemical Generation of Gold Nanoparticles in Langmuir–Blodgett Films. *Langmuir* **1998**, *14*, 708–713.
- (316) (a) Bourgoin, J.-P.; Kergueris, C.; Lefèvre, E.; Palacin, S. Langmuir–Blodgett Films of Thiol-Capped Gold Nanoclusters: Fabrication and Electrical Properties. *Thin Solid Films* **1998**, *327–329*, 515–519. (b) Swami, A.; Kumar, A.; Selvakannan, P. R.; Mandal, S.; Sastry, M. Langmuir–Blodgett Films of Laurylamine-Modified Hydrophobic Gold Nanoparticles Organized at the Air–Water Interface. *J. Colloid Interface Sci.* **2003**, *260*, 367–373.
- (317) (a) Brown, J. J.; Porter, J. A.; Daghighian, C. P.; Gibson, U. J. Ordered Arrays of Amphiphilic Gold Nanoparticles in Langmuir Monolayers. *Langmuir* **2001**, *17*, 7966–7969. (b) Sbrana, F.; Parodi, M. T.; Ricci, D.; Di Zitti, E.; Natale, C.; Thea, S. Assembling Thiolated Gold Nanoparticles in Compact Patterns: a Transmission Electron Microscopy and Scanning Probe Microscopy Investigation. *Mater. Sci. Eng. B* **2002**, *96*, 193–198.
- (318) Khomutov, G. B.; Kislov, V. V.; Gainutdinov, R. V.; Gubin, S. P.; Obydenov, A. Y.; Pavlov, S. A.; Sergeev-Cherenkov, A. N.; Soldatov, E. S.; Tolstikhina, A. L.; Trifonov, A. S. The Design, Fabrication and Characterization of Controlled-Morphology Nanomaterials and Functional Planar Molecular Nanocluster-Based Nanostructures. *Surf. Sci.* **2003**, *532–535*, 287–293.

- (319) (a) Zhao, S.-Y.; Lei, S.-B.; Chen, S.-H.; Ma, H.-Y.; Wang, S.-Y. Assembly of Two-Dimensional Ordered Monolayers of Nanoparticles by Electrophoretic Deposition. *Colloid Polym. Sci.* **2002**, *278*, 682–686. (b) Tanaka, H.; Mitsuishi, M.; Miyashita, T. Tailored-Control of Gold Nanoparticle Adsorption onto Polymer Nanosheets. *Langmuir* **2003**, *19*, 3103–3105.
- (320) Kumar, A.; Mandal, S.; Mathew, S. P.; Selvakannan, P. R.; Mandale, A. B.; Chaudhari, R. V.; Sastry, M. Benzene- and Anthracene-Mediated Assembly of Gold Nanoparticles at the Liquid Interface. *Langmuir* **2002**, *18*, 6478–6483.
- (321) (a) Krinke, T. J.; Deppert, K.; Magnusson, M. H.; Schmidt, F.; Fissan, H. Microscopic Aspects of the Deposition of Nanoparticles From the Gas Phase. *Aerosol Sci.* **2002**, *33*, 1341–1359. (b) Raguse, B.; Herrmann, J.; Stevens, G.; Myers, J.; Baxter, G.; Müller, K.-H.; Reda, T.; Molodyk, A.; Braach-Maksyvtis, V. Hybrid Nanoparticle Film Material. *J. Nanopart. Res.* **2002**, *4*, 137–143.
- (322) Shiigi, H.; Yamamoto, Y.; Yakabe, H.; Tokonami, S.; Nagaoka, T. Electrical Property and Water Repellency of a Networked Monolayer Film Prepared from Au Nanoparticles. *Chem. Commun.* **2003**, 1038–1039.
- (323) Akamatsu, K.; Deki, S. Characterization and Optical Properties of Gold Nanoparticles Dispersed in Nylon 11 Thin Films. *J. Mater. Chem.* **1997**, *7*, 1773–1777.
- (324) Akamatsu, K.; Deki, S. Dispersion of Gold Nanoparticles Into a Nylon 11 Thin Film During Heat Treatment: in situ Optical Transmission Study. *J. Mater. Chem.* **1998**, *8*, 637–640.
- (325) (a) Akamatsu, K.; Deki, S. TEM Investigation and Electron Diffraction Study on Dispersion of Gold Nanoparticles into a Nylon 11 Thin Film During Heat Treatment. *J. Colloid Interface Sci.* **1999**, *214*, 353–361. (b) Inoue, Y.; Fujii, M.; Inata, M.; Hayashi, S.; Yamamoto, K.; Akamatsu, K.; Deki, S. Single-Electron Tunneling Effects in Thin Nylon 11 Films Containing Gold Nanoparticles. *Thin Solid Films* **2000**, *372*, 169–172.
- (326) (a) Yao, H.; Momozawa, O.; Hamatani, T.; Kimura, K. Phase Transfer of Gold Nanoparticles Across a Water/Oil Interface by Stoichiometric Ion-Pair Formation on Particle Surfaces. *Bull. Chem. Soc. Jpn.* **2000**, *73*, 2675–2678. (b) Mayya, K. S.; Caruso, F. Phase Transfer of Surface-Modified Gold Nanoparticles by Hydrophobization with Alkylamines. *Langmuir* **2003**, *19*, 6987–6993. (c) Kaempfe, M.; Graener, H.; Kiesow, A.; Heilmann, A. Formation of Metal Particle Nanowires Induced by Ultrashort Laser Pulses. *Appl. Phys. Lett.* **2001**, *79*, 1876–1879.
- (327) (a) Dick, K.; Dhanasekaran, T.; Zhang, Z.; Meisel, D. Size-Dependent Melting of Silica-Encapsulated Gold Nanoparticles. *J. Am. Chem. Soc.* **2002**, *124*, 2312–2317. (b) Fu, G.; Cai, W.; Kann, C.; Li, C.; Fang, Q. Optical Study of the Ultrasonic Formation Process of Noble Metal Nanoparticles Dispersed Inside the Pores of Monolithic Mesoporous Silica. *J. Phys. D: Appl. Phys.* **2003**, *36*, 1382–1387.
- (328) (a) Sadtler, B.; Wei, A. Spherical Ensembles of Gold Nanoparticles on Silica: Electrostatic and Size Effects. *Chem. Commun.* **2002**, 1604–1605. (b) Zhu, H.; Lee, B.; Dai, S.; Oberbury, S. H. Co-Assembly Synthesis of Ordered Mesoporous Silica Materials Containing Au Nanoparticles. *Langmuir* **2003**, *19*, 3974–3980.
- (329) (a) Lu, Y.; Yin, Y.; Li, Z.-Y.; Xia, Y. Synthesis and Self-Assembly of Au@SiO₂ Core-Shell Colloids. *Nano Lett.* **2002**, *2*, 785–788. (b) Lu, X.; Hanrath, T.; Johnston, K. P.; Korgel, B. A. Growth of Single-Crystal Silicon Nanowires in Supercritical Solution from Tethered Gold Particles on a Silicon Substrate. *Nano Lett.* **2003**, *3*, 93–99.
- (330) (a) Schroedter, A.; Weller, H. Biofunctionalization of Silica-Coated CdTe and Gold Nanocrystals. *Nano Lett.* **2002**, *2*, 1363–1367. (b) Hu, M.; Wang, X.; Hartland, G. V.; Salgueiriño-Maceira, V.; Liz-Marzán, L. M. Heat Dissipation in Gold-Silica Core-Shell Nanoparticles. *Chem. Phys. Lett.* **2003**, *372*, 767–772.
- (331) Guari, Y.; Thieuleux, C.; Mehdi, A.; Reyé, C.; Corriu, R. J. P.; Gomez-Gallardo, S.; Philippot, K.; Chaudret, B. In Situ Formation of Gold Nanoparticles within Thiol Functionalized HMS-C₁₆ and SBA-15 Type Materials via an Organometallic Two-Step Approach. *Chem. Mater.* **2003**, *15*, 2017–2024.
- (332) (a) Nooney, R. I.; Dhanasekaran, T.; Chen, Y.; Josephs, R.; Ostafin, A. E. Self-Assembled Highly-Ordered Spherical Mesoporous Silica/Gold Nanocomposites. *Adv. Mater.* **2002**, *14*, 529–532. (b) Chen, W.; Zhang, J.-Y.; Di, Y.; Boyd, I. W. Photochemical Production of Gold Nanoparticles in Monolithic Porous Silica by Using a Novel Excimer Ultraviolet Source. *Inorg. Chem. Commun.* **2003**, *6*, 950–952.
- (333) (a) Fleming, M. S.; Walt, D. R. Stability and Exchange Studies of Alkanethiol Monolayers on Gold-Nanoparticle-Coated Silica Microspheres. *Langmuir* **2001**, *17*, 4836–4843. (b) Cheng, S.; Wei, Y.; Feng, Q.; Qiu, K.-Y.; Pang, J.-B.; Jansen, S. A.; Yin, R.; Ong, K. Facile Synthesis of Mesoporous Gold-Silica Nanocomposite Materials via Gold-Gel Process with Nonsurfactant Templates. *Chem. Mater.* **2003**, *15*, 1560–1566.
- (334) (a) Kobayashi, Y.; Corraera-Durante, M. A.; Liz-Marzán, L. M. Sol-Gel Processing of Silica-Coated Gold Nanoparticles. *Langmuir* **2001**, *17*, 6375–6379. (b) Lim, Y. T.; Park, O. O.; Jung, H.-T. Gold Nanolayer-Encapsulated Silica Particles Synthesized by Surface Seeding and Shell Growing Method: Near Infrared Responsive Materials. *J. Colloid Interface Sci.* **2003**, *263*, 449–453.
- (335) Petó, G.; Molnár, G. L.; Pászti, Z.; Geszti, O.; Beck, A.; Gucci, L. Electronic Structure of Gold Nanoparticles Deposited on SiO/Si(100). *Mater. Sci. Eng. C* **2002**, *19*, 95–99.
- (336) Caruso, F.; Spasova, M.; Salgueiriño-Maceira, V.; Liz-Marzán, L. M. Multilayer Assemblies of Silica-Encapsulated Gold Nanoparticles on Decomposable Colloid Templates. *Adv. Mater.* **2001**, *13*, 1090–1094.
- (337) García-Santamaría, F.; Salgueiriño-Maceira, V.; López, C.; Liz-Marzán, L. M. Synthetic Opals Based on Silica-Coated Gold Nanoparticles. *Langmuir* **2002**, *18*, 4519–4522.
- (338) Chen, W.; Cai, W.; Wang, G.; Zhang, L. Effects of Interface Interaction on the Mie Resonance Absorption of Gold Nanoparticles Dispersed within Pores of Mesoporous Silica. *Appl. Surf. Sci.* **2001**, *174*, 51–54.
- (339) Papernov, S.; Schmid, A. W. Correlations between Embedded Single Gold Nanoparticles in SiO₂ Thin Film and Nanoscale Crater Formation Induced by Pulsed-Laser Radiation. *J. Appl. Phys.* **2002**, *92*, 5720–5728.
- (340) Chen, W.; Cai, W.; Zhang, Z.; Zhang, L. A Convenient Synthetic Route to Gold Nanoparticles Dispersed within Mesoporous Silica. *Chem. Lett.* **2001**, 152–153.
- (341) Ila, D.; Williams, E. K.; Zimmerman, R. L.; Poker, D. B.; Hensley, D. K. Radiation Induced Nucleation of Nanoparticles in Silica. *Nucl. Instrum. Methods Phys. Res. B* **2002**, *166–167*, 845–850.
- (342) Abis, L.; Armelao, L.; Dell'Amico, D. B.; Calderazzo, F.; Garbassi, F.; Merigo, A.; Quadrelli, E. A. Gold Molecular Precursors and Gold-Silica Interactions. *J. Chem. Soc., Dalton Trans.* **2001**, 2704–2709.
- (343) Shi, H.; Zhang, L.; Cai, W. Preparation and Optical Absorption of Gold Nanoparticles within Pores of Mesoporous Silica. *Mater. Res. Bull.* **2000**, *35*, 1689–1695.
- (344) Selvan, S. T.; Nogami, M.; Nakamura, A.; Hamanaka, Y. A Facile Sol-Gel Method for the Encapsulation of Gold Nanoparticles in Silica Gels and their Optical Properties. *J. Non-Cryst. Solids* **1999**, *255*, 254–258.
- (345) Ghosh, A.; Patra, C. R.; Mukherjee, P.; Sastry, M.; Kumar, R. Preparation and Stabilization of Gold Nanoparticles Formed by in situ Reduction of Aqueous Chloroaurate Ions within Surface-Modified Mesoporous Silica. *Microporous Mesoporous Mater.* **2003**, *58*, 201–211.
- (346) Battaglin, G.; Boscolo-Boscoletto, A.; Mazzoldi, P.; Meneghini, C.; Arnold, G. W. Gold Nanocluster Formation in Silicate Glasses by Low Fluence Ion Implantation and Annealing. *Nucl. Instrum. Methods Phys. Res. B* **1996**, *116*, 527–530.
- (347) Innocenti, P.; Brusatin, G.; Martucci, A.; Urabe, K. Microstructural Characterization of Gold-Doped Silica-Titania Sol-Gel Films. *Thin Solid Films* **1996**, *279*, 23–28.
- (348) Coultard, I.; Degen, S.; Zhu, Y.-J.; Sham, T. K. Gold Nanoclusters Reductively Deposited on Porous Silicon: Morphology and Electronic Structures. *Can. J. Chem.* **1998**, *76*, 1707–1716.
- (349) Aihara, N.; Torigoe, K.; Esumi, K. Preparation and Characterization of Gold and Silver Nanoparticles in Layered Laponite Suspensions. *Langmuir* **1998**, *14*, 4945–4949.
- (350) Wescott, S. L.; Oldenburg, S. J.; Lee, T. R.; Halas, N. J. Formation and Adsorption of Clusters of Gold Nanoparticles onto Functionalized Silica Nanoparticle Surfaces. *Langmuir* **1998**, *14*, 5396–5401.
- (351) Kónya, Z.; Puentes, V. F.; Kiricsi, I.; Zhu, J.; Ager, J. W., III; Ko, M. K.; Frei, H.; Alivisatos, P.; Somorjai, G. A. Synthetic Insertion of Gold Nanoparticles into Mesoporous Silica. *Chem. Mater.* **2003**, *15*, 1242–1248.
- (352) Wang, J.; Zhu, T.; Song, J.; Liu, Z. Gold Nanoparticulate Films Bound to Silicon Surface with Self-Assembled Monolayers. *Thin Solid Films* **1998**, *327–329*, 591–594.
- (353) Bharathi, S.; Lev, O. Direct Synthesis of Gold Nanodispersions in Sol-Gel Derived Silicate Sols, Gels and Films. *Chem. Commun.* **1997**, 2303–2304.
- (354) Caruso, F. Nanoengineering of Particle Surfaces. *Adv. Mater.* **2001**, *13*, 11–22.
- (355) Liz-Marsan, L. M.; Griersig, M.; Mulvaney, P. Synthesis of Nanosized Gold-Silica Core-Shell Particles. *Langmuir* **1996**, *12*, 4329–4335.
- (356) Hall, S. R.; Davis, S. A.; Mann, S. Co-Condensation of Organosilica Hybrid Shells on Nanoparticle Templates: A Direct Synthetic Route to Functionalized Core-Shell Colloids. *Langmuir* **2000**, *16*, 1454–1456.
- (357) González-Rodríguez, B.; Salgueiriño-Maceira, V.; García-Santamaría, F.; Liz-Marzán, L. M. Fully Accessible Gold Nanoparticles within Ordered Macroporous Solids. *Nano Lett.* **2002**, *2*, 471–473.
- (358) Guari, Y.; Thieuleux, C.; Mehdi, A.; Reyé, C.; Corriu, R. J. P.; Gomez-Gallardo, S.; Philippot, K.; Chaudret, B.; Dutartre, R. In situ Formation of Gold Nanoparticles within Functionalized Ordered Mesoporous Silica via an Organometallic 'Chimie Douce' Approach. *Chem. Commun.* **2001**, 1374–1375.

- (359) Epifani, M.; Carliano, E.; Blasi, C.; Giannini, C.; Tapfer, L.; Vasanelli, L. Sol-Gel Processing of Au Nanoparticles in Bulk 10% B₂O₃-90% SiO₂ Glass. *Chem. Mater.* **2001**, *13*, 1533–1539.
- (360) Horváth, D.; Thfoin-Polisset, M.; Fraissard, J.; Gucci, L. Novel Preparation Method and Characterization of Au-Fe/HY Zeolite Containing Highly Stable Gold Nanoparticles Inside Zeolite Supercages. *Solid State Ionics* **2001**, *141–142*, 153–156.
- (361) Ng, L. N.; Zervas, M. N.; Wilkinson, J. S.; Luff, B. J. Manipulation of Colloidal Gold Nanoparticles in the Evanescent Field of a Channel Waveguide. *Appl. Phys. Lett.* **2000**, *76*, 1993–1995.
- (362) Oku, T.; Suganuma, K. Carbon Nanocage Structures Formed by One-Dimensional Self-Organization of Gold Nanoparticles. *Chem. Commun.* **1999**, 2355–2356.
- (363) Sawitowski, T.; Miquel, Y.; Heilmann, A.; Schmid, G. Optical Properties of Quasi One-Dimensional Chains of Gold Nanoparticles. *Adv. Funct. Mater.* **2001**, *11*, 435–440.
- (364) Reuter, T.; Vidoni, O.; Torma, V.; Schmid, G. Two-Dimensional Networks via Quasi One-Dimensional Arrangements of Gold Clusters. *Nano Lett.* **2002**, *2*, 709–711.
- (365) Blonder, R.; Sheeney, L.; Willner, I. Three-Dimensional Redox-Active Layered Composites of Au–Au, Ag–Ag and Au–Ag Colloids. *Chem. Commun.* **1998**, 1393–1394.
- (366) Gutiérrez-Wing, C.; Santiago, P.; Ascencio, J. A.; Camacho, A.; José-Yacamán, M. Self-Assembling of Gold Nanoparticles in One, Two, and Three Dimensions. *Appl. Phys. A* **2000**, *71*, 237–243.
- (367) Mafuné, F.; Kohno, J.-Y.; Takeda, Y.; Kondow, T. Nanoscale Soldering of Metal Nanoparticles for Construction of Higher-Order Structures. *J. Am. Chem. Soc.* **2003**, *125*, 1686–1687.
- (368) Oh, S.-K.; Kim, Y.-G.; Ye, H.; Crooks, R. M. Synthesis, Characterization, and Surface Immobilization of Metal Nanoparticles Encapsulated within Bifunctionalized Dendrimers. *Langmuir* **2003**, *19*, 10420–10425.
- (369) Liang, Z.; Susha, A. S.; Caruso, F. Metallodielectric Opals of Layer-by-Layer Processed Coated Colloids. *Adv. Mater.* **2002**, *14*, 1160–1164.
- (370) Powell, C.; Fenwick, N.; Bresme, F.; Quirke, N. Wetting of Nanoparticles and Nanoparticle Arrays. *Physicochem. Eng. Asp.* **2002**, *206*, 241–251.
- (371) Hall, S. R.; Shenton, W.; Engelhardt, H.; Mann, S. Site-Specific Organization of Gold Nanoparticles by Biomolecular Templating. *ChemPhysChem* **2001**, *n° 3*, 184–186.
- (372) (a) Khan, M. A.; Perruchot, C.; Armes, S. P.; Randall, D. P. Synthesis of Gold-Decorated Latexes via Conducting Polymer Redox Templates. *J. Mater. Chem.* **2001**, *11*, 2363–2372. (b) Liu, F.-K.; Chang, Y.-C.; Ko, F.-H.; Chu, T.-C.; Dai, B.-T. Rapid Fabrication of High Quality Self-Assembled Nanometer Gold Particles by Spin Coating Methodology. *Microelectron. Eng.* **2003**, *67–68*, 702–709.
- (373) Mott, N. F.; Gurney, N. W. *Electronic Processes in Ionic Crystals*; Oxford University Press: Oxford, 1948.
- (374) (a) Mulvaney, P. Surface Plasmon Spectroscopy of Nanosized Metal Particles. *Langmuir* **1996**, *12*, 788–800. (b) Mulvaney, P. In *Semiconductor Nanoclusters—Physical, Chemical and Catalytic Aspects*; Kamat, P. V., Meisel, D., Eds.; Elsevier: Amsterdam, 1997; pp 99–123.
- (375) *The Theory of the Photographic Process*, 4th ed; James, T. H., Ed.; MacMillan Press: New York, 1977.
- (376) Van der Hulst, H. C. *Light Scattering by Small Metal Particles*; Wiley: New York, 1957.
- (377) Kerker, M. *The Scattering of Light and Other Electromagnetic Radiation*; Academic Press: New York, 1969.
- (378) Bohren, C. F.; Huffman, D. R. *Absorption of Light by Small Particles*; Wiley: New York, 1983.
- (379) Mie, G. Beiträge zur Optik Trüber Medien, Speziell Kolloidaler Metallösungen. *Ann. Phys.* **1908**, *25*, 377–445.
- (380) Alvarez, M. M.; Khoury, J. T.; Schaaff, T. G.; Shafiqullin, M. N.; Vezmar, I.; Whetten, R. L. Optical Absorption Spectra of Nanocrystal Gold Molecules. *J. Phys. Chem. B* **1997**, *101*, 3706–3712.
- (381) Logunov, S. L.; Ahmadi, T. S.; El-Sayed, M. A.; Khoury, J. T.; Whetten, R. L. Electron Dynamics of Passivated Gold Nanocrystals Probed by Subpicosecond Transient Absorption Spectroscopy. *J. Phys. Chem. B* **1997**, *101*, 3713–3719.
- (382) (a) Schaaf, T. G.; Shafiqullin, M. N.; Khoury, J. T.; Vezmar, I.; Whetten, R. L.; Cullen, W. G.; First, P. N.; Gutiérrez-Wing, C.; Ascencio, J.; Jose-Yacamán, M. J. Isolation of Smaller Nanocrystal Au Molecules: Robust Quantum Effects in Optical Spectra. *J. Phys. Chem. B* **1997**, *101*, 7885–7891. (b) Zaitoun, M. A.; Mason, W. R.; Lin, C. T. Magnetic Circular Dichroism Spectra for Colloidal Gold Nanoparticles in Xerogels at 5.5 K. *J. Phys. Chem. B* **2001**, *105*, 6780–6784.
- (383) Melinger, J. S.; Kleiman, V. D.; McMorro, D.; Gröhn, F.; Bauer, B. J.; Amis, E. Ultrafast Dynamics of Gold-Based Nanocomposite Materials. *J. Phys. Chem. A* **2003**, *107*, 3424–3431.
- (384) Papavassiliou, G. C. Optical Properties of Small Inorganic and Organic Metal Particles. *Prog. Solid State Chem.* **1979**, *12*, 185–271.
- (385) Templeton, A. C.; Pietron, J. J.; Murray, R. W.; Mulvaney, P. Solvent Refractive Index and Core Charge Influences on the Surface Plasmon Adsorbance of Alkanethiolate Monolayer-Protected Gold Clusters. *J. Phys. Chem. B* **2000**, *104*, 564–570.
- (386) (a) Link, S.; El-Sayed, M. A. Size and Temperature Dependence of the Plasmon Absorption of Colloidal Gold Nanoparticles. *J. Phys. Chem. B* **1999**, *103*, 4212–4217. (b) Itoh, T.; Asahi, T.; Masuhara, H. Femtosecond Light Scattering Spectroscopy of Single Gold Nanoparticles. *Appl. Phys. Lett.* **2001**, *79*, 1667–1669. (c) Su, K.-H.; Wei, Q.-H.; Zhang, X.; Mock, J. J.; Smith, D. R.; Schulz, S. Interparticle Coupling Effects on Plasmon Resonance of Nanogold Particles. *Nano Lett.* **2003**, *3*, 1087–1090. (d) Rechberger, W.; Hohenau, A.; Leitner, A.; Krenn, J. R.; Lamprecht, B.; Aussenegg, F. R. Optical Properties of Two Interacting Gold Nanoparticles. *Opt. Commun.* **2003**, *220*, 137–141. (e) Link, S.; Mohamed, M. B.; El-Sayed, M. A. Simulation of the Optical Absorption Spectra of a Gold Nanorods as a Function of their Aspect Ratio and the Effect of the Medium Dielectric Constant. *J. Phys. Chem. B* **1999**, *103*, 3073. (f) Yan, B.; Yang, Y.; Wang, Y. Comment on “Simulation of the Optical Absorption Spectra of a Gold Nanorods as a Function of their Aspect Ratio and the Effect of the Medium Dielectric Constant”. *J. Phys. Chem. B* **2003**, *107*, 9159. (g) Swanson, N. L.; Billard, B. D. Optimization of Extinction from Surface Plasmon Resonances of Gold Nanoparticles. *Nanotechnology* **2003**, *14*, 353–357.
- (387) Ung, T.; Liz-Marzán, L. M.; Mulvaney, P. Gold Particles Thin Films. *Colloids Surf. A: Physicochem. Eng. Asp.* **2002**, *202*, 119–126.
- (388) Ung, T.; Giersig, M.; Dunstan, D.; Mulvaney, P. Spectroelectrochemistry of Colloidal Silver. *Langmuir* **1997**, *13*, 1773–1782.
- (389) Ung, T.; Liz-Marzán, L. M.; Mulvaney, P. Optical Properties of Thin Films of Au@SiO₂ Particles. *J. Phys. Chem. B* **2001**, *105*, 3441–3452.
- (390) Klar, T.; Perner, M.; Grosse, S.; von Plessen, G.; Spirkel, W.; Feldmann, J. Surface-Plasmon Resonances in Single Metallic Nanoparticles. *Phys. Rev. Lett.* **1998**, *80*, 4249–4252.
- (391) Al-Rawashdeh, N.; Foss, C. A., Jr. UV/Visible and Infrared Spectra of Polyethylene/Nanoscale Gold Rod Composite Films: Effects of Gold Particle Size, Shape and Orientation. *Nanostruct. Mater.* **1997**, *9*, 383–386.
- (392) Al-Rawashdeh, N. A. F.; Sandrock, M. L.; Seugling, C. J.; Foss, C. A., Jr. Visible Region Polarization Spectroscopic Studies of Template-Synthesized Gold Nanoparticles Oriented in Polyethylene. *J. Phys. Chem. B* **1998**, *102*, 361–371.
- (393) Linden, S.; Christ, A.; Kuhl, J.; Giessen, H. Selective Suppression of Extinction within the Plasmon Resonance of Gold Nanoparticles. *Appl. Phys. B* **2001**, *73*, 311–316.
- (394) Linden, S.; Kuhl, J.; Giessen, H. Controlling the Interaction between Light and Gold Nanoparticles: Selective Suppression of Extinction. *Phys. Rev. Lett.* **2001**, *86*, 4688–4691.
- (395) (a) Ahmadi, T. S.; Logunov, S. L.; El-Sayed, M. A. Picosecond Dynamics of Colloidal Gold Nanoparticles. *J. Phys. Chem. B* **1999**, *100*, 8059–8056. (b) Logunov, S. L.; Ahmadi, T. S.; El-Sayed, M. A. Electron Dynamics of Passivated Gold Nanocrystals Probed by Subpicosecond Transient Absorption Spectroscopy. *J. Phys. Chem. B* **1997**, *101*, 3713–3719. (c) Hartland, G. V.; Hu, M.; Sader, J. E. Softening of the Symmetric Breathing Mode in Gold Particles by Laser-Induced Heating. *J. Phys. Chem. B* **2003**, *107*, 7472–7478.
- (396) (a) Fujiwara, H.; Yanagida, S.; Kamat, P. V. Visible Laser Induced Fusion and Fragmentation of Thionicotinamide-Capped Gold Nanoparticles. *J. Phys. Chem. B* **1999**, *103*, 2589–2591.
- (397) Takeuchi, Y.; Ida, T.; Kimura, K. Colloidal Stability of Gold Nanoparticles in 2-Propanol Under Laser Irradiation. *J. Phys. Chem. B* **1997**, *101*, 1322–1327.
- (398) Satoh, N.; Hasegawa, H.; Tsujii, K.; Kimura, K. Photoinduced Coagulation of Au Nanocolloids. *J. Phys. Chem.* **1994**, *98*, 2143–2147.
- (399) Mafuné, F.; Kohno, J.-Y.; Takeda, Y.; Kondow, T. Dissociation and Aggregation of Gold Nanoparticles under Laser Irradiation. *J. Phys. Chem. B* **2001**, *105*, 9050–9056.
- (400) Westcott, S. L.; Oldenburg, S. J.; Lee, T. R.; Halas, N. J. Construction of Simple Gold Nanoparticle Aggregates with Controlled Plasmon-Plasmon Interactions. *Chem. Phys. Lett.* **1999**, *300*, 651–655.
- (401) Eck, D.; Helm, C. A.; Wagner, N. J.; Vaynberg, K. A. Plasmon Resonance Measurements of the Adsorption and Adsorption Kinetics of a Biopolymer onto Gold Nanocolloids. *Langmuir* **2001**, *17*, 957–960.
- (402) Chandrasekharan, N.; Kamat, P. V.; Hu, J.; Jones, G., II. Dye-Capped Gold Nanoclusters: Photoinduced Morphological Changes in Gold/Rhodamine 6G Nanoassemblies. *J. Phys. Chem. B* **2000**, *104*, 11103–11109.
- (403) Nath, N.; Chilkoti, A. Interfacial Phase Transition of an Environmentally Responsive Elastin Biopolymer Adsorbed on Functionalized Gold Nanoparticles Studied by Colloidal Surface Plasmon Resonance. *J. Am. Chem. Soc.* **2001**, *123*, 8197–8202.
- (404) Huang, S.; Minami, K.; Sakaue, H.; Shingubara, S.; Takahagi, T. Optical Spectroscopic Studies of the Dispersibility of Gold Nanoparticle solutions. *J. Appl. Phys.* **2002**, *92*, 7486–7490.

- (405) Swami, A.; Kumar, A.; Sastry, M. Formation of Water-Dispersible Gold Nanoparticles Using a Technique Based on Surface-Bound Interdigitated Bilayers. *Langmuir* **2003**, *19*, 1168–1172.
- (406) Thomas, K. G.; Zajicek, J.; Kamat, P. V. Surface Binding Properties of Tetraoctylammonium Bromide-Capped Gold Nanoparticles. *Langmuir* **2002**, *18*, 3722–3727.
- (407) (a) Malikova, N.; Pastoriza-Santos, I.; Schierhorn, M.; Kotov, N. A.; Liz-Marzán, L. M. Layer-by-Layer Assembled Mixed Spherical and Planar Gold Nanoparticles: Control of Interparticle Interactions. *Langmuir* **2002**, *18*, 3694–3697. (b) Aizpurua, J.; Hanarp, P.; Sutherland, D. S.; Käll, M.; Bruant, G. W.; Garcia de Abajo, F. J. Optical Properties of Gold Nanorings. *Phys. Rev. Lett.* **2003**, *90*, 057401-1–057401-4.
- (408) Huang, T.; Murray, R. W. Visible Luminescence of Water-Soluble Monolayer-Protected Gold Clusters. *J. Phys. Chem. B* **2001**, *105*, 12498–12502.
- (409) Hwang, Y.-N.; Jeong, D. H.; Shin, H. J.; Kim, D.; Jeoung, S. C.; Han, S. H.; Lee, J.-S.; Cho, G. Femtosecond Emission Studies of Gold Nanoparticles. *J. Phys. Chem. B* **2002**, *106*, 7581–7584.
- (410) Chen, M. M. Y.; Katz, A. Steady-State Fluorescence-Based Investigation of the Interaction between Protected Thiols and Gold Nanoparticles. *Langmuir* **2002**, *18*, 2413–2420.
- (411) Hu, J.; Zhang, J.; Liu, F.; Kittredge, K.; Whitesell, J. K.; Fox, M. A. Competitive Photochemical Reactivity in a Self-Assembled Monolayer on a Colloidal Gold Cluster. *J. Am. Chem. Soc.* **2001**, *123*, 1464–1470.
- (412) Wang, T.; Zhang, D.; Xu, W.; Yang, J.; Han, R.; Zhu, D. Preparation, Characterization, and Photophysical Properties of Alkanethiols with Pyrene Units-Capped Gold Nanoparticles: Unusual Fluorescence Enhancement for the Aged Solutions of These Gold Nanoparticles. *Langmuir* **2002**, *18*, 1840–1848.
- (413) Thomas, K. G.; Kamat, P. V. Making Gold Nanoparticles Glow: Enhanced Emission from a Surface-Bound Fluoroprobe. *J. Am. Chem. Soc.* **2000**, *122*, 2655–2656.
- (414) Sarathy, V. K.; Narayan, K. S.; Kim, J.; White, J. O. Novel Fluorescence and Morphological Structures in Gold Nanoparticles-Polyoctylthiophene Based Thin Films. *Chem. Phys. Lett.* **2000**, *318*, 543–548.
- (415) Xu, P.; Yanagi, H. Fluorescence Patterning in Dye-Doped Sol-Gel Films by Generation of Gold Nanoparticles. *Chem. Mater.* **1999**, *11*, 2626–2628.
- (416) Makarova, O. V.; Ostafin, A. E.; Miyoshi, H.; Norris, J. R., Jr.; Meisel, D. Adsorption and Encapsulation of Fluorescent Probes in Nanoparticles. *J. Phys. Chem. B* **1999**, *103*, 9080–9084.
- (417) Dulkeith, E.; Morteani, A. C.; Niedereichholz, T.; Klar, T. A.; Feldmann, J. Fluorescence Quenching of Dye Molecules near Gold Nanoparticles: Radiative and Nonradiative Effects. *Phys. Rev. Lett.* **2002**, *89*, 203002-1–203002-4.
- (418) Gu, T.; Whitesell, J. K.; Fox, M. A. Energy Transfer from a Surface-Bound Arene to the Gold Core in ω -Fluorenyl-Alkane-1-Thiolate Monolayer-Protected Gold Clusters. *Chem. Mater.* **2003**, *15*, 1358–1366.
- (419) Dubertret, B.; Calame, M.; Libchaber, A. J. Single-Mismatch Detection Using Gold-Quenched Fluorescent Oligonucleotides. *Nat. Biotechnol.* **2001**, *19*, 365–370.
- (420) Imahori, H.; Fukuzumi, S. Porphyrin Monolayer-Modified Gold Clusters as Photoactive Materials. *Adv. Mater.* **2001**, *13*, 1197–1199.
- (421) Imahori, H.; Arimura, M.; Hanada, T.; Nishimura, Y.; Yamazaki, I.; Sakata, Y.; Fukuzumi, S. Photoactive Three-Dimensional Monolayers: Porphyrin-Alkanethiolate-Stabilized Gold Clusters. *J. Am. Chem. Soc.* **2001**, *123*, 335–336.
- (422) Lakowitz, J. R. *Principles of Fluorescence Spectroscopy*; Kluwer: New York, 1999.
- (423) Wilcoxon, J. P.; Martin, J. E.; Parsapour, F.; Wiedenman, B.; Kelley, D. F. Photoluminescence From Nanosize Gold Clusters. *J. Chem. Phys.* **1998**, *108*, 9137–9143.
- (424) Mohamed, M. B.; Volkov, V.; Link, S.; El-Sayed, M. A. The 'lightning' Gold Nanorods: Fluorescence Enhancement of Over a Million Compared to the Gold Metal. *Chem. Phys. Lett.* **2000**, *317*, 517–523.
- (425) Bigioni, T. P.; Whetten, T. P.; Dag, O. Near-Infrared Luminescence from Small Gold Nanocrystals. *J. Phys. Chem. B* **2000**, *104*, 6983–6986.
- (426) Link, S.; El-Sayed, M. A. Shape and Size Dependence of Radiative, Non-Radiative and Photothermal Properties of Gold Nanocrystals. *Int. Rev. Phys. Chem.* **2000**, *19*, 3, 409–453.
- (427) Ipe, B. I.; Mahima, S.; Thomas, K. G. Light-Induced Modulation of Self-Assembly on Spiropyran-Capped Gold Nanoparticles: A Potential System for the Controlled Release of Amino Acid Derivatives. *J. Am. Chem. Soc.* **2003**, *125*, 7174–7175.
- (428) (a) Chen, S.; Huang, K. Electrochemical and Spectroscopic Studies of Nitrophenyl Moieties Immobilized on Gold Nanoparticles. *Langmuir* **2000**, *16*, 2014–2018. (b) Chen, S.; Yang, Y. Magnetochemistry of Gold Nanoparticle Quantized Capacitance Charging. *J. Am. Chem. Soc.* **2002**, *124*, 5280–5281. (c) Li, D.; Li, J. Preparation, Characterization and Quantized Capacitance of 3-Mercapto-1,2-Propanediol Monolayer Protected Gold Nanoparticles. *Chem. Phys. Lett.* **2003**, *372*, 668–673.
- (429) (a) Yang, Y.; Chen, S. Surface Manipulation of the Electronic Energy of Subnanometer-Sized Gold Clusters: An Electrochemical and Spectroscopic Investigation. *Nano Lett.* **2003**, *3*, 75–79. (b) Lee, D.; Donkers, R. L.; DeSimone, J. M.; Murray, R. W. Voltammetry and Electron-Transfer Dynamics in a Molecular Melt of a 1.2 nm Metal Quantum Dot. *J. Am. Chem. Soc.* **2003**, *125*, 1182–1183.
- (430) (a) Gittins, D. I.; Bethell, D.; Nichols, R. J.; Schiffrin, D. J. Redox-Connected Multilayers of Discrete Gold Particles: A Novel Electroactive Nanomaterial. *Adv. Mater.* **1999**, *11*, 737–740. (b) Sagara, T.; Kato, N.; Toyota, A.; Nakashima, N. Anomalous Electroreflectance and Absorption Spectra of Viologen Radical Cation in Close Proximity of Gold Nanoparticles at Electrified Interfaces. *Langmuir* **2002**, *18*, 6995–7001.
- (431) Kuwahara, Y.; Akiyama, T.; Yamada, S. Facile Fabrication of Photoelectrochemical Assemblies Consisting of Gold Nanoparticles and a Tris(2,2'-bipyridine)ruthenium(II)-Viologen Linked Thiol. *Langmuir* **2001**, *17*, 5714–5716.
- (432) Cheng, W.; Dong, S.; Wang, E. Gold Nanoparticles as Fine Tuners of Electrochemical Properties of the Electrode/Solution Interface. *Langmuir* **2002**, *18*, 9947–9952.
- (433) Labande, A.; Astruc, D. Colloids as Redox Sensors: Recognition of H_2PO_4^- and HSO_4^- by Amidoferrrocenylalkylthiol-Gold-Nanoparticles. *Chem. Commun.* **2000**, 1007–1008.
- (434) Horikoshi, T.; Itoh, M.; Kurihara, M.; Kubo, K.; Nishihara, H. Synthesis, Redox Behavior and Electrodeposition of Biferrocene-modified Gold Clusters. *J. Electroanal. Chem.* **1999**, *473*, 113–116.
- (435) Yamada, M.; Tadera, T.; Kubo, K.; Nishihara, H. *J. Phys. Chem. B* **2003**, *107*, 3703–3711.
- (436) Yamada, M.; Kubo, K.; Nishihara, H. Electroreductive Deposition of An Clusters Modified with an Anthraquinone Derivative. *Chem. Lett.* **1999**, 1335–1336.
- (437) Yamada, M.; Nishihara, H. Electrochemical Deposition of Metal Nanoparticles Functionalized with Multiple Redox Molecules. In *Dendrimers and Nanoscience*; Astruc, D., Ed.; Comptes-Rendus Chimie, Elsevier: Paris, 2003.
- (438) Ogawa, T.; Kobayashi, K.; Masuda, G.; Takase, T.; Maeda, S. Electronic Conductive Characteristics of Devices Fabricated with 1,10-Decanedithiol and Gold Nanoparticles Between 1- μm Electrode Gaps. *Thin Solid Films* **2001**, *393*, 374–378.
- (439) Chen, S.; Deng, F. Rectifying Nanoscale Electron Transfer by Viologen Moieties and Hydrophobic Electrolyte Ions. *Langmuir* **2002**, *18*, 8942–8948.
- (440) Yamada, M.; Nishihara, H. Electrochemical Construction of an Alternating Multi-Layered Structure of Palladium and Gold Nanoparticles Attached with Biferrocene Moieties. *Chem. Commun.* **2002**, 2578–2579.
- (441) (a) Fujihara, H.; Nakai, H. Fullerene-thiolate-Functionalized Gold Nanoparticles: A New Class of Surface-Confined Metal-C₆₀ Nanocomposites. *Langmuir* **2001**, *17*, 6393–6395. (b) Liljeroth, P.; Quinn, B. M.; Ruiz, V.; Kontturi, K. Charge Injection and Lateral Conductivity in Monolayers of Metallic Nanoparticles. *Chem. Commun.* **2003**, 1570–1571. (c) Zhang, P.; Kim, P. S.; Sham, T. K. Electrochemical Route for the Fabrication of Alkanethiolate-Capped Gold Nanoparticles. *Appl. Phys. Lett.* **2003**, *82*, 1470–1472. (d) Cheng, W.; Dong, S.; Wang, E. Site-Selective Self-Assembly of MPA-Bridged CuHCF Multilayers on APTMS-Supported Gold Colloid Electrodes. *Chem. Mater.* **2003**, *15*, 2495–2501. (e) Li, D.; Zhang, Y.; Li, J. Electrochemical Study of 4-Ferrocene Thiophenol Monolayers Assembled on Gold Nanoparticles. *Microelectron. Eng.* **2003**, *66*, 91–94.
- (442) (a) Park, S.; Yang, P.; Coorod, P.; Weaver, M. J. Transition Metal-Coated Nanoparticle Films: Vibrational Characterization with Surface-Enhanced Raman Scattering. *J. Am. Chem. Soc.* **2002**, *124*, 2428–2429. (b) Jakob, M.; Levanon, H.; Kamat, P. V. Charge Distribution between UV-Irradiated TiO₂ and Gold Nanoparticles: Determination of Shift in the Fermi Level. *Nano Lett.* **2003**, *3*, 353–358.
- (443) (a) Davidovic, D.; Tinkham, M. Coulomb Blockade and Discrete Energy Levels in Au Nanoparticles. *Appl. Phys. Lett.* **1998**, *73*, 3959–3961. Davidovic, D.; Tinkham, M. Spectroscopy, Interactions, and Level Splittings in Au Nanoparticles. *Phys. Rev. Lett.* **1999**, *83*, 1644–1647. (b) Zhang, J.; Lahtinen, R. M.; Kontturi, K.; Unwin, P. R.; Schiffrin, D. J. Electron-Transfer Reactions at Gold Nanoparticles. *Chem. Commun.* **2001**, 1818–1819.
- (444) (a) Zhang, P.; Sham, T. K. Tuning the Electronic Behavior of Au Nanoparticles with Capping Molecules. *Appl. Phys. Lett.* **2002**, *81*, 736–738. (b) Zhang, P.; Sham, T. K. X-Ray Studies of the Structure and Electronic Behavior of Alkanethiolate-Capped Gold Nanoparticles: The Interplay of Size and Surface Effects. *Phys. Rev. Lett.* **2003**, *90*, 245502-1–245502-4. (c) Huang, X.; Huang, H.; Wu, N.; Hu, R.; Zhu, T.; Liu, Z. Investigation of Structure and Chemical States of Self-Assembled Au Nanoscale Particles by Angle-Resolved X-Ray Photoelectron Spectroscopy. *Surf. Sci.* **2000**, *459*, 183–190.

- (445) Mohamed, M. B.; Ahmadi, T. S.; Link, S.; Braun, M.; El-Sayed, M. A. Hot Electron and Phonon Dynamics of Gold Nanoparticles Embedded in a Gel Matrix. *Chem. Phys. Lett.* **2001**, *343*, 55–63.
- (446) (a) Chen, Y.; Palmer, R. E.; Shelley, E. J.; Preece, J. A. HREELS Studies of Gold Nanoparticles with Dialkyl Sulphide Ligands. *Surf. Sci.* **2002**, *502–503*, 208–213. (b) Lin, H.-W.; Wang, X.-H.; Zhao, X.-J.; Li, J.; Wang, F.-S. Metal-Containing Molecular Wires and Their Electron Transportation Properties. *Synth. Met.* **2003**, *135–136*, 239–240.
- (447) (a) Petta, J. R.; Ralph, D. C. Studies of Spin–Orbit Scattering in Noble-Metal Nanoparticles Using Energy-Level Tunneling Spectroscopy. *Phys. Rev. Lett.* **2001**, *87*, 266801-1–266801-4. (b) Bieri, N. R.; Chung, J.; Haferl, S. E.; Poulidakos, D.; Grigoriopoulos, C. P. Microstructuring by Printing and Laser Curing of Nanoparticle Solutions. *Appl. Phys. Lett.* **2003**, *82*, 3529–3531.
- (448) (a) Montalti, M.; Prodi, L.; Zaccaroni, N.; Baxter, R.; Teobaldi, G.; Zerbetto, F. Kinetics of Place-Exchange Reactions of Thiols on Gold Nanoparticles. *Langmuir* **2003**, *19*, 5172–5174. (b) Song, Y.; Murray, R. W. Dynamics and Extent of Ligand Exchange Depend on Electronic Charge of Metal Nanoparticles. *J. Am. Chem. Soc.* **2002**, *124*, 7096–7102.
- (449) Zheng, W.; Maye, M. M.; Leibowitz, F. L.; Zhong, C.-J. Imparting Biomimetic Ion-Gating Recognition Properties to Electrodes with a Hydrogen-Bonding Structured Core–Shell Nanoparticle Network. *Anal. Chem.* **2000**, *72*, 2190–2199.
- (450) Zamborini, F. P.; Hicks, J. F.; Murray, R. W. Quantized Double Layer Charging of Nanoparticle Films Assembled Using Carboxylate/(Cu²⁺ or Zn²⁺)/Carboxylate Bridges. *J. Am. Chem. Soc.* **2000**, *122*, 4514–4515.
- (451) Wuelfling, W. P.; Zamborini, F. P.; Templeton, A. C.; Wen, X.; Yoon, H.; Murray, R. W. Monolayer-Protected Clusters: Molecular Precursors to Metal Films. *Chem. Mater.* **2001**, *13*, 87–95.
- (452) Chen, S.; Pei, R.; Dyer, D. J. Gold Nanoparticle Assemblies by Metal Ion-Pyridine Complexation and Their Rectified Quantized Charging in Aqueous Solutions. *J. Phys. Chem. B* **2002**, *106*, 1903–1908.
- (453) McIntosh, C. M.; Esposito, E. A.; Boal, A. K.; Simard, J. M.; Martin, C. T.; Rotello, V. M. Inhibition of DNA Transcription Using Cationic Mixed Monolayer Protected Gold Clusters. *J. Am. Chem. Soc.* **2001**, *123*, 7626–7629.
- (454) Pietron, J. J.; Murray, R. W. Mediated Electrocatalysis with Polyanthraquinone-Functionalized Monolayer-Protected Clusters. *J. Phys. Chem. B* **1999**, *103*, 4440–4446.
- (455) Miles, D. T.; Murray, R. W. Redox and Double-Layer Charging of Phenothiazine Functionalized Monolayer-Protected Clusters. *Anal. Chem.* **2001**, *73*, 921–929.
- (456) Brousseau, L. C., III; Zhao, D. A.; Shulz, D. A.; Felheim, D. L. pH-Gated Single-Electron Tunneling in Chemically Modified Gold Nanoclusters. *J. Am. Chem. Soc.* **1998**, *120*, 7645–7646.
- (457) Nakai, H.; Yoshihara, M.; Fujihara, H. New Electroactive Tetrathiafulvalene-Derivatized Gold Nanoparticles and Their Remarkably Stable Nanoparticle Films on Electrodes. *Langmuir* **1999**, *15*, 8574–8576.
- (458) Chen, S.; Huang, K. Electrochemical and Spectroscopic Studies of Nitrophenyl Moieties Immobilized on Gold Nanoparticles. *Langmuir* **2000**, *16*, 2014–2018.
- (459) Chandrasekharan, N.; Kamat, P. V. Improving the Photoelectrochemical Performance of Nanostructured TiO₂ Films by Adsorption of Gold Nanoparticles. *J. Phys. Chem. B* **2000**, *104*, 10851–10857.
- (460) (a) Sudeep, P. K.; Ipe, B. I.; Thomas, K. G.; George, M. V.; Barazzouk, S.; Hotchandani, S.; Kamat, P. V. Fullerene-Functionalized Gold Nanoparticles. A Self-Assembled Photoactive Antenna-Metal Nanocore Assembly. *Nano Lett.* **2002**, *2*, 29–35. (b) Thomas, K. G.; Ipe, B. I.; Sudeep, P. K. Photochemistry of Chromophore-Functionalized Gold Nanoparticles. *Pure Appl. Chem.* **2002**, *74*, 1731–1738.
- (461) (a) Kamat, P. V. Photophysical, Photochemical and Photocatalytic Aspects of Metal Nanoparticles. *J. Phys. Chem. B* **2002**, *2*, 7729–7744. (b) Dawson, A.; Kamat, P. V. Semiconductor-Metal Nanocomposites. Photoinduced Fusion and Photocatalysis of Gold-Capped TiO₂ (TiO₂/Gold) Nanoparticles. *J. Phys. Chem. B* **2001**, *105*, 960–966.
- (462) Hu, J.; Zhang, J.; Liu, F.; Kittredge, K.; Whitesell, J. K.; Fox, M. A. Competitive Photochemical Reactivity in a Self-Assembled Monolayer on a Colloidal Gold Cluster. *J. Am. Chem. Soc.* **2001**, *123*, 1464–1470.
- (463) Wang, G.; Zhang, J.; Murray, R. W. DNA Binding of an Ethidium Intercalator Attached to a Monolayer-Protected Gold Cluster. *Anal. Chem.* **2002**, *74*, 4320–4327.
- (464) Aguila, A.; Murray, R. W. Monolayer-Protected Clusters with Fluorescent Dansyl Ligands. *Langmuir* **2000**, *16*, 5949–5964.
- (465) Ipe, B. I.; Thomas, K. G.; Barazzouk, S.; Hotchandani, S.; Kamat, P. V. Photoinduced Charge Separation in a Fluorophore-Gold Nanoassembly. *J. Phys. Chem. B* **2002**, *106*, 18–21.
- (466) Evans, S. D.; Johnson, S. R.; Ringsdorf, R.; Williams, L. M.; Wolf, H. Photoswitching of Azobenzene Derivatives Formed on Planar and Colloidal Gold Surfaces. *Langmuir* **1998**, *14*, 6436–6440.
- (467) Imahori, H.; Arimura, M.; Hanada, T.; Nishimura, Y.; Yamazaki, I.; Sakata, Y.; Fukuzumi, S. Photoactive Three-Dimensional Monolayers: Porphyrin-Alkanethiolate-Stabilized Gold Clusters. *J. Am. Chem. Soc.* **2001**, *123*, 335–336.
- (468) Ionita, P.; Carageorghopol, A.; Gilbert, B. C.; Chechik, V. EPR Study of a Place-Exchange Reaction on Au Nanoparticles: Two Branches of a Disulfide Molecule Do Not Adsorb Adjacent to Each Other. *J. Am. Chem. Soc.* **2002**, *124*, 9048–9049.
- (469) Li, H.; Luk, Y.-Y.; Mrksich, M. Catalytic Asymmetric Dihydroxylation by Gold Colloids Functionalized with Self-Assembled Monolayers. *Langmuir* **1999**, *15*, 4957–4959.
- (470) Pasquato, L.; Rancan, F.; Scrimin, P.; Mancin, F.; Frigeri, C. N-Methylimidazole-Functionalized Gold Nanoparticles as Catalysts for Cleavage of a Carboxylic Acid Ester. *Chem. Commun.* **2000**, 2253–2254.
- (471) Warner, M. G.; Reed, S. M.; Hutchison, J. E. Small, Water-Soluble, Ligand-Stabilized Gold Nanoparticles Synthesized by Interfacial Ligand Exchange Reactions. *Chem. Mater.* **2000**, *12*, 3316–3320.
- (472) Gregori, L.; Hainfeld, J. F.; Simon, M. N.; Golbager, D. Binding of Amyloid β Protein to the 20 S Proteasome. *J. Biol. Chem.* **1997**, *272*, 58–62.
- (473) Alivisatos, A. P.; Johnsson, K. P.; Peng, X.; Wislon, T. E.; Loweth, C. J.; Bruchez, M. P., Jr.; Schultz, P. G. Organization of Nanocrystal Molecules Using DNA. *Nature* **1996**, *382*, 609–611.
- (474) Lipka, J. J.; Hainfeld, J. F.; Wall, J. S. Undecagold Labeling of a Glycoprotein: STEM Visualization of an Undecagoldphosphine Cluster Labeling the Carbohydrate Sites of Human Haptoglobin-Hemoglobin Complex. *J. Ultrastruct. Res.* **1983**, *84*, 120–129.
- (475) Templeton, A. C.; Hostetler, M. J.; Warmoth, E. K.; Chen, S.; Hartshorn, C. M.; Krishnamurthy, V. M.; Forbes, M. D. E.; Murray, R. W. Gateway Reactions to Diverse, Polyfunctional Monolayer-Protected Gold Clusters. *J. Am. Chem. Soc.* **1998**, *120*, 4845–4849.
- (476) Mandal, T. K.; Fleming, M. S.; Walt, D. R. Preparation of Polymer Coated Gold Nanoparticles by Surface-Confined Living Radical Polymerization at Ambient Temperature. *Nano Lett.* **2002**, *2*, 3–7.
- (477) Banerjee, S.; Wong, S. S. Synthesis and Characterization of Carbon Nanotube-Nanocrystal Heterostructures. *Nano Lett.* **2002**, *2*, 195–200.
- (478) Liu, J.; Rinzler, A. G.; Dai, H.; Hafner, J. H.; Bradley, R. K.; Boul, P. J.; Lu, A.; Iverson, T.; Shelimov, K.; Huffman, C. B.; Rodriguez-Macias, F.; Shon, Y.-S.; Lee, T. R.; Colbert, R. E.; Smalley, R. E. Fullerene Pipes. *Science* **1998**, *280*, 1253–1256.
- (479) Ronit, H.; Katz, E.; Willner, I. Magneto-Switchable Bioelectrocatalysis. *J. Am. Chem. Soc.* **2000**, *122*, 12053–12054.
- (480) Wu, M.; O'Neill, S. A.; Brousseau, L. C.; McConnell, W. P.; Schulz, D. A.; Linderman, R. J.; Feldheim, D. L. Synthesis of Nanometer-Sized Hollow Polymer Capsules from Alkanethiol-Coated Gold Particles. *Chem. Commun.* **2000**, 775–776.
- (481) Buining, P. A.; Humbel, B. M.; Philipse, A. P.; Verkleij, A. J. Preparation of Functional Silane-Stabilized Gold Colloids in the (Sub)nanometer Size Range. *Langmuir* **1997**, *13*, 3921–3926.
- (482) Pal, A. Photochemical Dissolution of Gold Nanoparticles by Bromine Containing Trihalomethanes (THMs) in an Aqueous Triton X-100 Medium and its Analytical Application. *J. Photochem. Photobiol.* **2001**, *142*, 59–65.
- (483) Sastry, M.; Rao, M.; Ganesh, K. N. Electrostatic Assembly of Nanoparticles and Biomacromolecules. *Acc. Chem. Res.* **2002**, *35*, 847–855.
- (484) Boal, A. K.; Rotello, V. M. Radial Control of Recognition and Redox Processes with Multivalent Nanoparticle Hosts. *J. Am. Chem. Soc.* **2002**, *124*, 5019–5024.
- (485) Fullam, S.; Rao, S. N.; Fitzmaurice, D. Noncovalent Self-Assembly of Silver Nanocrystal Aggregates in Solution. *J. Phys. Chem. B* **2000**, *104*, 6164–6173.
- (486) Pawsey, S.; McCormick, M.; De Paul, S.; Graf, R.; Lee, Y. S.; Reven, L.; Spiess, H. W. ¹H Fast MAS NMR Studies of Hydrogen-Bonding Interactions in Self-Assembled Monolayers. *J. Am. Chem. Soc.* **2003**, *125*, 4174–4184.
- (487) Zheng, W.; Maye, M. M.; Leibowitz, F. L.; Zhong, C.-J. An Infrared Reflectance Spectroscopic Study of a pH-tunable Network of Nanoparticles Linked by Hydrogen Bonding. *Analyst* **2000**, *125*, 17–20.
- (488) Zhang, F. X.; Zheng, W.; Maye, M. M.; Lou, Y.; Li, H.; Zhong, C.-J. An Infrared Reflection Spectroscopic Assessment of Interfacial Derivatization and Reactivity at Inter-Shell Linked Nanoparticle Films. *Langmuir* **2000**, *16*, 9639–9644.
- (489) Yonezawa, T.; Onoue, S.-Y.; Kimizuka, N. Formation of Nanoparticle Arrays at the Interlayer of Aqueous Phosphate Bilayers. *Chem. Lett.* **2002**, 528–529.
- (490) Fitzmaurice, D.; Rao, S. N.; Preece, J. A.; Stoddart, J. F.; Wenger, S.; Zaccaroni, N. Heterosupramolecular Chemistry: Programmed Pseudorotaxane Assembly at the Surface of a Nanocrystal. *Angew. Chem., Int. Ed.* **1999**, *38*, 1147–1150.
- (491) Hicks, J. F.; Shon, Y. S.; Murray, R. W. Layer-by-Layer Growth of Polymer/Nanoparticle Films Containing Monolayer-Protected Gold Clusters. *Langmuir* **2002**, *18*, 2288–2294.

- (492) Kumar, A.; Mandale, A. B.; Sastry, M. Sequential Electrostatic Assembly of Amine-Derivatized Gold and Carboxylic Acid-Derivatized Silver Colloidal Particles on Glass Substrates. *Langmuir* **2000**, *16*, 6921–6926.
- (493) Schmid, G.; Bäuml, M.; Beyrer, N. Ordered Two-Dimensional Monolayers of Au₅₅ Clusters. *Angew. Chem., Int. Ed.* **2000**, *39*, 181–183.
- (494) Boal, A. K.; Rotello, V. M. *Intra-* and *Intermonolayer* Hydrogen Bonding in Amide-Functionalized Alkanethiol Self-Assembled Monolayers on Gold Nanoparticles. *Langmuir* **2000**, *16*, 9527–9532.
- (495) Carroll, J. B.; Frankamp, B. L.; Rotello, V. M. Self-Assembly of Gold Nanoparticles Through Tandem Hydrogen Bonding and Polyoligosilsequioxane (POSS)-POSS Recognition Processes. *Chem. Commun.* **2002**, 1892–1893.
- (496) Paulini, R.; Frankamp, B. L.; Rotello, V. M. Effects of Branched Ligands on the Structure and Stability of Monolayers on Gold Nanoparticles. *Langmuir* **2002**, *18*, 2368–2373.
- (497) Zhang, Z.; Berg, A.; Levanon, H.; Fessenden, R. W.; Meisel, D. On the Interactions of Free Radicals with Gold Nanoparticles. *J. Am. Chem. Soc.* **2003**, *125*, 7959–7963.
- (498) Miller, S. R.; Gustowski, D. A.; Chen, Z.-H.; Gokel, G. W.; Echeogoyen, L.; Kaifer, A. E. Rationalization of the Unusual Electrochemical Behavior Observed in Lariat Ethers and Other Reducible Macrocyclic Systems. *Anal. Chem.* **1988**, *60*, 2021–2024.
- (499) Beer, P. D.; Gale, P. A. Anion Recognition and Sensing: The State of the Art and Future Perspectives. *Angew. Chem., Int. Ed.* **2001**, *40*, 486–516.
- (500) Valério, C.; Fillaut, J.-L.; Ruiz, J.; Guitard, J.; Blais, J.-C.; Astruc, D. The Dendritic Effect in Molecular Recognition: Ferrocene Dendrimers and their Use as Supramolecular Redox Sensors for the Recognition of Small Inorganic Anions. *J. Am. Chem. Soc.* **1997**, *119*, 2588–2589.
- (501) (a) Lehn, J.-M. *Supramolecular Chemistry: Concepts and Perspectives*; VCH: Weinheim, 1995. (b) Boal, A.; Ilhan, F.; Derouchey, J. E.; Thurn-Albrecht, T.; Russell, T. P.; Rotello, V. Self-assembly of nanoparticles into structured spherical and network aggregates. *Nature* **2000**, *404*, 746–748. (c) Jin, J.; Iyoda, T.; Cao, C.; Song, Y.; Jiang, L.; Li, T. J.; Zhu, D. B. Self-Assembly of Uniform Spherical Aggregates of Magnetic Nanoparticles through π - π Interactions. *Angew. Chem., Int. Ed.* **2001**, *40*, 2135–2138. (d) Liu, J.; Mendoza, S.; Roman, E.; Lynn, M. J.; Xu, R.; Kaifer, A. E. Cyclodextrin-Modified Gold Nanospheres. Host–Guest Interactions at Work to Control Colloidal Properties. *J. Am. Chem. Soc.* **1999**, *121*, 4304–4305. (e) Patil, V.; Mayya, K. S.; Pradhan, S. D.; Satry, M. Evidence for Novel Interdigitated Bilayer Formation of Fatty Acids during Three-Dimensional Self-Assembly on Silver Colloidal Particles. *J. Am. Chem. Soc.* **1997**, *119*, 9281–9282. (f) Caruso, F.; Caruso, R. A.; Mohwald, H. Nanoengineering of Inorganic and Hybrid Hollow Spheres by Colloidal Templating. *Science* **1998**, *282*, 1111–1114. (g) Naka, K.; Itoh, H.; Chujo, Y. Temperature-Dependent Reversible Self-Assembly of Gold Nanoparticles into Spherical Aggregates by Molecular Recognition between Pyrenyl and Dinitrophenyl Units. *Langmuir* **2003**, *19*, 5496–5501. (h) Shenton, W.; Davies, S. A.; Mann, S. Directed Self-Assembly of Nanoparticles into Macroscopic Materials Using Antibody–Antigen Recognition. *Adv. Mater.* **1999**, *11*, 449–452.
- (502) Watanabe, S.; Sonobe, M.; Arai, M.; Tazume, Y.; Matsuo, T.; Nakamura, T.; Yoshida, K. Enhanced Optical Sensing of Anions with Amide-Functionalized Gold Nanoparticles. *Chem. Commun.* **2002**, 2866–2867.
- (503) (a) Lin, S.-Y.; Liu, S.-W.; Lin, C.-M.; Chen, C.-H. Recognition of Potassium Ion in Water by 15-Crown-5 Functionalized Gold Nanoparticles. *Anal. Chem.* **2002**, *74*, 330–335. (b) Obare, S. O.; Hollowell, R. E.; Murphy, C. J. Sensing Strategy for Lithium Ion Based on Gold Nanoparticles. *Langmuir* **2002**, *18*, 10407–10410.
- (504) Kim, Y.; Johnson, R. C.; Hupp, J. T. Gold Nanoparticle-Based Sensing of “Spectroscopically Silent” Heavy Metal Ions. *Nano Lett.* **2001**, *1*, 165–167.
- (505) Frankamp, B. L.; Uzun, O.; Ilhan, F.; Boal, A. K.; Rotello, V. M. Recognition-Mediated Assembly of Nanoparticles into Micellar Structures with Diblock Copolymers. *J. Am. Chem. Soc.* **2002**, *124*, 892–893.
- (506) Xu, H.; Käll, M. Modeling the Optical Response of Nanoparticle-Based Surface Plasmon Resonance Sensors. *Sens. Actuators B* **2002**, *87*, 244–249.
- (507) (a) Zhang, H.-L.; Evans, S. D.; Henderson, J. R.; Miles, R. E.; Shen, T.-H. Vapour Sensing Using Surface Functionalized Gold Nanoparticles. *Nanotechnology* **2002**, *13*, 439–444. (b) Evans, S. D.; Johnson, S. R.; Cheng, Y. L.; Shen, T. Vapour Sensing Using Hybrid Organic–Inorganic Nanostructured Materials. *J. Mater. Chem.* **2000**, *10*, 183–188. (c) Ozsoz, M.; Erdem, A.; Kerman, K.; Ozkan, D.; Tugrul, B.; Topcuoglu, N.; Ekren, H.; Taylan, M. Electrochemical Genosensor Based on Colloidal Gold Nanoparticles for the Detection of Factor V Leiden Mutation Using Disposable Pencil Graphite Electrodes. *Anal. Chem.* **2003**, *75*, 2181–2187. (d) Liu, J.; Lu, Y. A Colorimetric Lead Biosensor Using DNzyme-Directed Assembly of Gold Nanoparticles. *J. Am. Chem. Soc.* **2003**, *125*, 6642–6643. (e) Fantuzzi, G.; Pengo, P.; Gomila, R.; Ballester, P.; Hunter, C. A.; Pasquato, L.; Scrimin, P. Multivalent Recognition of bis- and tris-Zn–Porphyrins by *N*-Methylimidazole Functionalized Gold Nanoparticles. *Chem. Commun.* **2003**, 1004–1005.
- (508) Mirkin, C. A.; Letsinger, R. L.; Mucic, R. C.; Storhoff, J. J. DNA-Based Method for Rationally Assembling Nanoparticles into Macroscopic Materials. *Nature* **1996**, *382*, 607–609.
- (509) Storhoff, J. J.; Mucic, R. C.; Mirkin, C. A. Strategies for Organizing Nanoparticles into Aggregate Structures and Functional Materials. *J. Clust. Sci.* **1997**, *8*, 179–216.
- (510) Elghanian, R.; Storhoff, J. J.; Mucic, R. C.; Letsinger, R. L.; Mirkin, C. A. Selective Colorimetric Detection of Polynucleotides Based on the Distance-Dependent Optical Properties of Gold Nanoparticles. *Science* **1997**, *277*, 1078–1081.
- (511) (a) Storhoff, J. J.; Elghanian, R.; Mucic, R. C.; Mirkin, C. A.; Letsinger, R. L. One-Pot Colorimetric Differentiation of Polynucleotides with Single Base Imperfections Using Gold Nanoparticle Probes. *J. Am. Chem. Soc.* **1998**, *120*, 1959–1964. (b) Mucic, R. C.; Storhoff, J. J.; Mirkin, C. A.; Letsinger, R. L. DNA-Directed Synthesis of Binary Nanoparticles Network Materials. *J. Am. Chem. Soc.* **1998**, *120*, 12674–12675.
- (512) Mitchell, G. P.; Mirkin, C. A.; Letsinger, R. L. Programmed Assembly of DNA Functionalized Quantum Dots. *J. Am. Chem. Soc.* **1999**, *121*, 8122–8123.
- (513) Reynolds, R. A.; Mirkin, C. A.; Letsinger, R. L. Homogeneous, Nanoparticle-Based Quantitative Colorimetric Detection of Oligonucleotides. *J. Am. Chem. Soc.* **2000**, *122*, 3795–3796.
- (514) Storhoff, J. J.; Lazarides, A. A.; Music, R. C.; Mirkin, C. A.; Letsinger, R. L.; Schatz, G. C. What Controls the Optical Properties of DNA-Linked Gold Nanoparticle Assemblies. *J. Am. Chem. Soc.* **2000**, *122*, 4640–4650.
- (515) Taton, T. A.; Mucic, R. C.; Mirkin, C. A.; Letsinger, R. L. The DNA-Mediated Formation of Supramolecular Mono- and Multilayered Nanoparticle Structures. *J. Am. Chem. Soc.* **2000**, *122*, 6305–6306.
- (516) Demers, L. M.; Mirkin, C. A.; Mucic, R. C.; Reynolds, R. A., III; Letsinger, R. L.; Elghanian, R.; Viswanadham, G. A Fluorescence-Based Method for Determining the Surface Coverage and Hybridization Efficiency of Thiol-Capped Oligonucleotides Bound to Gold Thin Films and Nanoparticles. *Anal. Chem.* **2000**, *72*, 5535–5541.
- (517) Storhoff, J. J.; Mirkin, C. A. Programmed Materials Synthesis with DNA. *Chem. Rev.* **1999**, *99*, 1849–1862.
- (518) (a) Lazarides, A. A.; Schatz, G. C. DNA-Linked Metal Nanosphere Materials: Structural Basis for the Optical Properties. *J. Phys. Chem. B* **2000**, *104*, 460–467. (b) Lazarides, A. A.; Schatz, G. C. DNA-Linked Metal Nanosphere Materials: Fourier Transform Solutions for the Optical Response. *J. Chem. Phys.* **2000**, *112*, 2987–2993.
- (519) Niemeyer, C. M.; Burger, W.; Peplies, J. Covalent DNA-Streptavidin Conjugates as Building Blocks for Novel Biometallic Nanostructures. *Angew. Chem., Int. Ed.* **1998**, *37*, 2265–2268.
- (520) (a) Niemeyer, C. M.; Ceyhan, B.; Gao, S.; Chi, L.; Peschel, S.; Simon, U. Site-Selective Immobilization of Gold Nanoparticles Functionalized with DNA Oligomers. *Colloid Polym. Sci.* **2001**, *279*, 68–72. (b) Peschel, S.; Ceyhan, B.; Niemeyer, C. M.; Gao, S.; Chi, L.; Simon, U. Immobilization of Gold Nanoparticles on Solid Supports Utilizing DNA Hybridization. *Mater. Sci. Eng. C* **2002**, *19*, 47–50.
- (521) Hölzel, R.; Gajovic-Eichelmann, N.; Bier, F. F. Oriented and Vectorial Immobilization of Linear M13 dsDNA between Interdigitated Electrodes Towards Single Molecule DNA Nanostructures. *Biosens. Bioelectron.* **2003**, *18*, 555–564.
- (522) Simon, U. In *Metal Clusters in Chemistry*; Braunstein, P., Oro, L., Raithby, P. R., Eds.; Wiley-VCH: Weinheim, 1999; p 1342.
- (523) Simon, U.; Schön, G. In *Handbook of Nanostructured Materials and Nanotechnology*; Nalwa, H. S., Ed.; Academic Press: San Diego, 1999; p 131.
- (524) Xiao, S.; Liu, F.; Rosen, A. E.; Hainfeld, J. F.; Seeman, N. C.; Musier-Forsyth, K.; Kiehl, R. A. Self-Assembly of Metallic Nanoparticle Arrays by DNA Scaffolding. *J. Nanopart. Res.* **2002**, *4*, 313–317.
- (525) Parak, W. J.; Pellegrino, T.; Micheel, C. M.; Gerion, D.; Williams, S. C.; Alivisatos, A. P. Conformation of Oligonucleotides Attached to Gold Nanocrystals Probed by Gel Electrophoresis. *Nano Lett.* **2003**, *3*, 33–36.
- (526) Storhoff, J. J.; Elghanian, R.; Mirkin, C. A.; Letsinger, R. L. Sequence-Dependent Stability of DNA-Modified Gold Nanoparticles. *Langmuir* **2002**, *18*, 6666–6670.
- (527) Park, S.-J.; Lazarides, A. A.; Mirkin, C. A.; Letsinger, R. L. Directed Assembly of Periodic Materials from Protein and Oligonucleotide-Modified Nanoparticle Building Blocks. *Angew. Chem., Int. Ed.* **2001**, *40*, 2909–2912.

- (528) Reynolds, R. A., III; Mirkin, C. A.; Letsinger, R. L. A Gold Nanoparticle/Latex Microsphere-Based Colorimetric Oligonucleotide Detection Methodology. *Pure Appl. Chem.* **2000**, *72*, 229–235.
- (529) Li, Z.; Jin, R.; Mirkin, C. A.; Letsinger, R. L. Multiple Thiol-Anchored Capped DNA-Gold Nanoparticle Conjugates. *Nucleic Acids Res.* **2002**, *30*, 1558–1562.
- (530) Harnack, O.; Ford, W. E.; Yasuda, A.; Wessels, J. M. Tris-(hydroxymethyl)phosphine-Capped Gold Particles Templated by DNA as Nanowire Precursors. *Nano Lett.* **2002**, *2*, 919–923.
- (531) Maeda, Y.; Tabata, H.; Kawai, T. Two-Dimensional Assembly of Gold Nanoparticles with a DNA Network Template. *Appl. Phys. Lett.* **2001**, *79*, 1181–1183.
- (532) Liu, T.; Tang, J.; Zhao, H.; Deng, Y.; Jiang, L. Particle Size Effect of the DNA Sensor Amplified with Gold Nanoparticles. *Langmuir* **2002**, *18*, 5624–5626.
- (533) Sauthier, M. L.; Carroll, R. L.; Gorman, C. B.; Franzen, S. Nanoparticle Layers Assembled through DNA Hybridization: Characterization and Optimization. *Langmuir* **2002**, *18*, 1825–1830.
- (534) Han, S.; Lin, J.; Satjapipat, M.; Baca, A. J.; Zhou, F. A Three-Dimensional Heterogeneous DNA Sensing Surface Formed by Attaching Oligodeoxynucleotide-Capped Gold Nanoparticles onto a Gold-Coated Quartz Crystal. *Chem. Commun.* **2001**, 609–610.
- (535) Zhao, H. Q.; Lin, L.; Li, J. R.; Tang, J. A.; Duan, M. X.; Jiang, L. DNA Biosensor with High Sensitivity Amplified by Gold Nanoparticles. *J. Nanopart. Res.* **2001**, *3*, 321–323.
- (536) Patolsky, F.; Ranjit, K. T.; Lichtenstein, A.; Willner, I. Dendritic of DNA Analysis by Oligonucleotide-Functionalized Au–Nanoparticles. *Chem. Commun.* **2000**, 1025–1026.
- (537) Yonezawa, T.; Onoue, S.-Y.; Kimizuka, N. Metal Coating of DNA Molecules by Cationic, Metastable Gold Nanoparticles. *Chem. Lett.* **2002**, 1172–1173.
- (538) Kumar, A.; Pattarkine, M.; Bhadhbade, M.; Mandale, A. B.; Ganesh, K. N.; Datar, S. S.; Dharmadhikari, C. V.; Sastry, M. Linear Superclusters of Colloidal Gold Particles by Electrostatic Assembly on DNA Templates. *Adv. Mater.* **2001**, *13*, 341–344.
- (539) (a) Sastry, M.; Kumar, A.; Datar, S.; Dharmadhikari, C. V.; Ganesh, K. DNA-Mediated Electrostatic Assembly of Gold Nanoparticles into Linear Arrays by a Simple Drop-Coating Procedure. *Appl. Phys. Lett.* **2001**, *78*, 2943–2945. (b) Hussain, N.; Singh, B.; Sakthivel, T.; Florence, A. T. Formulation and Stability of Surface-Tethered DNA-Gold-Dendron Nanoparticles. *Int. J. Pharm.* **2003**, *254*, 27–31. (c) Sato, K.; Hosokawa, K.; Maeda, M. Rapid Aggregation of Gold Nanoparticles Induced by Non-Cross-Linking DNA Hybridization. *J. Am. Chem. Soc.* **2003**, *125*, 8102–8103.
- (540) (a) Cao, Y. W. C.; Jin, R.; Mirkin, C. A. Nanoparticles with Raman Spectroscopic Fingerprints for DNA and RNA Detection. *Science* **2002**, *297*, 1536–1540.
- (541) (a) Park, S.-J.; Taton, T. A.; Mirkin, C. A. Array-Based Electrical Detection of DNA with Nanoparticle Probes. *Science* **2002**, *295*, 1503–1506. (b) Dong, W.-F.; Sukhorukov, G. B.; Möhwald, H. Enhanced Raman Imaging and Optical Spectra of Gold Nanoparticle Doped Microcapsules. *Phys. Chem. Chem. Phys.* **2003**, *5*, 3003–3012.
- (542) Hashimoto, K.; Ito, K.; Ishimori, Y. Sequence-Specific Gene Detection with a Gold Electrode Modified with DNA Probes and an Electrochemically Active Dye. *Anal. Chem.* **1994**, *66*, 3830–3833.
- (543) Millan, K. M.; Saraullo, A.; Mikkelsen, S. R. Voltammetric DNA Biosensor for Cystic Fibrosis Based on a Modified Carbon Paste Electrode. *Anal. Chem.* **1994**, *66*, 2943–2948.
- (544) (a) Wang, J.; Song, F.; Zhou, F. Silver-Enhanced Imaging of DNA Hybridization at DNA Microarrays with Scanning Electrochemical Microscopy. *Langmuir* **2002**, *18*, 6653–6658. (b) Iacopino, D.; Ongaro, A.; Nagle, L.; Eritja, R.; Fitzmaurice, D. Imaging the DNA and Nanoparticle Components of a Self-Assembled Nanoscale Architecture. *Nanotechnology* **2003**, *14*, 447–452.
- (545) Cai, H.; Wang, Y.; He, P.; Fang, Y. Electrochemical Detection of DNA Hybridization Based on Silver-Enhanced Gold Nanoparticle Label. *Anal. Chim. Acta* **2002**, *469*, 165–172.
- (546) Wang, J.; Xu, D.; Kawde, A.-N.; Polsky, R. Metal Nanoparticle-Based Electrochemical Stripping Potentiometric Detection of DNA Hybridization. *Anal. Chem.* **2001**, *73*, 5576–5581.
- (547) Gearheart, L. A.; Ploehn, H. J.; Murphy, C. J. Oligonucleotide Adsorption to Gold Nanoparticles: A Surface-Enhanced Raman Spectroscopy Study of Intrinsically Bent DNA. *J. Phys. Chem. B* **2001**, *105*, 12609–12615.
- (548) Csáki, A.; Möller, R.; Straube, W.; Köhler, J. M.; Fritzsche, W. DNA Monolayer on Gold Substrates Characterized by Nanoparticle Labeling and Scanning Force Microscopy. *Nucleic Acids Res.* **2001**, *29*, 1–5.
- (549) (a) Bogatyrev, V. A.; Dykman, L. A.; Krasnov, Ya. M.; Plotnikov, V. K.; Khlebtsov, N. G. Differential Light Scattering Spectroscopy for Studying Biospecific Assembling of Gold Nanoparticles with Protein or Oligonucleotide Probes. *Colloid J.* **2002**, *64*, 671–680. (b) Su, M.; Li, S.; Dravid, V. P. Microcantilever Resonance-Based DNA Detection with Nanoparticle Probes. *Appl. Phys. Lett.* **2003**, *82*, 3562–3564. (c) Liu, T.; Tang, J.; Han, M.; Jiang, L. A Novel Microgravimetric DNA Sensor with High Sensitivity. *Biochem. Biophys. Res. Commun.* **2003**, *304*, 98–100. (d) Glynou, K.; Ioannou, P. C.; Christopoulos, T. K.; Syriopoulou, V. Oligonucleotide-Functionalized Gold Nanoparticles as Probes in a Dry-Reagent Strip Biosensor for DNA Analysis by Hybridization. *Anal. Chem.* **2003**, *75*, 4155–4160. (e) Wang, J.; Li, J.; Baca, A.; Hu, J.; Zhou, F.; Yan, W.; Pang, D.-W. Amplified Voltammetric Detection of DNA Hybridization via Oxidation of Ferrocene Caps on Gold Nanoparticles/Streptavidin Conjugates. *Anal. Chem.* **2003**, *75*, 3941–3945. (f) Sandström, P.; Boncheva, M.; Åkerman, B. *Langmuir* **2003**, *19*, 6066–6071. (g) Zheng, M.; Davidson, F.; Huang, X. Ethylene Glycol Monolayer Protected Nanoparticles for Eliminating Nonspecific Binding with Biological Molecules. *J. Am. Chem. Soc.* **2003**, *125*, 7790–7791.
- (550) Natan, M. J.; Lyon, L. A. Surface Plasmon Resonance Biosensing with Colloidal Au Amplification. In *Metal Nanoparticles—Synthesis, Characterization and Applications*; Feldheim, D. L., Colby, A. F., Jr., Eds.; Marcel Dekker: New York, 2002; pp 183–205.
- (551) Thanh, N. T. K.; Rosenzweig, Z. Development of an Aggregation-Based Immunoassay for Anti-Protein A Using Gold Nanoparticles. *Anal. Chem.* **2002**, *74*, 1624–1628.
- (552) Zhang, C.; Zhang, Z.; Yu, B.; Shi, J.; Zhang, X. Application of the Biological Conjugate between Antibody and Colloid Au Nanoparticles as Analyte to Inductively Coupled Plasma Mass Spectrometry. *Anal. Chem.* **2002**, *74*, 96–99.
- (553) Schneider, B. H.; Dickinson, E. L.; Vach, M. D.; Hoijer, J. V.; Howard, L. V. Highly Sensitive Optical Chip Immunoassays in Human Serum. *Biosens. Bioelectron.* **2000**, *15*, 13–22.
- (554) Schneider, B. H.; Dickinson, E. L.; Vach, M. D.; Hoijer, J. V.; Howard, L. V. Optical Chip Immunoassay for hCG in Human Whole Blood. *Biosens. Bioelectron.* **2000**, *15*, 497–604.
- (555) Niemeyer, C. M. Nanoparticles, Proteins, and Nucleic Acids: Biotechnology Meets Materials Science. *Angew. Chem., Int. Ed.* **2001**, *40*, 4128–4158.
- (556) Taton, T. A. Nanostructures as Tailored Biological Probes. *Trends Biotechnol.* **2002**, *20*, 277–279.
- (557) Lin, C.-C.; Yeh, Y.-C.; Yang, C.-Y.; Chen, C.-L.; Chen, G.-F.; Chen, C.-C.; Wu, Y.-C. Selective Binding of Mannose-Encapsulated Gold Nanoparticles to Type 1 Pili in *Escherichia coli*. *J. Am. Chem. Soc.* **2002**, *124*, 3508–3509.
- (558) De la Fuente, J. M.; Barrientos, A. G.; Rojas, T. C.; Rojo, J.; Cañada, A.; Fernandez, A.; Penadés, S. Gold Glyconanoparticles as Water-Soluble Polyvalent Models To Study Carbohydrate Interactions. *Angew. Chem., Int. Ed. Engl.* **2001**, *40*, 2257–2261.
- (559) Rojas, T. C.; de la Fuente, J. M.; Barrientos, A. G.; Penadés, S.; Ponsónnet, L.; Fernández, A. Gold Glyconanoparticles as Building Blocks for Nanomaterials Design. *Adv. Mater.* **2002**, *14*, 585–588.
- (560) Esumi, K.; Hosoya, T.; Suzuki, A.; Torigoe, K. Spontaneous Formation of Gold Nanoparticles in Aqueous Solution of Sugar-Substituted Poly(amidoamine)dendrimers. *Langmuir* **2000**, *16*, 2978–2980.
- (561) (a) Wilson, R. Haptentylated Mercaptodextran-Coated Gold Nanoparticles for Biomolecular Assays. *Chem. Commun.* **2003**, 108–109. (b) Hone, D. C.; Haines, A. H.; Russell, D. A. Rapid, Quantitative Colorimetric Detection of a Lectin Using Mannose-Stabilized Gold Nanoparticles. *Langmuir* **2003**, *19*, 7141–7144. (c) Nolting, B.; Yu, J.-J.; Liu, G.-y.; Cho, S.-J.; Kaulzarich, S.; Gervay-Hague, J. Synthesis of Gold Glyconanoparticles and Biological Evaluation of Recombinant Gp 120 Interactions. *Langmuir* **2003**, *19*, 6465–6473.
- (562) Chow, G. M.; Markowitz, M. A.; Rayne, R.; Dunn, D. N.; Singh, A. Phospholipid Mediated Synthesis and Characterization of Gold Nanoparticles. *J. Colloid Interface Sci.* **1996**, *183*, 135–142.
- (563) Burkett, S. L.; Mann, S. Spatial Organization and Patterning of Gold Nanoparticles on Self-Assembled Biolipid Tubular Templates. *Chem. Commun.* **1996**, 321–322.
- (564) Forstner, M. B.; Käs, J.; Martin, D. Single Lipid Diffusion in Langmuir Monolayers. *Langmuir* **2001**, *17*, 567–570.
- (565) (a) Rautaray, D.; Kumar, A.; Reddy, S.; Sainkar, S. R.; Sastry, M. Morphology of BaSO₄ Crystals Grown on Templates of Varying Dimensionality: The Case of Cysteine-Capped Gold Nanoparticles (0-D), DNA (1-D), and Lipid Bilayer Stacks (2-D). *Cryst. Growth Des.* **2002**, *2*, 197–203. (b) Bhattacharya, S.; Srivastava, A. Synthesis and Characterization of Novel Cationic Lipid and Cholesterol-Coated Gold Nanoparticles and Their Interactions with Dipalmitoylphosphatidylcholine Membranes. *Langmuir* **2003**, *19*, 4439–4447.
- (566) Wong, M. S.; Cha, J. N.; Choi, K.-S.; Deming, T. J.; Stucky, G. D. Assembly of Nanoparticles into Hollow Spheres Using Block Copolypeptides. *Nano Lett.* **2002**, *2*, 583–587.
- (567) (a) Pengo, P.; Broxterman, Q. B.; Kaptein, B.; Pasquato, L.; Scrimin, P. Synthesis of a Stable Helical Peptide and Grafting on Gold Nanoparticles. *Langmuir* **2003**, *19*, 2521–2524. (b) Fan, J.; Chen, S.; Gao, Y. Coating Gold Nanoparticles with Peptide

- Molecules via a Peptide Elongation Approach. *Colloids Surf.* **2003**, *28*, 199–207.
- (568) Templeton, A. C.; Chen, S.; Gross, S. M.; Murray, R. W. Water-Soluble, Isolable Gold Clusters Protected by Tiopronin and Coenzyme A Monolayers. *Langmuir* **1999**, *15*, 66–76.
- (569) Templeton, A. C.; Cliffler, D. E.; Murray, R. W. Redox and Fluorophore Functionalization of Water-Soluble, Tiopronin-Protected Gold Clusters. *J. Am. Chem. Soc.* **1999**, *121*, 7081–7089.
- (570) Boal, A. K.; Rotello, V. M. Fabrication and Self-Optimization of Multivalent Receptors on Nanoparticle Scaffolds. *J. Am. Chem. Soc.* **2000**, *122*, 734–735.
- (571) Boal, A. K.; Rotello, V. M. Redox-Modulated Recognition of Flavin by Functionalized Gold Nanoparticles. *J. Am. Chem. Soc.* **1999**, *121*, 4914–4915.
- (572) Schroedter, A.; Weller, H. Ligand Design and Bioconjugation of Colloidal Gold Nanoparticles. *Angew. Chem., Int. Ed.* **2002**, *41*, 3218–3221.
- (573) Grabar, C. C.; Freeman, R. G.; Hommer, M. B.; Natan, M. J. Preparation and Characterization of Au Colloid Monolayers. *Anal. Chem.* **1995**, *67*, 735–743.
- (574) Su, X.; Yau Li, S. F.; O'Shea, S. J. Au Nanoparticle- and Silver-Enhancement Reaction-Amplified Microgravimetric Biosensor. *Chem. Commun.* **2001**, 755–756.
- (575) Himmelhaus, M.; Takei, H. Cap-Shaped Gold Nanoparticles for an Optical Biosensor. *Sens. Actuators B* **2000**, *63*, 24–30.
- (576) Bharathi, S.; Lev, O. Sol–Gel-Derived Nanocrystalline Gold-Silicate Composite Biosensor. *Anal. Commun.* **1998**, *35*, 29–31.
- (577) Gole, A.; Dash, C.; Soman, C.; Sainkar, S. R.; Rao, M.; Sastry, M. On the Preparation, Characterization, and Enzymatic Activity of Fungal Protease-Gold Colloid Bioconjugates. *Bioconjugate Chem.* **2001**, *12*, 684–690.
- (578) Jia, J.; Wang, B.; Wu, A.; Cheng, G.; Li, Z.; Dong, S. A Method to Construct a Third-Generation Horseradish Peroxidase Biosensor: Self-Assembling Gold Nanoparticles to Three-Dimensional Sol–Gel Network. *Anal. Chem.* **2002**, *74*, 2217–2223.
- (579) Hone, D. C.; Walker, P. I.; Evans-Gowing, R.; FitzGerald, S.; Beby, A.; Chambrier, I.; Cook, M. J.; Russell, D. A. Generation of Cytotoxic Singlet Oxygen via Phthalocyanine-Stabilized Gold Nanoparticles; A Potential Delivery Vehicle for Photodynamic Therapy. *Langmuir* **2002**, *18*, 2985–2987.
- (580) Gardea-Torresdey, J. L.; Parsons, J. G.; Gomez, E.; Peralta-Videa, J.; Troiani, H. E.; Santiago, P.; Yacaman, M. J. Formation and Growth of Au Nanoparticles inside Live Alfalfa Plants. *Nano Lett.* **2002**, *2*, 397–401.
- (581) Mukherjee, P.; Ahmad, A.; Mandal, D.; Senapati, S.; Sainkar, S. R.; Khan, M. I.; Ramani, R.; Parischa, R.; Ajayakumar, P. V.; Alam, M.; Sastry, M.; Kumar, R. Bioreduction of AuCl₄⁻ Ions by the Fungus *Verticillium sp.* and Surface Trapping of the Gold Nanoparticles Formed. *Angew. Chem., Int. Ed.* **2001**, *40*, 3585–3588.
- (582) (a) Hillyer, J. F.; Albrecht, R. M. Gastrointestinal Persorption and Tissue Distribution of Differently Sized Colloidal Gold Nanoparticles. *J. Pharm. Sci.* **2001**, *90*, 1927–1936. (b) Gardea-Torresdey, J. L.; Tiemann, K. J.; Dokken, K.; Tehuacanero, S.; José-Yacamán, M. Gold Nanoparticles Obtained by Bio-Precipitation from Gold (III) Solutions. *J. Nanopart. Res.* **1999**, *1*, 397–404. (c) Mukherjee, P.; Senapati, S.; Mandal, D.; Ahmad, A.; Khan, M. I.; Kumar, R.; Sastry, M. Extracellular Synthesis of Gold Nanoparticles by the Fungus *Fusarium oxysporum*. *ChemBioChem* **2002**, *461*–463.
- (583) (a) Mukhopadhyay, K.; Phadtare, S.; Vinod, V. P.; Kumar, A.; Rao, M.; Chaudhari, R. V.; Sastry, M. Gold Nanoparticles Assembled on Amine-Functionalized Na–Y Zeolite: A Biocompatible Surface for Enzyme Immobilization. *Langmuir* **2003**, *19*, 3858–3863. (b) Phadtare, S.; Kumar, A.; Vinod, V. P.; Dash, C.; Palaskar, D. V.; Rao, M.; Shukla, P. G.; Sivaram, S.; Sastry, M. Direct Assembly of Gold Nanoparticle “Shells” on Polyurethane Microsphere “Cores” and Their Application as Enzyme Immobilization Templates. *Chem. Mater.* **2003**, *15*, 1944–1949. (c) Dragnea, B.; Chen, C.; Kwak, E.-S.; Stein, B.; Kao, C. C. Gold Nanoparticles as Spectroscopic Enhancers for in Vitro Studies on Single Viruses. *J. Am. Chem. Soc.* **2003**, *125*, 6374–6375.
- (584) (a) Rautaray, D.; Kumar, A.; Reddy, S.; Sainkar, S. R.; Sastry, M. Morphology of BaSO₄ Crystals Grown on Templates of Varying Dimensionality: The Case of Cysteine-Capped Gold Nanoparticles (0-D), DNA (1-D), and Lipid Bilayer Stacks (2-D). *Cryst. Growth Des.* **2002**, *2*, 197–203. (b) Tchachenko, A. G.; Xie, H.; Coleman, D.; Glomm, W.; Ryan, J.; Anderson, M. F.; Franzen, S.; Feldheim, D. L. Multifunctional Gold Nanoparticle-Peptide Complexes for Nuclear Targeting. *J. Am. Chem. Soc.* **2003**, *125*, 4700–4701. (c) Li, Z.; Chung, S.-W.; Nam, J.-M.; Ginger, D. S.; Mirkin, C. A. Living Templates for the Hierarchical Assembly of Gold Nanoparticles. *Angew. Chem., Int. Ed.* **2003**, *42*, 2306–2309. (d) Shankar, S. S.; Ahmad, A.; Pasricha, R.; Sastry, M. Bioreduction of Chloroaurate ions by Geranium Leaves and its Endophytic Fungus Yields Gold Nanoparticles of Different Shapes. *J. Mater. Chem.* **2003**, *13*, 1822–1826.
- (585) Cha, D. Y.; Parravano, G. Surface Reactivity of Supported Gold. I. Oxygen Transfer Between Carbon Monoxide and Carbon Dioxide. *J. Catal.* **1970**, *18*, 200–211.
- (586) Parravano, G. Surface Reactivity of Supported Gold. II. Hydrogen Transfer Between Benzene and Cyclohexane. *J. Catal.* **1970**, *18*, 320–328.
- (587) Schwank, J.; Galvano, S.; Parravano, G. Isotopic Oxygen Exchange on Supported Ruthenium and Gold Catalysts. *J. Catal.* **1980**, *63*, 415–424.
- (588) Galvagno, S.; Parravano, G. Chemical Reactivity of Supported Gold. IV. Reduction of Nitric Oxide by Hydrogen. *J. Catal.* **1978**, *55*, 178–190.
- (589) (a) Haruta, M.; Kobayashi, T.; Sano, H.; Yamada, N. Novel Gold Catalysts for the Oxidation of Carbon Monoxide at a Temperature far below 0 °C. *Chem. Lett.* **1987**, 405–406. (b) Haruta, M.; Yamada, N.; Kobayashi, T.; Ijima, S. Gold Catalysts Prepared by Coprecipitation for Low-Temperature Oxidation of Hydrogen and of Carbon Monoxide. *J. Catal.* **1989**, *115*, 301–309.
- (590) Haruta, M. Size- and Support-Dependency in the Catalysis of Gold. *Catal. Today* **1997**, *36*, 153–166.
- (591) Ueda, A.; Oshima, T.; Haruta, M. Reduction of Nitrogen Monoxide with Propene in the Presence of Oxygen and Moisture Over Gold Supported on Metal Oxides. *Appl. Catal. B* **1997**, *12*, 81–93.
- (592) Andreeva, D.; Tabakova, T.; Idakiev, V.; Chistov, P.; Giovanoli, R. Au–Fe₂O₃ Catalyst for Water-Gas Shift Reaction Prepared by Deposition-Precipitation. *Appl. Catal. A* **1998**, *169*, 9–14.
- (593) Sakurai, H.; Haruta, M. Synergism in Methanol Synthesis from Carbon Dioxide Over Gold Catalysts Supported on Metal Oxides. *Catal. Today* **1996**, *29*, 361–365.
- (594) Valden, M.; Lai, X.; Goodman, D. W. Onset of Catalytic Activity of Gold Clusters on Titania with the Appearance of Nonmetallic Properties. *Science* **1998**, *281*, 1647–1650.
- (595) Haruta, M.; Ueda, A.; Tsubota, S.; Torres Sanchez, R. M. Low-Temperature Catalytic Combustion of Methanol and its Decomposed Derivatives Over Supported Gold Catalysts. *Catal. Today* **1996**, *29*, 443–447.
- (596) Yuan, Y.; Asakura, K.; Wan, H.; Tsai, K.; Iwasawa, Y. Supported Gold Catalysts Derived from Gold Complexes and As–Precipitated Metal Hydroxides, Highly Active for Low-Temperature CO Oxidation. *Chem. Lett.* **1996**, *9*, 755–756.
- (597) Kozlova, P.; Kozlov, I.; Sugiyama, S.; Matsui, Y.; Asakura, K.; Iwasawa, Y. Study of Gold Species in Iron-Oxide-Supported Gold Catalysts Derived from Gold-Phosphine Complex Au(PPh₃)(NO₃) and As–Precipitated Wet Fe(OH)₃. *J. Catal.* **1999**, *181*, 37–48.
- (598) Wagner, F. E.; Galvano, S.; Milone, C.; Visco, A. M. Mössbauer Characterization of Gold/Iron Oxide Catalysts. *J. Chem. Soc., Faraday Trans.* **1997**, *93*, 3403–3409.
- (599) Minico, S.; Sciere, S.; Crisafulli, C.; Visco, A. M.; Galvano, S. FT-IR Study of Au/Fe₂O₃ Catalysts for CO Oxidation at Low Temperature. *Catal. Lett.* **1997**, *47*, 273–276.
- (600) Guillemot, D.; Borovkov, V. B.; Polisset-Thofin, M.; Fraissard, J. Surface Characterization of Au/HY by ¹²⁹Xe NMR and Diffuse Reflectance IR Spectroscopy of Adsorbed CO. Formation of Electron-Deficient Gold Particles Inside HY Cavities. *J. Chem. Soc., Faraday Trans.* **1997**, *93*, 3587–3591.
- (601) Salmama, T. M.; Ohnishi, R.; Shido, T.; Ichikawa, M. Highly Selective Catalytic Reduction of NO by H₂ over Au(0) and Au(I) Impregnated in NaY Zeolite Catalysts. *J. Catal.* **1996**, *162*, 169–178.
- (602) Cunningham, D. A.; Vogel, W.; Kageyama, H.; Tsubota, S.; Haruta, M. The Relationship Between the Structure and Activity of Nanometer Size Gold When Supported on Mg(OH)₂. *J. Catal.* **1998**, *177*, 1–10.
- (603) Haruta, M. Novel Catalysis of Gold Deposited on Metal Oxides. *Catal. Surveys Jpn.* **1997**, *1*, 61–73.
- (604) Schubert, M. M.; Hacjenberg, S.; van Vee, A. C.; Muhler, M.; Plzak, V.; Behm, R. CO Oxidation over Supported Gold Catalysts—“Inert” and “Active” Support Materials and Their Role for the Oxygen Supply during Reaction. *J. Catal.* **2001**, *197*, 113–122.
- (605) Haruta, M.; Daté, M. Advances in the Catalysis of Au Nanoparticles. *Appl. Catal. A* **2001**, *222*, 427–437.
- (606) Bera, P.; Hedge, M. S. Characterization and Catalytic Properties of Combustion Synthesized Au/CeO₂ Catalyst. *Catal. Lett.* **2002**, *79*, 75–81.
- (607) (a) Bond, G. C.; Thompson, D. T. Catalysis by Gold. *Catal. Rev.-Sci. Eng.* **1999**, *41*, 319–388. (b) Bond, G. C.; Thompson, D. T. Gold-Catalyzed Oxidation of Carbon Monoxide. *Gold Bull.* **2000**, *33*, 41–51. (c) Fan, L.; Ichikuni, N.; Shimazu, S.; Uematsu, T. Preparation of Au/TiO₂ Catalysts by Suspension Spray Reaction Method and Their Catalytic Property for CO Oxidation. *Appl. Catal.* **2003**, *246*, 87–95.
- (608) Kozlov, A. I.; Kozlova, A. P.; Liu, H.; Iwasawa, Y. A New Approach to Active Supported Au Catalysts. *Appl. Catal. A* **1999**, *182*, 9–28.
- (609) Serna, R.; Missana, T.; Afonso, C. N.; Ballesteros, J. M.; Petford-Long, A. K.; Doole, R. C. Bi Nanocrystals Embedded in an

- Amorphous Ge Matrix Grown by Pulsed Laser Deposition. *Appl. Phys. A* **1998**, *66*, 43–47.
- (610) Horváth, D.; Tóth, L.; Gucci, L. Gold Nanoparticles: Effect of Treatment on Structure and Catalytic Activity of Au/Fe₂O₃ Catalyst Prepared by Co-Precipitation. *Catal. Lett.* **2000**, *67*, 117–128.
- (611) Gucci, L.; Horváth, D.; Pászti, Z.; Tóth, L.; Horváth, Z. E.; Karacs, A.; Petó, G. Modeling Gold Nanoparticles: Morphology, Electron Structure, and Catalytic Activity in CO Oxidation. *J. Phys. Chem. B* **2000**, *104*, 3183–3193.
- (612) Gucci, L.; Horváth, D.; Pászti, Z.; Petó, G. Effect of Treatments on Gold Nanoparticles Relation Between Morphology, Electron Structure and Catalytic Activity in CO Oxidation. *Catal. Today* **2002**, *72*, 101–105.
- (613) Petó, G.; Molnár, G. L.; Pászti, Z.; Geszti, O.; Beck, A.; Gucci, L. Electronic Structure of Gold Nanoparticles Deposited on SiO/Si(100). *Mater. Sci. Eng. C* **2002**, *19*, 95–99.
- (614) Gucci, L.; Petó, G.; Beck, A.; Frey, K.; Geszti, O.; Molnár, G.; Daróczy, C. Gold Nanoparticles Deposited on SiO₂/Si(100): Correlation Between Size, Electron Structure, and Activity in CO Oxidation. *J. Am. Chem. Soc.* **2003**, *125*, 4332–4337.
- (615) Kawasaki, T.; Takai, Y.; Shimizu, R. Distorted Surface and Interface Structures of Catalytic Gold Nanoparticles Observed by Spherical Aberration-Free Phase Electron Microscopy. *Appl. Phys. Lett.* **2001**, *79*, 3509–3511.
- (616) Finch, R. M.; Hodge, N. A.; Hutchings, G. J.; Meagher, A.; Pankhurst, Q. A.; Siddiqui, M. R. H.; Wagner, F. E.; Whyman, R. Identification of Active Phases in Au–Fe Catalysts for Low-Temperature CO Oxidation. *Phys. Chem. Chem. Phys.* **1999**, *1*, 485–489.
- (617) Okumura, M.; Tsubota, S.; Iwamoto, M.; Haruta, M. Chemical Vapor Deposition of Gold Nanoparticles on MCM-41 and Their Catalytic Activities for the Low-Temperature Oxidation of CO and of H₂. *Chem. Lett.* **1998**, 315–316.
- (618) Schimpf, S.; Lucas, M.; Mohr, C.; Rodemerck, U.; Brückner, A.; Radnik, J.; Hofmeister, H.; Claus, P. Supported Gold Nanoparticles: in Depth Catalyst Characterization and Application in Hydrogenation and Oxidation Reactions. *Catal. Today* **2002**, *72*, 63–78.
- (619) Grunwaldt, J.-D.; Kiener, C.; Wogerbauer, C.; Baiker, A. Preparation of Supported Gold Catalysts for Low-Temperature CO Oxidation via “Size-Controlled” Gold Colloids. *J. Catal.* **1999**, *181*, 223–232.
- (620) Boccuzzi, C. A.; Manzola, M. Au/TiO₂ Nanostructured Catalyst: Effects of Gold Particle Sizes on CO Oxidation at 90 K. *Mater. Sci. Eng. C* **2001**, *15*, 215–217.
- (621) Sayo, K.; Deki, S.; Hayashi, S. Novel Method for Preparation of a Nanosized Gold Catalyst Supported on TiO₂. *J. Colloid Interface Sci.* **1999**, *212*, 597–599.
- (622) Cataliotti, R. S.; Compagnini, G.; Crisafulli, C.; Minicò, S.; Pignataro, B.; Sassi, P.; Scire, S. Low-Frequency Raman Modes and Atomic Force Microscopy for the Size Determination of Catalytic Gold Clusters Supported on Iron Oxide. *Surf. Sci.* **2001**, *494*, 75–82.
- (623) Franceschetti, A.; Pennycook, S. J.; Pantelides, S. T. Oxygen Chemisorption on Au Nanoparticles. *Chem. Phys. Lett.* **2003**, *374*, 471–475.
- (624) Maye, M. M.; Lou, Y.; Zhong, C.-J. Core–Shell Gold Nanoparticle Assembly as Novel Electrocatalyst of CO Oxidation. *Langmuir* **2000**, *16*, 7520–7523.
- (625) Lou, Y.; Maye, M. M.; Han, L.; Luo, J.; Zhong, C. J. Gold–Platinum Alloy Nanoparticle Assembly as Catalyst for Methanol Electrooxidation. *Chem. Commun.* **2001**, 473–474.
- (626) Luo, J.; Maye, M. M.; Lou, Y.; Han, L.; Hepel, M.; Zhong, C. J. Catalytic Activation of Core–Shell Assembled Gold Nanoparticles as Catalyst for Methanol Electrooxidation. *Catal. Today* **2002**, *77*, 127–138.
- (627) (a) Luo, J.; Lou, Y.; Maye, M. M.; Zhong, C. J.; Hepel, M. An EQCN Assessment of Electrocatalytic Oxidation of Methanol at Nanostructured Au–Pt Alloy Nanoparticles. *Electrochem. Commun.* **2001**, *3*, 172–176. (b) Jaramillo, T. F.; Baeck, S.-H.; Cuenya, B. R.; McFarland, E. W. Catalytic Activity of Supported Au Nanoparticles Deposited from Block Copolymer Micelles. *J. Am. Chem. Soc.* **2003**, *125*, 7148–7149.
- (628) (a) Zhong, C.-J.; Maye, M. M. Core–Shell Assembled Nanoparticles as Catalysts. *Adv. Mater.* **2001**, *13*, n° 19, 1507–1511. (b) Zhang, Y.; Asahina, S.; Yoshihara, S.; Shirakashi, T. Oxygen Reduction on Au Nanoparticle Deposited Boron-Doped Diamond Films. *Electrochim. Acta* **2003**, *48*, 741–747.
- (629) El-Deab, M. S.; Ohsaka, T. An Extraordinary Electrocatalytic Reduction of Oxygen on Gold Nanoparticles-Electrodeposited Gold Electrodes. *Electrochem. Commun.* **2002**, *4*, 288–292.
- (630) Claus, P.; Brückner, A.; Mohr, C.; Hofmeister, H. Supported Gold Nanoparticles from Quantum Dot to Mesoscopic Size Scale: Effect of Electronic and Structural Properties on Catalytic Hydrogenation of Conjugated Functional Groups. *J. Am. Chem. Soc.* **2000**, *122*, 11430–11439.
- (631) Mohr, C.; Hofmeister, H.; Claus, P. The Influence of Real Structure of Gold Catalysts in the Partial Hydrogenation of Acrolein. *J. Catal.* **2002**, *213*, 86–94.
- (632) Mohr, C.; Hofmeister, H.; Radnik, J.; Claus, P. Identification of Active Sites in Gold-Catalyzed Hydrogenation of Acrolein. *J. Am. Chem. Soc.* **2003**, *125*, 1905–1911.
- (633) Mukherjee, P.; Patra, C. R.; Ghosh, A.; Kumar, R.; Sastry, M. Characterization and Catalytic Activity of Gold Nanoparticles Synthesized by Auto-reduction of Aqueous Chloroaurate Ions with Fumed Silica. *Chem. Mater.* **2002**, *14*, 1678–1684.
- (634) Bartz, M.; Küther, J.; Seshadri, R.; Tremel, W. Colloid-Bound Catalysts for Ring-Opening Metathesis Polymerization: A Combination of Homogeneous and Heterogeneous Properties. *Angew. Chem., Int. Ed.* **1998**, *37*, 2466–2468.
- (635) Kapoor, M. P.; Sinha, A. K.; Seelan, S.; Inagaki, S.; Tsubota, S.; Hoshida, H.; Haruta, M. Hydrophobicity Induced Vapor-Phase Oxidation of Propene Over Gold Supported on Titanium Incorporated Hybrid Mesoporous Silsesquioxane. *Chem. Commun.* **2002**, 2902–2903.
- (636) Bianchi, C. L.; Porta, F.; Prati, L.; Rossi, M. Selective Liquid-Phase Oxidation Using Gold Catalysts. *Topics Catal.* **2000**, *13*, 231–236.
- (637) Porta, F.; Prati, L.; Rossi, M. Metal Sols as a Useful Tool for Heterogeneous Gold Catalyst Preparation: Reinvestigation of a Liquid-Phase Oxidation. *Catal. Today* **2000**, *61*, 165–172.
- (638) Li, X.-M.; Paraschiv, V.; Huskens, J.; Reinhoudt, D. N. Sulfonic Acid-Functionalized Gold Nanoparticles: A Colloid-Bound Catalyst for Soft Lithographic Application on Self-Assembled Monolayers. *J. Am. Chem. Soc.* **2003**, *125*, 4279–4284.
- (639) (a) Troiani, H. E.; Camacho-Bragado, A.; Armendariz, V.; Torresday, J. L. G.; Yacaman, M. J. Synthesis of Carbon Anions by Gold Nanoparticles and Electron Irradiation. *Chem. Mater.* **2003**, *15*, 1029–1031. (b) Scire, S.; Minicò, S.; Crisafulli, C.; Satriano, C.; Pistone, A. Catalytic Combustion of Volatile Organic Compounds on Gold/Cerium Oxide Catalysts. *Appl. Catal. B: Environmental* **2003**, *40*, 43–49.
- (640) Hayakawa, K.; Yoshimura, T.; Esumi, K. Preparation of Gold Dendrimer Nanocomposites by Laser Irradiation and Their Catalytic Reduction of 4-Nitrophenol. *Langmuir* **2003**, *19*, 5517–5521.
- (641) Inouye, H.; Tanaka, K.; Tanahashi, I.; Hirao, K. Ultrafast Dynamics of Nonequilibrium Electrons in a Gold Nanoparticle System. *Phys. Rev. B* **1998**, *57*, 11334–11340.
- (642) Shen, Y. R. *The Principles of Nonlinear Optics*; Wiley: New York, 1984.
- (643) Ricard, D.; Roussignol, Ph.; Flytzanis, C. Surface-Mediated Enhancement of Optical Phase Conjugation in Metal Colloids. *Opt. Lett.* **1985**, *10*, 511–513.
- (644) Hache, F.; Ricard, D.; Flytzanis, C.; Kreibig, U. The Optical Kerr Effect in Small Metal Particles and Metal Colloids: The Case of Gold. *Appl. Phys. A* **1988**, *47*, 347–357.
- (645) Fukumi, K.; Chayahara, A.; Kadono, K.; Sakaguchi, T.; Horino, Y.; Miya, M.; Hahakawa, J.; Satou, M. Au⁺-Ion-Implanted Silica Glass with Non-Linear Optical Property. *Jpn. J. Appl. Phys.* **1991**, *30*, L742–L744.
- (646) Fukumi, K.; Chayahara, A.; Kadono, K.; Sakaguchi, T.; Horino, Y.; Miya, M.; Fujii, K.; Hayakawa, J.; Satou, M. Gold Nanoparticles Ion Implanted in Glass with Enhanced Nonlinear Optical Properties. *J. Appl. Phys.* **1994**, *75*, 3075–3080.
- (647) Sasai, J.; Hirao, K. Crystallization Effect on Non-Linear Optical Response of Silicate Glass and Glass-Ceramics Containing Gold Nanoparticles. *J. Non-Cryst. Solids* **2001**, *290*, 49–56.
- (648) Sasai, J.; Hirao, K. Relaxation Behavior of Nonlinear Optical Response in Borate Glasses Containing Gold Nanoparticles. *J. Appl. Phys.* **2001**, *89*, 4548–4553.
- (649) Inouye, H.; Kanemitsu, Y. Direct Observation of Nonlinear Effects in a One-Dimensional Photonic Crystal. *Appl. Phys. Lett.* **2003**, *82*, 1155–1157.
- (650) Shen, Y.-C.; Tang, Z.; Gui, M.; Cheng, J.; Wang, X.; Lu, Z. Nonlinear Optical Response of Colloidal Gold Nanoparticles Studied by Hyper-Rayleigh Scattering Technique. *Chem. Lett.* **2000**, 1140–1141.
- (651) Vargas-Baca, I.; Brown, A. P.; Andrews, M. P.; Galstian, T.; Li, Y.; Vali, H.; Kuzyk, M. G. Linear and Nonlinear Optical Responses of a Dye Anchored to Gold Nanoparticles Dispersed in Liquid and Polymeric Matrixes. *Can. J. Chem.* **2002**, *80*, 1625–1633.
- (652) Antoine, R.; Brevet, P. F.; Girault, H. H.; Bethell, D.; Schiffrin, D. J. Surface Plasmon Enhanced Non-Linear Optical Response of Gold Nanoparticles at the Air/Toluene Interface. *Chem. Commun.* **1997**, 1901–1902.
- (653) Novak, J. P.; Brousseau, L. C., III; Vance, F. W.; Johnson, R. C.; Lemon, B. I.; Hupp, J. T.; Feldheim, D. L. Nonlinear Optical Properties of Molecularly Bridged Gold Nanoparticle Arrays. *J. Am. Chem. Soc.* **2000**, *122*, 12029–12030.
- (654) Qu, S.; Song, Y.; Du, C.; Wang, Y.; Gao, Y.; Liu, S.; Li, Y.; Zhu, D. Nonlinear Optical Properties in Three Novel Nanocomposites with Gold Nanoparticles. *Opt. Commun.* **2001**, *196*, 317–323.

- (655) Qu, S.; Du, C.; Song, Y.; Wang, Y.; Gao, Y.; Liu, S.; Li, Y.; Zhu, D. Optical Nonlinearities and Optical Limiting Properties in Gold Nanoparticles Protected by Ligands. *Chem. Phys. Lett.* **2002**, *356*, 403–408.
- (656) Fang, H.; Du, C.; Qu, S.; Li, Y.; Song, Y.; Li, H.; Liu, H.; Zhu, D. Self-Assembly of the [60] Fullerene-Substituted Oligopyridines on Au Nanoparticles and the Optical Nonlinearities of the Nanoparticles. *Chem. Phys. Lett.* **2002**, *364*, 290–296.
- (657) Vance, F. W.; Lemon, B. I.; Hupp, J. T. Enormous Hyper-Rayleigh Scattering from Nanocrystalline Gold Particle Suspensions. *J. Phys. Chem. B* **1998**, *102*, 10091–10093.
- (658) Galletto, P.; Brevet, P. F.; Girault, H. H.; Antoine, R.; Broyer, M. Size Dependence of the Surface Plasmon Enhanced Second Harmonic Response of Gold Colloids: Towards a New Calibration Methodology. *Chem. Commun.* **1999**, 581–582.
- (659) Olsen, A. W.; Kafafi, Z. H. Gold Cluster-Laden Polydiacetylenes: Novel Materials for Nonlinear Optics. *J. Am. Chem. Soc.* **1991**, *113*, 7758–7760.
- (660) Neiman, B.; Grushka, E.; Lev, O. Use of Gold Nanoparticles to Enhance Capillary Electrophoresis. *Anal. Chem.* **2001**, *73*, 5220–5227.
- (661) Pumera, M.; Wang, J.; Grushka, E.; Polsky, R. Gold Nanoparticle-Enhanced Microchip Capillary Electrophoresis. *Anal. Chem.* **2001**, *73*, 5625–5628.
- (662) Krenn, J. R.; Salerno, M.; Felidj, N.; Lamprecht, B.; Schider, G.; Leitner, A.; Aussenegg, F. R.; Weeber, J. C.; Dereux, A.; Goudonnet, J. P. Light Field Propagation by Metal Micro- and Nanostructures. *J. Microsc.* **2001**, *202*, 122–128.
- (663) Ng, L. N.; Luff, B. J.; Zervas, M. N.; Wilkinson, J. S. Propulsion of Gold Nanoparticles on Optical Waveguides. *Opt. Commun.* **2002**, *208*, 117–124.
- (664) Park, J. H.; Lim, Y. T.; Park, O. O.; Kim, Y. C. Enhancement of Photostability in Blue-Light-Emitting Polymers Doped with Gold Nanoparticles. *Macromol. Rapid Commun.* **2003**, *24*, 331–334.
- (665) Recent miscellaneous references added in proof: (a) Lowe, L. B.; Brewer, S. H.; Krämer, S.; Fuierer, R. R.; Qian, G.; Agbasi-Porter, O.; Moses, C.; Franzen, S.; Feldheim, D. L. Laser-Induced Temperature Jump Electrochemistry on Gold Nanoparticles-Coated Electrodes. *J. Am. Chem. Soc.* **2003**, *125*, 14258–14259. (b) Olofsson, L.; Rindzevicius, T.; Pfeiffer, I.; Käll, M.; Höök, F. Surface-Based Gold Nanoparticle Sensors for Specific and Quantitative DNA Hybridization Detection. *Langmuir* **2003**, *19*, 10414–10419. (c) Wurz, G. A.; Hranisavljevic, J.; Wiederrecht, G. P. Electromagnetic Scattering Pathways for Metallic Nanoparticles: A Near-Field Optical Study. *Nano Lett.* **2003**, *3*, 1511–1516. (d) Addition, Suppression, and Inhibition in the Electrophoretic Deposition of Nanocrystal Mixture Films for CdSe Nanocrystals with $\gamma\text{-Fe}_2\text{O}_3$ and Au Nanocrystals. Islam, M. A.; Xia, Y.; Steigerwald, M. L.; Yin, M.; Liu, Z.; O'Brien, S.; Levicky, R.; Herman, I. P. *Nano Lett.* **2003**, *3*, 1603–1606.

CR030698+